

Nonlinear Optics

Christian Koos

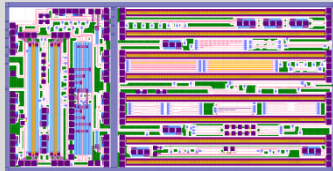
Institute of Photonics and Quantum Electronics (IPQ)
Institute of Microstructure Technology (IMT)



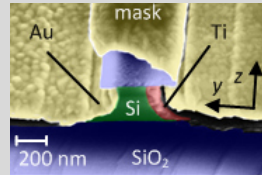
Lecture 1

Our research: Photonic Integration – Technologies and Applications

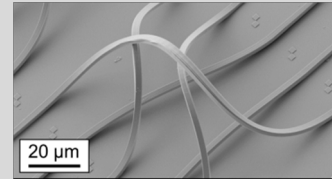
Photonic IC Design and Fabless Fabrication (IPQ)



Nanophotonic and Teratronic Devices (IMT)



3D Photonic Integration (IMT/IPQ)



~ 20 PhD candidates and postdocs
 11 tech./admin. staff
 ~ 15 students



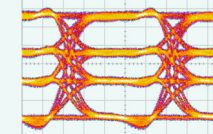
W. Freude



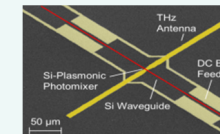
C. Koos



S. Randel



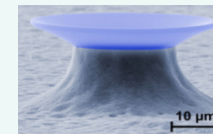
Optical Communications (IPQ)



Teratronic Signal Processing (IPQ/IMT)



Optical Metrology (IPQ)



Biophotonics (IMT)

DSPOC: Digital Signal Processing in Optical Communications (Workshop & Lecture by Prof. Sebastian Randel)



This course will provide practical knowledge about the design and implementation of digital-signal-processing (DSP) algorithms in optical communication systems. Topics will be introduced in lectures and applied in practical exercises in the computer lab using MATLAB. The course will cover the following topics:

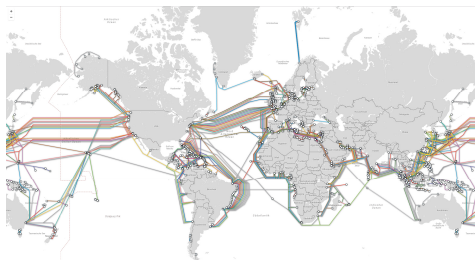
- Modulation formats, entropy, spectral efficiency, pulse shaping
- Noise sources and statistics
- Performance evaluation: Bit-error ratio, Q-Factor, OSNR-Penalty, Mutual Information, Monte Carlo Simulation
- Modeling systems with intensity modulation and direct detection
- Digital coherent receivers (carrier recovery, timing recovery, chromatic dispersion compensation, adaptive equalization)
- Impact and compensation of chromatic dispersion and polarization-mode dispersion
- System impact of fiber nonlinearities

Lecture (1 SWS): Tuesday 11:30-13:00

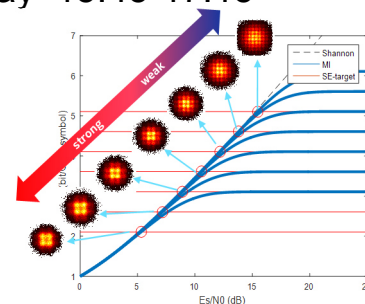
Building 20.40, Neuer Hörsaal (NH)

Workshop (2 SWS): Thursday 15:45-17:15

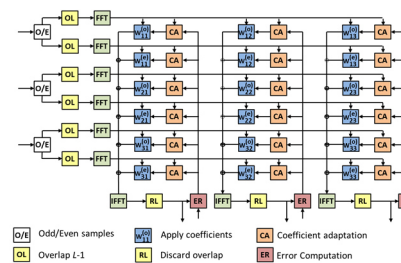
Building 20.21, SCC-PC-Pool L



<http://www.submarinecablemap.com/>



Probabilistic constellation shaping (figure from: F. Buchali NOKIA)



Adaptive MIMO equalizer



FPGA implementation www.xilinx.com



The need for high-speed optical communications



Papal election 2005
(Benedict XVI)

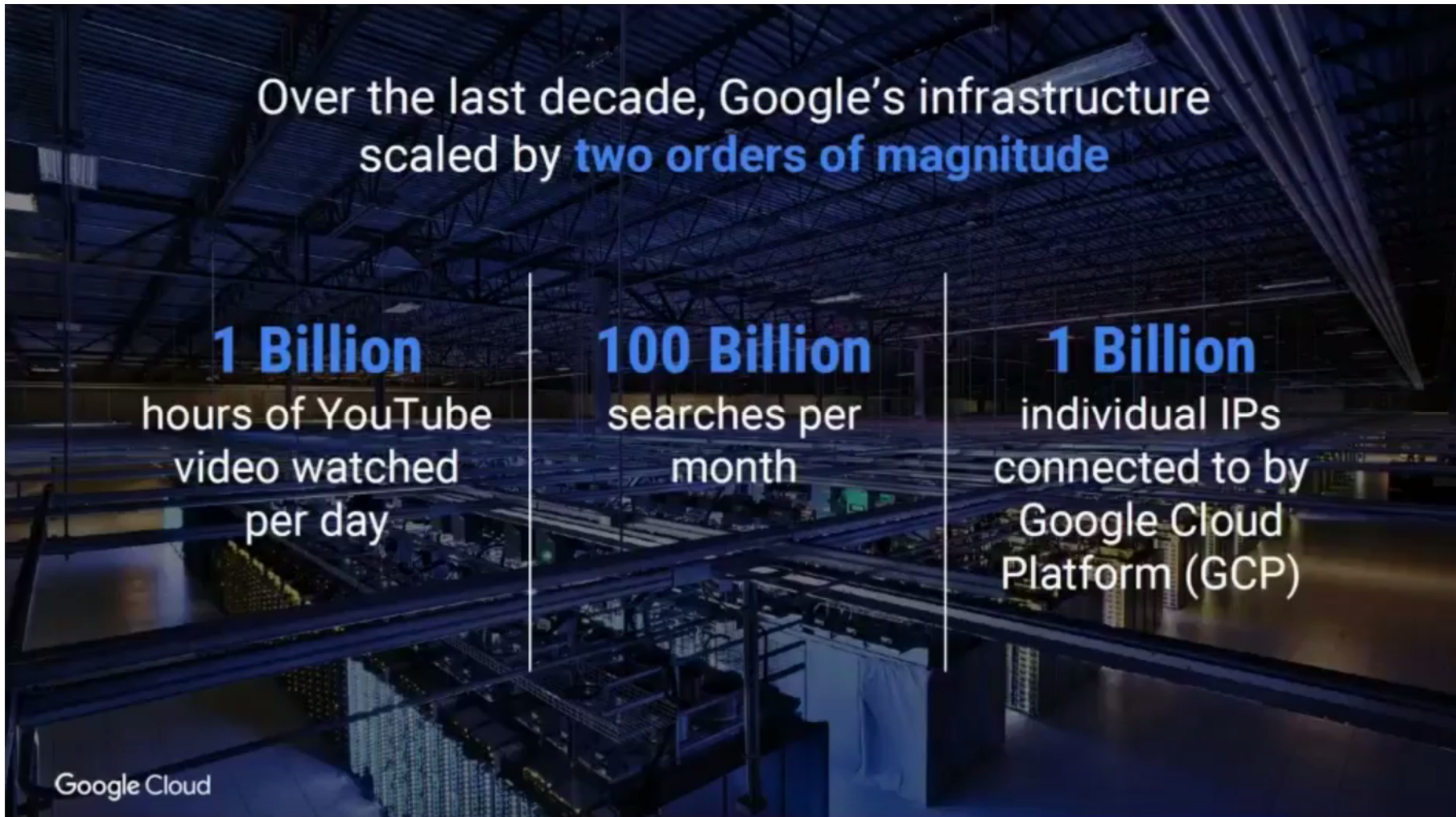


Papal election 2013
(Francis)

Our Research: Teratronics and Photonics

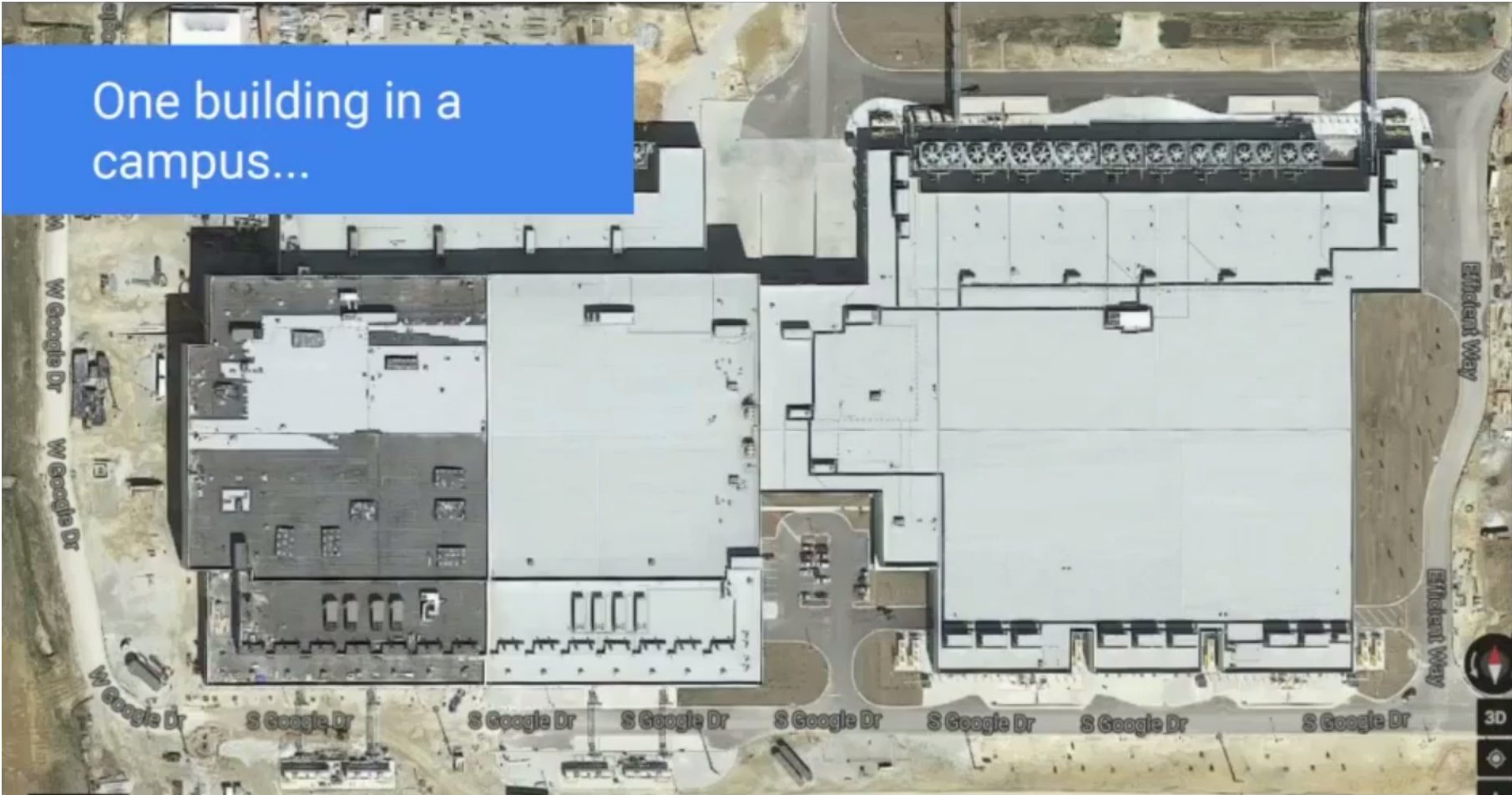


Capacity challenges in communication networks



Source: Urs Hölzle (Google employee No. 8, today: VP Technical Infrastructure), OFC 2017

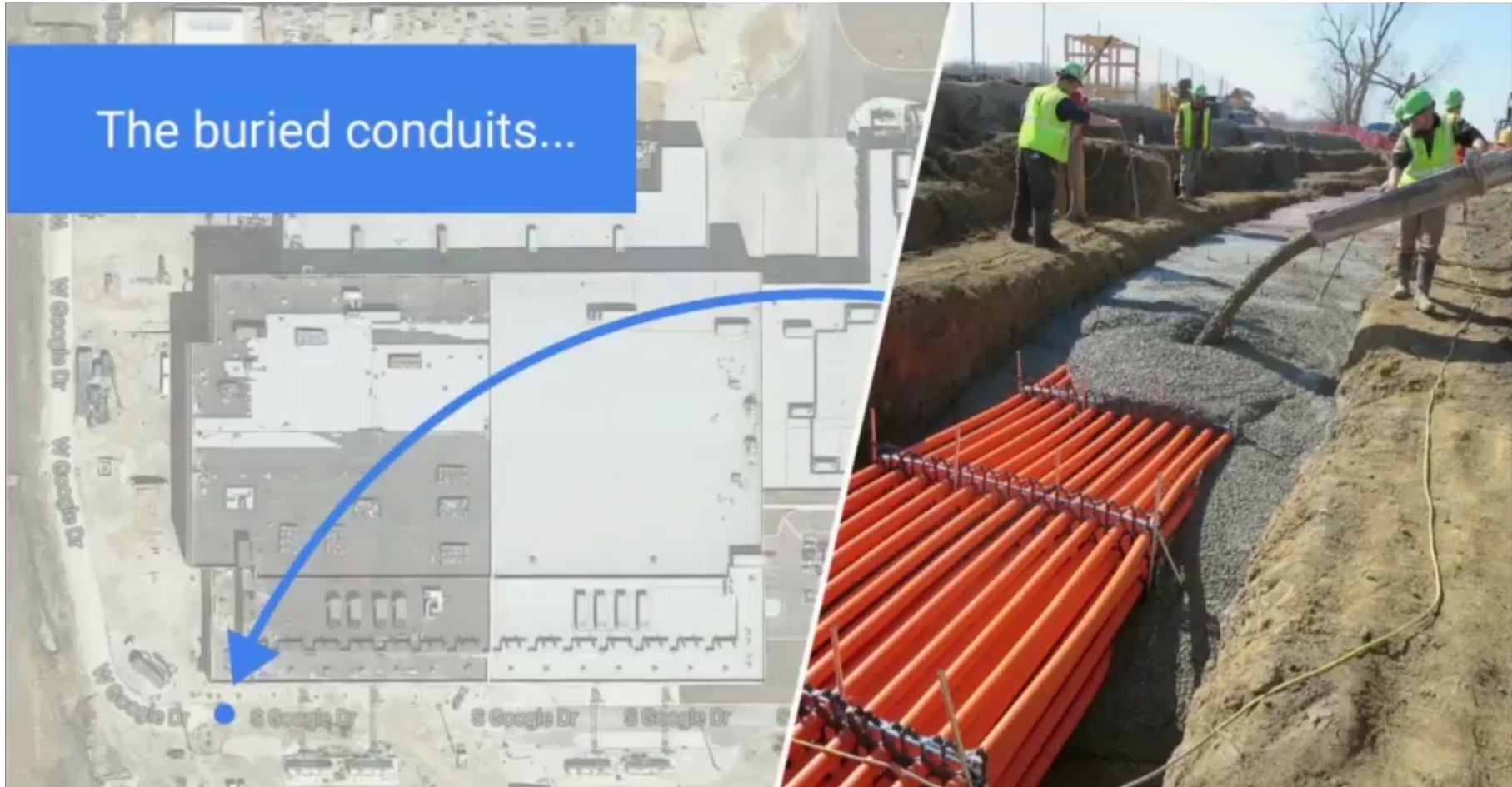
Connection of Data Centers through Campus-Area Networks



U. Hölzle, OFC 2017 Plenary Talk

Connection of Data Centers through Campus-Area Networks

KIT
Karlsruhe Institute of Technology



U. Hölzle, OFC 2017 Plenary Talk



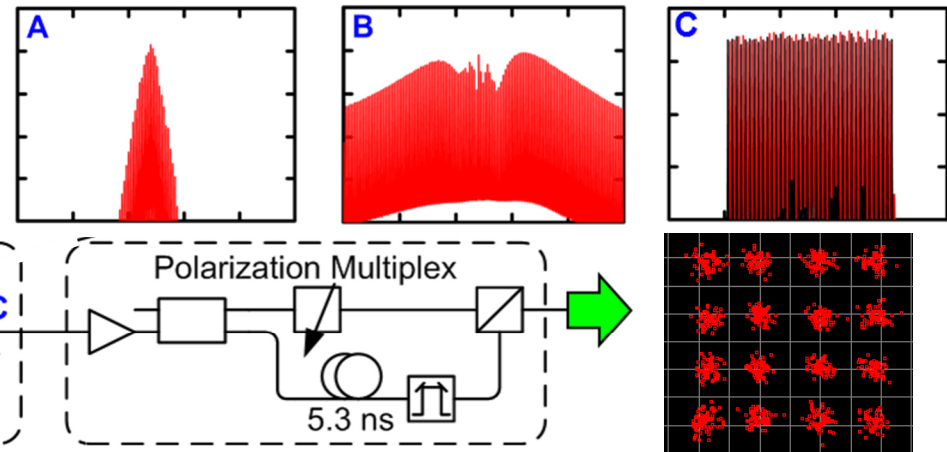
- ⇒ Further scaling requires increase of data rate per fiber
- ⇒ Massively parallel wavelength division multiplexing (WDM)

U. Hölzle, OFC 2017 Plenary Talk

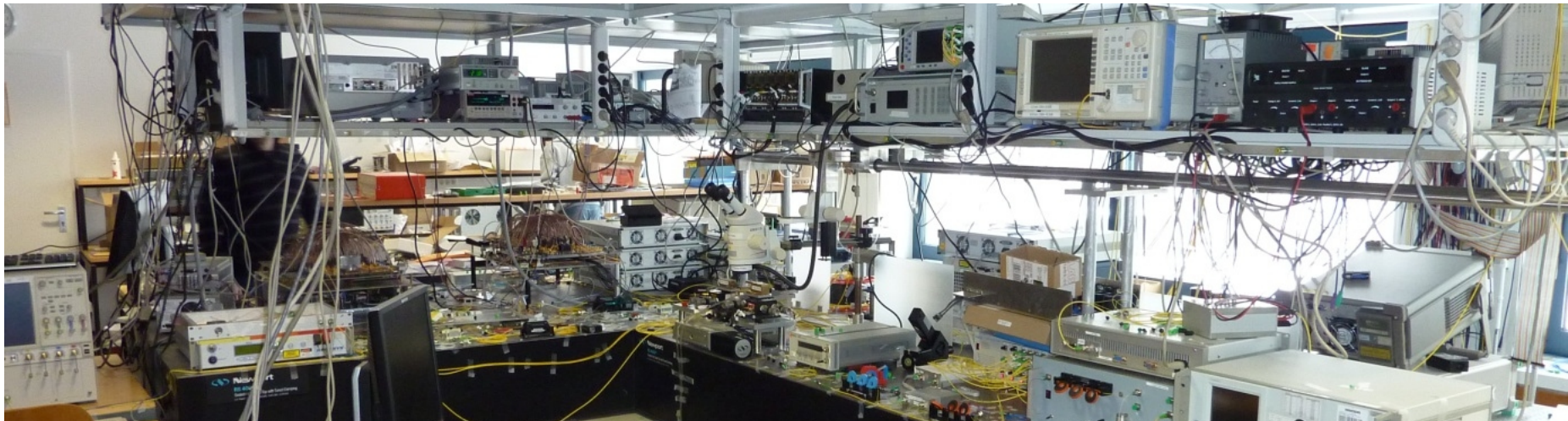
Massively parallel wavelength-division multiplexing (WDM) using optical frequency combs

Previous demonstration: Use frequency comb, generated by a mode-locked laser
 325 channels, 12.5 GBd,
 16 QAM, PoMUX \Rightarrow **32.5 Tbit/s**

Nonlinear Optics!



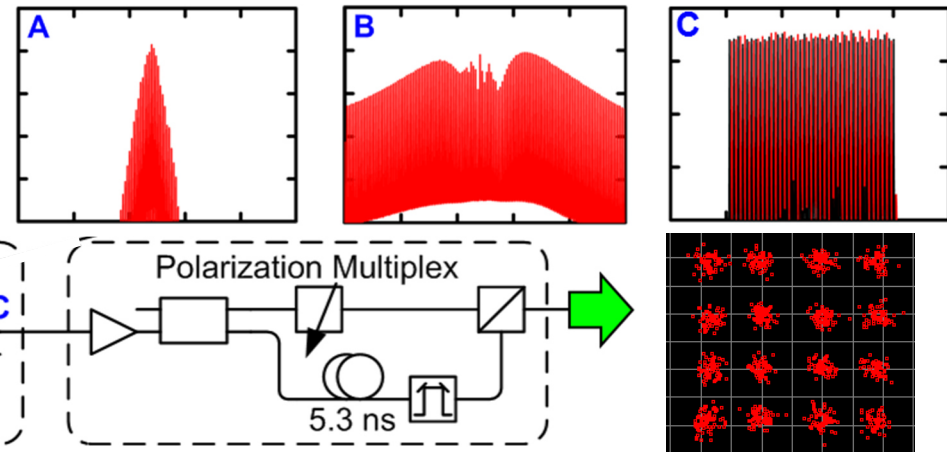
Hillerkuss *et al.*, Nat. Photon. 5, 364–371 (2011)



Massively parallel wavelength-division multiplexing (WDM) using optical frequency combs

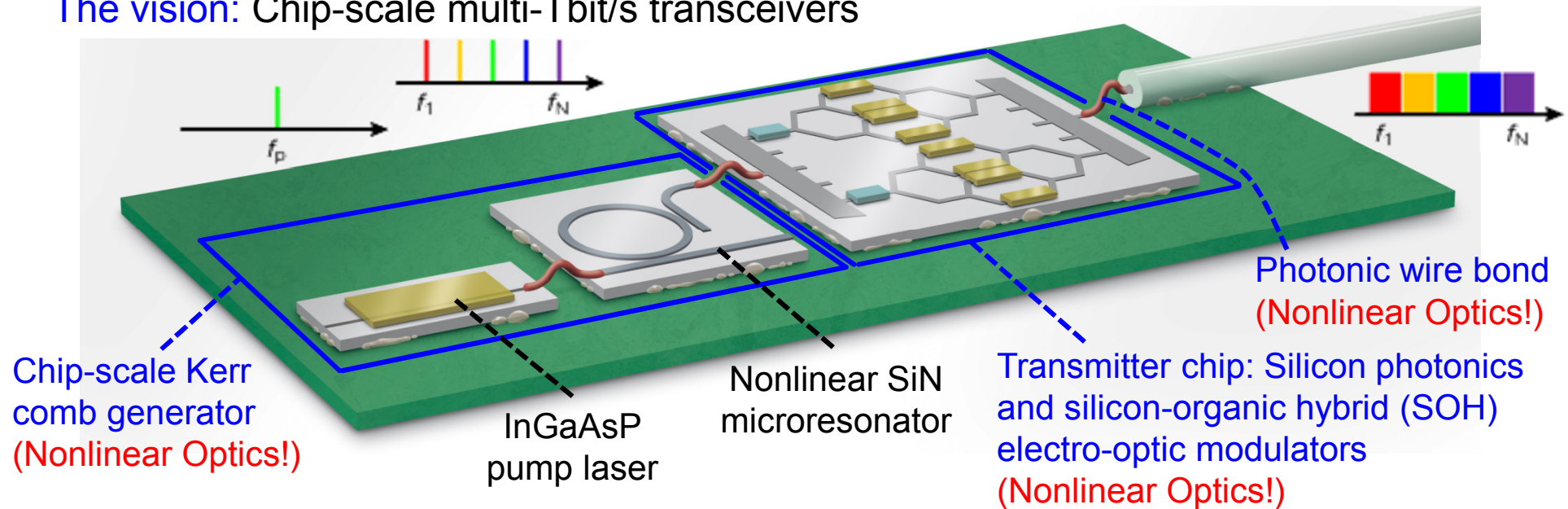
Previous demonstration: Use frequency comb, generated by a mode-locked laser
 325 channels, 12.5 GBd,
 16 QAM, PoMUX \Rightarrow **32.5 Tbit/s**

Nonlinear Optics!



Hillerkuss *et al.*, Nat. Photon. 5, 364–371 (2011)

The vision: Chip-scale multi-Tbit/s transceivers



Pfeifle *et al.*, Nat. Photon. 8, 375 - 380 (2014)

Contents

- **Linear and nonlinear optics:** Maxwell's equations and nonlinear optics, nonlinear wave equation, survey of nonlinear optical processes...
- **The nonlinear optical susceptibility:** Definition of the nonlinear optical susceptibility tensor, influence of spatial symmetry
- **Second-order nonlinear effects:** Linear electro-optic effect (Pockels effect), electro-optic modulators, difference-frequency generation and parametric amplification, phase matching
- **Acousto-optics:** Acousto-optic modulators, interaction of photons and phonons, Brillouin and Raman scattering
- **Third-order nonlinear effects:** Signal propagation in third-order nonlinear media, the nonlinear Schrödinger equation (NLSE); nonlinear signal processing, optical solitons and modulation instability

Further reading:

- R. W. Boyd. *Nonlinear Optics*. Academic Press, San Diego, 2003.
- G. P. Agrawal. *Nonlinear Fiber Optics*. Academic Press, 2013.
- G. I. Stegeman and R. A. Stegeman. *Nonlinear Optics: Phenomena, Materials, and Devices*, Wiley, 2012
- B. E. A. Saleh and M. C. Teich. *Fundamentals of Photonics*. John Wiley and Sons, 2007.
- Y. R. Shen. *Nonlinear Optics*. John Wiley and Sons, New York, 1984.

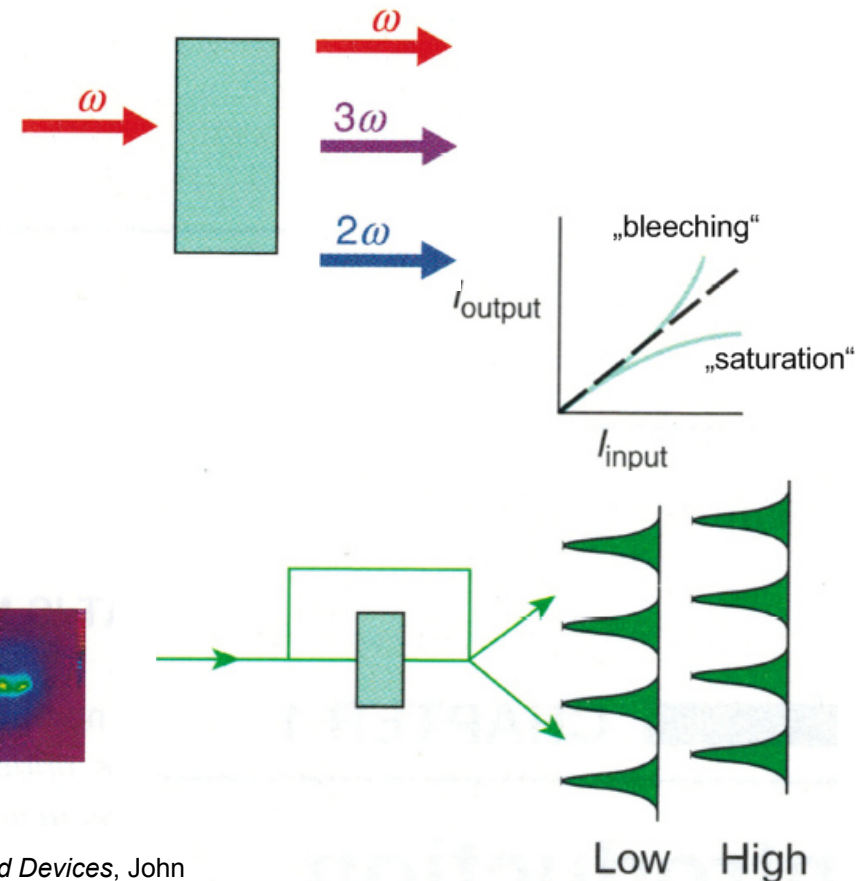
What is nonlinear optics?

“Nonlinear optics is the study of phenomena that occur as a consequence of the modification of optical properties by the presence of light“

Boyd, “Nonlinear Optics“, Academic Press 2003

Typical nonlinear-optical phenomena:

- Generation of new frequency components generation, e.g., third-harmonic generation (THG) or second-harmonic generation (SHG)
- Power-dependent transmission, e.g., nonlinear absorption or absorption bleaching
- Intensity-dependent interference
- Intensity-dependent beam profiles, e.g., due to self-focussing



Figures adapted from: Stegeman, *Nonlinear Optics: Phenomena, Materials, and Devices*, John Wiley & Sons, Hoboken, NJ. (2012).

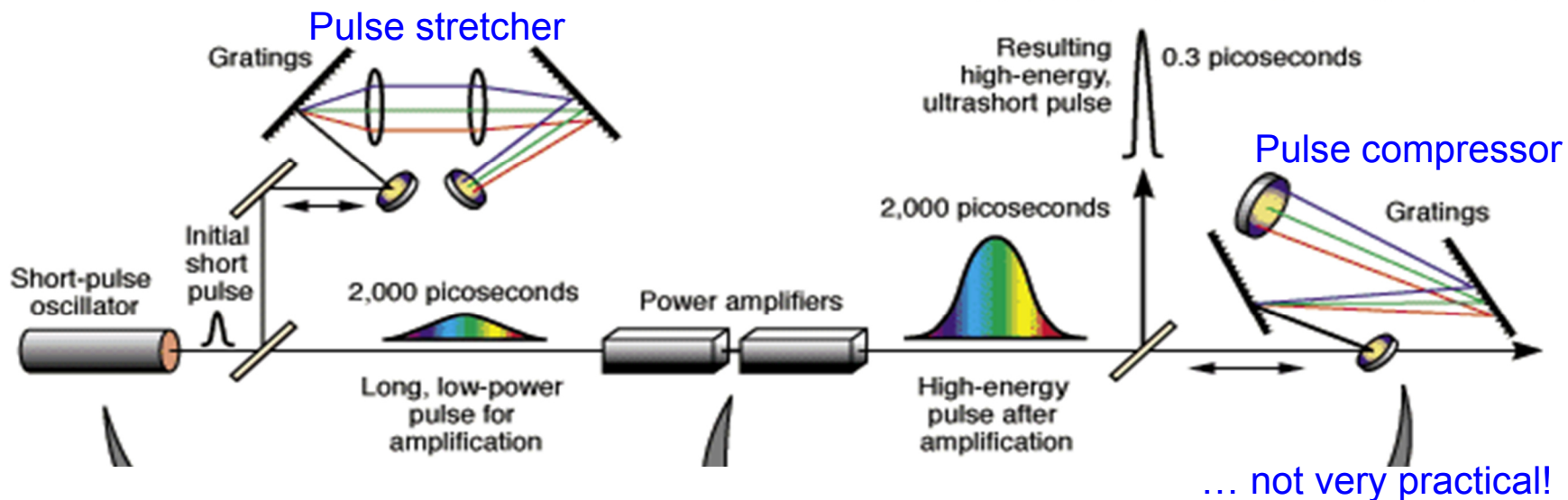
Generating high optical power: Pulsed laser sources

Important for observation of nonlinear optical phenomena: High intensities

- Exploit **pulsed lasers** with high peak power
- Use **strongly focused light** or **optical waveguides with small cross sections**

Nd: Glass Petawatt Laser, Lawrence Livermore Nat. Lab

- Peak power: ~ 2 PW
- Pulse stretching and recompression (factor 25000) to avoid damage of laser optics



Pulsed laser sources: Solid-state devices

Important for observation of nonlinear optical phenomena: High intensities

- Exploit **pulsed lasers** with high peak power
- Use **strongly focused light** or **optical waveguides with small cross sections**

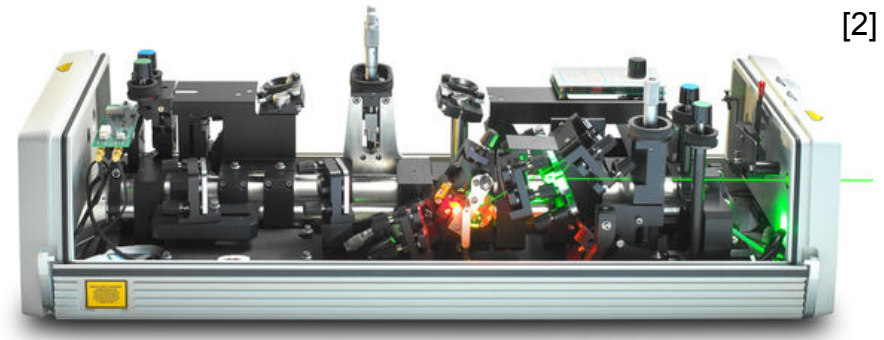


Picosecond laser (Lumentum)

- Pulse duration: 10 ps
- Wavelength: 1064 nm
- Repetition frequency: up to 8 MHz
- Average Power: up to 50 W
- Peak power: up to 20 MW

[1] <https://www.lumentum.com/en/products/laser-ultrafast-industrial-picoblade>

[2] <http://www.spectra-physics.com/products/ultrafast-lasers-for-scientific-research/>



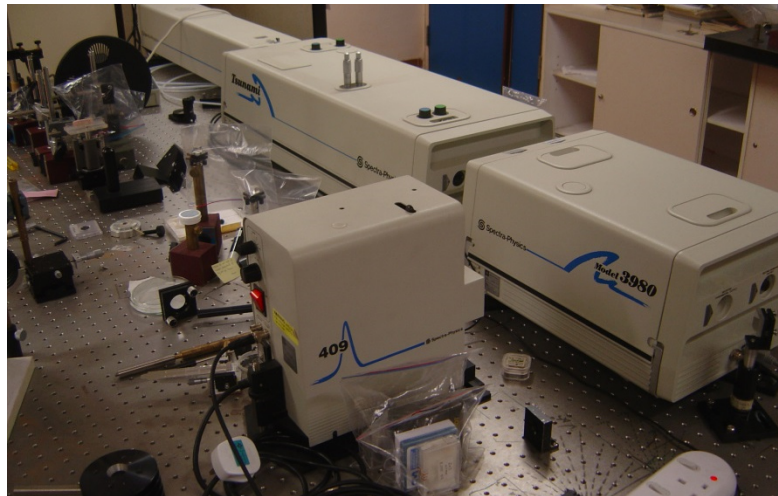
Ti: Sapphire laser oscillator (Spectra Physics)

- Pulse duration: < 100 fs
- Wavelength: ~ 800 nm
- Repetition frequency: 80 MHz
- Average Power: > 1.1 W
- Peak power: > 170 kW

Pulsed laser sources: Solid-state devices

Important for observation of nonlinear optical phenomena: High intensities

- Use **strongly focused light** or **optical waveguides with small cross sections**
- Exploit **pulsed lasers** with high peak power



Ti: Sapphire Laser (Spectra Physics)

- Pulse duration: < 100 fs
- Wavelength: ~ 800 nm
- Repetition frequency: 80 MHz
- Average power: > 4 W
- Peak power > 500 kW



Ergo-XG (Time-Bandwidth Products; now: Lumentum)

- Pulse duration: < 2 ps
- Wavelength: ~ 1550 nm
- Repetition frequency: 10 GHz
- Average power: > 50 mW
- Peak power > 2.5 W



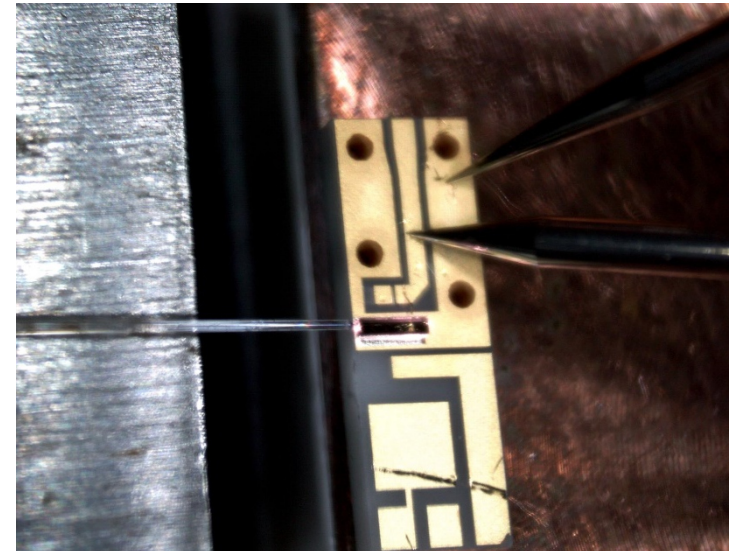
[1]

Fiber laser (Keopsys)

- Pulse duration: 0.5 ns to 200 ns
- Wavelength: ~ 1550 nm
- Repetition frequency: 10 Hz to 1 MHz
- Average power: up to 1.2 W
- Peak power: up to 15 kW

Mode-locked laser diode (III-V-labs)

- Pulse duration: ~ 1 ps
- Wavelength: 1550 nm
- Repetition frequency: up to 500 GHz
- Average Power: ~ 20 mW
- Peak power ~ 200 mW



[1] <http://www.bpress.cn/im/tag/Keopsys/>

Pulsed fiber lasers and mode-locked laser diodes



Fiber laser (Calmar)

- Pulse duration: 0.8 – 5 ps
- Wavelength: ~ 1550 nm
- Repetition frequency: 40 GHz
- Average Power: > 20 mW
- Peak power < 1 W

Mode-locked laser diode (III-V-labs)

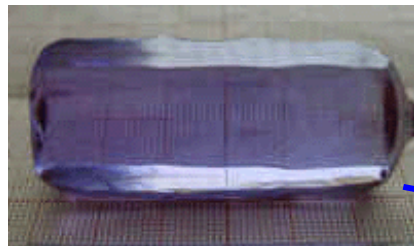
- Pulse duration: ~ 1 ps
- Wavelength: 1550 nm
- Repetition frequency: up to 500 GHz
- Average Power: ~ 20 mW
- Peak power ~ 200 mW



Special features of nonlinear-optical processes:

- Ultra-short response times (fs!) => Ultra-fast signal processing!
- Broadband => Light generation / amplification at wavelength ranges that cannot be accessed by other gain media

Example: Green laser pointer, based on second-harmonic generation of 1064 nm light



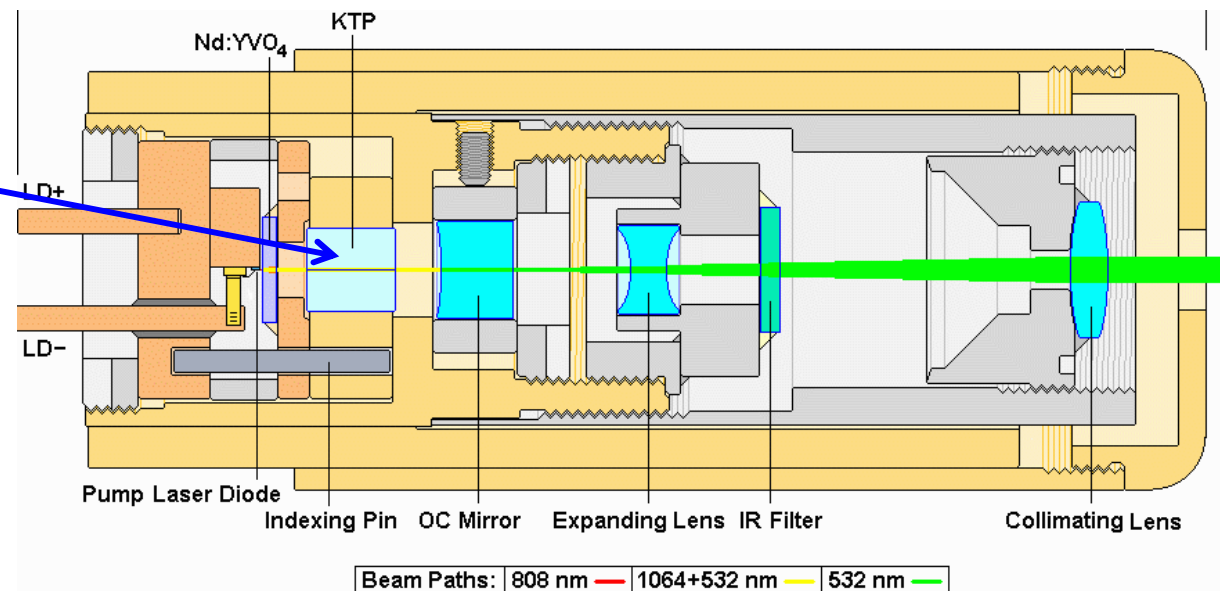
Nonlinear-optical crystal
(KTP = Kaliumtitanylphosphat)

DPSS: Diode-pumped
solid-state laser

Laser diode: 808 nm

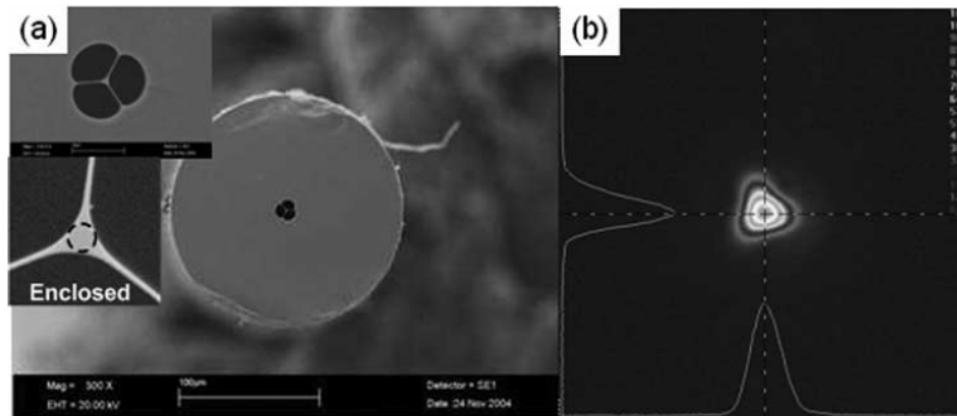
-> Nd:YVO₄-laser: 1064 nm

-> Second-harmonic generation (SHG) in nonlinear KTP crystal: 532 nm



Applications of nonlinear optics: Supercontinuum generation in highly nonlinear fibers

High index-contrast “small-core” fiber: High optical intensities in the waveguide core



Leong et al. Journ. Lightw. Technol., Vol. 24, No. 1 (2006)

- Solid core + low-index air cladding
 - Tight confinement of light within a small core area
- ⇒ **Strong nonlinear effects**; allows for supercontinuum generation!

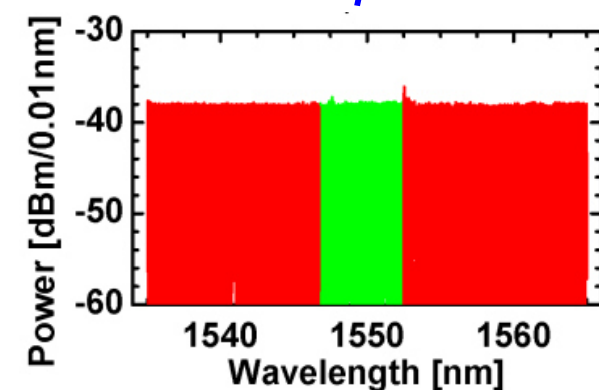
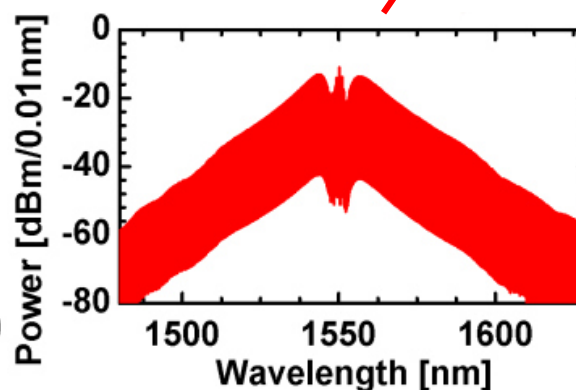
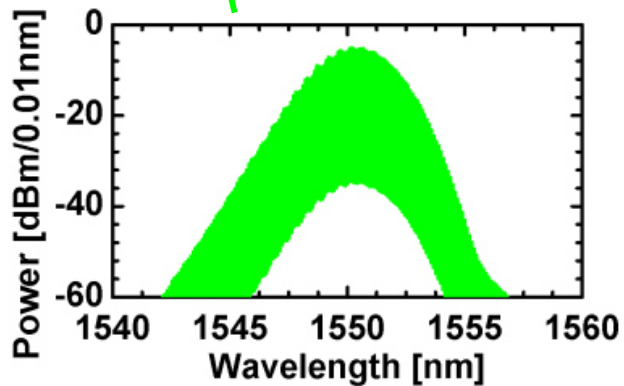
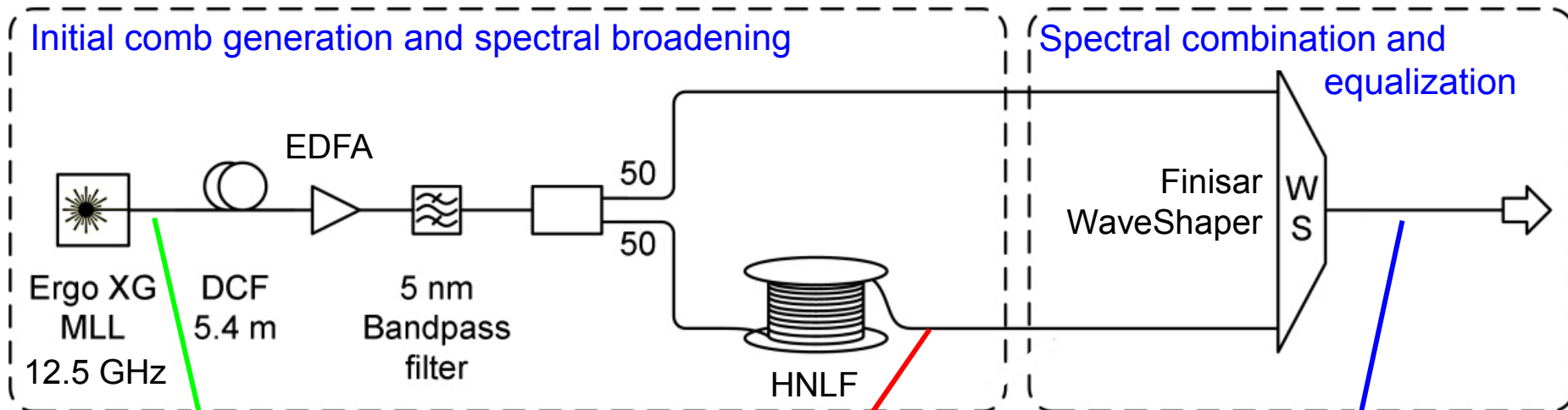


http://www.bath.ac.uk/physics/groups/cppm/nonlinear_pcf.php

Applications of nonlinear optics: Frequency comb generation for high-speed data transmission

Mode-locked laser + spectral broadening in highly nonlinear fiber (HNLF)

Problem: Spectral dips for SPM-induced phase shifts of $\Delta\Phi \geq 1.5 \pi$



⇒ 325 carriers with 12.5 GHz spacing, linewidth < 10 kHz

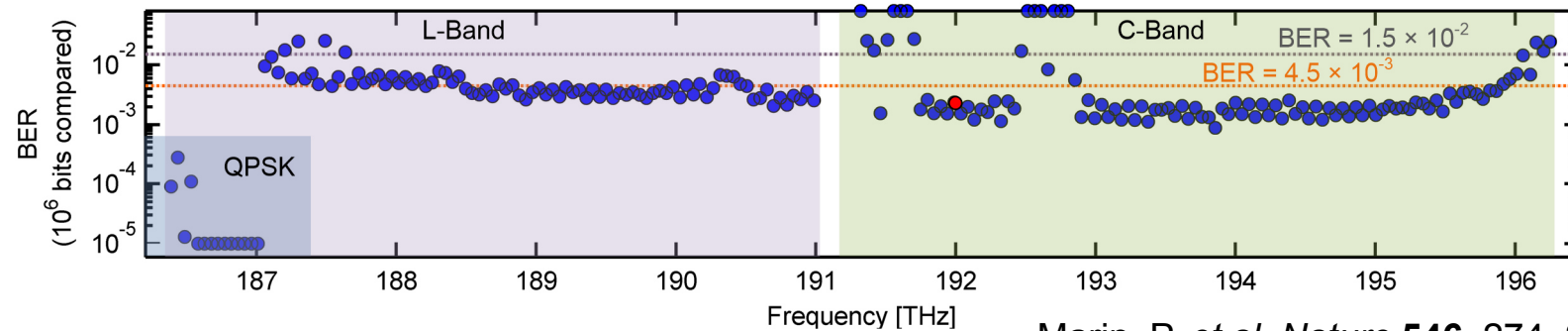
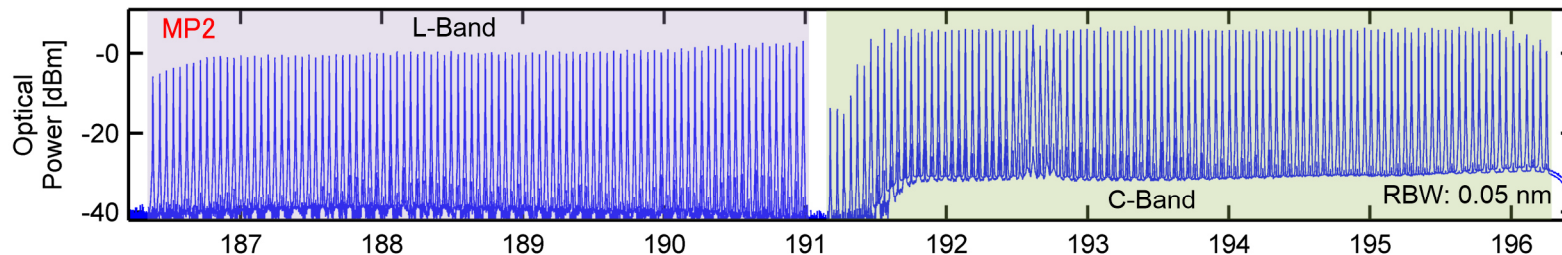
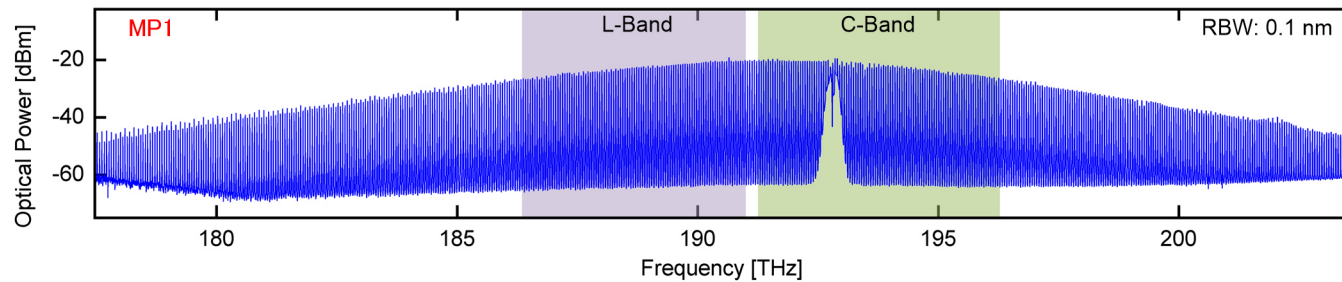
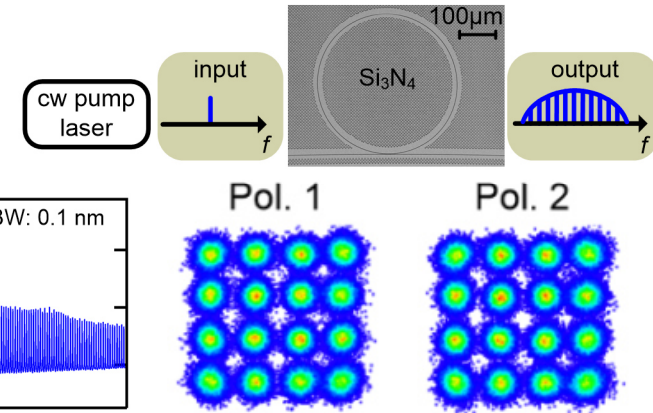
Hillerkuss *et al.*, J. Opt. Commun. Netw. 4, 715–723 (2012)

Applications of nonlinear optics: Kerr frequency comb generation for high-speed data transmission

Recent Achievements: Temporal dissipative integrated soliton frequency comb

- 179 Carriers from chip-scale comb sources,
- 40 GBd, 16 QAM, PoMUX \Rightarrow **50.2 Tbit/s**

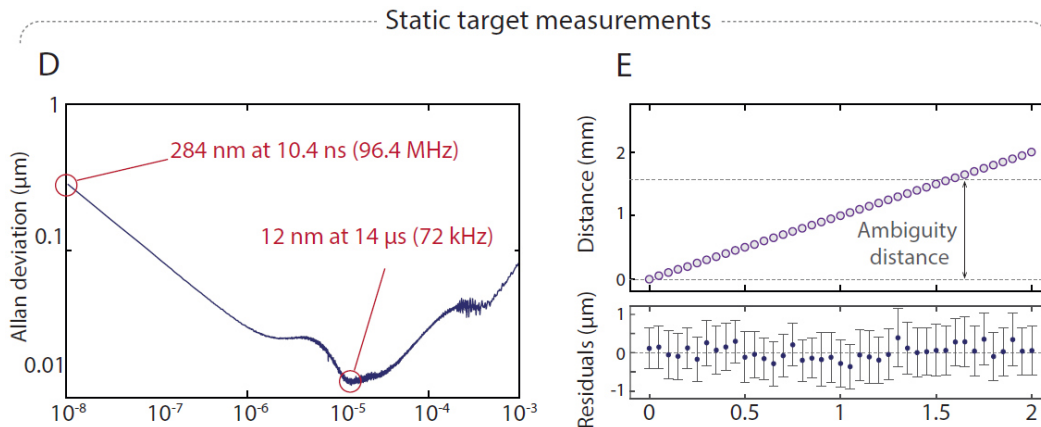
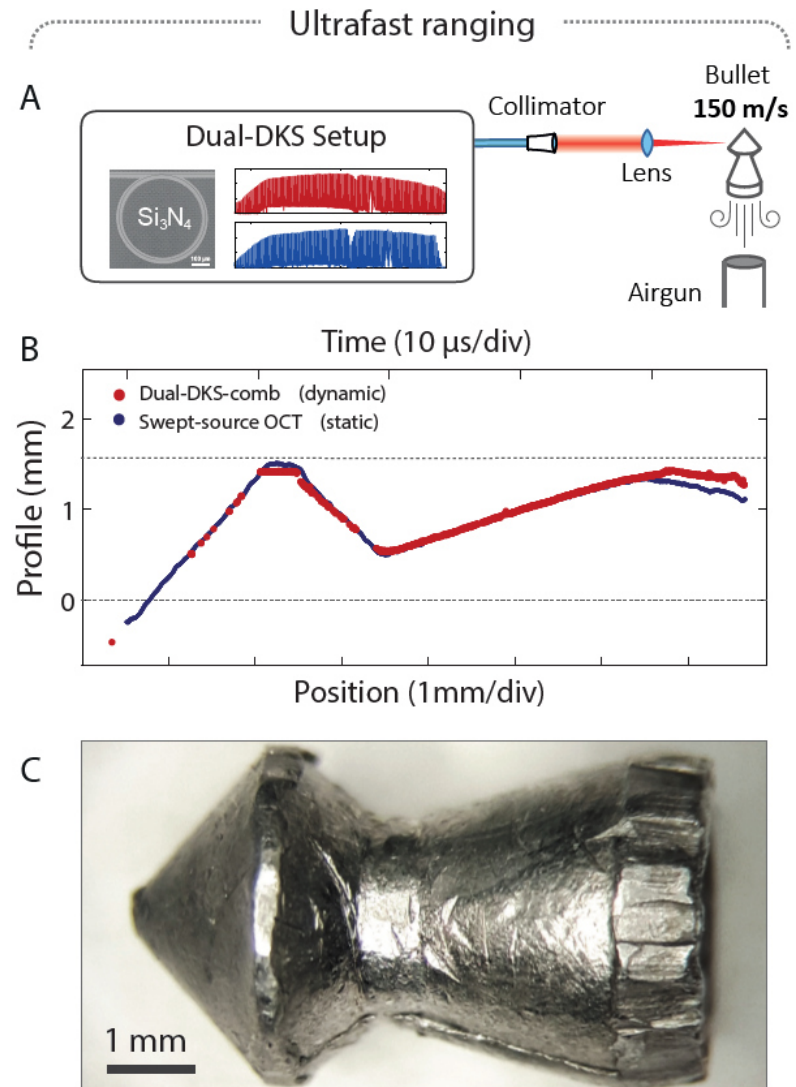
Chip-scale comb source



Marin, P. *et al. Nature* **546**, 274–279 (2017)

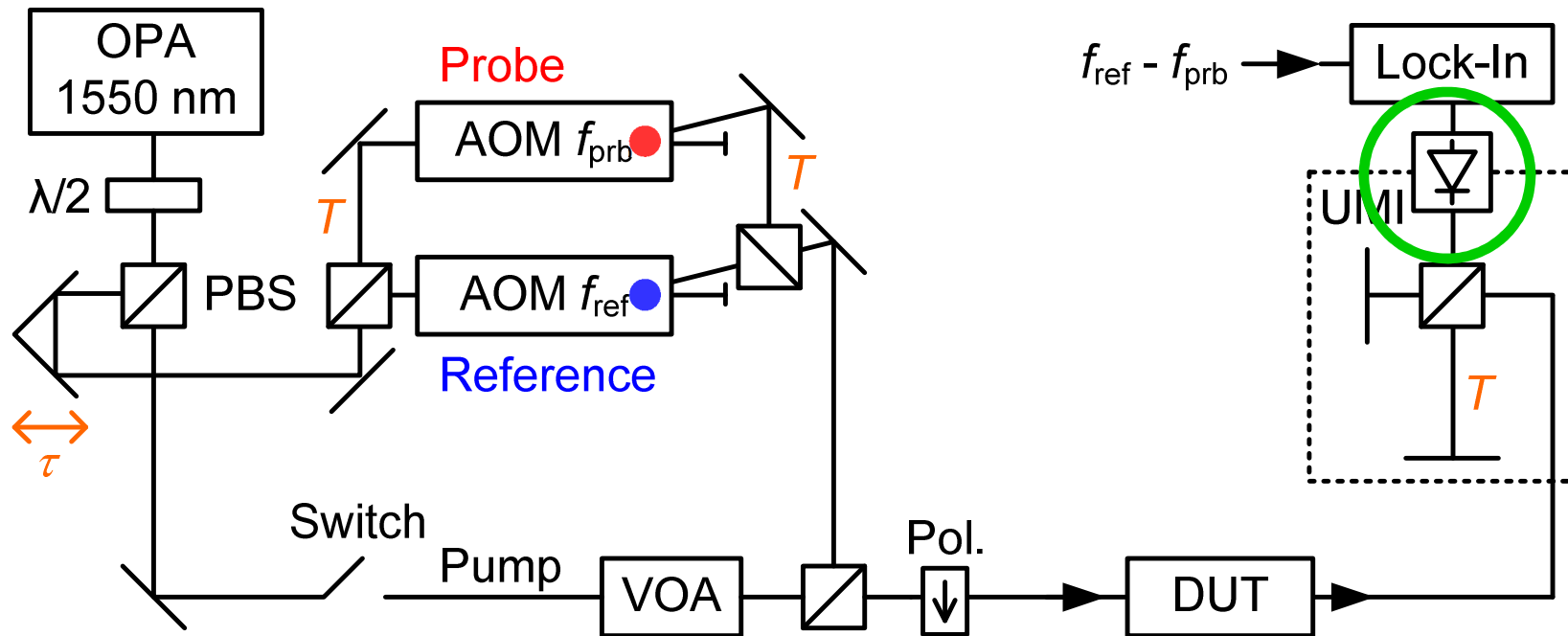
Applications of nonlinear optics: Kerr frequency comb generation for ultrafast optical ranging

- Unique combination of large free spectral range and large bandwidth enables ultrafast and precise optical distance measurements
- Demonstration of optical ranging at 100 MHz sampling rate, while keeping nm-precision in mm-range

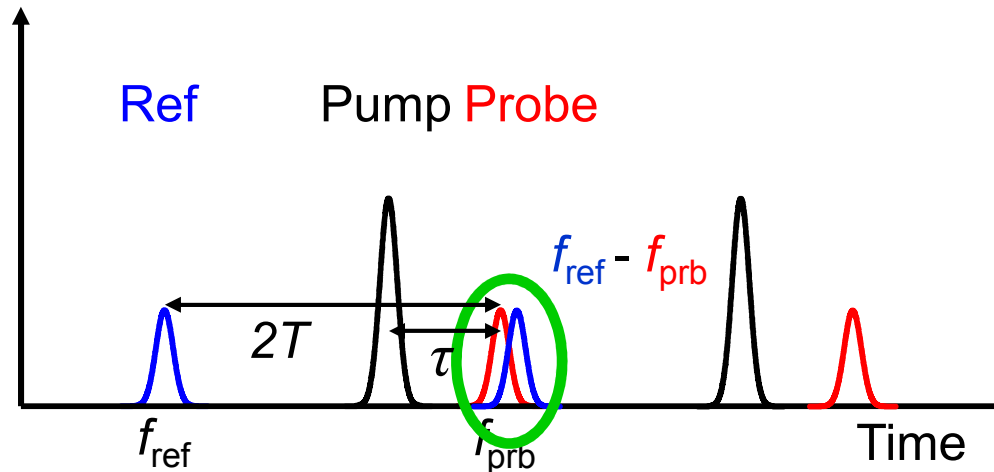


Trocha, P. *et al.*, *Science* **359**, 887–891 (2018)

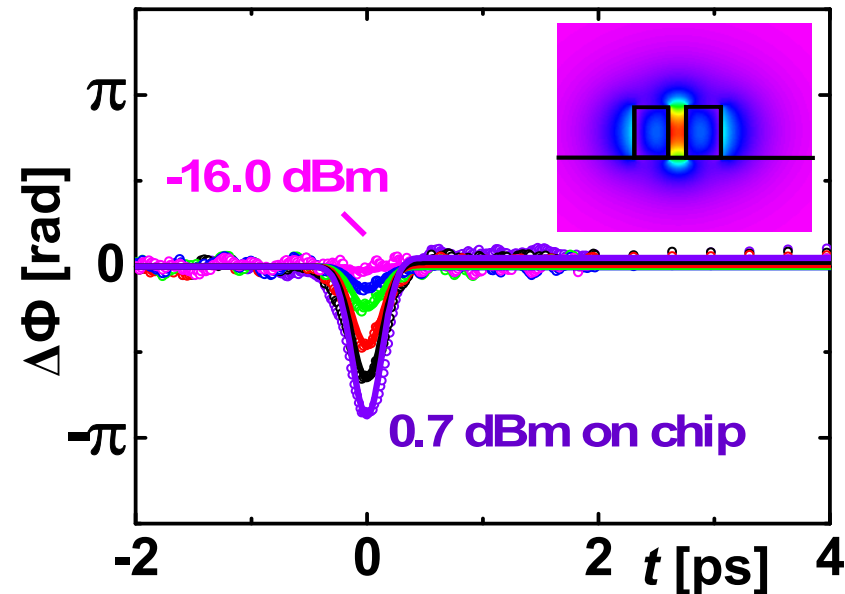
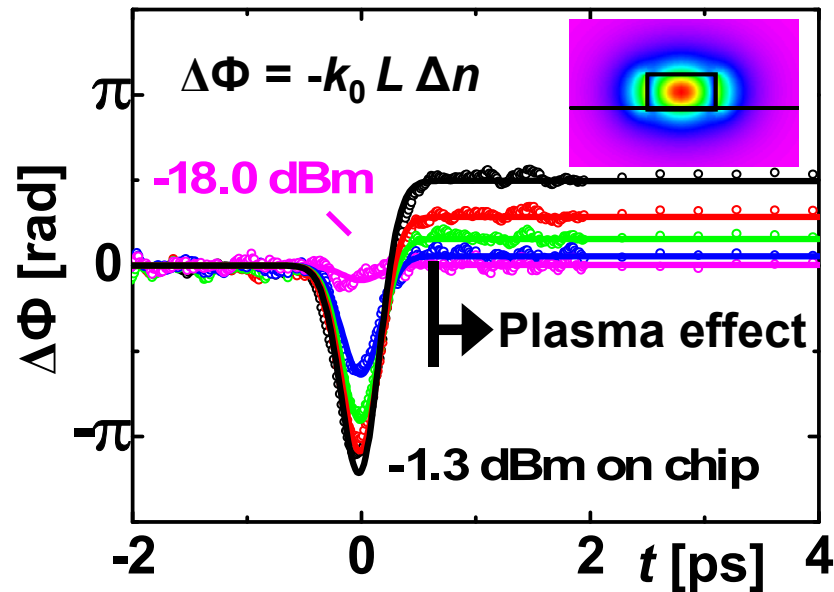
Ultra-fast all-optical switching: Pump-probe measurement of response times



Beat signal at difference frequency at $f_{\text{ref}} - f_{\text{prb}}$ detected by lock-in amplifier in amplitude and phase!



Applications of nonlinear optics: All-optical switching in nanophotonic silicon waveguides



SOI strip waveguides:

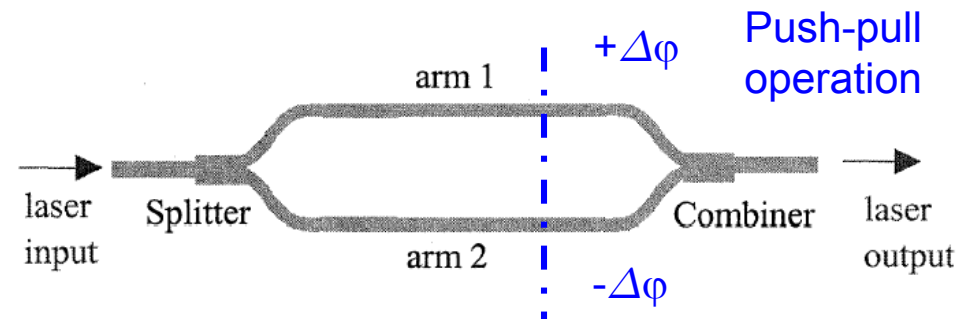
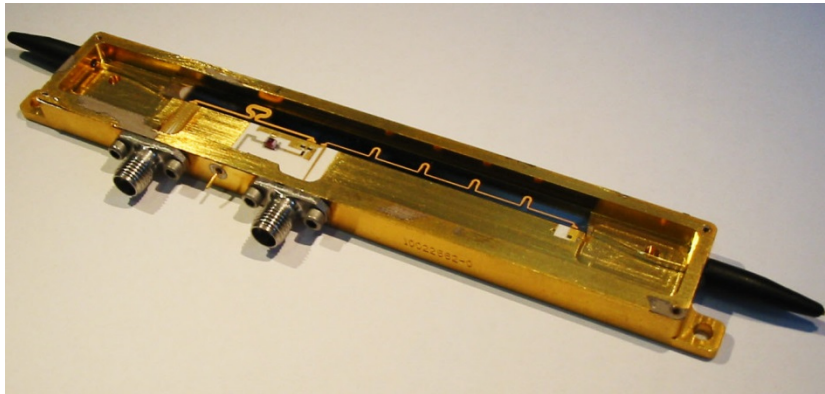
- Nonlinear response impaired by free carriers
- Free-carrier lifetime: $1.2 \pm 0.1 \text{ ns}$

Silicon-organic hybrid (SOH) slot waveguides:

- No impairment by free carriers
- Suitable for ultra-fast all-optical signal processing

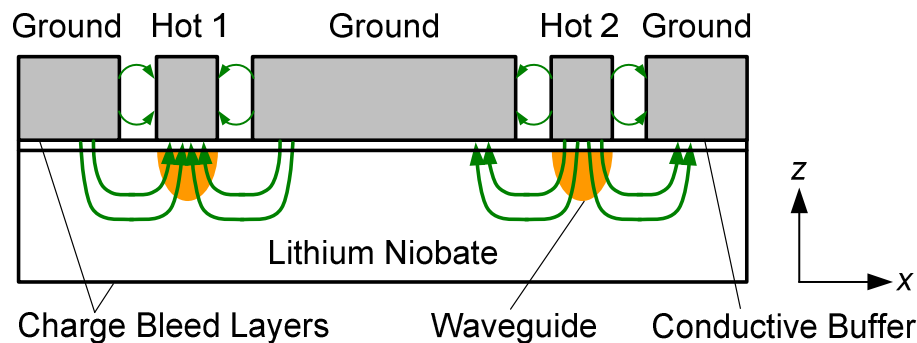
Koos *et al.*, Nature Photonics **3**, 216-218 (2009)
Vallaitis *et al.*, Opt. Expr. **17**, 17357–17368 (2009)

Applications of nonlinear optics: Lithium Niobate (LiNbO_3) electro-optic modulator



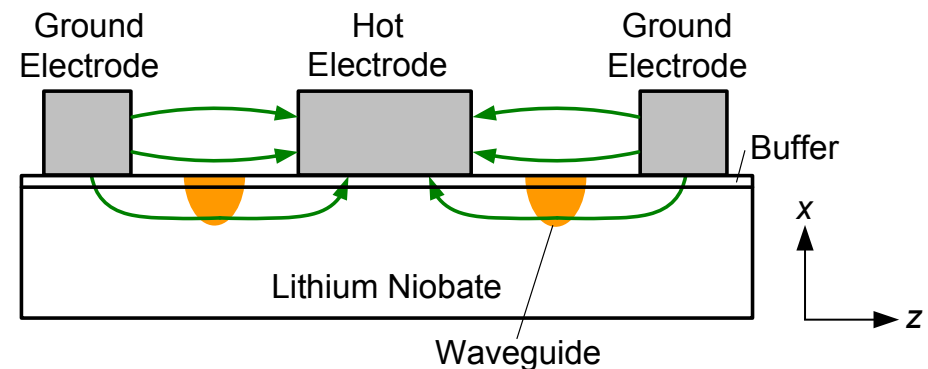
z-cut Lithium Niobate (LiNbO_3)

- Push-pull operation with RF-signals of opposite polarity
- Good overlap of RF-field and optical field → Low voltage; good electro-optic efficiency



x-cut Lithium Niobate

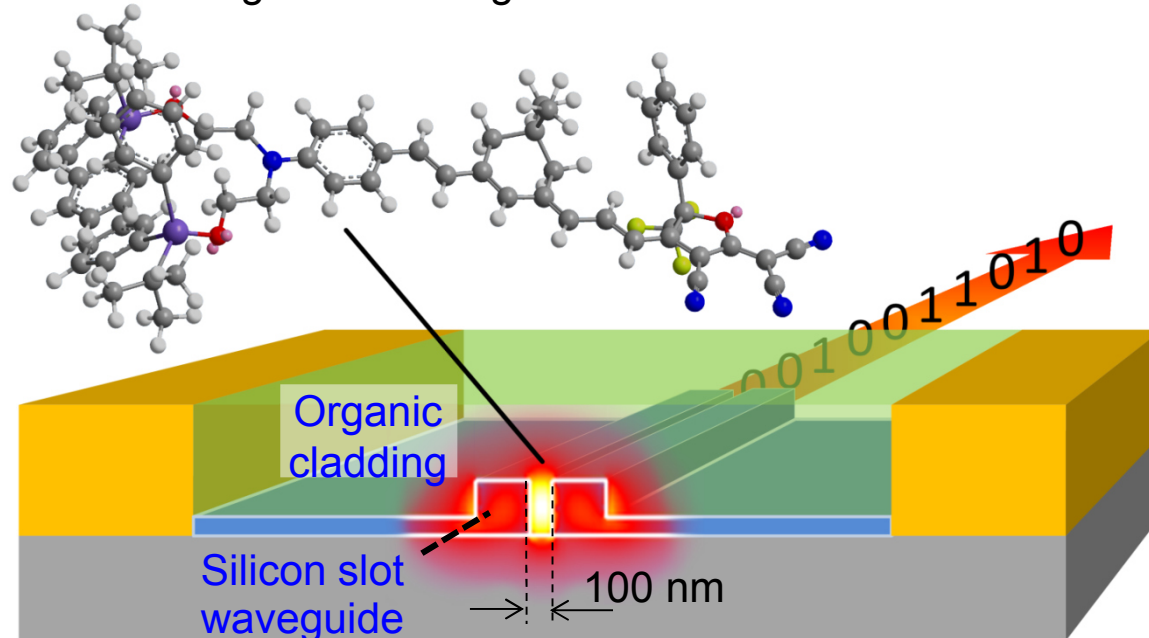
- Push-pull operation a single RF signal.
- Needs approx. 20% higher voltage compared to device on z-cut substrate



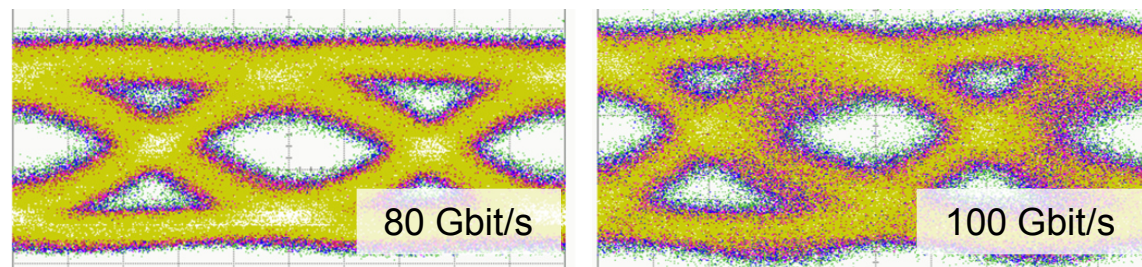
E. L. Wooten *et al.*, IEEE Journal of Selected Topics in Quantum Electronics 6 (1), Jan/Feb 2000, pp. 69 ff.

Applications of nonlinear optics: Silicon-organic hybrid (SOH) electro-optic modulators

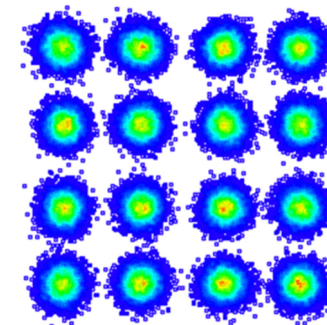
Silicon-organic hybrid (SOH) integration: Combine silicon-on-insulator (SOI) waveguides with functional organic cladding materials



- High speed: EO bandw. > 100 GHz
- Highly efficient: $U_{\pi}L \approx 0.5$ Vmm
- Record-low energy consumption
- No amplitude-phase coupling:
Enables higher-order modulation formats (16 QAM) at high symbol rates (up to 100 GBd)



SOH: 1.4 V_{pp}, 100 Gbit/s, 98 fJ/bit
Conventional: 5.1 V_{pp}, 80 Gbit/s, 1600 fJ/bit



SOH:
252 Gbit/s
 $U_{pp} \approx 1.0$ V
 $W_{bit} = 22$ fJ / bit

Conventional:
112 Gbit/s
 $U_{pp} \approx 5.0$ V
 $W_{bit} > 1000$ fJ / bit

Koos *et al.*, J. Lightw. Technol. **24**, 256-268 (2016)

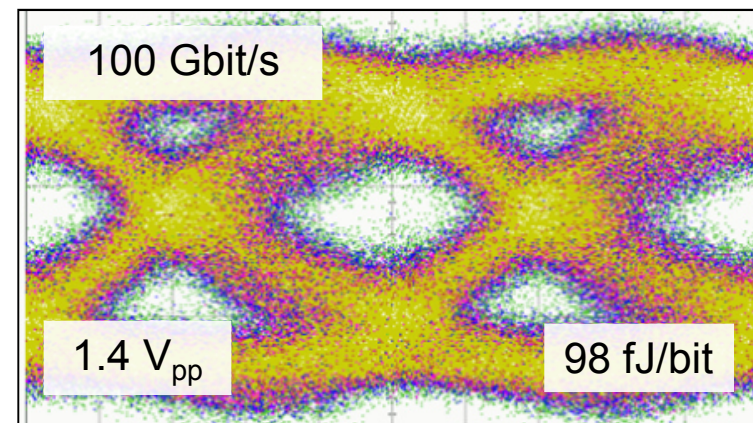
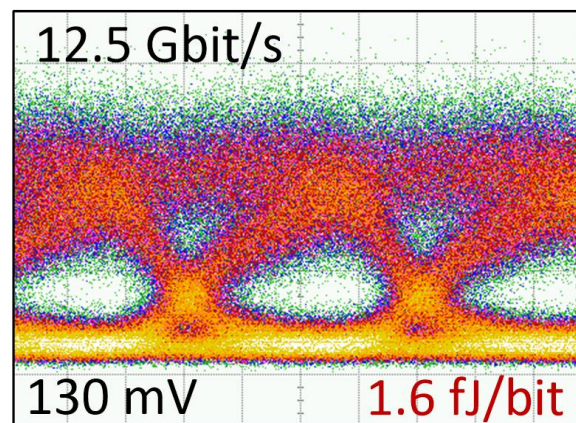
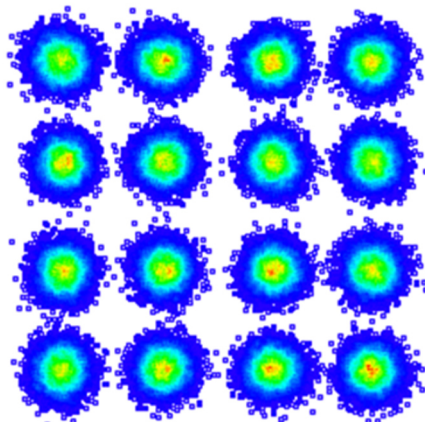
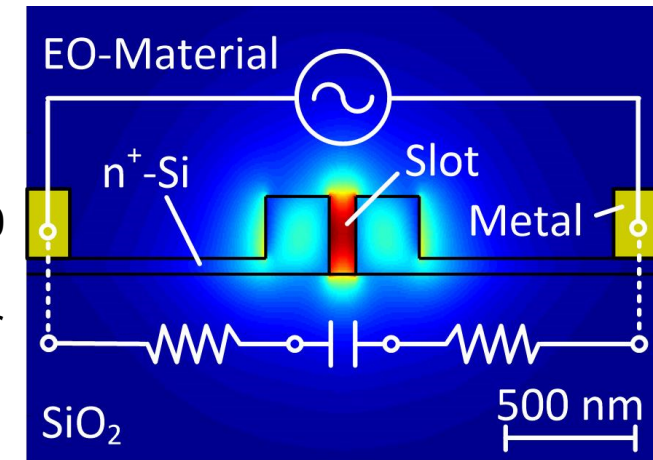
Koeber *et al.*, Light: Science & Applications **4**, e255, doi:10.1038/lsa.2015.28, (2015)

Wolf *et al.*, OFC 2017, paper Th5C.1. (postdeadline paper)

Applications of nonlinear optics: Silicon-organic hybrid (SOH) electro-optic modulators

Concept: Combine nanophotonic silicon waveguides with electro-optic organic cladding materials

- **High-speed modulation:** 3 dB bandwidth > 100 GHz (All-silicon devices: 30 GHz)
- **Highly efficient:** $U_{\pi}L < 1$ Vmm (All-silicon devices: $U_{\pi}L = 10 \dots 40$ V mm)
- **Lowest energy consumption** of a Mach-Zehnder modulator (MZM) in any material system:
< 2 fJ/bit (All-silicon MZM devices: 200 fJ/bit)
- **No amplitude-phase coupling:** Enables higher-order modulation formats (16 QAM)



Lauermann *et al.*, *Opt. Express* **22**, 29927–29936 (2014)

Koeber *et al.*, *Light: Science & Applications* **4**, e255, doi:10.1038/lsa.2015.28, (2015)

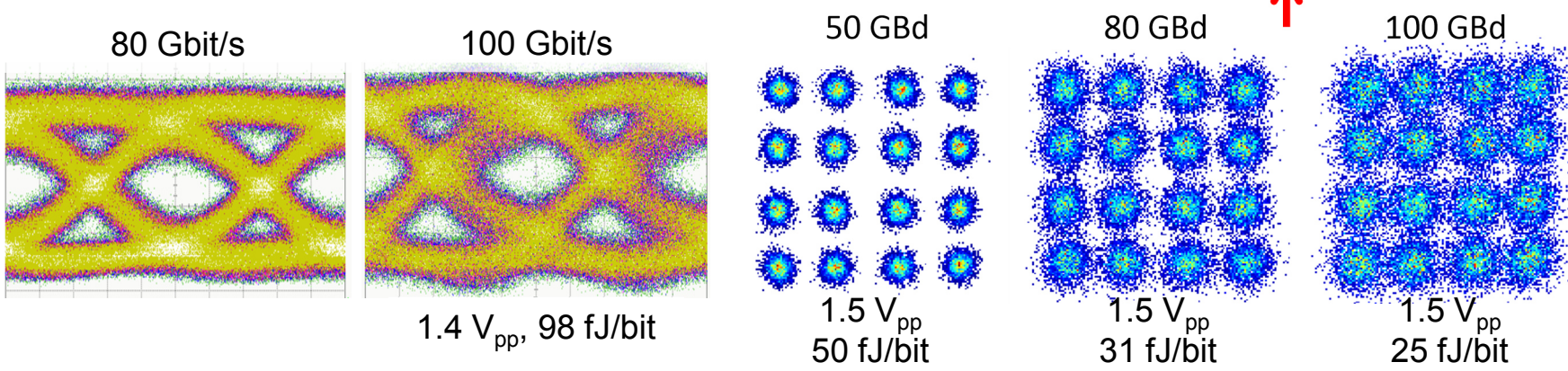
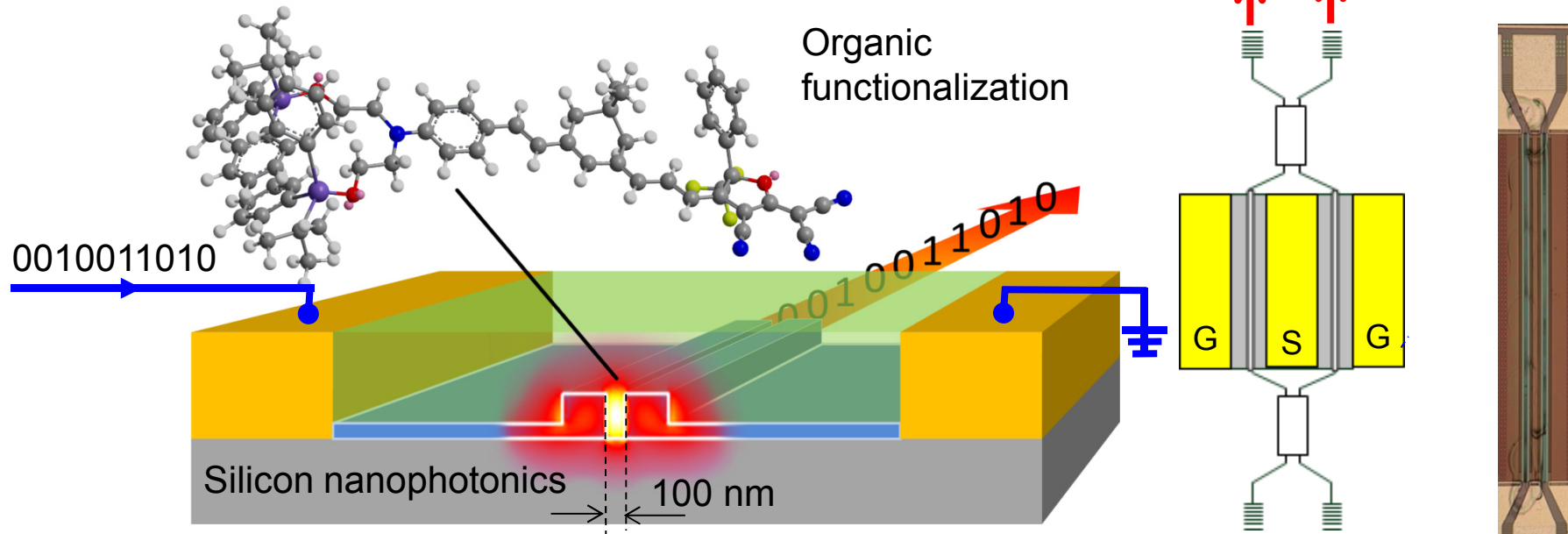
Lauermann *et al.*, *J. Lightw. Technol.* **33**, ,1210-1216 (2015)

Hartmann *et al.*, ECOC 2015, Post-deadline paper PDP1.4 (2015)

Silicon-Organic Hybrid (SOH) Integration

Concept: Combine nanophotonic silicon waveguides with electro-optic organic cladding materials

Mach-Zehnder modulators (MZM):



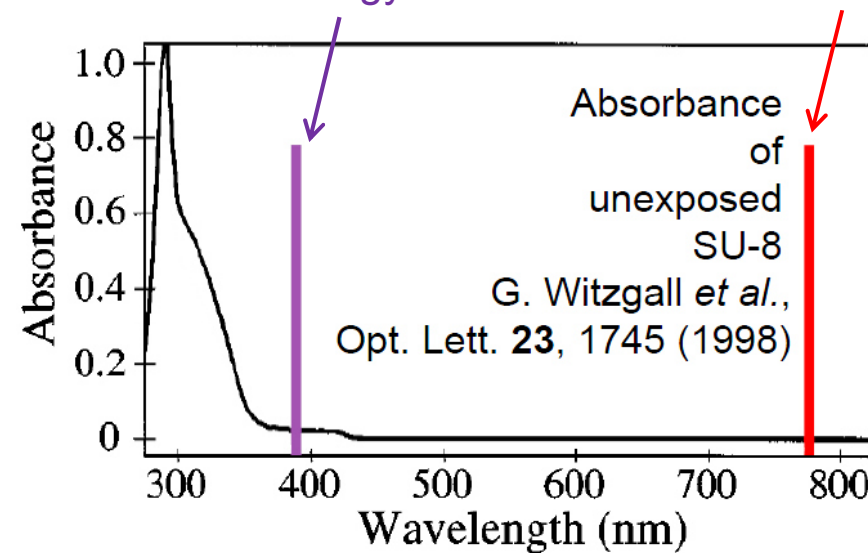
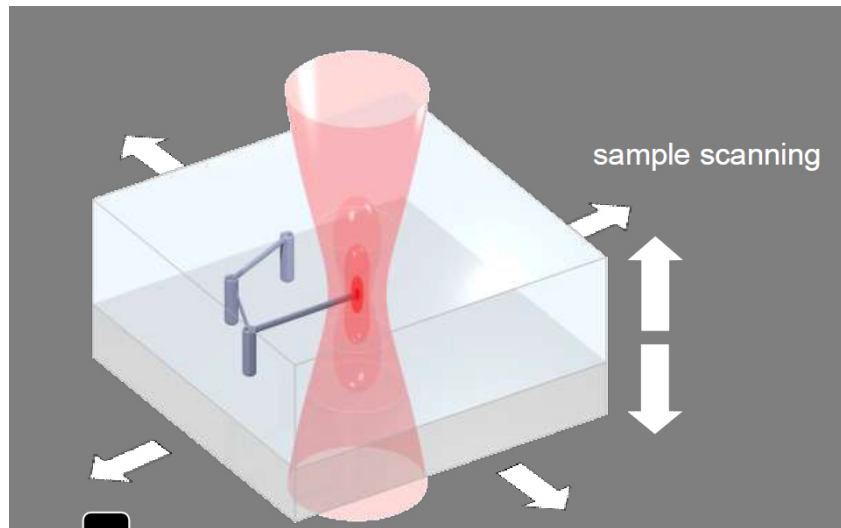
Applications of nonlinear optics: Direct-write 3D laser lithography



Nanoscribe GmbH (KIT start-up company):
3D structuring by **two-photon polymerization**

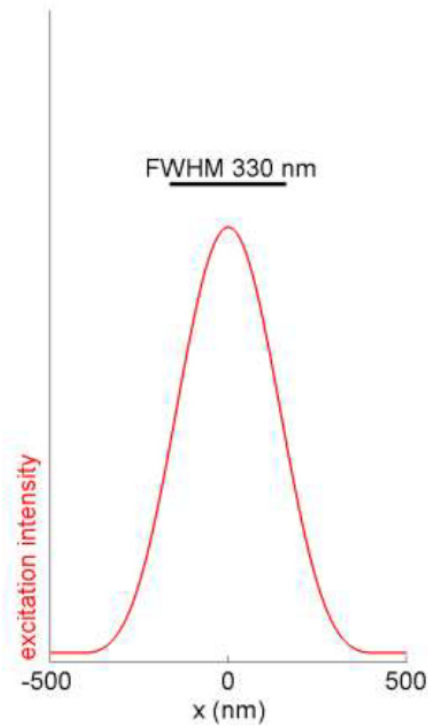
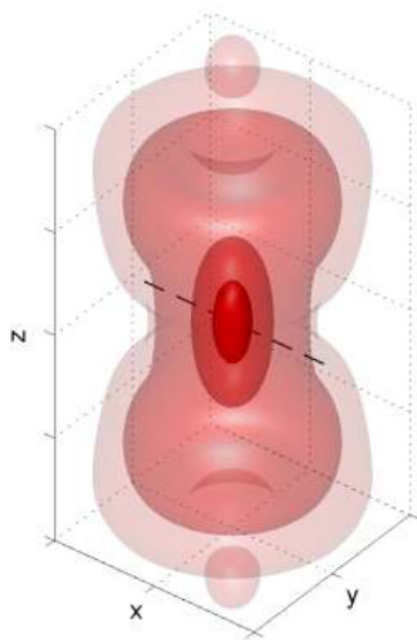
Equivalent wavelength
with double photon
energy

Exposure
wavelength (pulsed
Ti-sapphire laser)



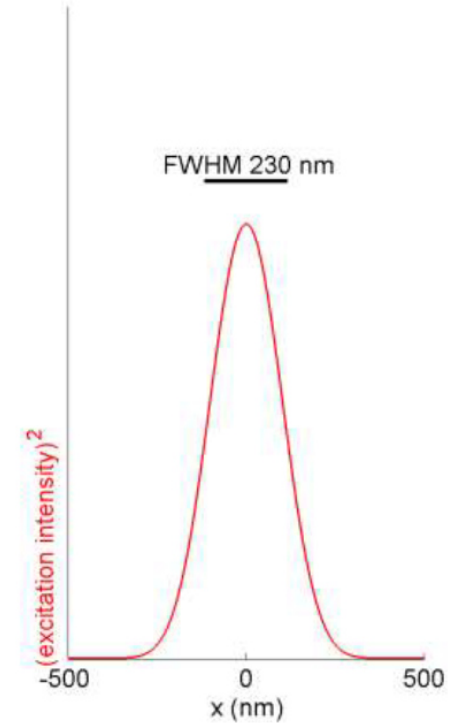
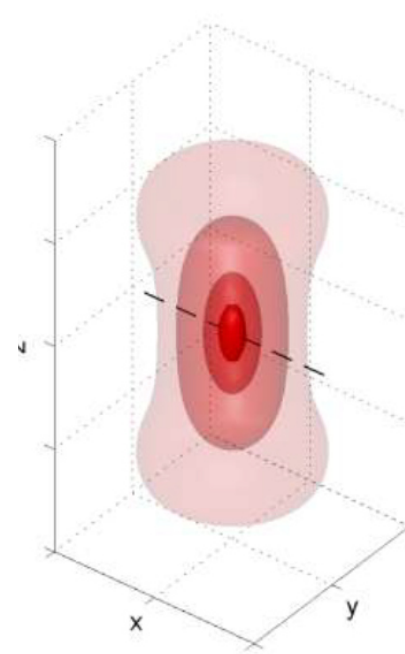
Polymerization by one- and two-photon absorption

Polymerization by one-photon absorption



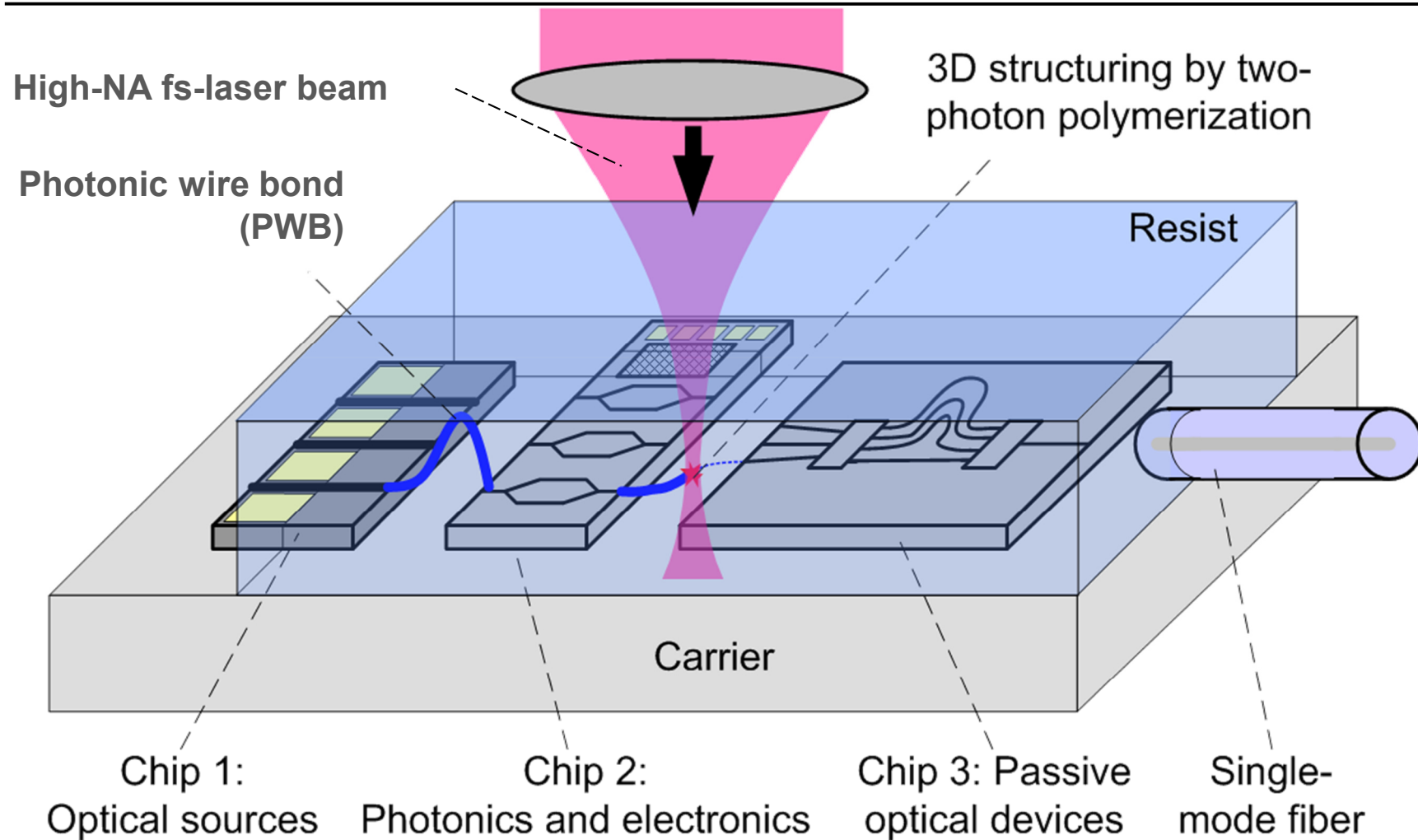
Polymerization by two-photon absorption:

- Increased resolution
- Suppression of beam side-lobes



Figures adapted from Nanoscribe GmbH

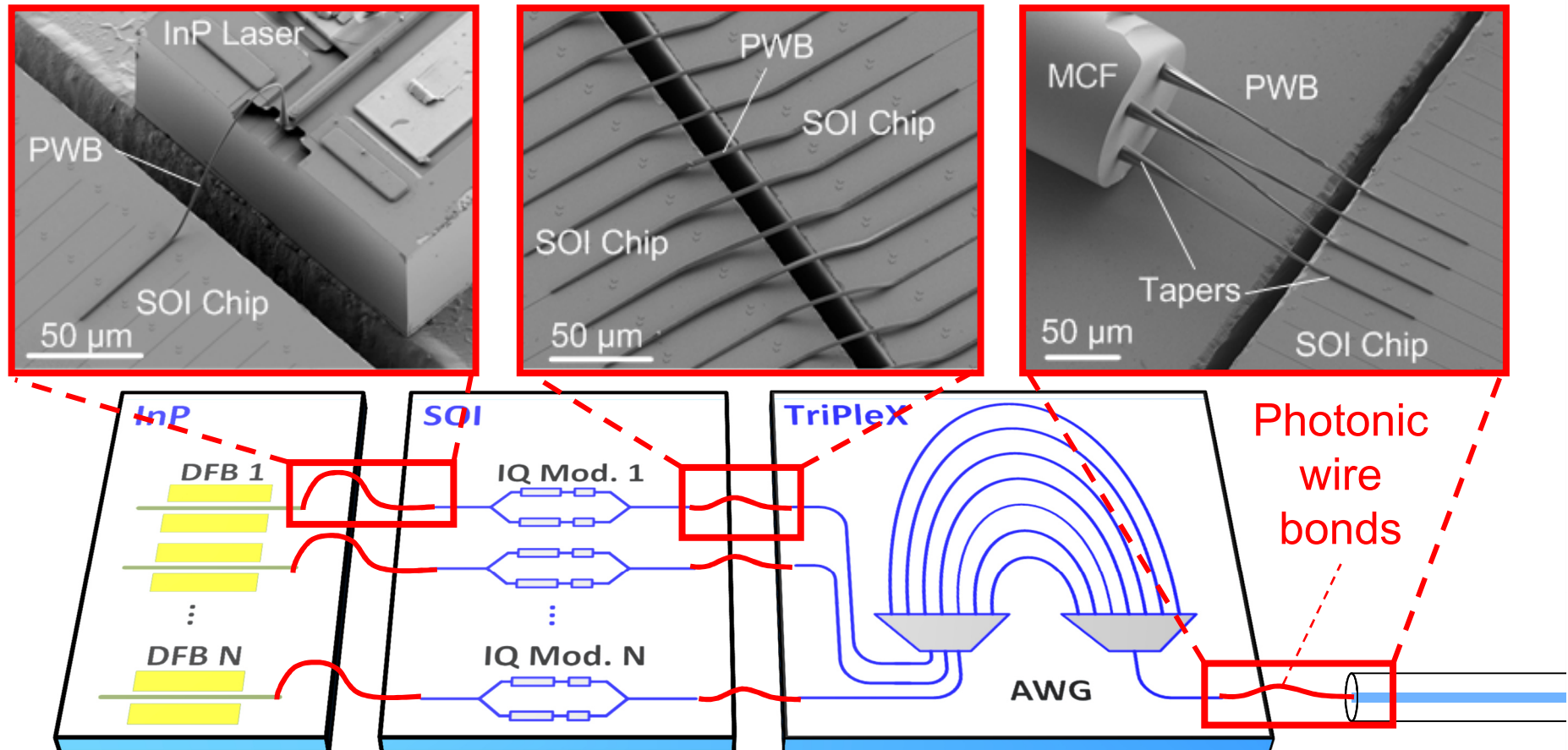
Photonic wire bonding: The concept



Lindenmann *et al.*, Opt. Express **20**, 17667-17677 (2012)

Photonic wire bonding and photonic multi-chip integration

Multi-chip integration: Assemble photonic systems from **discrete chips** that combine strengths of **different material platforms**

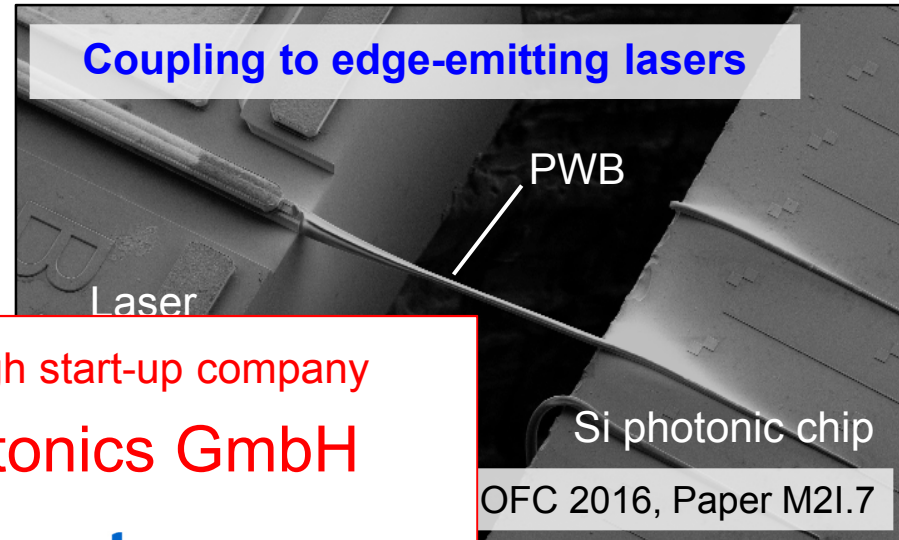
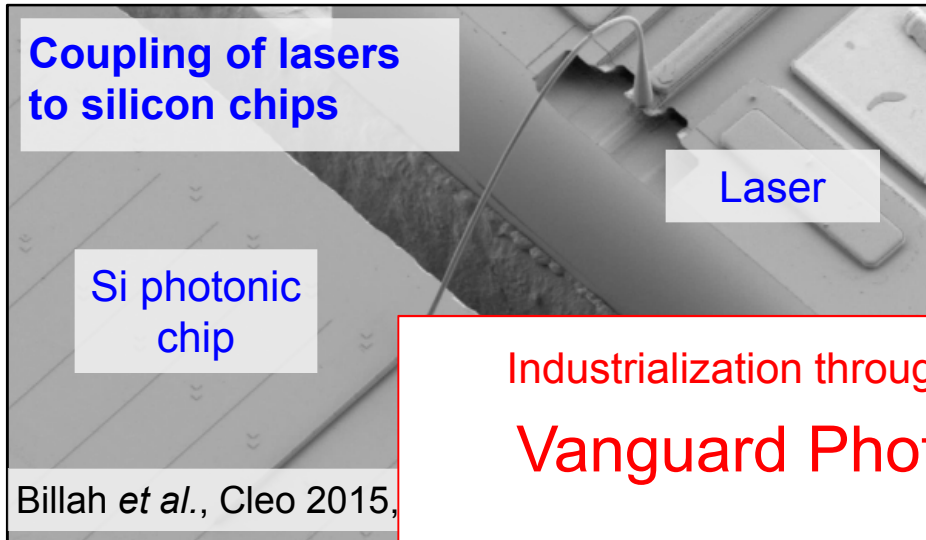


Lindenmann *et al.*, Opt. Express **20**, 17667-17677 (2012)

Lindenmann *et al.*, Journal of Lightw. Technology **33**, 755-760 (2015)

Billah *et al.*, Cleo 2015, Paper STu2F.2

Additive 3D nanofabrication of photonic devices



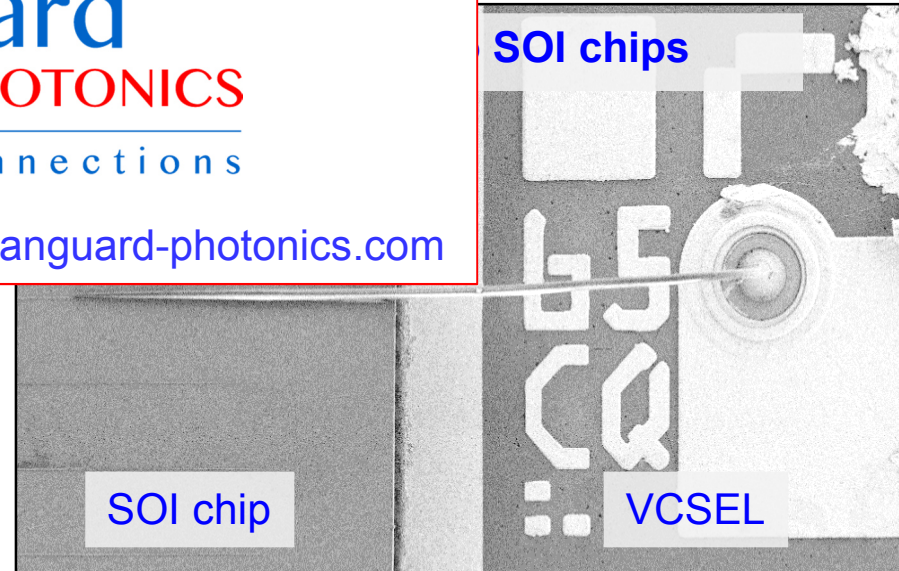
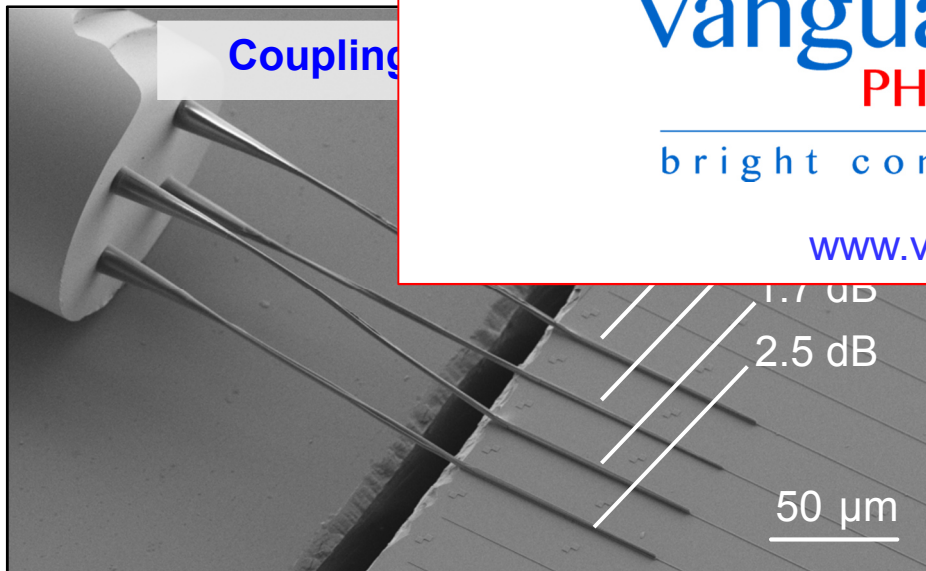
Industrialization through start-up company
Vanguard Photonics GmbH



vanguard
PHOTONICS

bright connections

www.vanguard-photonics.com



Linear and Nonlinear Optics

Maxwell's equations and electric polarization

Basic assumptions: No free charges, no currents
Nonmagnetic material

$$\begin{aligned}\nabla \cdot \mathbf{D}(\mathbf{r}, t) &= 0 & \mathbf{B}(\mathbf{r}, t) &= \mu_0 \mathbf{H}(\mathbf{r}, t) \\ \nabla \times \mathbf{E}(\mathbf{r}, t) &= -\frac{\partial \mathbf{B}(\mathbf{r}, t)}{\partial t} & \mathbf{D}(\mathbf{r}, t) &= \epsilon_0 \mathbf{E}(\mathbf{r}, t) + \mathbf{P}(\mathbf{r}, t) \\ \nabla \cdot \mathbf{B}(\mathbf{r}, t) &= 0 \\ \nabla \times \mathbf{H}(\mathbf{r}, t) &= \frac{\partial \mathbf{D}(\mathbf{r}, t)}{\partial t}\end{aligned}$$

Linear and nonlinear dielectric polarization:

- **Linear media:** Linear relationship between polarization \mathbf{P} and electric field \mathbf{E}
- **Nonlinear media:** Nonlinear relationship between \mathbf{P} and \mathbf{E}

Nonlinear Optics:

The field of nonlinear optics (often abbreviated as NLO) comprises the branch of optics that describes the behavior of light in nonlinear media, in which the dielectric polarization \mathbf{P} responds nonlinearly to the electric field \mathbf{E} of the light.

General case:
$$\mathbf{P}_L(\mathbf{r}, t) = \epsilon_0 \int_{-\infty}^{\infty} \iiint_{-\infty}^{\infty} \chi^{(1)}(\mathbf{r}, \mathbf{r}', t, t') \mathbf{E}(\mathbf{r}', t') d\mathbf{r}' dt'$$

3 x 3 - matrix

Time-invariant media
$$\mathbf{P}_L(\mathbf{r}, t) = \epsilon_0 \int_{-\infty}^{\infty} \iiint_{-\infty}^{\infty} \chi^{(1)}(\mathbf{r}, \mathbf{r}', \tau) \mathbf{E}(\mathbf{r}', t - \tau) d\mathbf{r}' d\tau$$

Media that are (additionally) local in space
$$\mathbf{P}_L(\mathbf{r}, t) = \epsilon_0 \int_{-\infty}^{\infty} \chi^{(1)}(\mathbf{r}, \tau) \mathbf{E}(\mathbf{r}, t - \tau) d\tau$$

scalar

Isotropic media:
$$\mathbf{P}_L(\mathbf{r}, t) = \epsilon_0 \int_{-\infty}^{\infty} \chi^{(1)}(\mathbf{r}, \tau) \mathbf{E}(\mathbf{r}, t - \tau) d\tau$$

Homogeneous media:
$$\mathbf{P}_L(\mathbf{r}, t) = \epsilon_0 \int_{-\infty}^{\infty} \chi^{(1)}(\tau) \mathbf{E}(\mathbf{r}, t - \tau) d\tau$$

Note: In these relations, χ represents the time-domain (susceptibility) **influence function of the medium**, and the units of χ depend on the relationship that is to be used. For time-invariant media that are local in space, the Fourier transform of $\chi(\mathbf{r}, \tau)$ with respect to τ leads to the frequency-dependent **electric susceptibility**.

Lecture 2

Maxwell's equations and electric polarization

Basic assumptions: No free charges, no currents
Nonmagnetic material

$$\begin{aligned}\nabla \cdot \mathbf{D}(\mathbf{r}, t) &= 0 & \mathbf{B}(\mathbf{r}, t) &= \mu_0 \mathbf{H}(\mathbf{r}, t) \\ \nabla \times \mathbf{E}(\mathbf{r}, t) &= -\frac{\partial \mathbf{B}(\mathbf{r}, t)}{\partial t} & \mathbf{D}(\mathbf{r}, t) &= \epsilon_0 \mathbf{E}(\mathbf{r}, t) + \mathbf{P}(\mathbf{r}, t) \\ \nabla \cdot \mathbf{B}(\mathbf{r}, t) &= 0 \\ \nabla \times \mathbf{H}(\mathbf{r}, t) &= \frac{\partial \mathbf{D}(\mathbf{r}, t)}{\partial t}\end{aligned}$$

Linear and nonlinear dielectric polarization:

- **Linear media:** Linear relationship between polarization \mathbf{P} and electric field \mathbf{E}
- **Nonlinear media:** Nonlinear relationship between \mathbf{P} and \mathbf{E}

Nonlinear Optics:

The field of nonlinear optics (often abbreviated as NLO) comprises the branch of optics that describes the behavior of light in nonlinear media, in which the dielectric polarization \mathbf{P} responds nonlinearly to the electric field \mathbf{E} of the light.

General case:
$$\mathbf{P}_L(\mathbf{r}, t) = \epsilon_0 \int_{-\infty}^{\infty} \iiint_{-\infty}^{\infty} \chi^{(1)}(\mathbf{r}, \mathbf{r}', t, t') \mathbf{E}(\mathbf{r}', t') d\mathbf{r}' dt'$$

3 x 3 - matrix

Time-invariant media
$$\mathbf{P}_L(\mathbf{r}, t) = \epsilon_0 \int_{-\infty}^{\infty} \iiint_{-\infty}^{\infty} \chi^{(1)}(\mathbf{r}, \mathbf{r}', \tau) \mathbf{E}(\mathbf{r}', t - \tau) d\mathbf{r}' d\tau$$

Media that are (additionally) local in space
$$\mathbf{P}_L(\mathbf{r}, t) = \epsilon_0 \int_{-\infty}^{\infty} \chi^{(1)}(\mathbf{r}, \tau) \mathbf{E}(\mathbf{r}, t - \tau) d\tau$$

scalar

Isotropic media:
$$\mathbf{P}_L(\mathbf{r}, t) = \epsilon_0 \int_{-\infty}^{\infty} \chi^{(1)}(\mathbf{r}, \tau) \mathbf{E}(\mathbf{r}, t - \tau) d\tau$$

Homogeneous media:
$$\mathbf{P}_L(\mathbf{r}, t) = \epsilon_0 \int_{-\infty}^{\infty} \chi^{(1)}(\tau) \mathbf{E}(\mathbf{r}, t - \tau) d\tau$$

Note: In these relations, χ represents the time-domain (susceptibility) **influence function of the medium**, and the units of χ depend on the relationship that is to be used. For time-invariant media that are local in space, the Fourier transform of $\chi(\mathbf{r}, \tau)$ with respect to τ leads to the frequency-dependent **electric susceptibility**.

Fourier transformation:

$$\Psi(t) = \frac{1}{2\pi} \int_{-\infty}^{+\infty} \tilde{\Psi}(\omega) e^{j\omega t} d\omega \quad \longleftrightarrow \quad \tilde{\Psi}(\omega) = \int_{-\infty}^{+\infty} \Psi(t) e^{-j\omega t} dt$$

Maxwell's equations for a linear time-invariant medium that is local in space:

$$\begin{aligned} \nabla \cdot \tilde{\mathbf{D}}(\mathbf{r}, \omega) &= 0 & \tilde{\mathbf{B}}(\mathbf{r}, \omega) &= \mu_0 \tilde{\mathbf{H}}(\mathbf{r}, \omega), \\ \nabla \times \tilde{\mathbf{E}}(\mathbf{r}, \omega) &= -j\omega \tilde{\mathbf{B}}(\mathbf{r}, \omega) & \tilde{\mathbf{D}}(\mathbf{r}, \omega) &= \epsilon_0 \tilde{\mathbf{E}}(\mathbf{r}, \omega) + \tilde{\mathbf{P}}(\mathbf{r}, \omega) \\ \nabla \cdot \tilde{\mathbf{B}}(\mathbf{r}, \omega) &= 0 \\ \nabla \times \tilde{\mathbf{H}}(\mathbf{r}, \omega) &= j\omega \tilde{\mathbf{D}}(\mathbf{r}, \omega), & \tilde{\mathbf{P}}_L(\mathbf{r}, \omega) &= \epsilon_0 \tilde{\chi}^{(1)}(\mathbf{r}, \omega) \tilde{\mathbf{E}}(\mathbf{r}, \omega) \end{aligned}$$

Note:

$\tilde{\chi}^{(1)}(\mathbf{r}, \omega)$ represents the Fourier transform of the time-domain influence function $\chi^{(1)}(\mathbf{r}, \tau)$ and is a complex quantity. It is also referred to as the electric susceptibility and often denoted as $\underline{\chi}^{(1)}(\mathbf{r}, \omega)$ without the tilde.

Maxwell's equations for complex time-domain amplitudes

Alternatively: Representation of harmonically oscillating field quantities by complex amplitudes of analytic time-domain signals rather than by Fourier transforms:

$$\mathbf{E}(\mathbf{r}, t) = \text{Re} \{ \underline{\mathbf{E}}(\mathbf{r}, \omega_0) \exp(j\omega_0 t) \}$$

Complex time-domain amplitude (a number, not a function of ω_0 !)

In linear optics, Maxwell's equations for complex time-domain amplitude are identical to those for Fourier transforms:

$$\nabla \cdot \underline{\mathbf{D}}(\mathbf{r}, \omega_0) = 0,$$

$$\nabla \times \underline{\mathbf{E}}(\mathbf{r}, \omega_0) = -j\omega_0 \underline{\mathbf{B}}(\mathbf{r}, \omega_0),$$

$$\nabla \cdot \underline{\mathbf{B}}(\mathbf{r}, \omega_0) = 0,$$

$$\nabla \times \underline{\mathbf{H}}(\mathbf{r}, \omega_0) = j\omega_0 \underline{\mathbf{D}}(\mathbf{r}, \omega_0).$$

$$\underline{\mathbf{B}}(\mathbf{r}, \omega_0) = \mu_0 \underline{\mathbf{H}}(\mathbf{r}, \omega_0),$$

$$\underline{\mathbf{D}}(\mathbf{r}, \omega_0) = \epsilon_0 \underline{\mathbf{E}}(\mathbf{r}, \omega_0) + \underline{\mathbf{P}}(\mathbf{r}, \omega_0).$$

$$\underline{\mathbf{P}}_{\perp}(\mathbf{r}, \omega_0) = \epsilon_0 \underline{\chi}^{(1)}(\mathbf{r}, \omega_0) \underline{\mathbf{E}}(\mathbf{r}, \omega_0)$$

where $\underline{\chi}^{(1)}(\mathbf{r}, \omega_0) = \tilde{\chi}^{(1)}(\mathbf{r}, \omega_0)$

Note:

- In nonlinear optics, it is important to discriminate between complex time-domain amplitudes of monochromatic waves, and Fourier transforms.
- Nonlinear optics mostly uses time-domain products of complex field amplitudes rather than Fourier transforms to avoid convolutions of signal spectra in the frequency domain.

Fourier transform of time-domain influence function $\chi(t)$.

Constitutive relations and complex refractive index

Constitutive relations:

$$\begin{aligned}\underline{\mathbf{D}}(\mathbf{r}, \omega) &= \epsilon_0 \underline{\mathbf{E}}(\mathbf{r}, \omega) + \underline{\mathbf{P}}(\mathbf{r}, \omega) \\ &= \epsilon_0 \left(1 + \underline{\chi}^{(1)}(\mathbf{r}, \omega) \right) \underline{\mathbf{E}}(\mathbf{r}, \omega) \\ &= \epsilon_0 \underline{\epsilon}_r(\mathbf{r}, \omega) \underline{\mathbf{E}}(\mathbf{r}, \omega) \\ &= \epsilon_0 \underline{n}^2(\mathbf{r}, \omega) \underline{\mathbf{E}}(\mathbf{r}, \omega)\end{aligned}$$

Complex dielectric constant and refractive index :

$$\underline{\epsilon}_r(\mathbf{r}, \omega) = 1 + \underline{\chi}(\mathbf{r}, \omega) = \underline{n}^2(\mathbf{r}, \omega)$$

Convention: Positive values of n_i (ϵ_{ri}) are assigned to lossy media, negative values correspond to optical gain!

$$\begin{aligned}\underline{n} &= n - j n_i, \\ \epsilon_r &= n^2 - n_i^2, \\ n^2 &= \frac{1}{2} \epsilon_r \left(1 + \sqrt{1 + \epsilon_{ri}^2 / \epsilon_r^2} \right), \\ n &\approx \sqrt{\epsilon_r} \quad (\text{for } |\epsilon_{ri}| \ll \epsilon_r) \\ n &\approx \sqrt{|\epsilon_{ri}|} / 2 \quad (\text{for } |\epsilon_{ri}| \gg \epsilon_r)\end{aligned}$$

$$\begin{aligned}\underline{\epsilon}_r &= \epsilon_r - j \epsilon_{ri}, \\ \epsilon_{ri} &= 2n n_i, \\ n_i &= \epsilon_{ri} / (2n), \\ n_i &\approx \epsilon_{ri} / (2\sqrt{\epsilon_r}), \\ n_i &\approx \text{sgn}(\epsilon_{ri}) \sqrt{|\epsilon_{ri}|} / 2.\end{aligned}$$

Basic relations of vector calculus

Linearität

1. $\nabla(\alpha\Phi + \beta\Psi) = \alpha \nabla\Phi + \beta \nabla\Psi$
2. $\nabla \cdot (\alpha \mathbf{F} + \beta \mathbf{G}) = \alpha \nabla \cdot \mathbf{F} + \beta \nabla \cdot \mathbf{G}$
3. $\nabla \times (\alpha \mathbf{F} + \beta \mathbf{G}) = \alpha \nabla \times \mathbf{F} + \beta \nabla \times \mathbf{G}$

Operation auf Produkten

4. $\nabla(\Phi\Psi) = \Phi \nabla\Psi + \Psi \nabla\Phi$
5. $\nabla(\mathbf{F} \cdot \mathbf{G}) = (\mathbf{F} \cdot \nabla)\mathbf{G} + (\mathbf{G} \cdot \nabla)\mathbf{F} + \mathbf{F} \times (\nabla \times \mathbf{G}) + \mathbf{G} \times (\nabla \times \mathbf{F})$
6. $\nabla \cdot (\Phi \mathbf{F}) = \Phi \nabla \cdot \mathbf{F} + (\nabla\Phi) \cdot \mathbf{F}$
7. $\nabla \cdot (\mathbf{F} \times \mathbf{G}) = \mathbf{G} \cdot \nabla \times \mathbf{F} - \mathbf{F} \cdot \nabla \times \mathbf{G}$
8. $\nabla \times (\Phi \mathbf{F}) = \Phi \nabla \times \mathbf{F} + (\nabla\Phi) \times \mathbf{F}$
9. $\nabla \times (\mathbf{F} \times \mathbf{G}) = (\mathbf{G} \cdot \nabla)\mathbf{F} - (\mathbf{F} \cdot \nabla)\mathbf{G} + \mathbf{F}(\nabla \cdot \mathbf{G}) - \mathbf{G}(\nabla \cdot \mathbf{F})$

Zweifache Anwendung von ∇

10. $\nabla \cdot (\nabla \times \mathbf{F}) = 0$
11. $\nabla \times (\nabla\Phi) = \mathbf{0}$
12. $\nabla \times (\nabla \times \mathbf{F}) = \nabla(\nabla \cdot \mathbf{F}) - \nabla^2 \mathbf{F}$

- $$\begin{aligned} \text{grad}(\alpha\Phi + \beta\Psi) &= \alpha \text{grad } \Phi + \beta \text{grad } \Psi \\ \text{div}(\alpha \mathbf{F} + \beta \mathbf{G}) &= \alpha \text{div } \mathbf{F} + \beta \text{div } \mathbf{G} \\ \text{rot}(\alpha \mathbf{F} + \beta \mathbf{G}) &= \alpha \text{rot } \mathbf{F} + \beta \text{rot } \mathbf{G} \end{aligned}$$

- $$\begin{aligned} \text{grad}(\Phi\Psi) &= \Phi \text{grad } \Psi + \Psi \text{grad } \Phi \\ \text{grad}(\mathbf{F} \cdot \mathbf{G}) &= (\mathbf{F} \cdot \text{grad})\mathbf{G} + \\ &\quad + (\mathbf{G} \cdot \text{grad})\mathbf{F} + \mathbf{F} \times \text{rot } \mathbf{G} + \mathbf{G} \times \text{rot } \mathbf{F} \\ \text{div}(\Phi \mathbf{F}) &= \Phi \text{div } \mathbf{F} + \mathbf{F} \cdot \text{grad } \Phi \\ \text{div}(\mathbf{F} \times \mathbf{G}) &= \mathbf{G} \cdot \text{rot } \mathbf{F} - \mathbf{F} \cdot \text{rot } \mathbf{G} \\ \text{rot}(\Phi \mathbf{F}) &= \Phi \text{rot } \mathbf{F} + (\text{grad } \Phi) \times \mathbf{F} \\ \text{rot}(\mathbf{F} \times \mathbf{G}) &= (\mathbf{G} \cdot \text{grad})\mathbf{F} - \\ &\quad - (\mathbf{F} \cdot \text{grad})\mathbf{G} + \mathbf{F} \text{div } \mathbf{G} - \mathbf{G} \text{div } \mathbf{F} \end{aligned}$$

- $$\begin{aligned} \text{div rot } \mathbf{F} &= 0 \\ \text{rot grad } \Phi &= \mathbf{0} \\ \text{rot rot } \mathbf{F} &= \text{grad div } \mathbf{F} - \Delta \mathbf{F} \end{aligned}$$

Rade / Westergren, Mathematische Formeln, Springer

Wave equation and plane waves

Wave equation in homogeneous media:

$$\nabla^2 \underline{\mathbf{E}}(\mathbf{r}, \omega) + k_0^2 \epsilon_r(\omega) \underline{\mathbf{E}}(\mathbf{r}, \omega) = 0$$

$$\nabla^2 \underline{\mathbf{H}}(\mathbf{r}, \omega) + k_0^2 \epsilon_r(\omega) \underline{\mathbf{H}}(\mathbf{r}, \omega) = 0 \quad \text{where} \quad k_0 = \frac{\omega}{c}$$

Solution for homogeneous media: Plane waves

$$\underline{\mathbf{E}}(\mathbf{r}, t) = \text{Re} \left\{ \underline{\mathbf{E}}(\mathbf{r}, \omega) e^{j\omega t} \right\} = \text{Re} \left\{ \underline{\mathbf{E}}_0 e^{j(\omega t - \underline{\mathbf{k}}\mathbf{r})} \right\}$$

$$\underline{\mathbf{H}}(\mathbf{r}, t) = \text{Re} \left\{ \underline{\mathbf{H}}(\mathbf{r}, \omega) e^{j\omega t} \right\} = \text{Re} \left\{ \underline{\mathbf{H}}_0 e^{j(\omega t - \underline{\mathbf{k}}\mathbf{r})} \right\} \quad \text{where} \quad \underline{\mathbf{k}}^2 = k_0^2 \epsilon_r(\omega)$$

Properties of plane waves:

- $\underline{\mathbf{k}}$, $\underline{\mathbf{E}}_0$, and $\underline{\mathbf{H}}_0$ are mutually connected and form an orthogonal right-handed system:

$$\begin{aligned} \underline{\mathbf{k}} \cdot \underline{\mathbf{E}}_0 &= 0 & \underline{\mathbf{H}}_0 &= \frac{1}{\omega \mu_0} \underline{\mathbf{k}} \times \underline{\mathbf{E}}_0 & \underline{\mathbf{E}}_0 &= -\frac{1}{\omega \epsilon_0 \epsilon_r} \underline{\mathbf{k}} \times \underline{\mathbf{H}}_0 \\ \underline{\mathbf{k}} \cdot \underline{\mathbf{H}}_0 &= 0 \end{aligned}$$

- The attenuation of a plane wave is linked to the imaginary part n_i of the complex refractive index. For a plane wave propagating in positive z-direction, the power decays as $e^{-\alpha z}$, where the attenuation constant α is given by

$$\alpha = 2k_0 n_i$$

Note: A positive value of n_i corresponds to a positive attenuation coefficient α and therefore to optical loss.

Wave equation and plane waves in isotropic media

General form:

$$\nabla^2 \underline{\mathbf{E}}(\mathbf{r}, \omega) + \nabla \left(\frac{\nabla \underline{\epsilon}_r(\mathbf{r}, \omega)}{\underline{\epsilon}_r(\mathbf{r}, \omega)} \cdot \underline{\mathbf{E}}(\mathbf{r}, \omega) \right) + k_0^2 \underline{\epsilon}_r(\mathbf{r}, \omega) \underline{\mathbf{E}}(\mathbf{r}, \omega) = 0$$

$$\nabla^2 \underline{\mathbf{H}}(\mathbf{r}, \omega) + \frac{\nabla \underline{\epsilon}_r(\mathbf{r}, \omega)}{\underline{\epsilon}_r(\mathbf{r}, \omega)} \times (\nabla \times \underline{\mathbf{H}}(\mathbf{r}, \omega)) + k_0^2 \underline{\epsilon}_r(\mathbf{r}, \omega) \underline{\mathbf{H}}(\mathbf{r}, \omega) = 0$$

where $k_0 = \frac{\omega}{c}$

Homogeneous (and weakly inhomogeneous) media: ϵ can be assumed constant (approximately constant within distances of the order of a wavelength)

$$\nabla^2 \underline{\mathbf{E}}(\mathbf{r}, \omega) + k_0^2 \underline{\epsilon}_r(\mathbf{r}, \omega) \underline{\mathbf{E}}(\mathbf{r}, \omega) = 0$$

$$\nabla^2 \underline{\mathbf{H}}(\mathbf{r}, \omega) + k_0^2 \underline{\epsilon}_r(\mathbf{r}, \omega) \underline{\mathbf{H}}(\mathbf{r}, \omega) = 0$$

Solution for homogeneous media: Plane waves

$$\underline{\mathbf{E}}(\mathbf{r}, t) = \text{Re} \left\{ \underline{\mathbf{E}}(\mathbf{r}, \omega) e^{j\omega t} \right\} = \text{Re} \left\{ \underline{\mathbf{E}}_0 e^{j(\omega t - \underline{\mathbf{k}}\mathbf{r})} \right\}$$

$$\underline{\mathbf{H}}(\mathbf{r}, t) = \text{Re} \left\{ \underline{\mathbf{H}}(\mathbf{r}, \omega) e^{j\omega t} \right\} = \text{Re} \left\{ \underline{\mathbf{H}}_0 e^{j(\omega t - \underline{\mathbf{k}}\mathbf{r})} \right\}$$

where $\underline{\mathbf{k}}^2 = k_0^2 \underline{\epsilon}_r(\omega)$

- \mathbf{k} , \mathbf{E}_0 , and \mathbf{H}_0 are mutually connected and form an orthogonal right-handed system:

$$\mathbf{k} \cdot \mathbf{E}_0 = 0$$

$$\mathbf{k} \cdot \mathbf{H}_0 = 0$$

$$\mathbf{H}_0 = \frac{1}{\omega\mu_0} \mathbf{k} \times \mathbf{E}_0$$

$$\mathbf{E}_0 = -\frac{1}{\omega\epsilon_0\epsilon_r} \mathbf{k} \times \mathbf{H}_0$$

- The attenuation of a plane wave is linked to the imaginary part n_i of the complex refractive index. For a plane wave propagating in positive z -direction, the power decays as $e^{-\alpha z}$, where the attenuation constant α is given by

$$\alpha = 2k_0 n_i$$

Note: A positive value of n_i corresponds to a positive attenuation coefficient α and therefore to optical loss.

Analytic time-domain signals

In nonlinear optics, **complex amplitudes of monochromatic electromagnetic waves** are usually considered rather than Fourier spectra:

$$\psi(t) = \text{Re} \left\{ \underline{\psi}(\omega_0) \exp(j\omega_0 t) \right\}$$

⇒ If only the real part has a physical meaning, what is the role of the imaginary part?

Recall: For a real time-domain signal $\psi(t) \in \mathbb{R}$, the Fourier spectrum $\tilde{\psi}(\omega)$ has Hermitian symmetry,

$$\tilde{\psi}(\omega) = \tilde{\psi}^*(-\omega).$$

Removing the redundant left part of the spectrum corresponds to adding an imaginary part to the time-domain signal that corresponds to the **Hilbert transform of the real part**,

$$\underline{\psi}(t) = \psi(t) + j \left(\psi(t) \star \frac{1}{\pi t} \right),$$

Hilbert transform
↙

$\underline{\psi}(t)$ is referred to as the **analytic representation** of a real-valued time-domain function $\psi(t)$.

Kramers-Kronig relations

Recall: The electric susceptibility is the Fourier transform of a **causal** influence function in time domain.

$$\mathbf{P}(t) = \epsilon_0 \int_{-\infty}^{\infty} \chi(\tau) \mathbf{E}(t - \tau) d\tau \quad \circ \text{---} \bullet \quad \underline{\mathbf{P}}(\omega) = \epsilon_0 \underline{\chi}(\omega) \underline{\mathbf{E}}(\omega)$$

$$\chi(\tau) = 0 \quad \text{for} \quad \tau < 0 \quad \tilde{\chi}(\omega) = \chi(\omega) + j\chi_i(\omega)$$

As a consequence, the real and the imaginary part of the complex susceptibility are connected by the **Hilbert transform**,

“**Cauchy principal value**”, i.e., the integration boundaries must approach the singularity “symmetrically” from both sides.

$$\chi(\omega) = -\frac{1}{\pi} \mathcal{P} \int_{-\infty}^{\infty} \frac{\chi_i(\omega_0)}{\omega_0 - \omega} d\omega_0$$

$$\chi_i(\omega) = \frac{1}{\pi} \mathcal{P} \int_{-\infty}^{\infty} \frac{\chi(\omega_0)}{\omega_0 - \omega} d\omega_0$$

Making further use of the fact that $\chi(t)$ is real, the **Kramers-Kronig relations** can be derived,

$$\chi(\omega) = -\frac{2}{\pi} \mathcal{P} \int_0^{\infty} \frac{\omega_0 \chi_i(\omega_0)}{\omega_0^2 - \omega^2} d\omega_0$$

$$\chi_i(\omega) = \frac{2}{\pi} \mathcal{P} \int_0^{\infty} \frac{\omega \chi(\omega_0)}{\omega_0^2 - \omega^2} d\omega_0$$

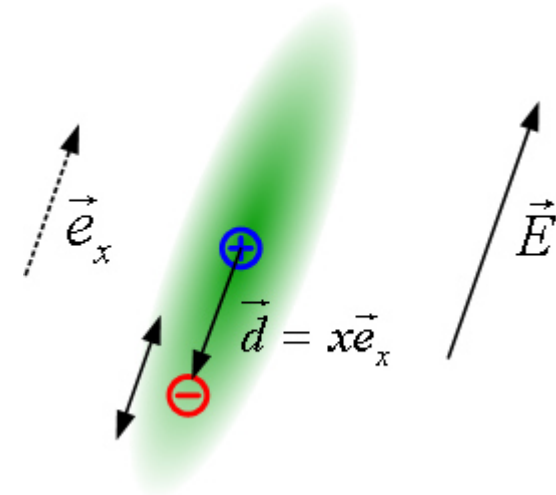
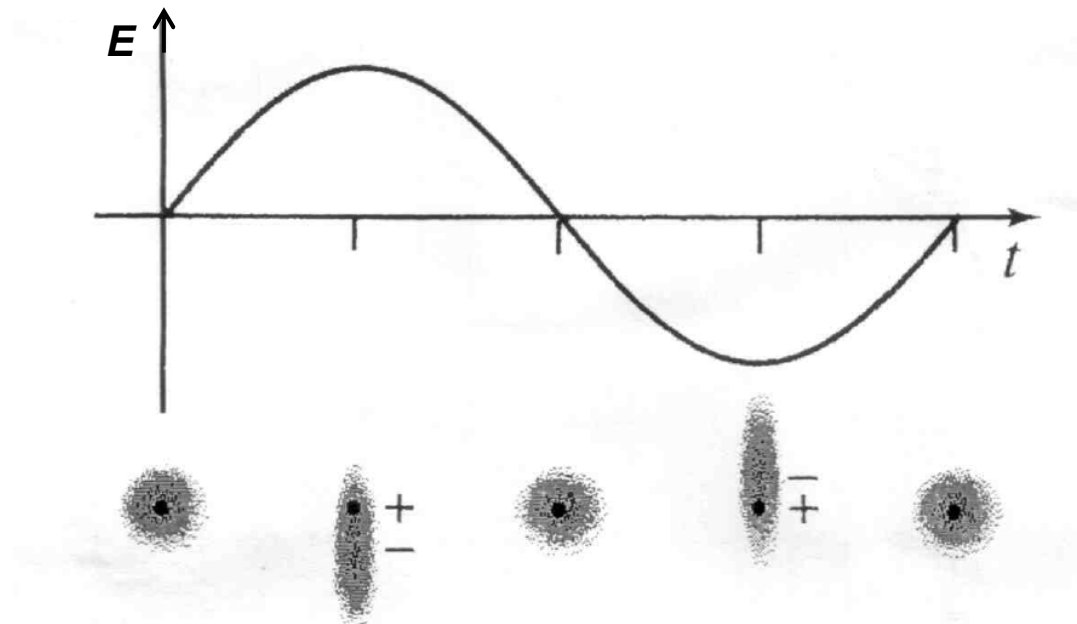
- The refractive index of a medium can be calculated from its absorption spectrum and vice versa. **Absorption and dispersion are intimately related by fundamental principles.**
- An “ideal” dispersionless lossless medium cannot exist:

$$\chi(\omega) = -\frac{1}{\pi} \mathcal{P} \int_{-\infty}^{\infty} \frac{\chi_i(\omega_0)}{\omega_0 - \omega} d\omega_0 \quad (1)$$

$$\chi_i(\omega) = \frac{1}{\pi} \mathcal{P} \int_{-\infty}^{\infty} \frac{\chi(\omega_0)}{\omega_0 - \omega} d\omega_0 \quad (2)$$

For constant $\chi(f)$, i.e., $\chi(f) = \epsilon_r(f) - 1 = \text{const}_f$, we find $\chi_i(f) = \epsilon_{ri}(f) = 0$ from Eq. (1), which implies $\chi(f) = 0$ and $\epsilon_r(f) = 1$, Eq. (2). Real media always have loss (or gain) in some frequency ranges, and the real part of the susceptibility is always frequency dependent. $\chi(f) = \text{const}_f$ and $\chi_i = 0$ is only possible in certain frequency ranges.

Lorentz oscillator model of bound charges



Equation of motion for bound charges:

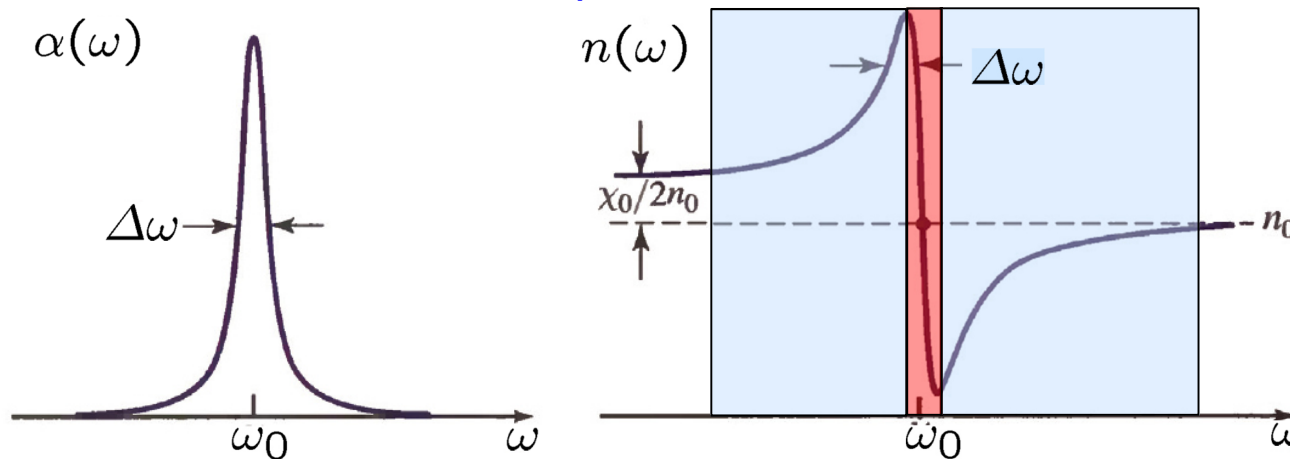
$$m_e \frac{d^2 x}{dt^2} = -e E_x - m_e \omega_r^2 x - m_e \gamma_r \frac{dx}{dt}$$

Complex electric susceptibility:

$$\begin{aligned} \underline{\chi}(\omega) &= \chi_0 \frac{\omega_r^2}{\omega_r^2 - \omega^2 + j\omega\gamma_r} \\ &= \frac{(\omega_r^2 - \omega^2) \omega_r^2}{(\omega_r^2 - \omega^2)^2 + \omega^2 \gamma_r^2} \chi_0 - j \frac{\omega \gamma_r \omega_r^2}{(\omega_r^2 - \omega^2)^2 + \omega^2 \gamma_r^2} \chi_0, \quad \chi_0 = \frac{e^2 N}{\epsilon_0 m_e \omega_r^2} \end{aligned}$$

Refractive index and absorption

Refractive index and absorption near a resonance:

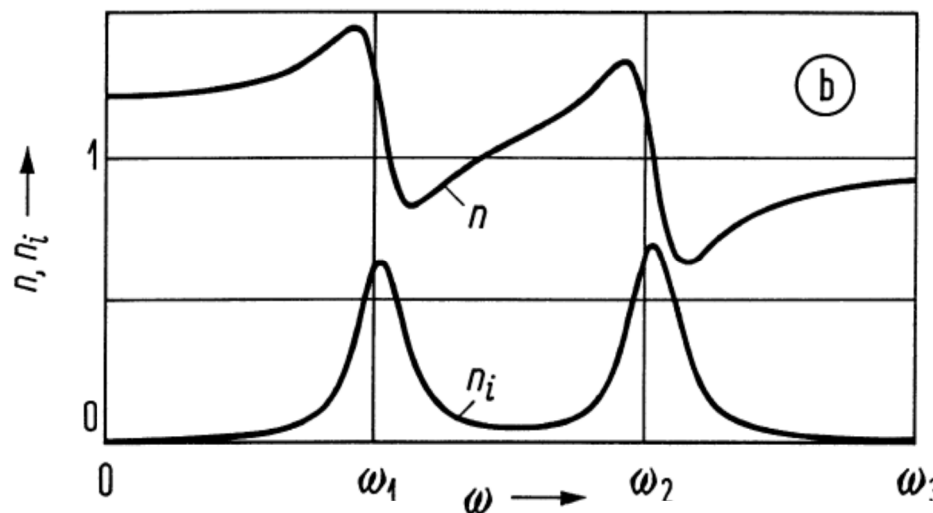


Adapted from Saleh, B. E. A. & Teich, M. C. (2007), *Fundamentals of Photonics*, John Wiley & Sons, Hoboken, NJ.

$$n \approx \sqrt{1 + \chi}$$

$$n_i \approx -\frac{\chi_i}{2n}, \quad \alpha = 2k_0 n_i$$

Real media often have several resonances, each of which contributes to the refractive index and to the absorption:



$$\chi(\omega) = \sum_{\nu} \frac{(\omega_{r\nu}^2 - \omega^2) \omega_r^2}{(\omega_{r\nu}^2 - \omega^2)^2 + \omega^2 \gamma_{r\nu}^2} \chi_{0\nu}$$

$$\chi_i(\omega) = -\sum_{\nu} \frac{\omega \gamma_{r\nu} \omega_{r\nu}^2}{(\omega_{r\nu}^2 - \omega^2)^2 + \omega^2 \gamma_{r\nu}^2} \chi_{0\nu}$$

Complex electric susceptibility far from resonance ($|\omega_r - \omega| \gg \gamma_r$):

$$\underline{\chi}(\omega) \approx \frac{\omega_r^2}{\omega_r^2 - \omega^2} \chi_0$$

$\Rightarrow \chi$ is approximately real, absorption is small. Contributions from multiple resonances lead to so-called **Sellmeier equations**:

$$n^2 = 1 + \chi = 1 + \sum_{\nu} \chi_{0\nu} \frac{f_{\nu}^2}{f_{\nu}^2 - f^2} = 1 + \sum_{\nu} \chi_{0\nu} \frac{\lambda^2}{\lambda^2 - \lambda_{\nu}^2}$$

For **Sellmeier coefficients** $\chi_{0\nu}$ and λ_{ν} , see reference books on optical materials or material databases, e.g.,

- Palik, E. D. (1998), *Handbook of Optical Constants of Solids*, Academic Press, San Diego, CA
- The Landolt Börnstein Database, <http://materials.springer.com/>

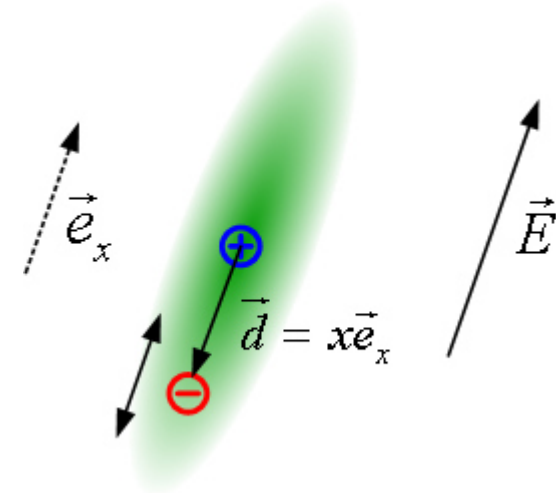
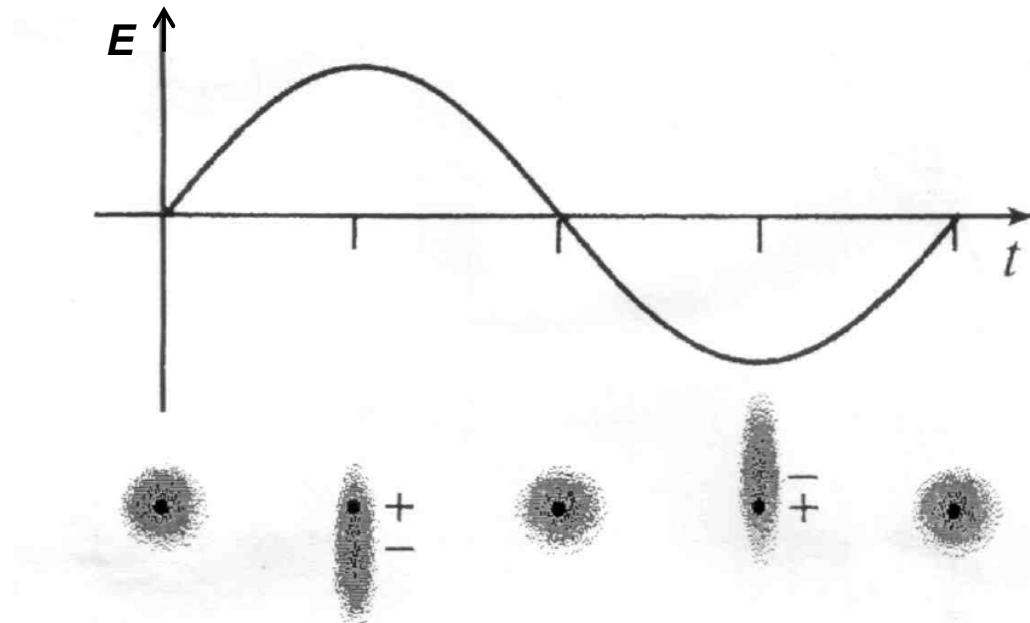
Sellmeier coefficients of various materials

Material	Sellmeier Equation (Wavelength λ in μm)	Wavelength Range (μm)
Fused silica	$n^2 = 1 + \frac{0.6962\lambda^2}{\lambda^2 - (0.06840)^2} + \frac{0.4079\lambda^2}{\lambda^2 - (0.1162)^2} + \frac{0.8975\lambda^2}{\lambda^2 - (9.8962)^2}$	0.21–3.71
Si	$n^2 = 1 + \frac{10.6684\lambda^2}{\lambda^2 - (0.3015)^2} + \frac{0.0030\lambda^2}{\lambda^2 - (1.1347)^2} + \frac{1.5413\lambda^2}{\lambda^2 - (1104.0)^2}$	1.36–11
GaAs	$n^2 = 3.5 + \frac{7.4969\lambda^2}{\lambda^2 - (0.4082)^2} + \frac{1.9347\lambda^2}{\lambda^2 - (37.17)^2}$	1.4–11
BBO	$n_o^2 = 2.7359 + \frac{0.01878}{\lambda^2 - 0.01822} - 0.01354\lambda^2$ $n_e^2 = 2.3753 + \frac{0.01224}{\lambda^2 - 0.01667} - 0.01516\lambda^2$	0.22–1.06
KDP	$n_o^2 = 1 + \frac{1.2566\lambda^2}{\lambda^2 - (0.09191)^2} + \frac{33.8991\lambda^2}{\lambda^2 - (33.3752)^2}$ $n_e^2 = 1 + \frac{1.1311\lambda^2}{\lambda^2 - (0.09026)^2} + \frac{5.7568\lambda^2}{\lambda^2 - (28.4913)^2}$	0.4–1.06
LiNbO ₃	$n_o^2 = 2.3920 + \frac{2.5112\lambda^2}{\lambda^2 - (0.217)^2} + \frac{7.1333\lambda^2}{\lambda^2 - (16.502)^2}$ $n_e^2 = 2.3247 + \frac{2.2565\lambda^2}{\lambda^2 - (0.210)^2} + \frac{14.503\lambda^2}{\lambda^2 - (25.915)^2}$	0.4–3.1

Saleh, B. E. A. & Teich, M. C. (2007), *Fundamentals of Photonics*, John Wiley & Sons, Hoboken, NJ.

Lecture 3

Lorentz oscillator model of bound charges



Equation of motion for bound charges:

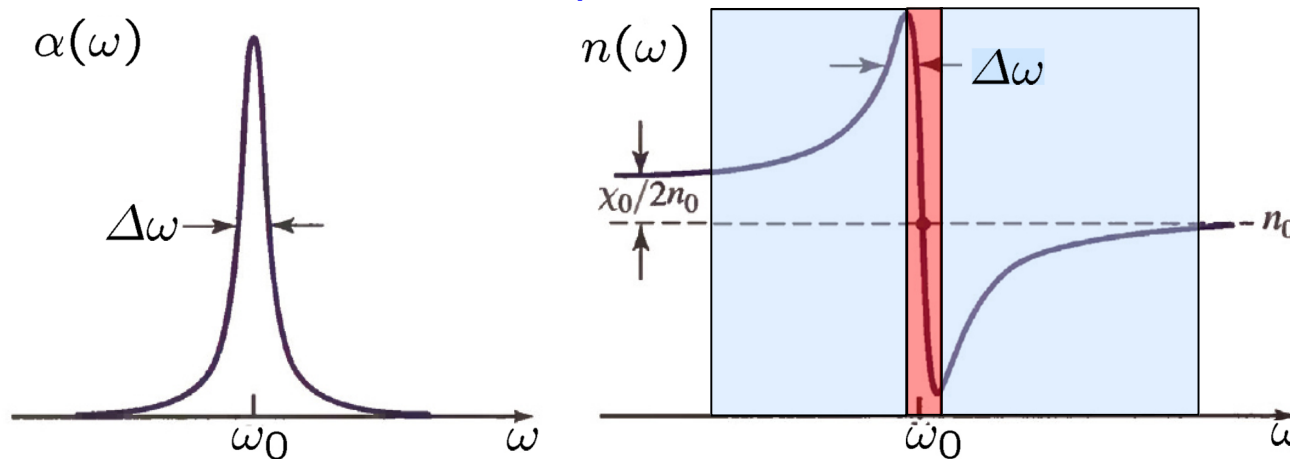
$$m_e \frac{d^2 x}{dt^2} = -e E_x - m_e \omega_r^2 x - m_e \gamma_r \frac{dx}{dt}$$

Complex electric susceptibility:

$$\begin{aligned} \underline{\chi}(\omega) &= \chi_0 \frac{\omega_r^2}{\omega_r^2 - \omega^2 + j\omega\gamma_r} \\ &= \frac{(\omega_r^2 - \omega^2) \omega_r^2}{(\omega_r^2 - \omega^2)^2 + \omega^2 \gamma_r^2} \chi_0 - j \frac{\omega \gamma_r \omega_r^2}{(\omega_r^2 - \omega^2)^2 + \omega^2 \gamma_r^2} \chi_0, \quad \chi_0 = \frac{e^2 N}{\epsilon_0 m_e \omega_r^2} \end{aligned}$$

Refractive index and absorption

Refractive index and absorption near a resonance:

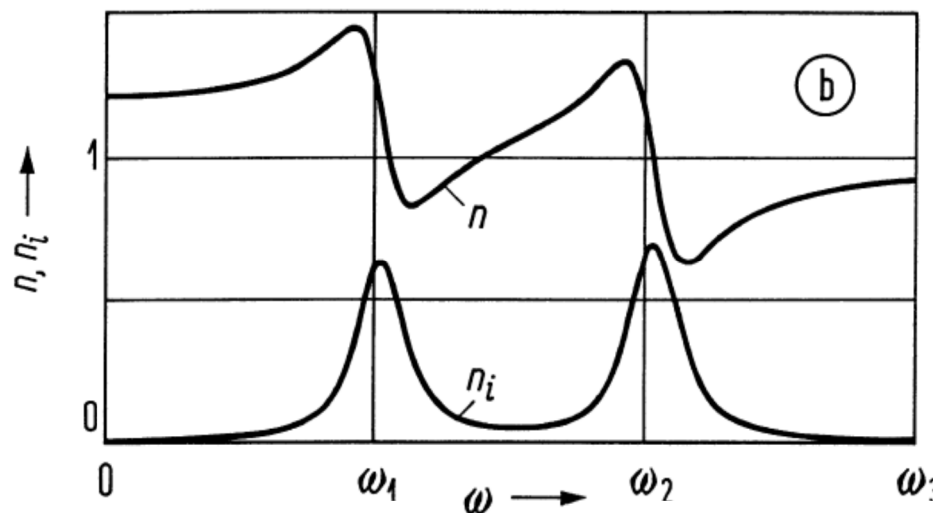


Adapted from Saleh, B. E. A. & Teich, M. C. (2007), *Fundamentals of Photonics*, John Wiley & Sons, Hoboken, NJ.

$$n \approx \sqrt{1 + \chi}$$

$$n_i \approx -\frac{\chi_i}{2n}, \quad \alpha = 2k_0 n_i$$

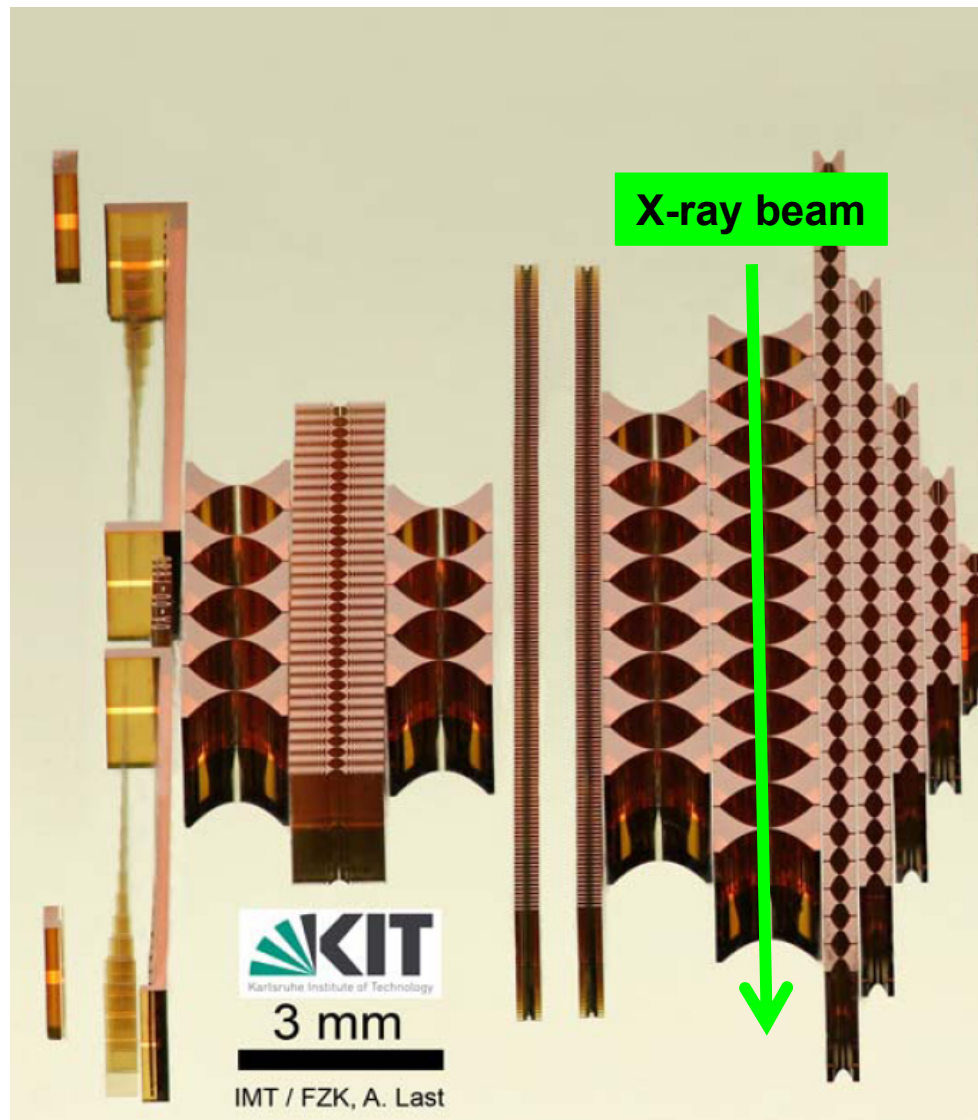
Real media often have several resonances, each of which contributes to the refractive index and to the absorption:



$$\chi(\omega) = \sum_{\nu} \frac{(\omega_{r\nu}^2 - \omega^2) \omega_r^2}{(\omega_{r\nu}^2 - \omega^2)^2 + \omega^2 \gamma_{r\nu}^2} \chi_{0\nu}$$

$$\chi_i(\omega) = -\sum_{\nu} \frac{\omega \gamma_{r\nu} \omega_{r\nu}^2}{(\omega_{r\nu}^2 - \omega^2)^2 + \omega^2 \gamma_{r\nu}^2} \chi_{0\nu}$$

Example: X-ray lenses



$$\chi(\omega) = \frac{(\omega_r^2 - \omega^2) \omega_r^2}{(\omega_r^2 - \omega^2)^2 + \omega^2 \gamma_r^2} \chi_0$$
$$\chi_i(\omega) = -\frac{\omega \gamma_r \omega_r^2}{(\omega_r^2 - \omega^2)^2 + \omega^2 \gamma_r^2} \chi_0$$

At very high frequencies ($\omega \gg \omega_r$):

$n < 1$

⇒ Focussing lenses must have concave form!

n very close to 1 ($1 - n \approx 10^{-6}$)

⇒ Needs lots of lenses to obtain sufficient refraction.

Complex electric susceptibility far from resonance ($|\omega_r - \omega| \gg \gamma_r$):

$$\underline{\chi}(\omega) \approx \frac{\omega_r^2}{\omega_r^2 - \omega^2} \chi_0$$

$\Rightarrow \chi$ is approximately real, absorption is small. Contributions from multiple resonances lead to so-called **Sellmeier equations**:

$$n^2 = 1 + \chi = 1 + \sum_{\nu} \chi_{0\nu} \frac{f_{\nu}^2}{f_{\nu}^2 - f^2} = 1 + \sum_{\nu} \chi_{0\nu} \frac{\lambda^2}{\lambda^2 - \lambda_{\nu}^2}$$

For **Sellmeier coefficients** $\chi_{0\nu}$ and λ_{ν} , see reference books on optical materials or material databases, e.g.,

- Palik, E. D. (1998), *Handbook of Optical Constants of Solids*, Academic Press, San Diego, CA
- The Landolt Börnstein Database, <http://materials.springer.com/>

Sellmeier coefficients of various materials

Material	Sellmeier Equation (Wavelength λ in μm)	Wavelength Range (μm)
Fused silica	$n^2 = 1 + \frac{0.6962\lambda^2}{\lambda^2 - (0.06840)^2} + \frac{0.4079\lambda^2}{\lambda^2 - (0.1162)^2} + \frac{0.8975\lambda^2}{\lambda^2 - (9.8962)^2}$	0.21–3.71
Si	$n^2 = 1 + \frac{10.6684\lambda^2}{\lambda^2 - (0.3015)^2} + \frac{0.0030\lambda^2}{\lambda^2 - (1.1347)^2} + \frac{1.5413\lambda^2}{\lambda^2 - (1104.0)^2}$	1.36–11
GaAs	$n^2 = 3.5 + \frac{7.4969\lambda^2}{\lambda^2 - (0.4082)^2} + \frac{1.9347\lambda^2}{\lambda^2 - (37.17)^2}$	1.4–11
BBO	$n_o^2 = 2.7359 + \frac{0.01878}{\lambda^2 - 0.01822} - 0.01354\lambda^2$ $n_e^2 = 2.3753 + \frac{0.01224}{\lambda^2 - 0.01667} - 0.01516\lambda^2$	0.22–1.06
KDP	$n_o^2 = 1 + \frac{1.2566\lambda^2}{\lambda^2 - (0.09191)^2} + \frac{33.8991\lambda^2}{\lambda^2 - (33.3752)^2}$ $n_e^2 = 1 + \frac{1.1311\lambda^2}{\lambda^2 - (0.09026)^2} + \frac{5.7568\lambda^2}{\lambda^2 - (28.4913)^2}$	0.4–1.06
LiNbO ₃	$n_o^2 = 2.3920 + \frac{2.5112\lambda^2}{\lambda^2 - (0.217)^2} + \frac{7.1333\lambda^2}{\lambda^2 - (16.502)^2}$ $n_e^2 = 2.3247 + \frac{2.2565\lambda^2}{\lambda^2 - (0.210)^2} + \frac{14.503\lambda^2}{\lambda^2 - (25.915)^2}$	0.4–3.1

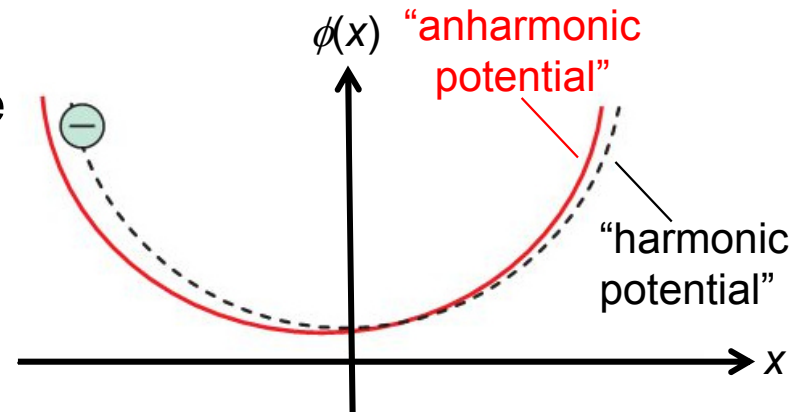
Saleh, B. E. A. & Teich, M. C. (2007), *Fundamentals of Photonics*, John Wiley & Sons, Hoboken, NJ.

Nonlinear optics: Anharmonic oscillator model

Lorentz model (linear optics):

Linear relationship between restoring force and displacement, corresponding to a **quadratic potential** (“harmonic potential”)

⇒ **Harmonic oscillator** as first-order approximation for small amplitudes.



General case (nonlinear optics):

Higher-order (e.g., cubic) terms in the potential (“anharmonic potential”) lead to nonlinear (e.g., quadratic) relationship between restoring force and displacement.

⇒ **Anharmonic oscillator:**

$$m_e \frac{d^2 x}{dt^2} = -eE_x - m_e \gamma_r \frac{dx}{dt} - m_e \omega_r^2 x - ax^2 - bx^3$$

For $E_x = \text{Re} \{ \underline{E}_x \exp(j\omega_0 t) \}$: Polarization contains **new spectral components** at $\omega = 0, \omega = \omega_0, \omega = 2\omega_0, \omega = 3\omega_0 \dots$

Nonlinear wave equation: Basic assumptions

- Decompose electric polarization into a **strong linear** and a **weak nonlinear contribution**:

$$\mathbf{P}(\mathbf{r}, t) = \mathbf{P}_L(\mathbf{r}, t) + \mathbf{P}_{NL}(\mathbf{r}, t)$$

$$\text{where } |\mathbf{P}_{NL}(\mathbf{r}, t)| \ll |\mathbf{P}_L(\mathbf{r}, t)|.$$

⇒ The nonlinear polarization can be treated as a **small perturbation** of the linear polarization, leading to **plane-wave-like solutions with weakly space and time-dependent amplitudes** (“**slowly varying envelope approximation**”, SVEA)

- Assume that the medium is operated **far away from any electronic resonances** such that the **electric susceptibility is real and independent of frequency**,

$$\underline{\chi}^{(1)}(\mathbf{r}, \omega_l) \approx \chi^{(1)}(\mathbf{r}) \in \mathbb{R}.$$

We can then relate the instantaneous linear polarization directly to the instantaneous electric field in the time domain, neglecting any memory of the medium,

$$\mathbf{P}_L(\mathbf{r}, t) = \epsilon_0 \chi^{(1)}(\mathbf{r}) \mathbf{E}(\mathbf{r}, t)$$

Nonlinear wave equation

⇒ Wave equation for **inhomogeneous nonlinear media**:

$$\nabla \times \nabla \times \mathbf{E}(\mathbf{r}, t) + \mu_0 \epsilon_0 \epsilon_r \frac{\partial^2 \mathbf{E}(\mathbf{r}, t)}{\partial t^2} = -\mu_0 \frac{\partial^2 \mathbf{P}_{\text{NL}}(\mathbf{r}, t)}{\partial t^2}$$

Simplification for **isotropic homogeneous nonlinear media**:

$$\nabla^2 \mathbf{E}(\mathbf{r}, t) - \frac{n^2}{c^2} \frac{\partial^2 \mathbf{E}(\mathbf{r}, t)}{\partial t^2} = \mu_0 \frac{\partial^2 \mathbf{P}_{\text{NL}}(\mathbf{r}, t)}{\partial t^2}.$$

Simplifying assumptions:

- **Linearly polarized, “plane-wave-like” fields** (Without loss of generality: Polarization along x, propagation along z)
⇒ Represent by scalar field quantities $E(z, t)$ and $P(z, t)$
- Polarization **responds instantaneously** to applied electric field (“memory-less material”)
⇒ Expand nonlinear time-domain relationship between P and E into a **power series of scalar quantities**:

$$\begin{aligned} P(z, t) &= \epsilon_0 \chi^{(1)} E(z, t) + \epsilon_0 \chi^{(2)} E^2(z, t) + \epsilon_0 \chi^{(3)} E^3(z, t) + \dots \\ &= P_L(z, t) + P_{\text{NL}}(z, t) \end{aligned}$$

$$P_L(z, t) = \epsilon_0 \chi^{(1)} E(z, t)$$

$$P_{\text{NL}}(z, t) = \epsilon_0 \chi^{(2)} E^2(z, t) + \epsilon_0 \chi^{(3)} E^3(z, t) + \dots$$

Representation of nonlinear polarization

Example: Second-order nonlinear polarization

Assume **superposition of two monochromatic plane waves**, oscillating with frequency ω_1 and ω_2 :

$$E(z, t) = \frac{1}{2} (\underline{E}(\omega_1) \exp(j(\omega_1 t - k_1 z)) + \underline{E}(\omega_2) \exp(j(\omega_2 t - k_2 z)) + \text{c.c.}).$$

⇒ The **second-order nonlinear polarization** contains components at all sum and difference frequencies:

$$P_{\text{NL}}(z, t) = \frac{1}{4} \epsilon_0 \chi^{(2)} \left(\underline{E}_1^2 e^{j2(\omega_1 t - k_1 z)} + \text{c.c.} \right. \\ \left. + \underline{E}_2^2 e^{j2(\omega_2 t - k_2 z)} + \text{c.c.} \right. \\ \left. + 2 |\underline{E}_1|^2 + 2 |\underline{E}_2|^2 \right. \\ \left. + 2 \underline{E}_1 \underline{E}_2 e^{j((\omega_1 + \omega_2)t - (k_1 + k_2)z)} + \text{c.c.} \right. \\ \left. + 2 \underline{E}_1 \underline{E}_2^* e^{j((\omega_1 - \omega_2)t - (k_1 - k_2)z)} + \text{c.c.} \right)$$

}

Second-harmonic generation (SHG)

}

Optical rectification (OR)

}

Sum and difference frequency generation (SFG, DFG)

Note: The individual expressions of the second-order polarization exhibit plane wave-like space and time dependences. However, the wavenumbers differ from that of a plane electromagnetic wave at the same frequency, $k(\omega_1) + k(\omega_2) \neq k(\omega_1 + \omega_2)$.

Solution of nonlinear wave equation: Slowly-varying envelope approximation (SVEA)

Solution ansatz:

- Represent electric field $E(z,t)$ and nonlinear polarization $P_{\text{NL}}(z,t)$ as a superposition of plane-wave-like fields, oscillating at different frequencies ω_l
- Introduce (weakly) **time- and space-dependent amplitudes** to account for nonlinear interaction

$$E(z,t) = \frac{1}{2} \left(\sum_l \underline{E}(z,t,\omega_l) \exp(j(\omega_l t - k_l z)) + \text{c.c.} \right)$$

Complex conjugate of preceding expression.

$$P_{\text{NL}}(z,t) = \frac{1}{2} \left(\sum_l \underline{P}_{\text{NL}}(z,t,\omega_l) \exp(j(\omega_l t - k_{p,l} z)) + \text{c.c.} \right)$$

where

$$\left| \frac{\partial^2 \underline{E}(z,t,\omega_l)}{\partial t^2} \right| \ll \omega_l \left| \frac{\partial \underline{E}(z,t,\omega_l)}{\partial t} \right|,$$

$$\left| \frac{\partial^2 \underline{E}(z,t,\omega_l)}{\partial z^2} \right| \ll k_l \left| \frac{\partial \underline{E}(z,t,\omega_l)}{\partial z} \right|.$$

Slowly-varying envelope approximation (SVEA): The envelope $\underline{E}(z,t,\omega_l)$ and $\underline{P}(z,t,\omega_l)$ vary much “slower” with z and t than the respective carrier wave.

⇒ First-order DEq for describing **evolution of the envelope $\underline{E}(z,t,\omega_l)$:**

$$\frac{\partial \underline{E}(z,t,\omega_l)}{\partial z} + \frac{n}{c} \frac{\partial \underline{E}(z,t,\omega_l)}{\partial t} = -j \frac{\omega_l}{2\epsilon_0 c n} \underline{P}_{\text{NL}}(z,t,\omega_l) e^{-j(k_{p,l} - k_l)z}.$$

Lecture 4

Nonlinear wave equation

⇒ Wave equation for **inhomogeneous nonlinear media**:

$$\nabla \times \nabla \times \mathbf{E}(\mathbf{r}, t) + \mu_0 \epsilon_0 \epsilon_r \frac{\partial^2 \mathbf{E}(\mathbf{r}, t)}{\partial t^2} = -\mu_0 \frac{\partial^2 \mathbf{P}_{\text{NL}}(\mathbf{r}, t)}{\partial t^2}$$

Simplification for **isotropic homogeneous nonlinear media**:

$$\nabla^2 \mathbf{E}(\mathbf{r}, t) - \frac{n^2}{c^2} \frac{\partial^2 \mathbf{E}(\mathbf{r}, t)}{\partial t^2} = \mu_0 \frac{\partial^2 \mathbf{P}_{\text{NL}}(\mathbf{r}, t)}{\partial t^2}.$$

Simplifying assumptions:

- **Linearly polarized, “plane-wave-like” fields** (Without loss of generality: Polarization along x, propagation along z)
⇒ Represent by scalar field quantities $E(z, t)$ and $P(z, t)$
- Polarization **responds instantaneously** to applied electric field (“memory-less material”)
⇒ Expand nonlinear time-domain relationship between P and E into a **power series** of scalar quantities:

$$\begin{aligned} P(z, t) &= \epsilon_0 \chi^{(1)} E(z, t) + \epsilon_0 \chi^{(2)} E^2(z, t) + \epsilon_0 \chi^{(3)} E^3(z, t) + \dots \\ &= P_L(z, t) + P_{\text{NL}}(z, t) \end{aligned}$$

$$P_L(z, t) = \epsilon_0 \chi^{(1)} E(z, t)$$

$$P_{\text{NL}}(z, t) = \epsilon_0 \chi^{(2)} E^2(z, t) + \epsilon_0 \chi^{(3)} E^3(z, t) + \dots$$

Representation of nonlinear polarization

Example: Second-order nonlinear polarization

Assume **superposition of two monochromatic plane waves**, oscillating with frequency ω_1 and ω_2 :

$$E(z, t) = \frac{1}{2} (\underline{E}(\omega_1) \exp(j(\omega_1 t - k_1 z)) + \underline{E}(\omega_2) \exp(j(\omega_2 t - k_2 z)) + \text{c.c.}).$$

⇒ The **second-order nonlinear polarization** contains components at all sum and difference frequencies:

$$P_{\text{NL}}(z, t) = \frac{1}{4} \epsilon_0 \chi^{(2)} \left(\underline{E}_1^2 e^{j2(\omega_1 t - k_1 z)} + \text{c.c.} \right. \\ \left. + \underline{E}_2^2 e^{j2(\omega_2 t - k_2 z)} + \text{c.c.} \right. \\ \left. + 2 |\underline{E}_1|^2 + 2 |\underline{E}_2|^2 \right. \\ \left. + 2 \underline{E}_1 \underline{E}_2 e^{j((\omega_1 + \omega_2)t - (k_1 + k_2)z)} + \text{c.c.} \right. \\ \left. + 2 \underline{E}_1 \underline{E}_2^* e^{j((\omega_1 - \omega_2)t - (k_1 - k_2)z)} + \text{c.c.} \right)$$

}

Second-harmonic generation (SHG)

}

Optical rectification (OR)

}

Sum and difference frequency generation (SFG, DFG)

Note: The individual expressions of the second-order polarization exhibit plane wave-like space and time dependences. However, the wavenumbers differ from that of a plane electromagnetic wave at the same frequency, $k(\omega_1) + k(\omega_2) \neq k(\omega_1 + \omega_2)$.

Solution of nonlinear wave equation: Slowly-varying envelope approximation (SVEA)

Solution ansatz:

- Represent electric field $E(z,t)$ and nonlinear polarization $P_{\text{NL}}(z,t)$ as a superposition of plane-wave-like fields, oscillating at different frequencies ω_l
- Introduce (weakly) **time- and space-dependent amplitudes** to account for nonlinear interaction

$$E(z,t) = \frac{1}{2} \left(\sum_l \underline{E}(z,t,\omega_l) \exp(j(\omega_l t - k_l z)) + \text{c.c.} \right)$$

Complex conjugate of preceding expression.

$$P_{\text{NL}}(z,t) = \frac{1}{2} \left(\sum_l \underline{P}_{\text{NL}}(z,t,\omega_l) \exp(j(\omega_l t - k_{p,l} z)) + \text{c.c.} \right)$$

where

$$\left| \frac{\partial^2 \underline{E}(z,t,\omega_l)}{\partial t^2} \right| \ll \omega_l \left| \frac{\partial \underline{E}(z,t,\omega_l)}{\partial t} \right|,$$

$$\left| \frac{\partial^2 \underline{E}(z,t,\omega_l)}{\partial z^2} \right| \ll k_l \left| \frac{\partial \underline{E}(z,t,\omega_l)}{\partial z} \right|.$$

Slowly-varying envelope approximation (SVEA): The envelope $\underline{E}(z,t,\omega_l)$ and $\underline{P}(z,t,\omega_l)$ vary much “slower” with z and t than the respective carrier wave.

⇒ First-order DEq for describing **evolution of the envelope $\underline{E}(z,t,\omega)$:**

$$\frac{\partial \underline{E}(z,t,\omega_l)}{\partial z} + \frac{n}{c} \frac{\partial \underline{E}(z,t,\omega_l)}{\partial t} = -j \frac{\omega_l}{2\epsilon_0 c n} \underline{P}_{\text{NL}}(z,t,\omega_l) e^{-j(k_{p,l} - k_l)z}.$$

Retarded time frame

Use a **retarded time frame** to represent electric field and nonlinear polarization:

$$t' = t - \frac{nz}{c},$$
$$z' = z,$$
$$\underline{E}(z, t, \omega_l) = \underline{E}'(z, t - \frac{nz}{c}, \omega_l).$$

⇒ **First-order DEq:**

$$\frac{\partial \underline{E}'(z', t', \omega_l)}{\partial z'} = -j \frac{\omega_l}{2\epsilon_0 cn} \underline{P}'_{NL}(z', t', \omega_l) e^{-j(k_{p,l} - k_l)z'}.$$

- Nonlinear polarization $\underline{P}'_{NL}(z', t', \omega_l)$ acts as a **source for new frequency components**
- Depending of the **relative phase** between $\underline{P}'_{NL}(z', t', \omega_l)$ and $\underline{E}'(z', t', \omega_l)$, the nonlinear polarization can cause **amplification, absorption or phase shifts**.
- Efficient nonlinear interaction requires proper **phase matching**, $k_{p,l} - k_l \approx 0$

⇒ **SPM/XPM**

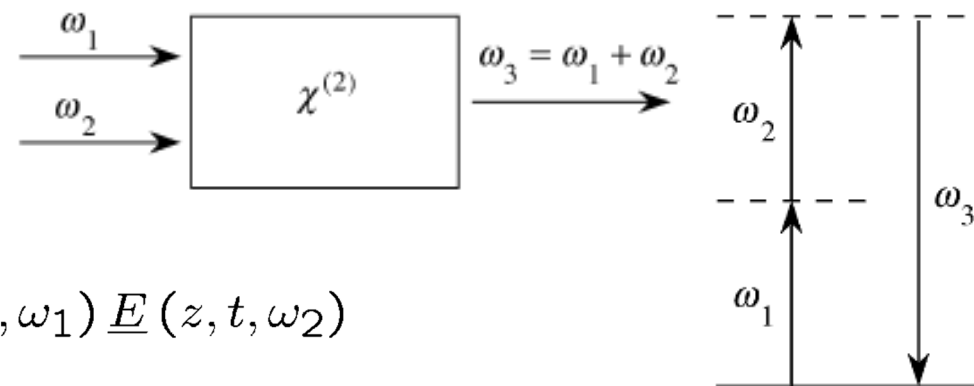
Second-order nonlinear processes

Recall: Frequency components of second-order nonlinear polarization for superposition of two monochromatic waves with frequencies ω_1 and ω_2 :

$$P_{\text{NL}}(z, t) = \frac{1}{4} \epsilon_0 \chi^{(2)} \left(\underline{E}_1^2 e^{j2(\omega_1 t - k_1 z)} + \underline{E}_2^2 e^{j2(\omega_2 t - k_2 z)} + 2|\underline{E}_1|^2 + 2|\underline{E}_2|^2 + 2\underline{E}_1 \underline{E}_2 e^{j((\omega_1 + \omega_2)t - (k_1 + k_2)z)} + 2\underline{E}_1 \underline{E}_2^* e^{j((\omega_1 - \omega_2)t - (k_1 - k_2)z)} + \text{c.c.} \right)$$

Sum-frequency generation (SFG):

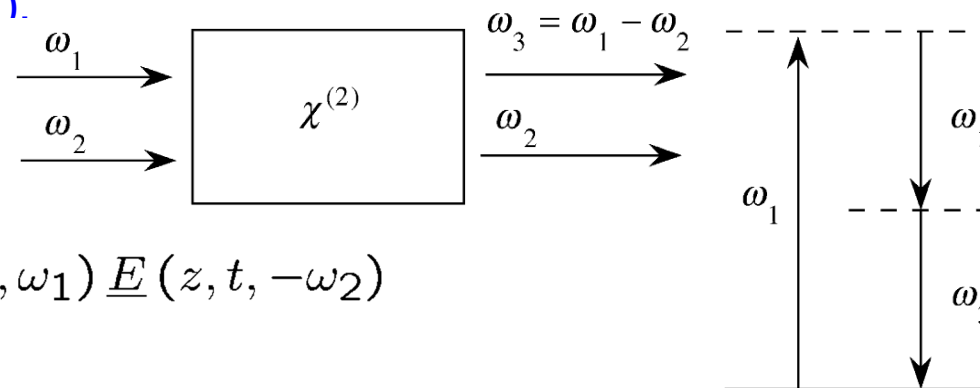
$$\omega_p = \omega_1 + \omega_2, k_p = k_1 + k_2$$



$$\underline{P}_{\text{NL}}(z, t, \omega_1 + \omega_2) = \epsilon_0 \chi^{(2)} \underline{E}(z, t, \omega_1) \underline{E}(z, t, \omega_2)$$

Difference-frequency generation (DFG):

$$\omega_p = \omega_1 - \omega_2, k_p = k_1 - k_2$$

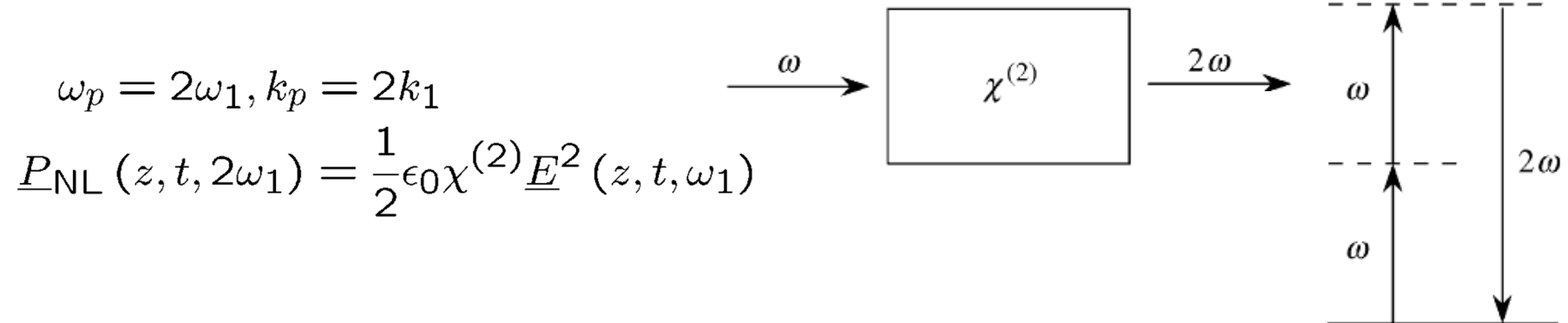


$$\underline{P}_{\text{NL}}(z, t, \omega_1 - \omega_2) = \epsilon_0 \chi^{(2)} \underline{E}(z, t, \omega_1) \underline{E}(z, t, -\omega_2)$$

Figures adapted from Boyd, Nonlinear Optics

Second-order nonlinear processes

Second-harmonic generation (SHG):



Optical rectification (OR):

$$\omega_p = 0, k_p = 0$$
$$P_{\text{NL}}(z, t, 0) = \frac{1}{2}\epsilon_0\chi^{(2)}\underline{E}(z, t, \omega_1)\underline{E}(z, t, -\omega_1)$$

Frequency components at $\omega = 0$
need special consideration (will be
explained later!)

Figures adapted from Boyd, Nonlinear Optics

Third-order nonlinear processes

Consider a superposition of three plane oscillating at frequencies ω_1 , ω_2 and ω_3 :

$$E(z, t) = \frac{1}{2} \left(\underline{E}_1 e^{j(\omega_1 t - k_1 z)} + \underline{E}_2 e^{j(\omega_2 t - k_2 z)} + \underline{E}_3 e^{j(\omega_3 t - k_3 z)} + \text{c.c.} \right),$$

$$\Rightarrow P_{\text{NL}}(z, t) = \frac{1}{2} \epsilon_0 \chi^{(3)} \left(\underbrace{\frac{1}{4} \underline{E}_1^3 e^{j(3\omega_1 t - 3k_1 z)} + \dots + \text{c.c.}}_{\text{THG}} \right. \\ \left. + \underbrace{\frac{3}{4} \underline{E}_1^2 \underline{E}_2 e^{j((2\omega_1 + \omega_2)t - (2k_1 + k_2)z)} + \dots + \text{c.c.}}_{\text{degenerate FWM}} \right. \\ \left. + \underbrace{\frac{6}{4} \underline{E}_1 \underline{E}_2 \underline{E}_3 e^{j((\omega_1 + \omega_2 + \omega_3)t - (k_1 + k_2 + k_3)z)} + \text{c.c.}}_{\text{non-degenerate FWM}} \right. \\ \left. + \underbrace{\frac{3}{4} |\underline{E}_1|^2 \underline{E}_1 e^{j(\omega_1 t - k_1 z)} + \dots + \text{c.c.}}_{\text{SPM}} \right. \\ \left. + \underbrace{\frac{6}{4} |\underline{E}_2|^2 \underline{E}_1 e^{j(\omega_1 t - k_1 z)} + \dots + \text{c.c.}}_{\text{XPM}} \right. \\ \left. + \underbrace{\frac{3}{4} \underline{E}_1^2 \underline{E}_2^* e^{j((2\omega_1 - \omega_2)t - (2k_1 - k_2)z)} + \dots + \text{c.c.}}_{\text{degenerate FWM}} \right. \\ \left. + \underbrace{\frac{6}{4} \underline{E}_1 \underline{E}_2 \underline{E}_3^* e^{j((\omega_1 + \omega_2 - \omega_3)t - (k_1 + k_2 - k_3)z)} + \dots + \text{c.c.}}_{\text{non-degenerate FWM}} \right).$$

Third-harmonic generation (THG)

Four-wave mixing (FWM)

Self-phase modulation (SPM)

Cross-phase modulation (XPM)

Four-wave mixing (FWM)

Summary of third-order nonlinear processes

Process	Abbreviation	Involved frequencies	Degeneracy factor D
Third-harmonic generation	THG	$(+\omega_1, +\omega_1, +\omega_1)$	1
Self-phase modulation	SPM	$(+\omega_1, -\omega_1, +\omega_1)$	3
Cross-phase modulation	XPM	$(+\omega_2, -\omega_2, +\omega_1)$	6
Non-degenerate four-wave mixing	(non-degenerate) FWM	$(+\omega_1, +\omega_2, +\omega_3)$	6
		$(+\omega_1, +\omega_2, -\omega_3)$	6
Degenerate four-wave mixing	(degenerate) FWM	$(+\omega_1, +\omega_1, +\omega_2)$	3
		$(+\omega_1, +\omega_1, -\omega_2)$	3

Note: Degeneracy factor D corresponds to the number of distinct permutations of the triple set of involved frequencies

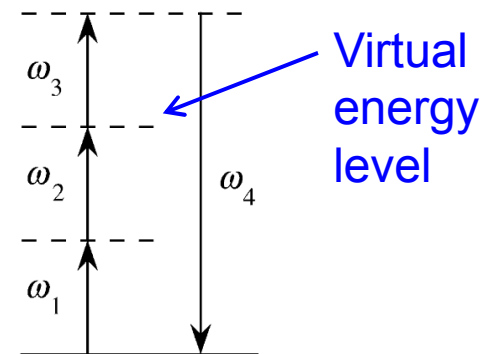
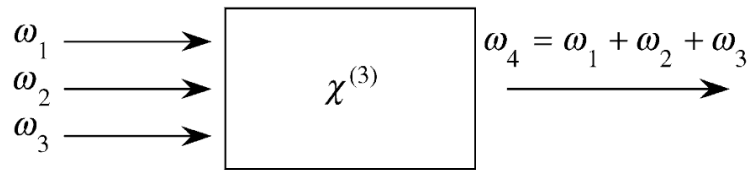
Third-order nonlinearities: Nondegenerate FWM

Generation of one new photon (third-order sum frequency generation):

$$\omega_p = \omega_1 + \omega_2 + \omega_3, \quad k_p = k_1 + k_2 + k_3$$

$$P_{\text{FWM}}(z, t, \omega_p = \omega_1 + \omega_2 + \omega_3) = \frac{6}{4} \epsilon_0 \chi^{(3)} \underline{E}(z, t, \omega_1) \underline{E}(z, t, \omega_2) \underline{E}(z, t, \omega_3).$$

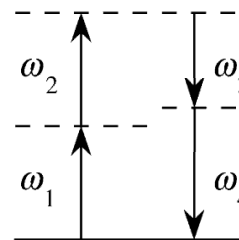
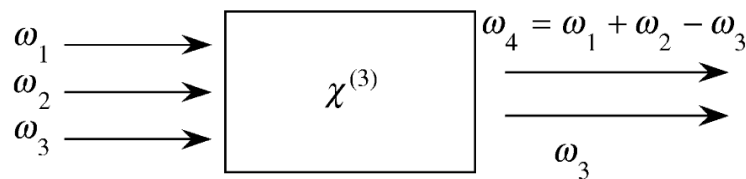
(a)



Generation of two new photons:

$$\omega_p = \omega_1 + \omega_2 - \omega_3, \quad k_p = k_1 + k_2 - k_3$$

$$P_{\text{FWM}}(z, t, \omega_p = \omega_1 + \omega_2 - \omega_3) = \frac{6}{4} \epsilon_0 \chi^{(3)} \underline{E}(z, t, \omega_1) \underline{E}(z, t, \omega_2) \underline{E}^*(z, t, \omega_3)$$



Figures adapted from
Boyd, Nonlinear Optics

Third-order nonlinearities: Degenerate FWM

Generation of one new photon (third-order sum frequency generation):

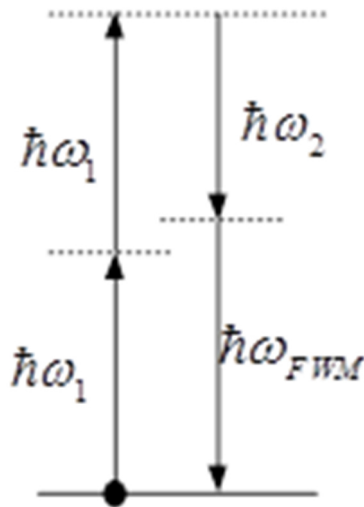
$$\omega_p = 2\omega_1 + \omega_2, \quad k_p = 2k_1 + k_2$$

$$\underline{P}_{\text{FWM}}(z, t, \omega_p = 2\omega_1 + \omega_2) = \frac{3}{4}\epsilon_0\chi^{(3)}\underline{E}^2(z, t, \omega_1)\underline{E}(z, t, \omega_2).$$

Generation of two new photons:

$$\omega_p = 2\omega_1 - \omega_2, \quad k_p = 2k_1 - k_2$$

$$\underline{P}_{\text{FWM}}(z, t, \omega_p = 2\omega_1 - \omega_2) = \frac{3}{4}\epsilon_0\chi^{(3)}\underline{E}^2(z, t, \omega_1)\underline{E}^*(z, t, \omega_2)$$

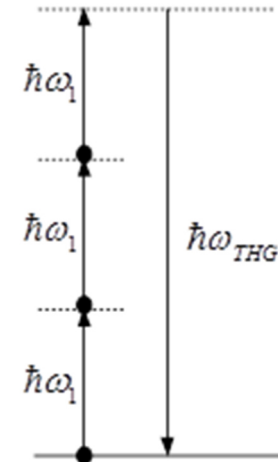


Third-order nonlinearities: THG, XPM, and SPM

Third-harmonic generation (THG):

$$\omega_p = 3\omega_1, k_p = 3k_1$$

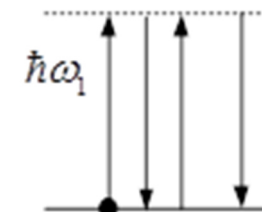
$$\underline{P}_{\text{THG}}(z, t, 3\omega_1) = \frac{1}{4}\epsilon_0\chi^{(3)}\underline{E}^3(z, t, \omega_1)$$



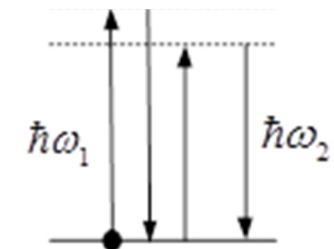
Cross-phase modulation (XPM) and self-phase modulation (SPM)

$$\omega_p = \omega_1, k_p = k_1$$

$$\underline{P}_{\text{SPM}}(z, t, \omega_1) = \frac{3}{4}\epsilon_0\chi^{(3)}|\underline{E}(z, t, \omega_1)|^2\underline{E}(z, t, \omega_1) \quad \text{SPM}$$

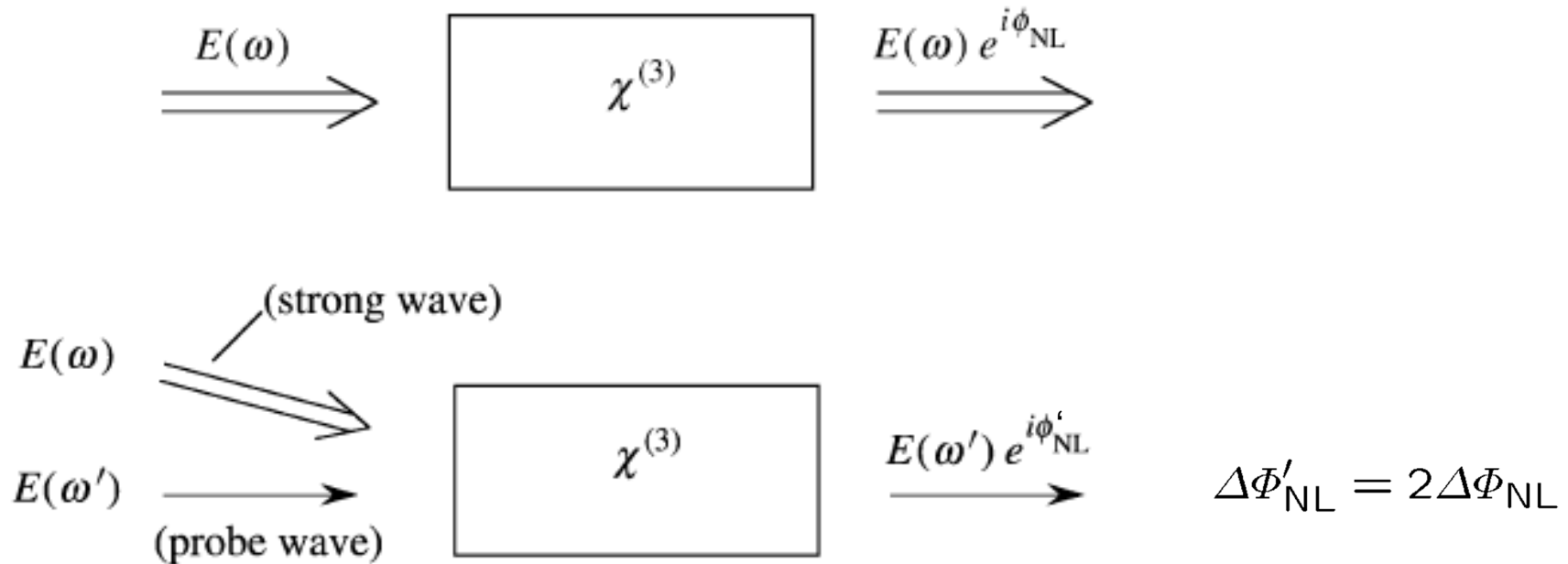


$$\underline{P}_{\text{XPM}}(z, t, \omega_1) = \frac{6}{4}\epsilon_0\chi^{(3)}|\underline{E}(z, t, \omega_2)|^2\underline{E}(z, t, \omega_1) \quad \text{XPM}$$



⇒ [Nonlinear wave equation](#)

Example: SPM and XPM



The intensity-dependent refractive index leads to modulation of a light beam by itself (SPM) or by another beam of light (XPM). For the same intensity of the modulating beam, the effect of XPM is twice as large as SPM!

Figure adapted from
Boyd, Nonlinear Optics

Kerr effect and intensity-dependent refractive index

Consider a **single monochromatic wave at frequency ω_1** in a third-order nonlinear medium
 \Rightarrow **SPM is the dominant nonlinear effect!**

$$\frac{\partial \underline{E}(z, t, \omega_1)}{\partial z} = -j \frac{3\omega_1 \chi^{(3)}}{8cn(\omega_1)} |\underline{E}(z, t, \omega_1)|^2 \underline{E}(z, t, \omega_1)$$

\Rightarrow SPM causes a **negative phase shift that is proportional to the square of the field magnitude, i.e., proportional to the intensity**. This can be interpreted as an **intensity-dependent refractive index**.

$$n(z, t, \omega_1) = n_0(\omega_1) + n_2 I(z, t, \omega_1)$$

where $n_2 = \frac{3Z_0}{4n_0^2} \chi^{(3)}$. **Kerr coefficient**

Note: For a superposition of two waves oscillating at frequencies ω_1 and ω_2 , the refractive index seen by wave 1 will also be influenced by **cross-phase modulation (XPM)** due to wave 2. Note that **XPM has twice the degeneracy factor of SPM**.

$$n(z, t, \omega_1) = n_0(\omega_1) + n_2 (I(z, t, \omega_1) + 2I(z, t, \omega_2)).$$

Third-order nonlinear coefficients of various materials

Material	n_0	$\chi^{(3)}$ (m^2/V^2)	n_2 (cm^2/W)
<i>Crystals</i>			
Al ₂ O ₃	1.8	3.1×10^{-22}	2.9×10^{-16}
CdS	2.34	9.8×10^{-20}	5.1×10^{-14}
Diamond	2.42	2.5×10^{-21}	1.3×10^{-15}
GaAs	3.47	1.4×10^{-18}	3.3×10^{-13}
Ge	4.0	5.6×10^{-19}	9.9×10^{-14}
LiF	1.4	6.2×10^{-23}	9.0×10^{-17}
Si	3.4	2.8×10^{-18}	2.7×10^{-14}
TiO ₂	2.48	2.1×10^{-20}	9.4×10^{-15}
ZnSe	2.7	6.2×10^{-20}	3.0×10^{-14}
<i>Glasses</i>			
Fused silica	1.47	2.5×10^{-22}	3.2×10^{-16}
As ₂ S ₃ glass	2.4	4.1×10^{-19}	2.0×10^{-13}
BK-7	1.52	2.8×10^{-22}	3.4×10^{-16}
BSC	1.51	5.0×10^{-22}	6.4×10^{-16}
Pb Bi gallate	2.3	2.2×10^{-20}	1.3×10^{-14}
SF-55	1.73	2.1×10^{-21}	2.0×10^{-15}
SF-59	1.953	4.3×10^{-21}	3.3×10^{-15}
<i>Nanoparticles</i>			
CdSSe in glass	1.5	1.4×10^{-20}	1.8×10^{-14}
CS 3-68 glass	1.5	1.8×10^{-16}	2.3×10^{-10}
Gold in glass	1.5	2.1×10^{-16}	2.6×10^{-10}
<i>Polymers</i>			
<i>Polydiacetylenes</i>			
PTS		8.4×10^{-18}	3.0×10^{-12}
PTS		-5.6×10^{-16}	-2.0×10^{-10}
9BCMU			2.7×10^{-18}
4BCMU	1.56	-1.3×10^{-19}	-1.5×10^{-13}

Material	n_0	$\chi^{(3)}$ (m^2/V^2)	n_2 (cm^2/W)
<i>Liquids</i>			
Acetone	1.36	1.5×10^{-21}	2.4×10^{-15}
Benzene	1.5	9.5×10^{-22}	1.2×10^{-15}
Carbon disulfide	1.63	3.1×10^{-20}	3.2×10^{-14}
CCl ₄	1.45	1.1×10^{-21}	1.5×10^{-15}
Diiodomethane	1.69	1.5×10^{-20}	1.5×10^{-14}
Ethanol	1.36	5.0×10^{-22}	7.7×10^{-16}
Methanol	1.33	4.3×10^{-22}	6.9×10^{-16}
Nitrobenzene	1.56	5.7×10^{-20}	6.7×10^{-14}
Water	1.33	2.5×10^{-22}	4.1×10^{-16}
<i>Other materials</i>			
Air	1.0003	1.7×10^{-25}	5.0×10^{-19}
Ag		2.8×10^{-19}	
Au		7.6×10^{-19}	

^a This table assumes the definition of the third-order susceptibility $\chi^{(3)}$ used in this book, as given for instance by Eq. (1.1.2) or by Eq. (1.3.21). This definition is consistent with that introduced by Bloembergen (1964). Some workers use an alternative definition which renders their values four times smaller. In compiling this table we have converted the literature values when necessary to the present definition.

The quantity n_2 is the coefficient of the intensity-dependent refractive index which is defined such that $n = n_0 + n_2 I$, where n_0 is the linear refractive index and I is the laser intensity. The relation between n_2 and $\chi^{(3)}$ is consequently $n_2 = 12\pi^2 \chi^{(3)} / n_0^2$. When the intensity is measured in W/cm^2 and $\chi^{(3)}$ is measured in electrostatic units (esu), that is, in $\text{cm}^2 \text{statvolt}^{-2}$, the relation between n_2 and $\chi^{(3)}$ becomes $n_2 (\text{cm}^2/\text{W}) = 0.0395 \chi^{(3)} (\text{esu}) / n_0^2$. The quantity β is the coefficient describing two-photon absorption.

Note: Even though Boyd uses a different definition for complex electric field amplitudes, the values for $\chi^{(3)}$ and n_2 are consistent with the definitions used in this lecture. Adapted from Boyd, Nonlinear Optics

Lecture 5

Retarded time frame

Use a **retarded time frame** to represent electric field and nonlinear polarization:

$$t' = t - \frac{nz}{c},$$
$$z' = z,$$
$$\underline{E}(z, t, \omega_l) = \underline{E}'(z, t - \frac{nz}{c}, \omega_l).$$

⇒ **First-order DEq:**

$$\frac{\partial \underline{E}'(z', t', \omega_l)}{\partial z'} = -j \frac{\omega_l}{2\epsilon_0 cn} \underline{P}'_{NL}(z', t', \omega_l) e^{-j(k_{p,l} - k_l)z'}.$$

- Nonlinear polarization $\underline{P}'_{NL}(z', t', \omega_l)$ acts as a **source for new frequency components**
- Depending of the **relative phase** between $\underline{P}'_{NL}(z', t', \omega_l)$ and $\underline{E}'(z', t', \omega_l)$, the nonlinear polarization can cause **amplification, absorption or phase shifts**.
- Efficient nonlinear interaction requires proper **phase matching**, $k_{p,l} - k_l \approx 0$

⇒ **SPM/XPM**

Kerr effect and intensity-dependent refractive index

Consider a **single monochromatic wave at frequency ω_1** in a third-order medium
 \Rightarrow **SPM is the dominant nonlinear effect!**

$$\frac{\partial \underline{E}(z, t, \omega_1)}{\partial z} = -j \frac{3\omega_1 \chi^{(3)}}{8cn(\omega_1)} |\underline{E}(z, t, \omega_1)|^2 \underline{E}(z, t, \omega_1)$$

\Rightarrow SPM causes a **negative phase shift that is proportional to the square of the field magnitude, i.e., proportional to the intensity**. This can be interpreted as an **intensity-dependent refractive index**.

$$n(z, t, \omega_1) = n_0(\omega_1) + n_2 I(z, t, \omega_1)$$

$$\text{where } n_2 = \frac{3Z_0}{4n_0^2} \chi^{(3)}. \quad \text{Kerr coefficient}$$

Note: For a superposition of two waves oscillating at frequencies ω_1 and ω_2 , the refractive index seen by wave 1 will also be influenced by **cross-phase modulation (XPM)** due to wave 2. Note that **XPM has twice the degeneracy factor of SPM**.

$$n(z, t, \omega_1) = n_0(\omega_1) + n_2 (I(z, t, \omega_1) + 2I(z, t, \omega_2)).$$

Parametric processes:

- Quantum state of the material remains unchanged
- No transfer of energy, momentum, or angular momentum between the optical field and the material => **Momentum and energy conservation:**

$$\sum_i \omega_i = \sum_f \omega_f, \quad \sum_i k_i = \sum_f k_f,$$

- Given by **real part of complex susceptibility**
- **Note:** Quantum system can be removed from a real energy state only for brief time intervals Δt , in which it resides in a **so-called virtual energy level:**

$$\Delta t \Delta W < \hbar$$

⇒ Ultra-fast response!

- **Examples:** SFG, SHG, DFG, THG, SPM, XPM, FWM

Nonparametric processes:

- **Transfer** of a quantum system from one real level to another
- Sum of photon energies is **not conserved**
- Given by **imaginary part of complex susceptibility**
- **Examples:** Two-photon absorption (TPA)

Two-photon absorption

Recall: Relations for cross-phase modulation (XPM) and self-phase modulation (SPM)
 Here: Consider case of complex nonlinear susceptibility $\chi^{(3)}$

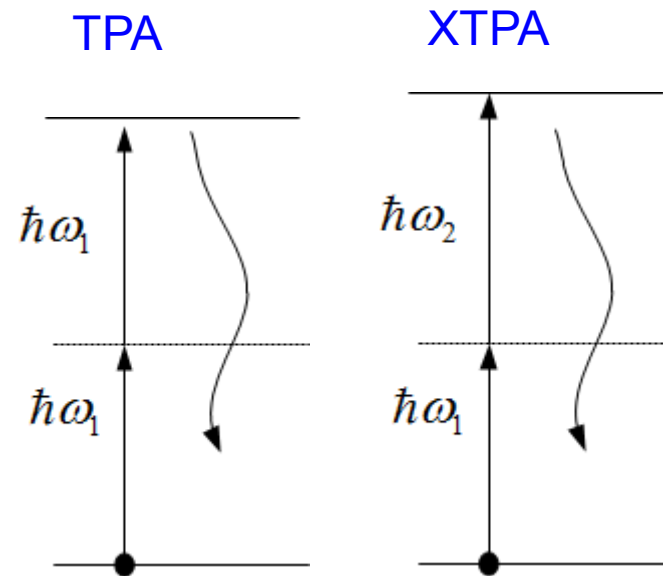
$$\frac{\partial \underline{E}(z, t, \omega_1)}{\partial z} = -j \frac{3\omega_l}{8cn} \chi^{(3)} |\underline{E}(z, t, \omega_1)|^2 \underline{E}(z, t, \omega_1),$$

$$\frac{\partial \underline{E}(z, t, \omega_1)}{\partial z} = -j \frac{3\omega_l}{4cn} \chi^{(3)} |\underline{E}(z, t, \omega_2)|^2 \underline{E}(z, t, \omega_1).$$

⇒ Imaginary part of $\chi^{(3)}$ leads to change of amplitude

⇒ Two-photon absorption (TPA) and cross-two-photon absorption (XTPA)

$$\frac{\partial I(\omega_1)}{\partial z} \propto \chi_i^{(3)} (I^2(\omega_1) + 2I(\omega_1)I(\omega_2))$$



So far: Time-domain treatment of special case of nonlinear polarization

- Instantaneous response of the nonlinear polarization with respect to the E-field
- Linearly polarized fields that are represented by scalar field quantities

⇒ Taylor series in the time domain:

$$P(z, t) = \epsilon_0 \chi^{(1)} E(z, t) + \epsilon_0 \chi^{(2)} E^2(z, t) + \epsilon_0 \chi^{(3)} E^3(z, t) + \dots$$

Now: General case

- Non-instantaneous response of the optical field (nonlinear material with memory)
⇒ Volterra series in the time domain
- Vectorial field quantities
⇒ Volterra kernel of the n -th order nonlinear susceptibility is represented as a tensor of rank $n+1$

$$P_{q_0}^{(n)}(t) = \epsilon_0 \sum_{q_1, \dots, q_n} \int_{-\infty}^{+\infty} \dots \int_{-\infty}^{+\infty} \chi_{q_0:q_1q_2\dots q_n}^{(n)}(\tau_1, \dots, \tau_n) E_{q_1}(t - \tau_1) \dots E_{q_n}(t - \tau_n) d\tau_1 \dots d\tau_n.$$

$q_0, q_1, \dots, q_n \in \{x, y, z\}$ denote the various vectorial components of the electric field, the polarization, and the corresponding elements of the susceptibility tensor.

Short-form tensor notation

Replace sum over tensor elements and vectorial components by a short-form notation

Second-order nonlinear susceptibility:

$$P_q^{(2)}(t) = \epsilon_0 \sum_{r,s} \iint_{\tau_1, \tau_2} \chi_{q:r,s}^{(2)}(\tau_1, \tau_2) E_r(t - \tau_1) E_s(t - \tau_2) d\tau_1 d\tau_2,$$

$$\mathbf{P}^{(2)}(t) = \epsilon_0 \iint_{\tau_1, \tau_2} \chi^{(2)}(\tau_1, \tau_2) : \mathbf{E}(t - \tau_1) \mathbf{E}(t - \tau_2) d\tau_1 d\tau_2,$$

where $\chi^{(2)} : \mathbf{E}\mathbf{E} = \sum_{q,r,s} e_q \chi_{q:r,s}^{(2)} E_r E_s,$

Short-form notation of tensor product contains summation over all vector components and tensor elements

General case:

$$\underline{\chi}^{(n)} : \mathbf{E}(\tau_1) \mathbf{E}(\tau_2) \dots \mathbf{E}(\tau_n) = \sum_{q_0, q_1, \dots, q_n} e_{q_0} \chi_{q_0:q_1 q_2 \dots q_n}^{(n)} E_{q_1}(\tau_1) E_{q_2}(\tau_2) \dots E_{q_n}(\tau_n)$$

where $q_0, q_1, \dots, q_n \in \{x, y, z\}$

Consider simplified case of second-order nonlinearity:

$$P_q^{(2)}(t) = \epsilon_0 \sum_{r,s} \iint_{\tau_1, \tau_2} \chi_{q:r,s}^{(2)}(\tau_1, \tau_2) E_r(t - \tau_1) E_s(t - \tau_2) d\tau_1 d\tau_2,$$

$$\tilde{P}_q^{(2)}(\omega) = \frac{1}{2\pi} \epsilon_0 \sum_{r,s} \int_{\omega_1} \tilde{\chi}_{q:r,s}^{(2)}(\omega_1, \omega - \omega_1) \tilde{E}_r(\omega_1) \tilde{E}_s(\omega - \omega_1) d\omega_1$$

where
$$\tilde{\chi}_{q:r,s}^{(2)}(\omega_1, \omega_2) = \iint_{\tau_1, \tau_2} \chi_{q:r,s}^{(2)}(\tau_1, \tau_2) e^{-j\omega_1\tau_1} e^{-j\omega_2\tau_2} d\tau_1 d\tau_2$$

General case:

$$\tilde{P}_{q_0}^{(n)}(\omega) = \frac{\epsilon_0}{(2\pi)^{n-1}} \sum_{q_1, \dots, q_n} \int_{-\infty}^{+\infty} \dots \int_{-\infty}^{+\infty} \tilde{\chi}_{q_0:q_1, \dots, q_n}^{(n)} \left(\omega : \omega_1, \dots, \omega_{n-1}, \omega - \sum_{m=1}^{n-1} \omega_m \right) \times \tilde{E}_{q_1}(\omega_1) \dots \tilde{E}_{q_{n-1}}(\omega_{n-1}) \tilde{E}_{q_n}(\omega - \sum_{m=1}^{n-1} \omega_m) d\omega_1 \dots d\omega_{n-1}$$

Summation over all vector components
Involved frequencies must sum up to ω

where

$$\tilde{\chi}_{q_0:q_1, q_2, \dots, q_n}^{(n)}(\sum_{m=1}^n \omega_m : \omega_1, \dots, \omega_n) = \int_{-\infty}^{+\infty} \dots \int_{-\infty}^{+\infty} \chi_{q_0:q_1, \dots, q_n}^{(n)}(\tau_1, \dots, \tau_n) e^{-j\omega_1\tau_1} \dots e^{-j\omega_n\tau_n} d\tau_1 \dots d\tau_n$$

Example: Second-order nonlinearities

$$\mathbf{P}^{(2)}(t) = \epsilon_0 \iint_{\tau_1, \tau_2} \chi^{(2)}(\tau_1, \tau_2) : \mathbf{E}(t - \tau_1) \mathbf{E}(t - \tau_2) d\tau_1 d\tau_2$$

$$\mathbf{E}(t) = \frac{1}{2} \sum_{m=-M}^M \underline{\mathbf{E}}(\omega_m) e^{j\omega_m t} \quad \text{where} \quad \omega_{-m} = -\omega_m, \quad \omega_0 = 0$$

$$\underline{\mathbf{E}}(\omega_{-m}) = \underline{\mathbf{E}}^*(\omega_m).$$

For now: No involvement of DC fields, $\underline{\mathbf{E}}(\omega_0) = 0$

$$\Rightarrow \mathbf{P}^{(2)}(t) = \frac{1}{4} \epsilon_0 \sum_{l, m} \tilde{\chi}^{(2)}(\omega_\Sigma : \omega_l, \omega_m) : \underline{\mathbf{E}}(\omega_l) \underline{\mathbf{E}}(\omega_m) e^{j(\omega_l + \omega_m)t}$$

Introduce complex time-domain amplitudes for nonlinear polarization:

$$\mathbf{P}^{(2)}(t) = \frac{1}{2} \sum_{p=-M}^M \underline{\mathbf{P}}^{(2)}(\omega_p) e^{j\omega_p t}$$

$$\Rightarrow \underline{\mathbf{P}}^{(2)}(\omega_p) = \frac{1}{2} \epsilon_0 \sum_{\mathcal{S}(\omega_p)} \underline{\chi}^{(2)}(\omega_p : \omega_l, \omega_m) : \underline{\mathbf{E}}(\omega_l) \underline{\mathbf{E}}(\omega_m)$$

where $\mathcal{S}(\omega_p) = \{(l, m) | \omega_l + \omega_m = \omega_p\}$

Third- and higher-order nonlinearities

Complex time-domain amplitude of third-order nonlinear polarization:

$$\underline{\mathbf{P}}^{(3)}(\omega_p) = \frac{1}{4}\epsilon_0 \sum_{\mathbb{S}(\omega_p)} \underline{\chi}^{(3)}(\omega_p : \omega_l, \omega_m, \omega_n) : \underline{\mathbf{E}}(\omega_l)\underline{\mathbf{E}}(\omega_m)\underline{\mathbf{E}}(\omega_n)$$

where $\mathbb{S}(\omega_p) = \{(l, m, n) | \omega_l + \omega_m + \omega_n = \omega_p\}$.

Complex time-domain amplitude of n -th nonlinear polarization:

$$\underline{\mathbf{P}}^{(n)}(\omega_p) = \frac{1}{2^{n-1}}\epsilon_0 \sum_{\mathbb{S}(\omega_p)} \underline{\chi}^{(n)}(\omega_p : \omega_{l_1}, \dots, \omega_{l_n}) : \underline{\mathbf{E}}(\omega_{l_1}) \dots \underline{\mathbf{E}}(\omega_{l_n}),$$

where $\mathbb{S}(\omega_p) = \{(l_1, \dots, l_n) | \omega_{l_1} + \dots + \omega_{l_n} = \omega_p\}$

Zero frequencies and DC fields...

Problem: Inconsistencies of time-domain representations with respect to zero frequencies $\omega_0 = 0$ and the associated DC fields

⇒ Use more rigorous definition of time-domain signals and complex amplitudes:

$$\begin{aligned} \underline{\mathbf{E}}(\mathbf{r}, t) &= \frac{1}{2} \left(\sum_{l=-N}^N (1 + \delta_{l,0}) \underline{\mathbf{E}}(\mathbf{r}, \omega_l) e^{j\omega_l t} \right) \\ \underline{\mathbf{P}}(\mathbf{r}, t) &= \frac{1}{2} \left(\sum_{l=-N}^N (1 + \delta_{l,0}) \underline{\mathbf{P}}(\mathbf{r}, \omega_l) e^{j\omega_l t} \right) \end{aligned} \quad \text{where} \quad \begin{aligned} \omega_{-l} &= -\omega_l, \\ \underline{\mathbf{E}}(\omega_{-l}) &= \underline{\mathbf{E}}^*(\omega_l), \\ \omega_0 &= 0, \\ \underline{\mathbf{E}}(\omega_0) &\in \mathbb{R}, \\ \delta_{l,0} &= \begin{cases} 1 & \text{for } l = 0 \\ 0 & \text{else} \end{cases} . \end{aligned}$$

Complex time-domain amplitude of n -th nonlinear polarization:

$$\underline{\mathbf{P}}^{(n)}(\omega_p) = \frac{1}{2^{n-1} \epsilon_0} \sum_{\mathbb{S}(\omega_p)} \frac{(1 + \delta_{l_1,0}) \dots (1 + \delta_{l_n,0})}{1 + \delta_{p,0}} \underline{\chi}^{(n)}(\omega_p : \omega_{l_1}, \dots, \omega_{l_n}) : \underline{\mathbf{E}}(\omega_{l_1}) \dots \underline{\mathbf{E}}(\omega_{l_n})$$

Examples:

Optical rectification (OR): $\underline{\mathbf{P}}^{(2)}(\omega_3 = 0) = \frac{1}{2} \epsilon_0 \underline{\chi}^{(2)}(0 : \omega_1, -\omega_1) : \underline{\mathbf{E}}(\omega_1) \underline{\mathbf{E}}^*(\omega_1)$

Electro-optic Kerr effect

(Quadratic electro-optic effect): $\underline{\mathbf{P}}^{(3)}(\omega_1) = 3 \epsilon_0 \underline{\chi}^{(3)}(\omega_1 : \omega_1, 0, 0) : \underline{\mathbf{E}}(\omega_1) \underline{\mathbf{E}}(0) \underline{\mathbf{E}}(0)$

Lecture 6

Zero frequencies and DC fields...

Problem: Inconsistencies of time-domain representations with respect to zero frequencies $\omega_0 = 0$ and the associated static (“DC”) fields

⇒ Use more rigorous definition of time-domain signals and complex amplitudes:

$$\begin{aligned} \underline{\mathbf{E}}(\mathbf{r}, t) &= \frac{1}{2} \left(\sum_{l=-N}^N (1 + \delta_{l,0}) \underline{\mathbf{E}}(\mathbf{r}, \omega_l) e^{j\omega_l t} \right) \\ \underline{\mathbf{P}}(\mathbf{r}, t) &= \frac{1}{2} \left(\sum_{l=-N}^N (1 + \delta_{l,0}) \underline{\mathbf{P}}(\mathbf{r}, \omega_l) e^{j\omega_l t} \right) \end{aligned} \quad \text{where} \quad \begin{aligned} \omega_{-l} &= -\omega_l, \\ \underline{\mathbf{E}}(\omega_{-l}) &= \underline{\mathbf{E}}^*(\omega_l), \\ \omega_0 &= 0, \\ \underline{\mathbf{E}}(\omega_0) &\in \mathbb{R}, \\ \delta_{l,0} &= \begin{cases} 1 & \text{for } l = 0 \\ 0 & \text{else} \end{cases} . \end{aligned}$$

Complex time-domain amplitude of n -th nonlinear polarization:

$$\underline{\mathbf{P}}^{(n)}(\omega_p) = \frac{1}{2^{n-1} \epsilon_0} \sum_{\mathbb{S}(\omega_p)} \frac{(1 + \delta_{l_1,0}) \dots (1 + \delta_{l_n,0})}{1 + \delta_{p,0}} \underline{\chi}^{(n)}(\omega_p : \omega_{l_1}, \dots, \omega_{l_n}) : \underline{\mathbf{E}}(\omega_{l_1}) \dots \underline{\mathbf{E}}(\omega_{l_n})$$

Examples:

Optical rectification (OR): $\underline{\mathbf{P}}^{(2)}(\omega_3 = 0) = \frac{1}{2} \epsilon_0 \underline{\chi}^{(2)}(0 : \omega_1, -\omega_1) : \underline{\mathbf{E}}(\omega_1) \underline{\mathbf{E}}^*(\omega_1)$

Electro-optic Kerr effect

(Quadratic electro-optic effect): $\underline{\mathbf{P}}^{(3)}(\omega_1) = 3 \epsilon_0 \underline{\chi}^{(3)}(\omega_1 : \omega_1, 0, 0) : \underline{\mathbf{E}}(\omega_1) \underline{\mathbf{E}}(0) \underline{\mathbf{E}}(0)$

- **Causality:**

$$\chi_{q_0:q_1q_2\dots q_n}^{(n)}(\tau_1, \tau_2, \dots, \tau_n) = 0 \quad \text{for} \quad \tau_1 < 0 \vee \tau_2 < 0 \dots \vee \tau_n < 0.$$

⇒ Frequency-domain relationships (Kramers-Kronig relations) exist for some nonlinear optical processes, but not for all!

- **Reality of fields:** Electromagnetic field quantities must be represented by real numbers in the time domain!

⇒ Positive- and negative-frequency components of the complex susceptibility tensor are the complex conjugate of each other:

$$\underline{\mathbf{E}}(\omega_l) = \underline{\mathbf{E}}^*(-\omega_l) \quad \underline{\mathbf{P}}(\omega_l) = \underline{\mathbf{P}}^*(-\omega_l)$$

$$\underline{\chi}_{q_0:q_1q_2\dots q_n}^{(n)}(\omega_\Sigma : \omega_1, \omega_2, \dots, \omega_n) = \left[\underline{\chi}_{q_0:q_1q_2\dots q_n}^{(n)}(-\omega_\Sigma : -\omega_1, -\omega_2, \dots, -\omega_n) \right]^*$$

- **Intrinsic permutation symmetry:**

Nonlinear susceptibility tensor element remains unchanged if frequency arguments $\omega_1 \dots \omega_n$ (not: ω_Σ) and corresponding Cartesian indices are swapped simultaneously

$$\underline{\chi}_{q_0:q_1\dots q_iq_j\dots q_n}^{(n)}(\omega_\Sigma : \omega_1, \dots, \omega_i, \omega_j, \dots, \omega_n) = \underline{\chi}_{q_0:q_n\dots q_jq_i\dots q_1}^{(n)}(\omega_\Sigma : \omega_n, \dots, \omega_j, \omega_i, \dots, \omega_1)$$

- **Symmetries for lossless media:**

All components of the nonlinear susceptibility tensor are real:

$$\underline{\chi}_{q_0:q_1\dots q_i q_j\dots q_n}^{(n)}(\omega_\Sigma : \omega_1, \dots, \omega_i, \omega_j, \dots, \omega_n) \in \mathbb{R}$$

Permutation symmetry holds also for the resulting frequency ω_Σ

Note: Signs must be changed appropriately when interchanging the first argument with any other argument.

$$\tilde{\chi}_{q_0:q_1\dots q_i\dots q_n}^{(n)}(\omega_\Sigma : \omega_1, \dots, \omega_i, \dots, \omega_n) = \tilde{\chi}_{q_i:q_1\dots q_0\dots q_n}^{(n)}(\omega_i : -\omega_1, \dots, \omega_\Sigma, \dots, -\omega_n)$$

- **Kleinman's symmetry:**

Operated at frequencies far below their lowest resonance frequency

⇒ The medium is lossless and the nonlinear susceptibility is essentially independent of frequency.

⇒ The frequency arguments can be permuted without permuting the indices:

$$\underline{\chi}_{q_0:q_1\dots q_i q_j\dots q_n}^{(n)}(\omega_\Sigma : \omega_1, \dots, \omega_i, \omega_j, \dots, \omega_n) = \underline{\chi}_{q_0:q_1\dots q_i q_j\dots q_n}^{(n)}(\omega_\Sigma : \omega_1, \dots, \omega_j, \omega_i, \dots, \omega_n)$$

Assumption: Kleinman symmetry applies, i.e., frequency arguments can be permuted without permuting the corresponding vector indices.

⇒ Exploit permutability of last two frequency arguments to introduce **contracted notation**:

$$\underline{\chi}_{q:r,s}^{(2)} \mapsto d_{ql} = \frac{1}{2} \underline{\chi}_{q:r,s}^{(2)} \quad \begin{matrix} rs & xx & yy & zz & yz, zy & xz, zx & xy, yx \\ l & 1 & 2 & 3 & 4 & 5 & 6 \end{matrix}$$

Represent nonlinear susceptibility tensor as a (3×6) – matrix:

$$\mathbf{d} = \begin{pmatrix} d_{x1} & d_{x2} & d_{x3} & d_{x4} & d_{x5} & d_{x6} \\ d_{y1} & d_{y2} & d_{y3} & d_{y4} & d_{y5} & d_{y6} \\ d_{z1} & d_{z2} & d_{z3} & d_{z4} & d_{z5} & d_{z6} \end{pmatrix}$$

Exploitation of full Kleinman symmetry: Only 10 independent elements

$$\mathbf{d} = \begin{pmatrix} d_{x1} & d_{x2} & d_{x3} & d_{x4} & d_{x5} & d_{x6} \\ d_{x6} & d_{y2} & d_{y3} & d_{y4} & d_{x4} & d_{x2} \\ d_{x5} & d_{y4} & d_{z3} & d_{y3} & d_{x3} & d_{x4} \end{pmatrix}$$

Second-harmonic generation (SHG):

$$\begin{pmatrix} \underline{P}_x^{(2)}(2\omega_1) \\ \underline{P}_y^{(2)}(2\omega_1) \\ \underline{P}_z^{(2)}(2\omega_1) \end{pmatrix} = \epsilon_0 \begin{pmatrix} d_{x1} & d_{x2} & d_{x3} & d_{x4} & d_{x5} & d_{x6} \\ d_{x6} & d_{y2} & d_{y3} & d_{y4} & d_{x4} & d_{x2} \\ d_{x5} & d_{y4} & d_{z3} & d_{y3} & d_{x3} & d_{x4} \end{pmatrix} \begin{pmatrix} \underline{E}_x^2(\omega_1) \\ \underline{E}_y^2(\omega_1) \\ \underline{E}_z^2(\omega_1) \\ 2\underline{E}_y(\omega_1)\underline{E}_z(\omega_1) \\ 2\underline{E}_x(\omega_1)\underline{E}_z(\omega_1) \\ 2\underline{E}_x(\omega_1)\underline{E}_y(\omega_1) \end{pmatrix}$$

Sum-frequency generation (SFG):

$$\begin{pmatrix} \underline{P}_x^{(2)}(\omega_3) \\ \underline{P}_y^{(2)}(\omega_3) \\ \underline{P}_z^{(2)}(\omega_3) \end{pmatrix} = 2\epsilon_0 \begin{pmatrix} d_{x1} & d_{x2} & d_{x3} & d_{x4} & d_{x5} & d_{x6} \\ d_{x6} & d_{y2} & d_{y3} & d_{y4} & d_{x4} & d_{x2} \\ d_{x5} & d_{y4} & d_{z3} & d_{y3} & d_{x3} & d_{x4} \end{pmatrix} \begin{pmatrix} \underline{E}_x(\omega_1)\underline{E}_x(\omega_2) \\ \underline{E}_y(\omega_1)\underline{E}_y(\omega_2) \\ \underline{E}_z(\omega_1)\underline{E}_z(\omega_2) \\ \underline{E}_y(\omega_1)\underline{E}_z(\omega_2) + \underline{E}_z(\omega_1)\underline{E}_y(\omega_2) \\ \underline{E}_x(\omega_1)\underline{E}_z(\omega_2) + \underline{E}_z(\omega_1)\underline{E}_x(\omega_2) \\ \underline{E}_x(\omega_1)\underline{E}_y(\omega_2) + \underline{E}_y(\omega_1)\underline{E}_x(\omega_2) \end{pmatrix}$$

Exploitation of spatial symmetries

Neumann's principle: If a crystal is invariant with respect to certain geometric transformations, any of its physical properties must also be invariant with respect to the same transformations.

⇒ Investigate influence of spatial symmetries on susceptibility tensor

Idea:

- Consider coordinate transformation from a coordinate system (x,y,z) to a coordinate system (x',y',z') that leaves the crystal lattice unchanged
- Since this does not change the physical situation, the tensor elements must be invariant under this coordinate transformation.

Einstein notation: Comprises summation over all unpaired subscripts on the right-hand side.

Coordinate transformation:

$$\begin{pmatrix} E'_{x'} \\ E'_{y'} \\ E'_{z'} \end{pmatrix} = \begin{pmatrix} T_{x'x} & T_{x'y} & T_{x'z} \\ T_{y'x} & T_{y'y} & T_{y'z} \\ T_{z'x} & T_{z'y} & T_{z'z} \end{pmatrix} \begin{pmatrix} E_x \\ E_y \\ E_z \end{pmatrix} \quad E'_{q'} = T_{q'q} E_q$$

For orthogonal transformations (reflection, inversion, rotation):

$$\mathbf{T}^{-1} = \mathbf{T}^T \quad (T^{-1})_{qq'} = T_{q'q}$$

$$\Rightarrow \chi_{q'_0:q'_1\dots q'_n}^{(n)} = T_{q'_0q_0} T_{q'_1q_1} \cdots T_{q'_nq_n} \chi_{q_0:q_1\dots q_n}^{(n)}$$

i.e., susceptibility tensor of rank (n+1) transforms like (n+1)-fold product of coordinates

Centro-symmetric media are invariant with respect to an inversion of coordinates:

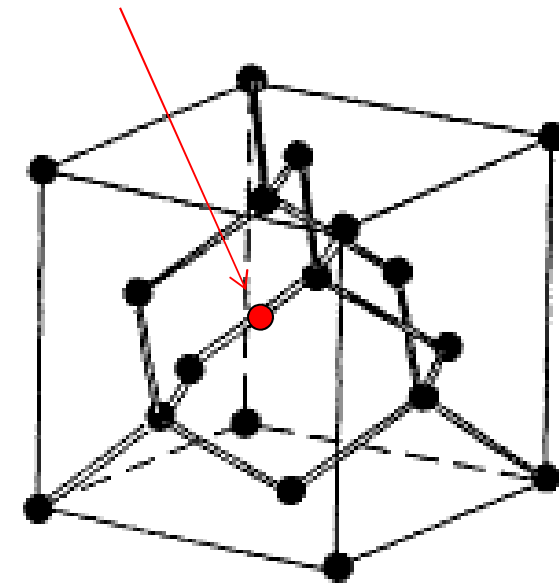
$$T_{q'q} = -\delta_{q'q}$$

$$\Rightarrow \chi_{q_0:q_1\dots q_n}^{(n)} = (-1)^{n+1} \chi_{q_0:q_1\dots q_n}^{(n)}$$

i.e., for even orders n all susceptibility tensor elements must vanish. **Centro-symmetric media do not exhibit any second-order (even-order) nonlinearity!**

Note: The same applies to amorphous materials with randomly oriented molecules that do not feature any preferential direction. Even though the microscopic structure of the material is not centro-symmetric, the macroscopic structural properties are defined as an average over random orientations of molecules and do hence not change upon inversion of coordinates.

Inversion point: Mid-point of nearest-neighbour bonds!



Example: Diamond lattice (e.g., silicon); features inversion symmetry.

Needed: Coordinate transformations with respect to which the crystal lattice remains unchanged

⇒ Categorization of crystals by their symmetry properties:

- 32 crystal classes, characterized by 32 point groups
- 5 cubic point groups, 27 non-cubic point groups
- Point group: Set of symmetry operations that leave the crystal lattice unchanged
- Nomenclature of point groups by Schoenflies notation or international notation

Figure adapted from Ashcroft/ Mermin, Solid State Physics

5 cubic crystallographic point groups

Schoenflies notation

(O = octahedral symmetry group, i.e., rotation axes of an octahedron or cube)

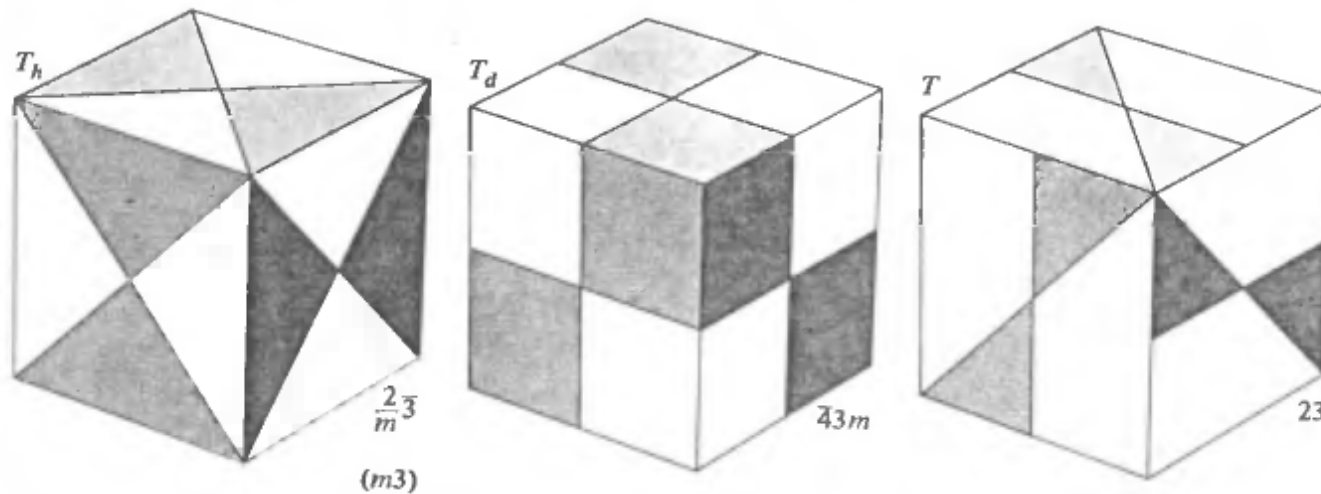
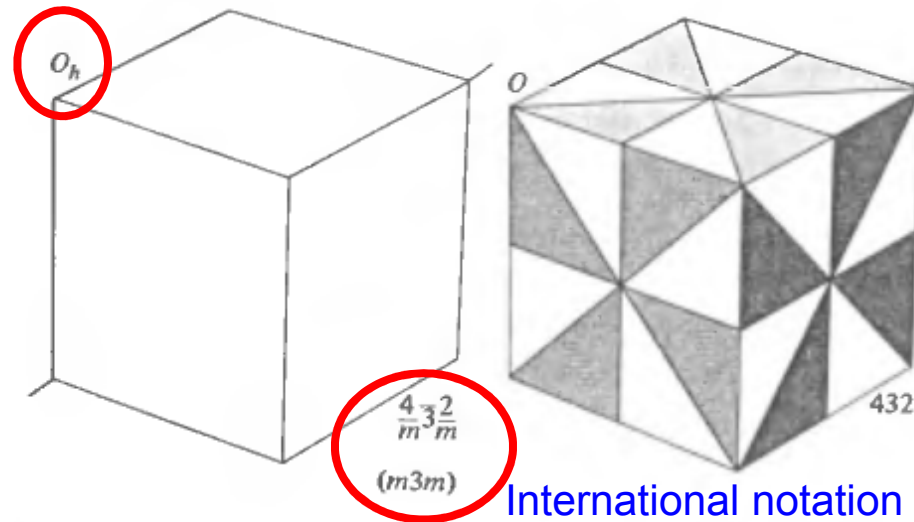


Figure adapted from Ashcroft/ Mermin, Solid State Physics

Lecture 7

Exploitation of spatial symmetries

Neumann's principle: If a crystal is invariant with respect to certain geometric transformations, any of its physical properties must also be invariant with respect to the same transformations.

⇒ Investigate influence of spatial symmetries on susceptibility tensor

Idea:

- Consider coordinate transformation from a coordinate system (x,y,z) to a coordinate system (x',y',z') that leaves the crystal lattice unchanged
- Since this does not change the physical situation, the tensor elements must be invariant under this coordinate transformation.

Einstein notation: Comprises summation over all unpaired subscripts on the right-hand side.

Coordinate transformation:

$$\begin{pmatrix} E'_{x'} \\ E'_{y'} \\ E'_{z'} \end{pmatrix} = \begin{pmatrix} T_{x'x} & T_{x'y} & T_{x'z} \\ T_{y'x} & T_{y'y} & T_{y'z} \\ T_{z'x} & T_{z'y} & T_{z'z} \end{pmatrix} \begin{pmatrix} E_x \\ E_y \\ E_z \end{pmatrix} \quad E'_{q'} = T_{q'q} E_q$$

For orthogonal transformations (reflection, inversion, rotation):

$$\mathbf{T}^{-1} = \mathbf{T}^T \quad (T^{-1})_{qq'} = T_{q'q}$$

$$\Rightarrow \chi_{q'_0:q'_1\dots q'_n}^{(n)} = T_{q'_0q_0} T_{q'_1q_1} \cdots T_{q'_nq_n} \chi_{q_0:q_1\dots q_n}^{(n)}$$

i.e., susceptibility tensor of rank (n+1) transforms like (n+1)-fold product of coordinates

Centro-symmetric media are invariant with respect to an inversion of coordinates:

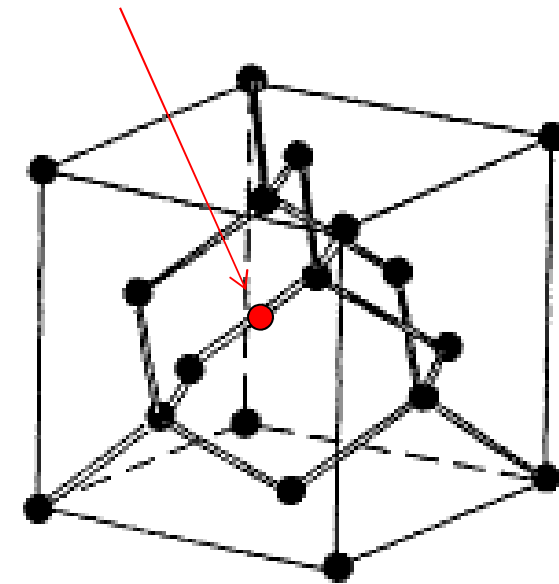
$$T_{q'q} = -\delta_{q'q}$$

$$\Rightarrow \chi_{q_0:q_1\dots q_n}^{(n)} = (-1)^{n+1} \chi_{q_0:q_1\dots q_n}^{(n)}$$

i.e., for even orders n all susceptibility tensor elements must vanish. **Centro-symmetric media do not exhibit any second-order (even-order) nonlinearity!**

Note: The same applies to amorphous materials with randomly oriented molecules without preferential direction. Even though the microscopic structure of the material is not centro-symmetric, the macroscopic structural properties are defined as an average over random orientations of molecules and do hence not change upon inversion of coordinates.

Inversion point: Mid-point of nearest-neighbour bonds!



Example: Diamond lattice (e.g., silicon); features inversion symmetry.

Needed: Coordinate transformations with respect to which the crystal lattice remains unchanged

⇒ Categorization of crystals by their symmetry properties:

- 32 crystal classes, characterized by 32 point groups
- 5 cubic point groups, 27 non-cubic point groups
- Point group: Set of symmetry operations that leave the crystal lattice unchanged
- Nomenclature of point groups by Schoenflies notation or international notation

Figure adapted from Ashcroft/ Mermin, Solid State Physics

5 cubic crystallographic point groups

Schoenflies notation

(O = octahedral symmetry group, i.e., rotation axes of an octahedron or cube)

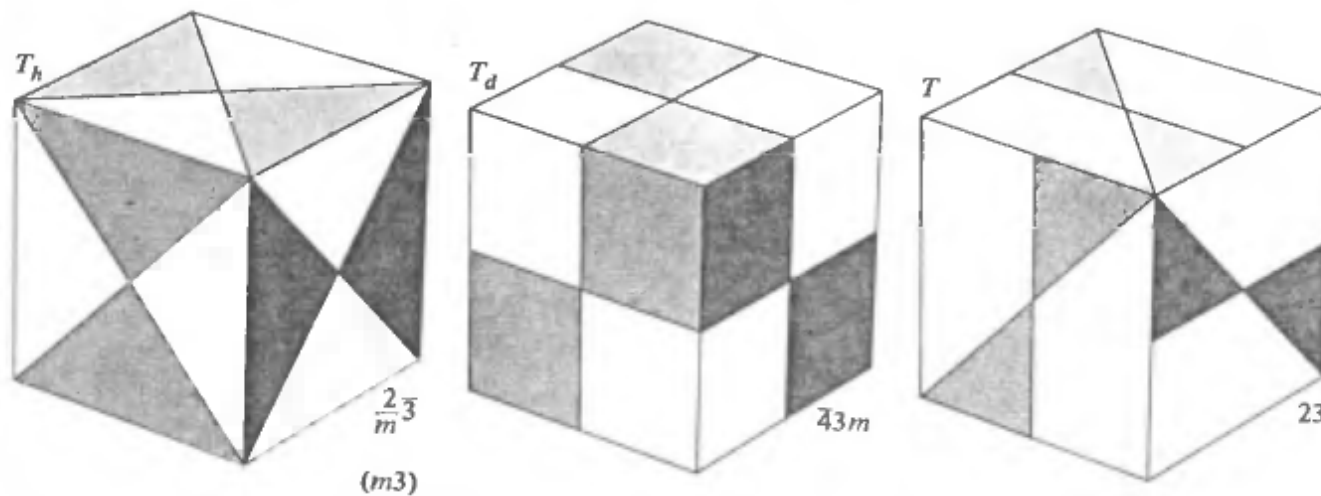
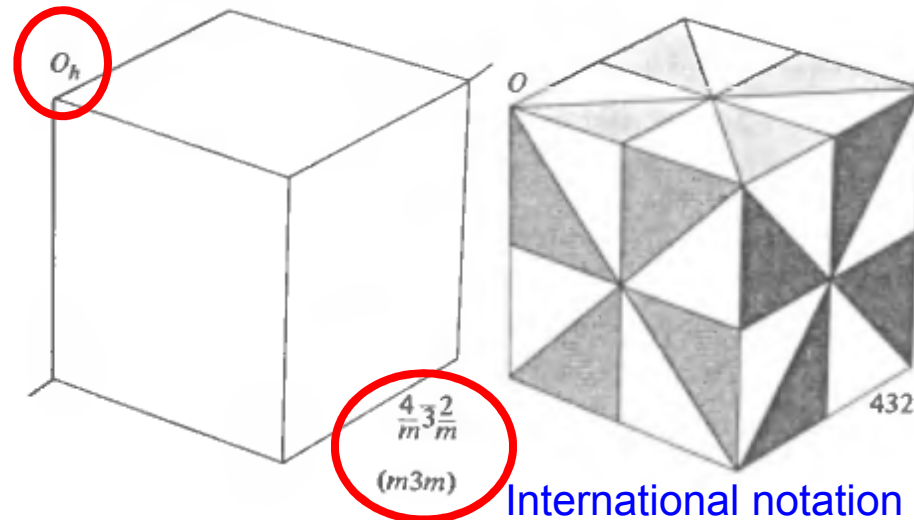


Figure adapted from Ashcroft/ Mermin, Solid State Physics

27 noncubic crystallographic point groups

Schoenflies	Hexagonal	Tetragonal	Trigonal	Orthorhombic	Monoclinic	Triclinic	International
C_n	C_6  6	C_4  4	C_3  3		C_2  2	C_1  1	n
C_{nv}	C_{6v}  6 mm	C_{4v}  4 mm	C_{3v}  3 m	C_{2v}  2 mm			
C_{nh}	C_{6h}  6/ m	C_{4h}  4/ m			C_{2h}  2/ m		n/m
	C_{3h}  $\bar{6}$				C_{1h} ($\bar{2}$)  m		\bar{n}
S_n		S_4  4	S_6  (C_{3i}) 3			S_2  (C_i) 1	

Schoenflies	Hexagonal	Tetragonal	Trigonal	Orthorhombic	Monoclinic	Triclinic	International
D_n	D_6  622	D_4  422	D_3  32	D_2  (V) 222			$n22$ (n even) $n2$ (n odd)
D_{nh}	D_{6h}  6/ mmm	D_{4h}  4/ mmm		D_{2h} (mmm)  (V_h) 2/ mmm			$\frac{n}{m} \frac{2}{m} \frac{2}{m}$ (n/mmm)
	D_{3h}  $\bar{6}2m$						$\bar{n}2m$ (n even)
D_{nd}		D_{2d}  (V_d) 422	D_{2d} ($\bar{3}m$)  $\bar{3} \frac{2}{m}$				$\bar{n} \frac{2}{m}$ (n odd)

Schoenflies notation:

C_n : n -fold rotation axis

C_{nh} : n -fold rotation axis + horizontal mirror plane

C_{nv} : n -fold rotation axis + n vertical mirror planes

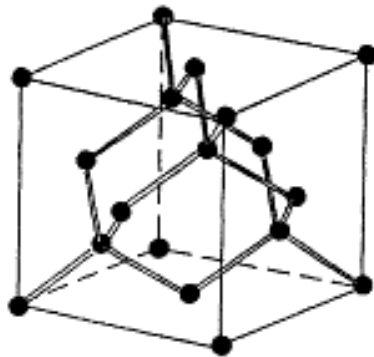
S_{2n} : $2n$ -fold rotation-reflection axis

... => see Ashcroft Mermin for more information!

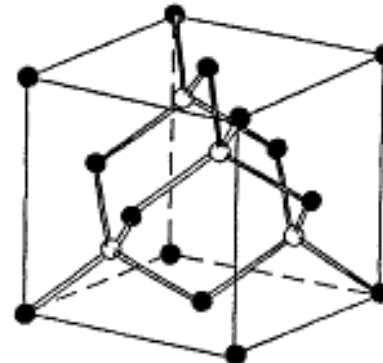
Figure adapted from Ashcroft/ Mermin, Solid State Physics

Second-order susceptibility for the 32 crystal classes

Crystal System	Crystal Class	Nonvanishing Tensor Elements	Crystal System	Crystal Class	Nonvanishing Tensor Elements
Triclinic	$1 = C_1$	All elements are independent and nonzero	Cubic	$432 = O$	$xyz = -xzy = yzx = -yxz = zxy = -zyx$
	$\bar{1} = S_2$	Each element vanishes		$\bar{4}3m = T_d$	$xyz = xzy = yzx = yxz = zxy = zyx$
Monoclinic	$2 = C_2$	$xyz, xzy, xxy, xyx, yxx, yyy, yzz, yzx, yxz, zyz, zzy, zxy, zyx$ (twofold axis parallel to \hat{y})		$23 = T$	$xyz = yzx = zxy, xzy = yxz = zyx$
	$m = C_{1h}$	$xxx, xyy, xzz, xzx, xxz, yyz, yzy, yxy, yyx, zxx, zyy, zzz, zzx, zxz$ (mirror plane perpendicular to \hat{y})	$m\bar{3} = T_h, m\bar{3}m = O_h$	Each element vanishes	
	$2/m = C_{2h}$	Each element vanishes	Trigonal	$3 = C_3$	$xxx = -xyy = -yyz = -yxy, xyz = -yxz, xzy = xzx = yzy, xxz = yyz, yyy = -yxx = -xxy = -zxx = zyy, zzz, zxy = -zyx$
Orthorhombic	$222 = D_2$	$xyz, xzy, yzx, yxz, zxy, zyx$		$32 = D_3$	$xxx = -xyy = -yyx = -yxy, xyz = -yxz, xzy = -yzx, zxy = -zyx$
	$mm2 = C_{2v}$	$xzx, xxz, yyz, yzy, zxx, zyy, zzz$		$3m = C_{3v}$	$xzx = yzy, xxz = yyz, zxx = zyy, zzz, yyy = -yxx = -xxy = -xyx$ (mirror plane perpendicular to \hat{x})
	$mmm = D_{2h}$	Each element vanishes	$\bar{3} = S_6, \bar{3}m = D_{3d}$	Each element vanishes	
Tetragonal	$4 = C_4$	$xyz = -yxz, xzy = -yzx, xzx = yzy, xxz = yyz, zxx = zyy, zzz, zxy = -zyx$	Hexagonal	$6 = C_6$	$xyz = -yxz, xzy = -yzx, xzx = yzy, xxz = yyz, zxx = zyy, zzz, zxy = -zyx$
	$\bar{4} = S_4$	$xyz = yxz, xzy = yzx, xzx = -yzy, xxz = -yyz, zxx = -zyy, zxy = zyx$		$\bar{6} = C_{3h}$	$xxx = -xyy = -yxy = -yyx, yyy = -yxx = -xxy = -xyx$
	$422 = D_4$	$xyz = -yxz, xzy = -yzx, zxy = -zyx$		$622 = D_6$	$xyz = -yxz, xzy = -yzx, zxy = -zyx$
	$4mm = C_{4v}$	$xzx = yzy, xxz = yyz, zxx = zyy, zzz$		$6mm = C_{6v}$	$xzx = yzy, xxz = yyz, zxx = zyy, zzz$
	$\bar{4}2m = D_{2d}$	$xyz = yxz, xzy = yzx, zxy = zyx$		$\bar{6}m2 = D_{3h}$	$yyy = -yxx = -xxy = -xyx$
	$4/m = C_{4h}$	Each element vanishes		$6/m = C_{6h}$	Each element vanishes
$4/mmm = D_{4h}$	Each element vanishes	$6/mmm = D_{6h}$	Each element vanishes		



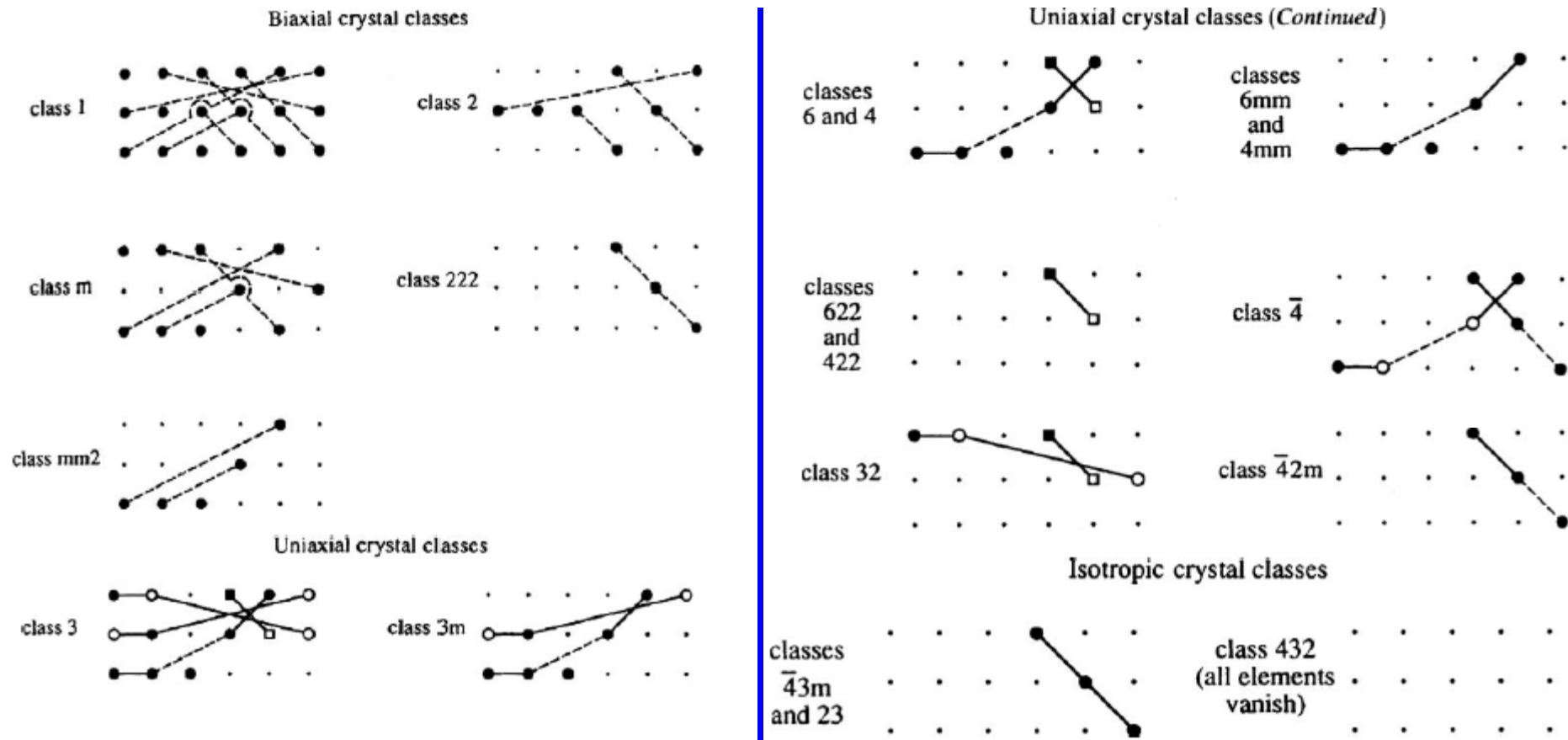
Diamond structure, e.g., Si
 $m\bar{3} = O_h$
 \Rightarrow All second-order elements vanish!



Zincblende structure, e.g., GaAs
 $\bar{4}3m$
 \Rightarrow 6 nonzero elements, which are all identical,
 $xyz = xzy = yzx = yxz = zxy = zyx$

Figures adapted from Boyd, Nonlinear Optics

Second-order susceptibility in contracted notation



Explanation:

- Small dot: Zero coefficient; large dot: Nonzero coefficient
- Square: Coefficient is zero if Kleinman symmetry applies
- Connected symbols: Numerically equal coefficients; open-symbol coefficients are opposite in sign with respect to the connected closed-symbol coefficient.
- Dashed connections: Valid only for the case of Kleinman symmetry

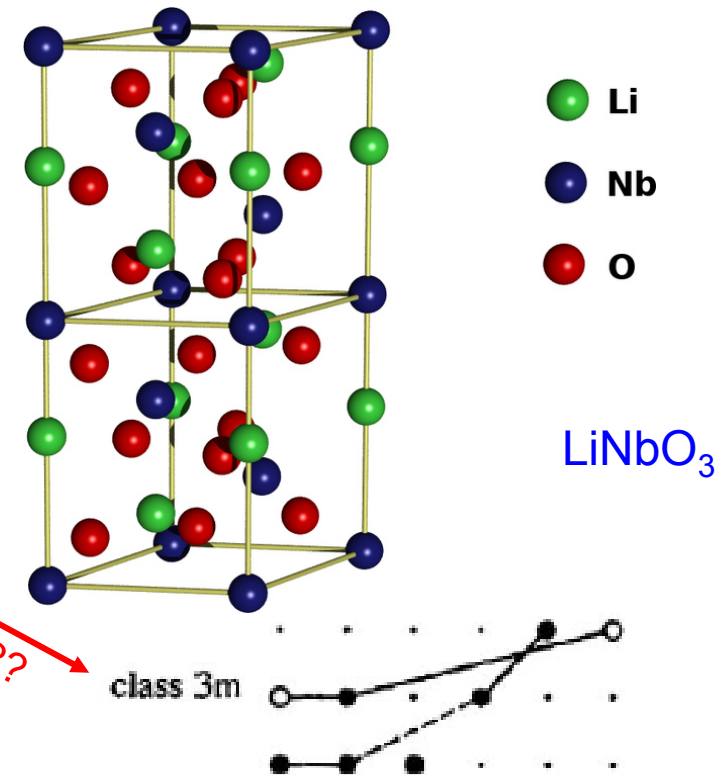
Figure adapted from Boyd, Nonlinear Optics

Second-order nonlinear susceptibilities for several crystals

Material	Point Group	d_{ij} (pm/V)
Ag ₃ AsS ₃ (proustite)	$3m = C_{3v}$	$d_{22} = 18$ $d_{15} = 11$
AgGaSe ₂	$\bar{4}2m = D_{2d}$	$d_{36} = 33$
AgSbS ₃ (pyrargyrite)	$3m = C_{3v}$	$d_{15} = 8$ $d_{22} = 9$
beta-BaB ₂ O ₄ (BBO) (beta barium borate)	$3m = C_{3v}$	$d_{22} = 2.2$
CdGeAs ₂	$\bar{4}2m = D_{2d}$	$d_{36} = 235$
CdS	$6mm = C_{6v}$	$d_{33} = 78$ $d_{31} = -40$
GaAs	$\bar{4}3m$	$d_{36} = 370$
KH ₂ PO ₄ (KDP)	$2m$	$d_{36} = 0.43$
KD ₂ PO ₄ (KD*P)	$2m$	$d_{36} = 0.42$
LiIO ₃	$6 = C_6$	$d_{15} = -5.5$ $d_{31} = -7$
LiNbO ₃	$3m = C_{3v}$	$d_{32} = -30$ $d_{31} = -5.9$
Quartz	$32 = D_3$	$d_{11} = 0.3$ $d_{14} = 0.008$

Watch out for

- unspecified wavelengths...
- typos...



Notes: Values are obtained from a variety of sources. Some of the more complete tabulations are those of R.L. Sutherland (1996), that of A.V. Smith, and the data sheets of Cleveland Crystals, Inc.

To convert to the gaussian system, multiply each entry by $(3 \times 10^{-8})/4\pi = 2.386 \times 10^{-9}$ to obtain d in esu units of cm/statvolt.

In any system of units, $\chi^{(2)} = 2d$ by convention.

Figures adapted from Boyd, Nonlinear Optics

Other values from the literature:
 $d_{22} \approx 3\text{pm/V}$; $d_{31} \approx -5\text{ pm/V}$; $d_{33} \approx -25\text{ pm/V}$

Third-order susceptibility tensor for various crystal classes

Isotropic

There are 21 nonzero elements, of which only 3 are independent. They are:

$$\begin{aligned} \chi_{yyzz} &= \chi_{zzyy} = \chi_{zzxx} = \chi_{xxzz} = \chi_{xxyy} = \chi_{yyxx}, \\ \chi_{yzzy} &= \chi_{zyzy} = \chi_{zxzx} = \chi_{zxzx} = \chi_{xyxy} = \chi_{yxyx}, \\ \chi_{zzzy} &= \chi_{yyyz} = \chi_{xxzx} = \chi_{zzzx} = \chi_{xyyx} = \chi_{xyyx}; \end{aligned}$$

and

$$\chi_{xxxx} = \chi_{yyyy} = \chi_{zzzz} = \chi_{xxyy} + \chi_{xyxy} + \chi_{yyxx}.$$

Cubic

For the two classes 23 and $m\bar{3}$, there are 21 nonzero elements, of which only 7 are independent. They are:

$$\begin{aligned} \chi_{xxxx} &= \chi_{yyyy} = \chi_{zzzz}, \\ \chi_{yyzz} &= \chi_{zzxx} = \chi_{xxyy}, \\ \chi_{zzyy} &= \chi_{xxzz} = \chi_{yyxx}, \\ \chi_{yzzy} &= \chi_{zxzx} = \chi_{xyxy}, \\ \chi_{zyzy} &= \chi_{zxzx} = \chi_{xyxy}, \\ \chi_{zzzy} &= \chi_{xxzx} = \chi_{xyyx}, \\ \chi_{yyyz} &= \chi_{xxzx} = \chi_{xyyx}. \end{aligned}$$

For the three classes 432 , $\bar{4}3m$, and $m\bar{3}m$, there are 21 nonzero elements, of which only 4 are independent. They are:

$$\begin{aligned} \chi_{xxxx} &= \chi_{yyyy} = \chi_{zzzz}, \\ \chi_{yyzz} &= \chi_{zzyy} = \chi_{zzxx} = \chi_{xxzz} = \chi_{xxyy} = \chi_{yyxx}, \\ \chi_{yzzy} &= \chi_{zyzy} = \chi_{zxzx} = \chi_{zxzx} = \chi_{xyxy} = \chi_{yxxy}, \\ \chi_{zzzy} &= \chi_{yyyz} = \chi_{xxzx} = \chi_{zzzx} = \chi_{xyyx} = \chi_{xyyx}. \end{aligned}$$

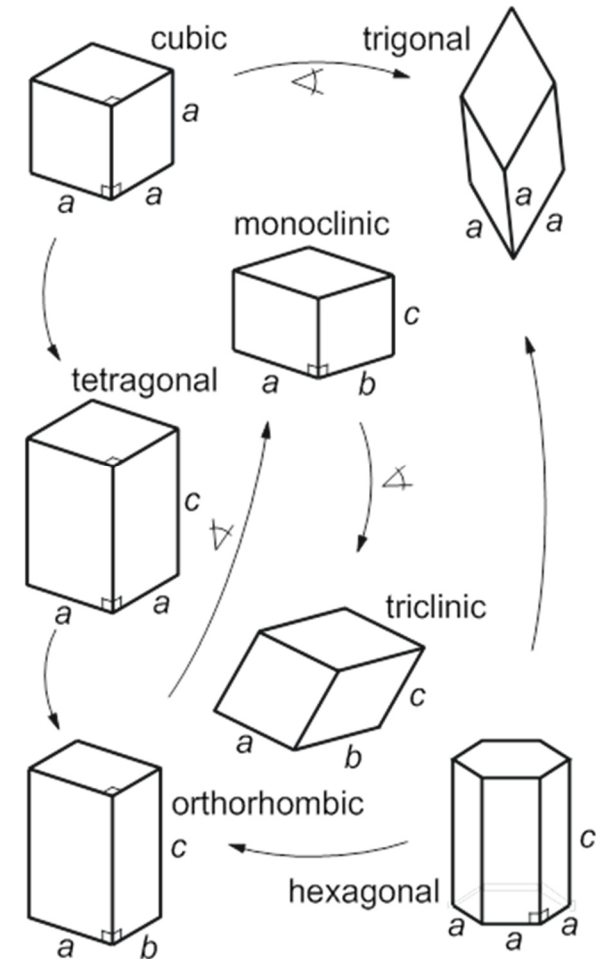


Figure adapted from Boyd, Nonlinear Optics

Third-order susceptibility tensor for various crystal classes

Hexagonal

For the three classes 6 , $\bar{6}$, and $6/m$, there are 41 nonzero elements, of which only 19 are independent.

They are:

$$\left. \begin{aligned} &zzzz, \\ &xxxx = yyyy = xxxy + xyxx + xyxy, \end{aligned} \right\} \begin{cases} xxxy = yyxx, \\ xyxx = yxyx, \\ xyxy = yxyx, \end{cases}$$

$$\begin{aligned} &yyzz = xxzz, & &xyzz = -yxzz, \\ &zzyy = zzxx, & &zzxy = -zzyx, \\ &zyyz = zxxz, & &zxyz = -zyxz, \\ &yzyy = xzxx, & &xzzy = -yzzx, \\ &yzyz = xzxx, & &xzzy = -yzzx, \\ &zzyy = zxzx, & &zxzy = -zyzx, \end{aligned}$$

$$xxxx = -yyyy = yyxy + yxyx + xyxy, \quad \left\{ \begin{aligned} &yyxy = -xyxx, \\ &yxyx = -xyxx, \\ &xyxy = -xyxx. \end{aligned} \right.$$

For the four classes 622 , $6mm$, $6/mmm$, and $\bar{6}m2$, there are 21 nonzero elements, of which only 10 are independent. They are:

$$\left. \begin{aligned} &zzzz, \\ &xxxx = yyyy = xxxy + xyxx + xyxy, \end{aligned} \right\} \begin{cases} xxxy = yyxx, \\ xyxx = yxyx, \\ xyxy = yxyx, \end{cases}$$

$$\begin{aligned} &yyzz = xxzz, \\ &zzyy = zzxx, \\ &zyyz = zxxz, \\ &yzyy = xzxx, \\ &yzyz = xzxx, \\ &zzyy = zxzx. \end{aligned}$$

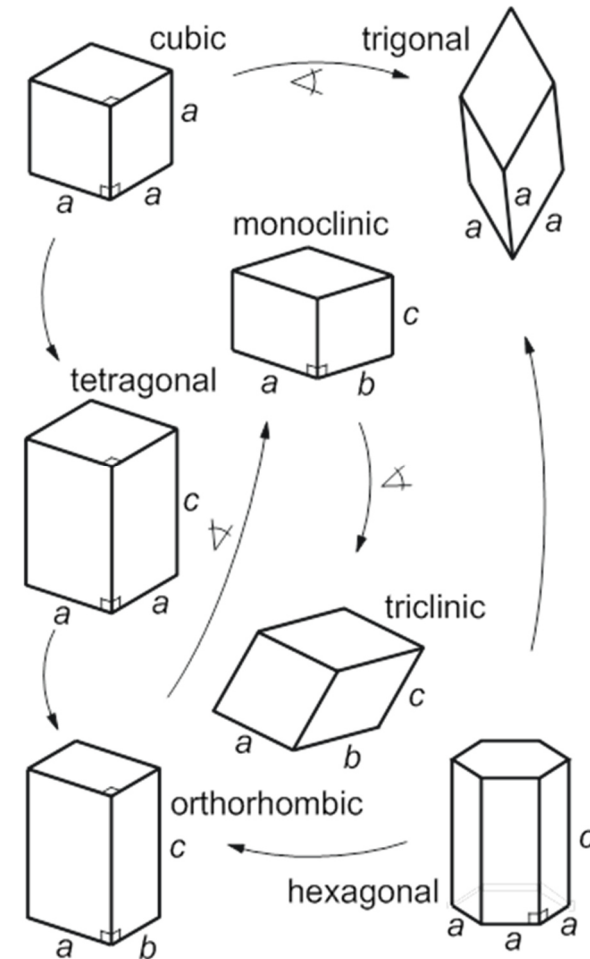


Figure adapted from Boyd, Nonlinear Optics

Third-order susceptibility tensor for various crystal classes

Trigonal

For the two classes 3 and $\bar{3}$, there are 73 nonzero elements, of which only 27 are independent. They are:

$$\begin{aligned} & zzzz, \\ & xxxx = yyyy = xxxy + xyxx + xyxy, \end{aligned} \quad \begin{cases} xxyy = yyxx, \\ xyyx = yxxy, \\ xyxy = yxyx, \end{cases}$$

$$\begin{aligned} & yyzz = xxzz, & xyzz = -yxzz, \\ & zzyy = zzxx, & zzyx = -zzyx, \\ & zyyz = zxxz, & zxyx = -zyxz, \\ & yzzx = xzzx, & xzzy = -yzzx, \\ & yzyz = xzxx, & xzyx = -yzxz, \\ & zyzx = xzxx, & zxyx = -zyxz, \end{aligned}$$

$$xxxy = -yyyy = yyxy + yxyx + xyxy, \quad \begin{cases} yyxy = -xxyx, \\ yxyx = -xyxx, \\ xyyy = -yxxx. \end{cases}$$

$$\begin{aligned} & yyyz = -yxxz = -xyxz = -xxyx, \\ & yyzy = -yxzx = -xyzx = -xxzy, \\ & yzyy = -yzxx = -xzyx = -xzxy, \\ & zyyy = -zyxx = -zxyx = -zxyx, \\ & xxxz = -xyyz = -xyyz = -yyxz, \\ & xxzx = -xyzy = -yxzy = -yyzx, \\ & xzxx = -yzxy = -yzxy = -xzyy, \\ & zxxx = -zxyy = -zyxy = -zyyx. \end{aligned}$$

For the three classes $3m$, $\bar{3}m$, and 32 , there are 37 nonzero elements, of which only 14 are independent. They are:

$$\begin{aligned} & zzzz, \\ & xxxx = yyyy = xxxy + xyxx + xyxy, \end{aligned} \quad \begin{cases} xxyy = yyxx, \\ xyyx = yxxy, \\ xyxy = yxyx, \end{cases}$$

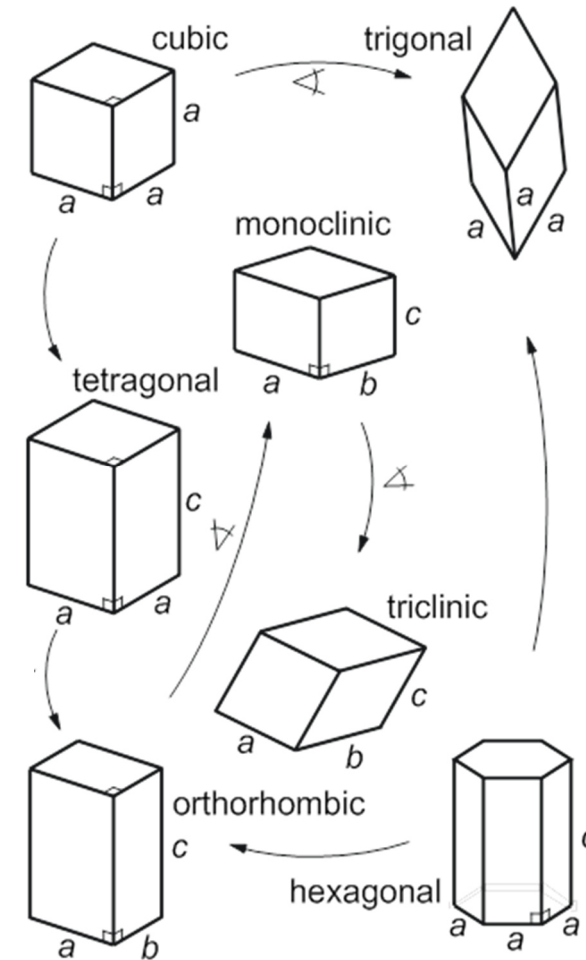


Figure adapted from Boyd, Nonlinear Optics

Third-order susceptibility tensor for various crystal classes

$$\begin{aligned}
 yyzz = xxzz, \quad xxxz = -xyyz = -yxzy = -yyxz, \\
 zzyy = zzxx, \quad xxzx = -xyzy = -yxzy = -yyzx, \\
 zyyz = zxxz, \quad xzxx = -xzyy = -yzxy = -yzyx, \\
 yzzz = xzzx, \quad zxxx = -zxyy = -zyxy = -zyyx, \\
 yzyz = xzxx, \\
 zyzy = zxzx.
 \end{aligned}$$

Tetragonal

For the three classes 4 , $\bar{4}$, and $4/m$, there are 41 nonzero elements, of which only 21 are independent. They are:

$$\begin{aligned}
 &xxxx = yyyy, \quad zzzz, \\
 &zzxx = zzyy, \quad xyzz = -yxzz, \quad xxyy = yyxx, \quad xxyx = -yyyx, \\
 &xxzz = zzxy, \quad ztxy = -zzyx, \quad xyxy = yxyx, \quad xxyx = -yyxy, \\
 &zxzx = zyzy, \quad xzyz = -yzxz, \quad xyyx = yxxy, \quad xyxx = -yxxy, \\
 &xzxz = yzyz, \quad zxyx = -zyzx, \quad yxxx = -xyyy, \\
 &zxzx = zyzy, \quad zxyx = -zyzx, \\
 &xxzx = yzzy, \quad xzzy = -yzzx.
 \end{aligned}$$

For the four classes 422 , $4mm$, $4/mmm$, and $\bar{4}2m$, there are 21 nonzero elements, of which only 11 are independent. They are:

$$\begin{aligned}
 &xxxx = yyyy, \quad zzzz, \\
 &yyzz = xxzz, \quad yzzy = xzxx, \quad xxyy = yyxx, \\
 &zzyy = zzxx, \quad yzyz = xzxx, \quad xyxy = yxyx, \\
 &zyyz = zxxz, \quad zyzy = zxzx, \quad xyyx = yxxy.
 \end{aligned}$$

Monoclinic

For the three classes 2 , m , and $2/m$, there are 41 independent nonzero elements, consisting of:

- 3 elements with indices all equal,
- 18 elements with indices equal in pairs,
- 12 elements with indices having two y's one x, and one z,
- 4 elements with indices having three x's and one z,
- 4 elements with indices having three z's and one x.

Orthorhombic

For all three classes, 222 , $mm2$, and mmm , there are 21 independent nonzero elements, consisting of:

- 3 elements with indices all equal,
- 18 elements with indices equal in pairs.

Triclinic

For both classes, 1 and $\bar{1}$, there are 81 independent nonzero elements.

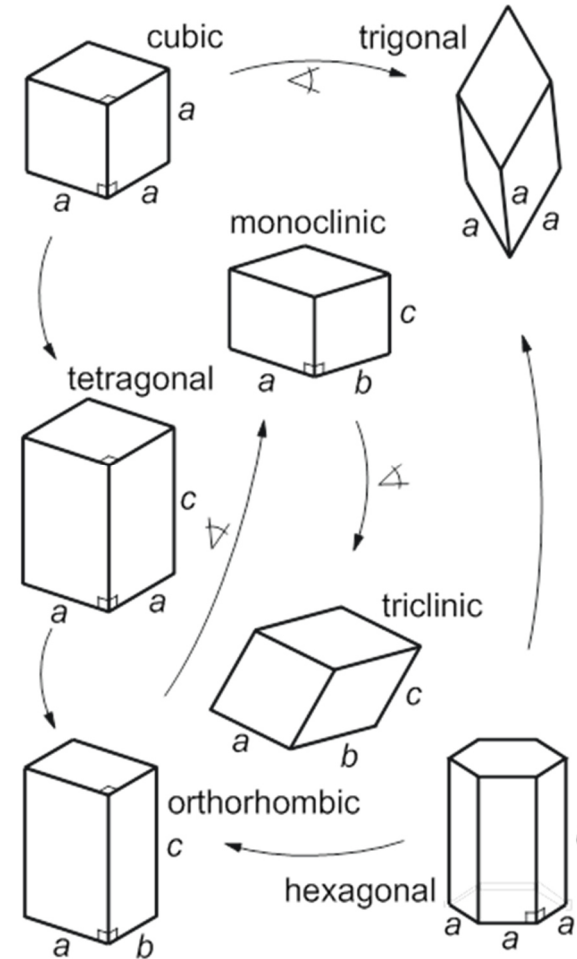


Figure adapted from Boyd, Nonlinear Optics

Second-order nonlinear effects

Note: Second-order nonlinear effects predominantly exist in anisotropic materials!
 \Rightarrow Need to study **wave propagation in linear anisotropic materials** first!

Representation by **permittivity tensor**: (3x3)-matrix

$$\underline{\mathbf{D}} = \epsilon_0 \underline{\epsilon_r} \underline{\mathbf{E}}, \quad \underline{\epsilon_r} = \mathbf{I} + \underline{\chi}$$

For lossless reciprocal media (no magneto-optic effect): $\epsilon_{ij} = \epsilon_{ji} \in \mathbb{R}$

\Rightarrow Representation in diagonal form with respect to principal axes of the crystal:

$$\begin{pmatrix} \underline{D}_x \\ \underline{D}_y \\ \underline{D}_z \end{pmatrix} = \epsilon_0 \begin{pmatrix} \epsilon_{xx} & 0 & 0 \\ 0 & \epsilon_{yy} & 0 \\ 0 & 0 & \epsilon_{zz} \end{pmatrix} \begin{pmatrix} \underline{E}_x \\ \underline{E}_y \\ \underline{E}_z \end{pmatrix} = \epsilon_0 \begin{pmatrix} n_1^2 & 0 & 0 \\ 0 & n_2^2 & 0 \\ 0 & 0 & n_3^2 \end{pmatrix} \begin{pmatrix} \underline{E}_x \\ \underline{E}_y \\ \underline{E}_z \end{pmatrix},$$

Alternatively: Representation by **impermeability tensor** η :

$$\underline{\mathbf{E}} = \frac{1}{\epsilon_0} \underline{\eta} \underline{\mathbf{D}}.$$

$$\begin{pmatrix} \underline{E}_x \\ \underline{E}_y \\ \underline{E}_z \end{pmatrix} = \frac{1}{\epsilon_0} \begin{pmatrix} \eta_{xx} & 0 & 0 \\ 0 & \eta_{yy} & 0 \\ 0 & 0 & \eta_{zz} \end{pmatrix} \begin{pmatrix} \underline{D}_x \\ \underline{D}_y \\ \underline{D}_z \end{pmatrix} = \frac{1}{\epsilon_0} \begin{pmatrix} \frac{1}{n_1^2} & 0 & 0 \\ 0 & \frac{1}{n_2^2} & 0 \\ 0 & 0 & \frac{1}{n_3^2} \end{pmatrix} \begin{pmatrix} \underline{D}_x \\ \underline{D}_y \\ \underline{D}_z \end{pmatrix}.$$

Biaxial, uniaxial, and isotropic crystals

Form of permittivity and impermeability tensor is **constrained by symmetry of the crystal**
⇒ **3 different categories**; depending on their representation with respect to the principal axes:

Biaxial crystals:

- Three different principal refractive indices, $n_1 \neq n_2 \neq n_3$

$$\underline{\epsilon}_r = \begin{pmatrix} n_1^2 & 0 & 0 \\ 0 & n_2^2 & 0 \\ 0 & 0 & n_3^2 \end{pmatrix}$$

Uniaxial crystals:

- Two orthogonal directions, along which refractive indices are equal.

⇒ **Ordinary indices** $n_o = n_1 = n_2$

- Third index: **Extraordinary index** $n_e = n_3$
- Positive uniaxial: $n_e > n_o$
- Negative uniaxial: $n_e < n_o$
- Note: Uniaxial crystals exhibit a single axis with threefold, four-fold, or six-fold symmetry.

$$\underline{\epsilon}_r = \begin{pmatrix} n_o^2 & 0 & 0 \\ 0 & n_o^2 & 0 \\ 0 & 0 & n_e^2 \end{pmatrix}$$

Isotropic crystals:

- Higher symmetry, e.g., due to a cubic unit cell.
- All three indices are equal

$$\underline{\epsilon}_r = \begin{pmatrix} n^2 & 0 & 0 \\ 0 & n^2 & 0 \\ 0 & 0 & n^2 \end{pmatrix}$$

Permeability tensors for different crystal classes

Representation of $\underline{\epsilon}_r$ with respect to the **coordinates of the unit cell** (not necessarily the principal axes of the permittivity tensor!)

isotropic	$\begin{bmatrix} xx & 0 & 0 \\ 0 & xx & 0 \\ 0 & 0 & xx \end{bmatrix}$	cubic
uniaxial	$\begin{bmatrix} xx & 0 & 0 \\ 0 & xx & 0 \\ 0 & 0 & zz \end{bmatrix}$	tetragonal trigonal hexagonal
biaxial	$\begin{bmatrix} xx & 0 & 0 \\ 0 & yy & 0 \\ 0 & 0 & zz \end{bmatrix}$	orthorhombic
	$\begin{bmatrix} xx & 0 & xz \\ 0 & yy & 0 \\ xz & 0 & zz \end{bmatrix}$	monoclinic
	$\begin{bmatrix} xx & xy & xz \\ xy & yy & yz \\ xz & yz & zz \end{bmatrix}$	triclinic

The seven crystal classes and their hierarchy:

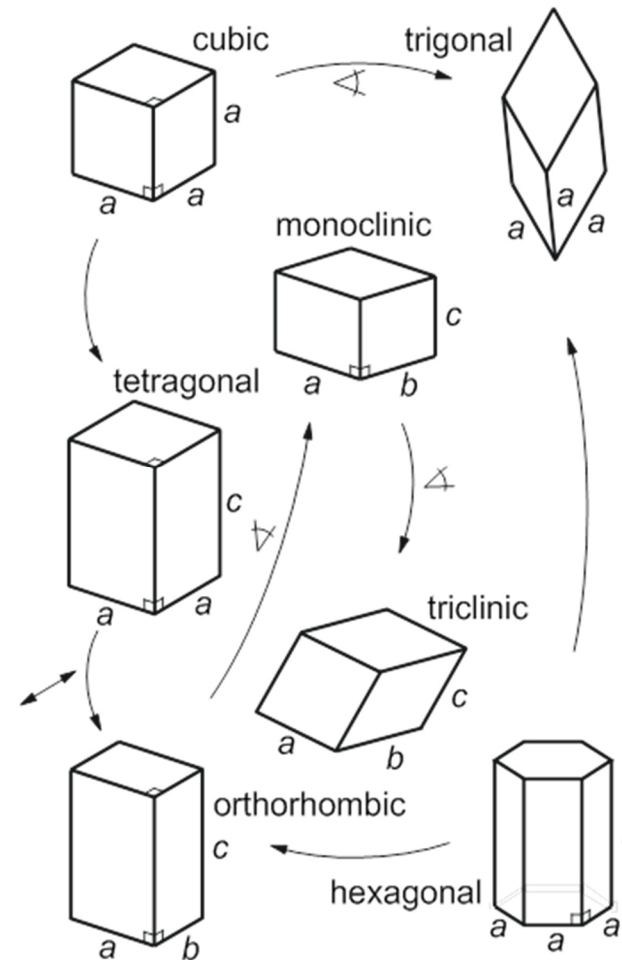
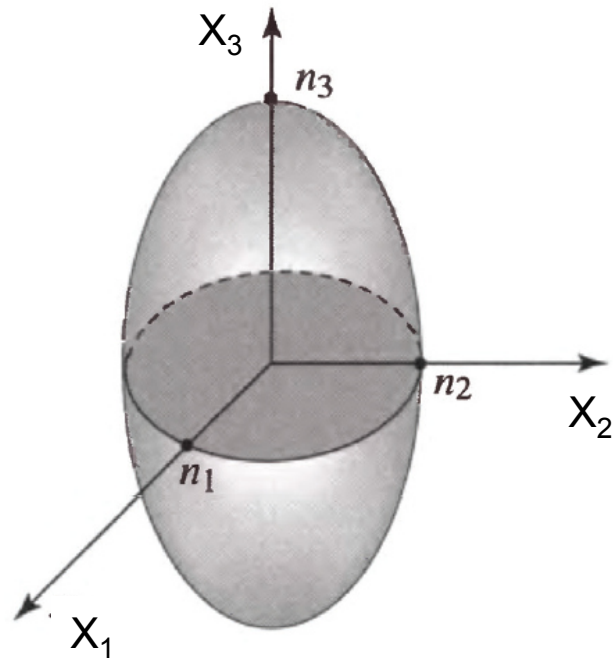


Figure adapted from Ashcroft/ Mermin, Solid State Physics



Index ellipsoid (optical indicatrix): Quadratic representation of the electric impermeability tensor.

$$\sum_{i,j} \eta_{ij} X_i X_j = 1$$

Representation with respect to the principal axes of the crystal:

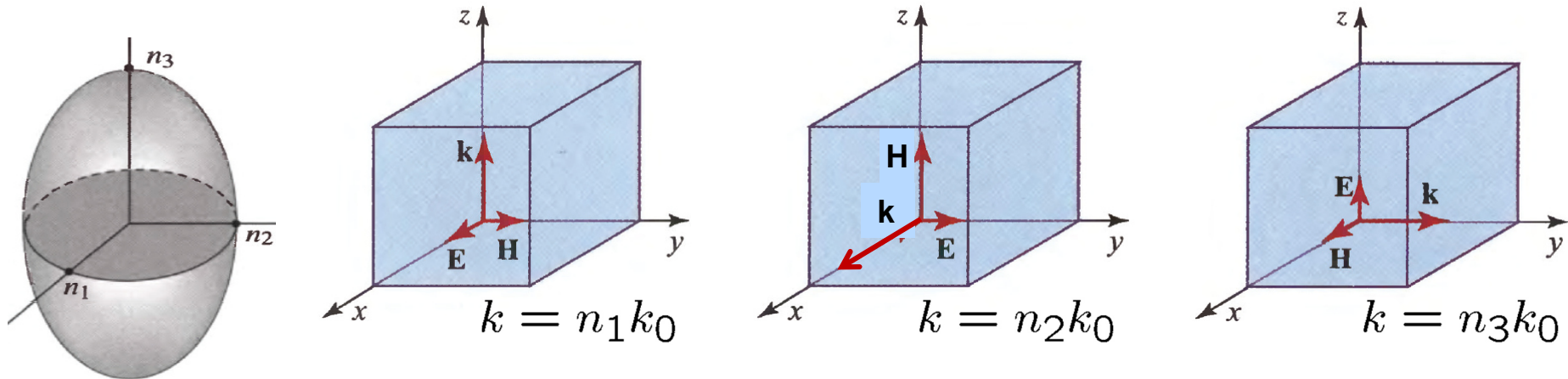
$$\frac{X_1^2}{n_1^2} + \frac{X_2^2}{n_2^2} + \frac{X_3^2}{n_3^2} = 1$$

X_1, X_2, X_3 = principal axes of the crystal
 n_1, n_2, n_3 = principal refractive indices

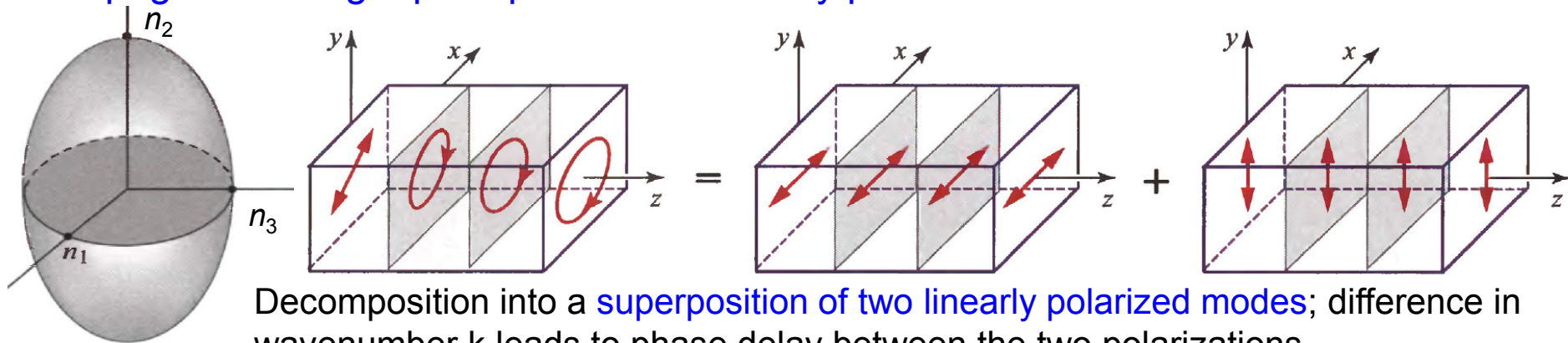
Figure adapted from Saleh/Teich, Fundamentals of Photonics

Wave propagation in anisotropic crystals

Propagation and polarization along a principal axis (“normal modes”): $k_i = n_i k_0$



Propagation along a principal axis – arbitrary polarization direction:



Decomposition into a **superposition of two linearly polarized modes**; difference in wavenumber k leads to phase delay between the two polarizations,

$$\Delta\Phi = -k_0 (n_2 - n_1) z$$

Figures adapted from Saleh/Teich, Fundamentals of Photonics

Wave propagation in anisotropic crystals

Propagation in arbitrary direction – fundamental properties:

Isotropic media

$$\underline{\mathbf{H}} \parallel \underline{\mathbf{B}}$$

$$\underline{\mathbf{E}} \parallel \underline{\mathbf{D}}$$

$\underline{\mathbf{k}}$, $\underline{\mathbf{E}}$, $\underline{\mathbf{H}}$ are mutually orthogonal and form a right-handed set

$$\underline{\mathbf{k}} \parallel \underline{\mathbf{S}}$$

Anisotropic media

$$\underline{\mathbf{H}} \parallel \underline{\mathbf{B}}$$

$$\underline{\mathbf{E}} \not\parallel \underline{\mathbf{D}} \quad \underline{\mathbf{D}} = \epsilon_0 \epsilon_r \underline{\mathbf{E}},$$

$$\underline{\mathbf{E}} = \frac{1}{\epsilon_0} \underline{\eta} \underline{\mathbf{D}}.$$

$\underline{\mathbf{k}}$, $\underline{\mathbf{D}}$, $\underline{\mathbf{H}}$ are mutually orthogonal and form a right-handed set

$$\underline{\mathbf{k}} \not\parallel \underline{\mathbf{S}}$$

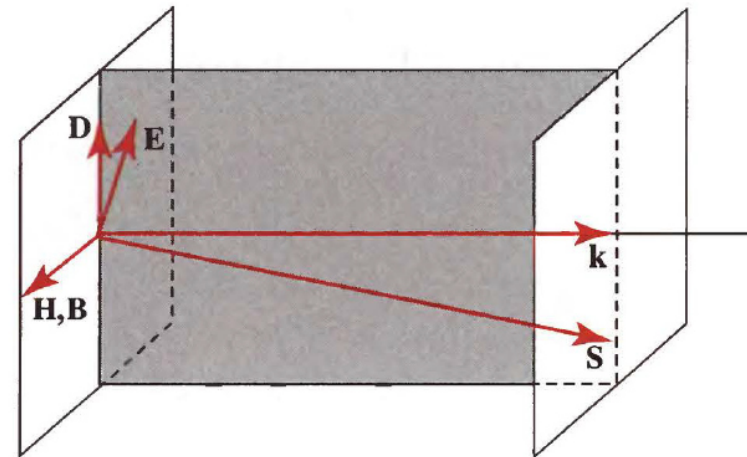


Figure adapted from Saleh/Teich, Fundamentals of Photonics

Normal modes for propagation in arbitrary direction

Plane-wave ansatz for the fields:

$$\underline{\mathbf{E}} = \underline{\mathbf{E}}_0 e^{-j\mathbf{k}\cdot\mathbf{r}} \quad \underline{\mathbf{H}} = \underline{\mathbf{H}}_0 e^{-j\mathbf{k}\cdot\mathbf{r}} \quad \underline{\mathbf{D}} = \underline{\mathbf{D}}_0 e^{-j\mathbf{k}\cdot\mathbf{r}}.$$

Insert into Maxwell's equations:

$$\begin{aligned} -j\mathbf{k} \times \underline{\mathbf{E}} &= -j\omega\mu_0\underline{\mathbf{H}}, & \underline{\mathbf{E}} &= \frac{1}{\epsilon_0}\underline{\eta}\underline{\mathbf{D}}. \\ -j\mathbf{k} \times \underline{\mathbf{H}} &= j\omega\underline{\mathbf{D}}. & \text{Note: } \underline{\mathbf{A}} \times \underline{\mathbf{B}} \times \underline{\mathbf{C}} &= \underline{\mathbf{B}} (\underline{\mathbf{A}}^T \underline{\mathbf{C}}) - \underline{\mathbf{C}} (\underline{\mathbf{A}}^T \underline{\mathbf{B}}) \end{aligned}$$

Wave equation for $\underline{\mathbf{D}}$:

$$-\mathbf{k} \times (\mathbf{k} \times (\underline{\eta}\underline{\mathbf{D}})) = k_0^2 \underline{\mathbf{D}}$$

Transform to implicit equation that relates the dielectric displacement vector $\underline{\mathbf{D}}$ to the corresponding propagation constant k :

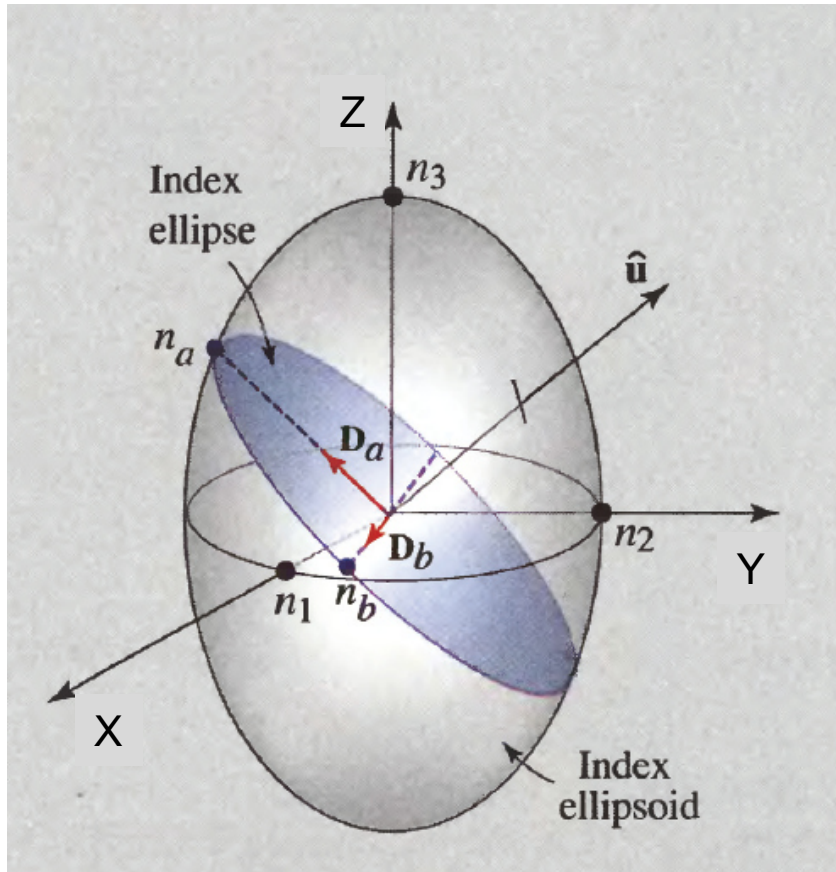
$$\underline{\mathbf{D}}^T \underline{\eta} \underline{\mathbf{D}} = \frac{k_0^2}{\mathbf{k}^T \mathbf{k}} \underline{\mathbf{D}}^T \underline{\mathbf{D}}$$

$$\frac{X^2}{n_1^2} + \frac{Y^2}{n_2^2} + \frac{Z^2}{n_3^2} = 1 \quad \text{where} \quad X = \frac{k D_x}{k_0 D}, \quad Y = \frac{k D_y}{k_0 D}, \quad Z = \frac{k D_z}{k_0 D},$$

Index ellipsoid / optical indicatrix

$$D = \sqrt{\underline{\mathbf{D}}^T \underline{\mathbf{D}}} \quad k = \sqrt{\mathbf{k}^T \mathbf{k}}$$

Determining normal modes from the index ellipsoid



Given: Propagation direction of the optical wave,

$$\mathbf{u} = \frac{\mathbf{k}}{|\mathbf{k}|}$$

Wanted: Effective refractive indices n_a and n_b of the normal modes and corresponding displacement vectors $\underline{\mathbf{D}}_a$ and $\underline{\mathbf{D}}_b$ (or their normalized counterparts $(X, Y, Z)^T$)

Solution:

- Draw a plane passing through the origin of the index ellipsoid, normal to \mathbf{u} . The intersection of the plane with the ellipsoid produces the **index ellipse**.
- The half-lengths of the major and minor axes of the index ellipse are the **refractive indexes n_a and n_b of the two normal modes**, that propagate like plane waves (without derivation).
- The directions of the major and minor axes of the index ellipse are the **directions of the vectors $\underline{\mathbf{D}}_a$ and $\underline{\mathbf{D}}_b$** for the normal modes. These directions are orthogonal.
- The vectors $\underline{\mathbf{E}}_a$ and $\underline{\mathbf{E}}_b$ are derived from $\underline{\mathbf{D}}_a$ and $\underline{\mathbf{D}}_b$

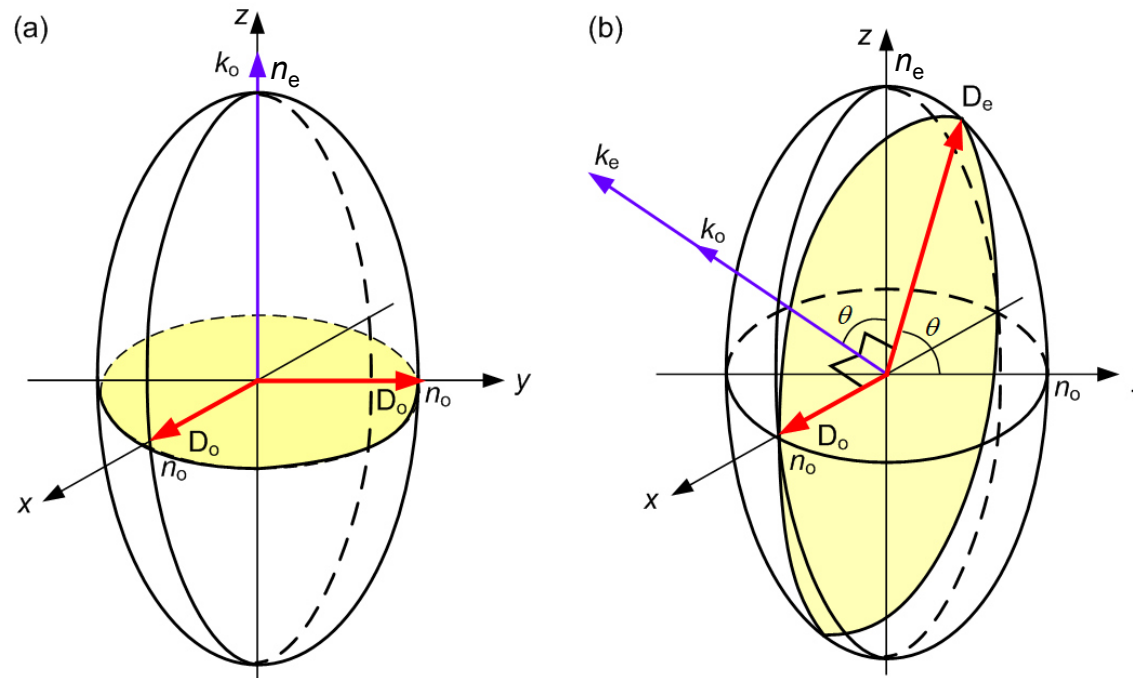
$$\underline{\mathbf{D}} = \epsilon_0 \underline{\epsilon}_r \underline{\mathbf{E}}, \quad \underline{\mathbf{E}} = \frac{1}{\epsilon_0} \underline{\eta} \underline{\mathbf{D}}.$$

Figure adapted from Saleh/Teich, Fundamentals of Photonics

Uniaxial crystals

$$n_1 = n_2 = n_o \text{ and } n_3 = n_e$$

⇒ Index ellipsoid is rotationally symmetric with respect to the Z-axis



Normal modes:

- Ordinary mode: $n_a = n_o$
- Extraordinary mode: $n_b = n(\theta)$, where

$$\frac{1}{n^2(\theta)} = \frac{\sin^2(\theta)}{n_e^2} + \frac{\cos^2(\theta)}{n_o^2}$$

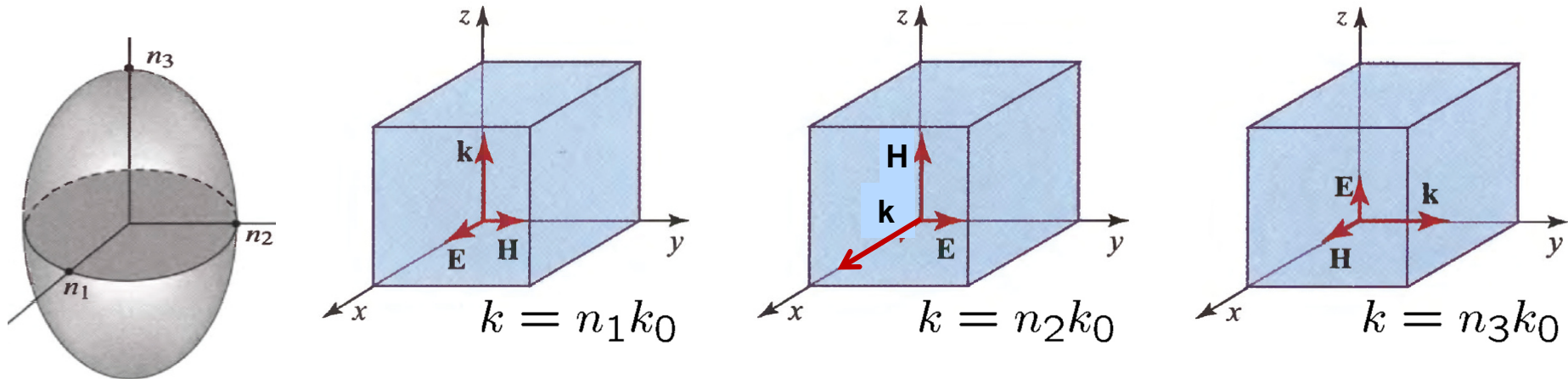
- Walk-off angle ρ between the electric field \underline{E}_e and the dielectric displacement \underline{D}_e :

$$\cos(\rho) = \frac{\underline{E}_b^T \underline{D}_b}{|\underline{E}_b| |\underline{D}_b|} = \frac{n_e^2 \cos^2(\theta) + n_o^2 \sin^2(\theta)}{\sqrt{n_e^4 \cos^2(\theta) + n_o^4 \sin^2(\theta)}}$$

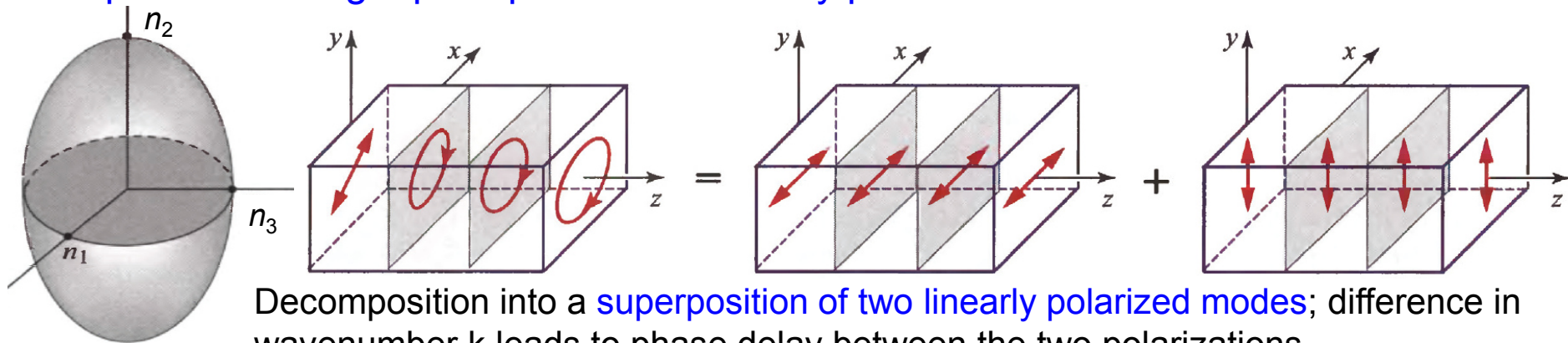
Lecture 8

Wave propagation in anisotropic crystals

Propagation and polarization along a principal axis (“normal modes”): $k_i = n_i k_0$



Propagation along a principal axis – arbitrary polarization direction:

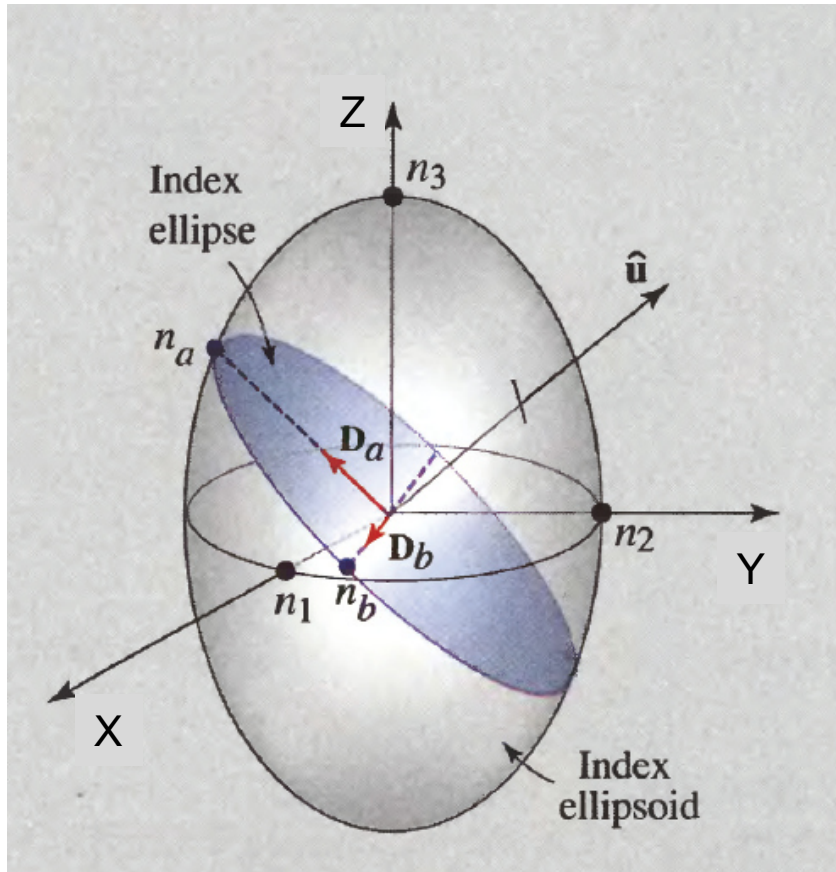


Decomposition into a **superposition of two linearly polarized modes**; difference in wavenumber k leads to phase delay between the two polarizations,

$$\Delta\Phi = -k_0 (n_2 - n_1) z$$

Figures adapted from Saleh/Teich, Fundamentals of Photonics

Determining normal modes from the index ellipsoid



Given: Propagation direction of the optical wave,

$$\mathbf{u} = \frac{\mathbf{k}}{|\mathbf{k}|}$$

Wanted: Effective refractive indices n_a and n_b of the normal modes and corresponding displacement vectors $\underline{\mathbf{D}}_a$ and $\underline{\mathbf{D}}_b$

Solution:

- Draw a plane passing through the origin of the index ellipsoid, normal to \mathbf{u} . The intersection of the plane with the ellipsoid produces the **index ellipse**.
- The half-lengths of the major and minor axes of the index ellipse are the **refractive indexes n_a and n_b of the two normal modes**, that propagate like plane waves (without derivation).
- The directions of the major and minor axes of the index ellipse are the **directions of the vectors $\underline{\mathbf{D}}_a$ and $\underline{\mathbf{D}}_b$** for the normal modes. These directions are orthogonal.
- The vectors $\underline{\mathbf{E}}_a$ and $\underline{\mathbf{E}}_b$ are derived from $\underline{\mathbf{D}}_a$ and $\underline{\mathbf{D}}_b$

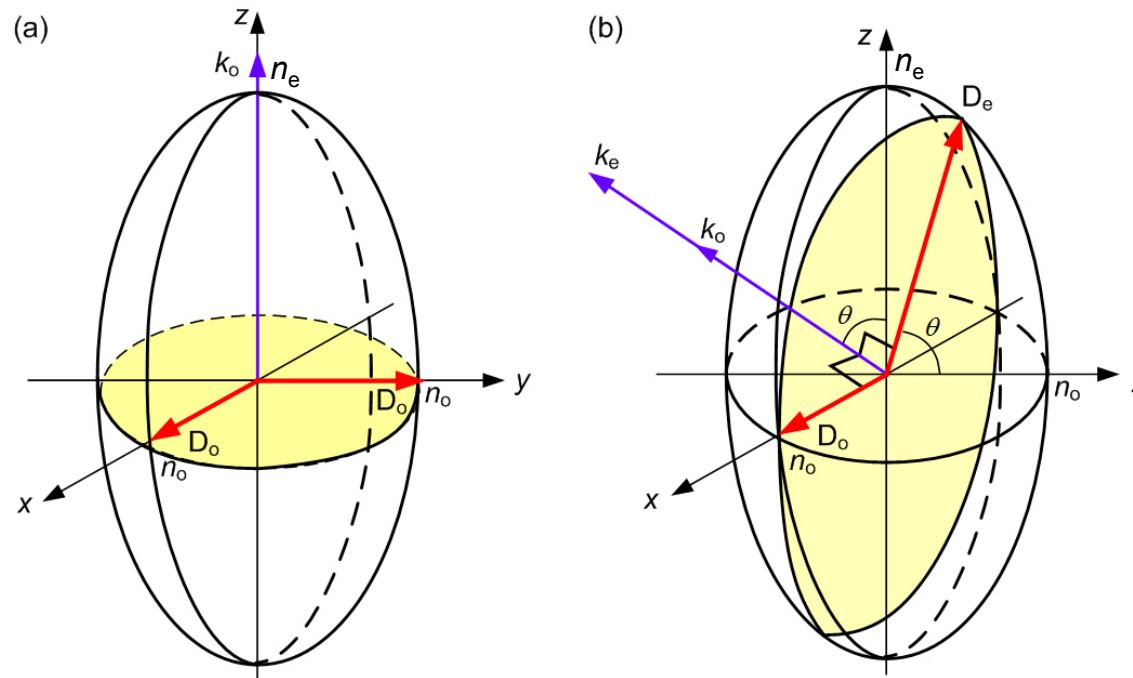
$$\underline{\mathbf{D}} = \epsilon_0 \underline{\epsilon}_r \underline{\mathbf{E}}, \quad \underline{\mathbf{E}} = \frac{1}{\epsilon_0} \underline{\eta} \underline{\mathbf{D}}.$$

Figure adapted from Saleh/Teich, Fundamentals of Photonics

Uniaxial crystals

$$n_1 = n_2 = n_o \text{ and } n_3 = n_e$$

⇒ Index ellipsoid is rotationally symmetric with respect to the Z-axis



Normal modes:

- Ordinary mode: $n_a = n_o$
- Extraordinary mode: $n_b = n(\theta)$, where

$$\frac{1}{n^2(\theta)} = \frac{\sin^2(\theta)}{n_e^2} + \frac{\cos^2(\theta)}{n_o^2}$$

- Walk-off angle ρ between the electric field \underline{E}_e and the dielectric displacement \underline{D}_e :

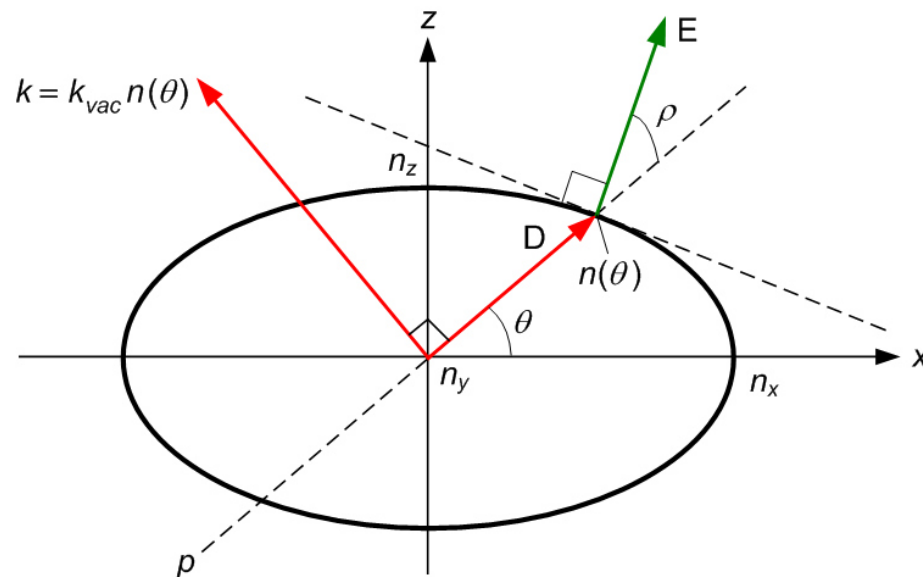
$$\cos(\rho) = \frac{\underline{E}_b^T \underline{D}_b}{|\underline{E}_b| |\underline{D}_b|} = \frac{n_e^2 \cos^2(\theta) + n_o^2 \sin^2(\theta)}{\sqrt{n_e^4 \cos^2(\theta) + n_o^4 \sin^2(\theta)}}$$

Graphical derivation of electric field directions from the index ellipsoid

Consider **gradient** of implicit representation of index ellipsoid:

$$\mathbf{n} = \text{grad} \left(\frac{X^2}{n_1^2} + \frac{Y^2}{n_2^2} + \frac{Z^2}{n_3^2} \right) = 2 \begin{pmatrix} \frac{X}{n_1^2} \\ \frac{Y}{n_2^2} \\ \frac{Z}{n_3^2} \end{pmatrix} = \frac{2k}{k_0 D} \begin{pmatrix} \frac{D_x}{n_1^2} \\ \frac{D_y}{n_2^2} \\ \frac{D_z}{n_3^2} \end{pmatrix} = \frac{2k\epsilon_0}{k_0 D} \underline{E},$$

=> **Surface normal of the index ellipsoid defines direction of the electric field \underline{E}**



Note: For uniaxial crystals, $E \parallel D$ for ordinary modes, but not for extraordinary modes

⇒ For a given direction of \mathbf{k} , the walk-off angle ρ between \mathbf{E} and \mathbf{D} corresponds also to the walk-off between the Poynting vector of the ordinary and the extraordinary beam

Linear electro-optic effect / Pockels effect

Index ellipsoid in coordinate system of crystal unit cell:

$$\eta_{ij} = \begin{pmatrix} \frac{1}{n^2} \\ \frac{1}{n^2} \\ \frac{1}{n^2} \\ \frac{1}{n^2} \\ \frac{1}{n^2} \\ \frac{1}{n^2} \end{pmatrix}_h \quad \begin{matrix} ij & 11 & 22 & 33 & 23, 32 & 13, 31 & 12, 21 \\ h & 1 & 2 & 3 & 4 & 5 & 6 \end{matrix}$$

$$\left(\frac{1}{n^2}\right)_1 X^2 + \left(\frac{1}{n^2}\right)_2 Y^2 + \left(\frac{1}{n^2}\right)_3 Z^2 + 2\left(\frac{1}{n^2}\right)_4 YZ + 2\left(\frac{1}{n^2}\right)_5 XZ + 2\left(\frac{1}{n^2}\right)_6 XY = 1$$

Nonlinear interaction: Express elements of the impermeability tensor as a power series in the strength of the external electric components E_k

$$\eta_{ij} = \eta_{ij}^{(0)} + \sum_k r_{ijk} E_k + \sum_{k,l} s_{ijkl} E_k E_l + \dots$$

Using **contracted notation**, the third-rank electro-optic tensor r_{ijk} can be expressed as a **two-dimensional (6×3)-matrix r_{hk}** :

$$\begin{pmatrix} \Delta \left(\frac{1}{n^2}\right)_1 \\ \Delta \left(\frac{1}{n^2}\right)_2 \\ \Delta \left(\frac{1}{n^2}\right)_3 \\ \Delta \left(\frac{1}{n^2}\right)_4 \\ \Delta \left(\frac{1}{n^2}\right)_5 \\ \Delta \left(\frac{1}{n^2}\right)_6 \end{pmatrix} = \begin{pmatrix} r_{11} & r_{12} & r_{13} \\ r_{21} & r_{22} & r_{23} \\ r_{31} & r_{32} & r_{33} \\ r_{41} & r_{42} & r_{43} \\ r_{51} & r_{52} & r_{53} \\ r_{61} & r_{62} & r_{63} \end{pmatrix} \begin{pmatrix} E_1 \\ E_2 \\ E_3 \end{pmatrix}.$$

Electro-optic tensor for different crystal classes

Form of the electro-optic tensor r_{hk} is restricted by the symmetry of the underlying crystal lattice:

$$r_{ij} = \begin{bmatrix} 0 & 0 & 0 \\ 0 & 0 & 0 \\ 0 & 0 & 0 \\ r_{41} & 0 & 0 \\ 0 & r_{41} & 0 \\ 0 & 0 & r_{63} \end{bmatrix} \quad (\text{for class } \bar{4}2m),$$

$$r_{ij} = \begin{bmatrix} 0 & -r_{22} & r_{13} \\ 0 & r_{22} & r_{13} \\ 0 & 0 & r_{33} \\ 0 & r_{42} & 0 \\ r_{42} & 0 & 0 \\ r_{22} & 0 & 0 \end{bmatrix} \quad (\text{for class } 3m),$$

$$r_{ij} = \begin{bmatrix} 0 & 0 & r_{13} \\ 0 & 0 & r_{13} \\ 0 & 0 & r_{33} \\ 0 & r_{42} & 0 \\ r_{42} & 0 & 0 \\ 0 & 0 & 0 \end{bmatrix} \quad (\text{for class } 4mm).$$

Figures adapted from Boyd,
Nonlinear Optics

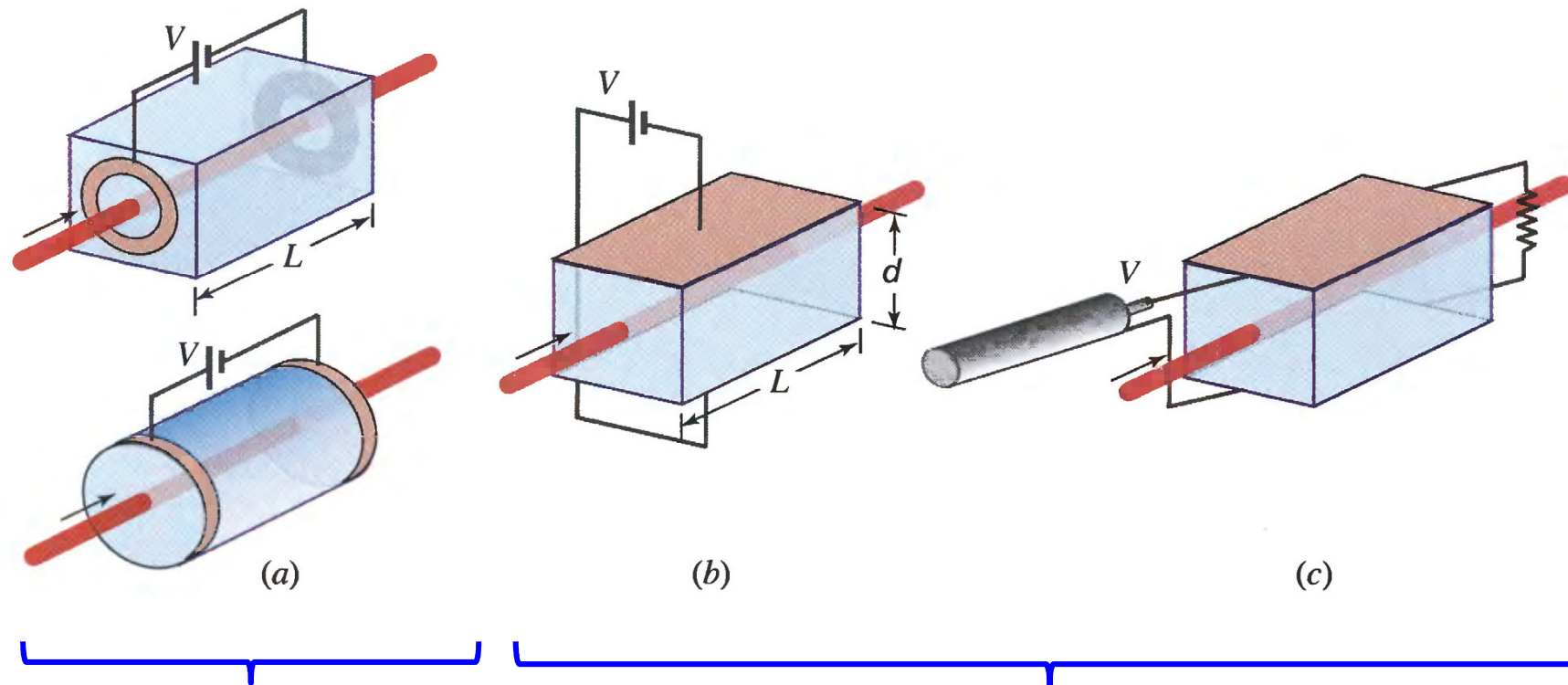
Material	Point Group	Electrooptic Coefficients (10^{-12} m/V)	Refractive Index
Potassium dihydrogen phosphate, KH_2PO_4 (KDP)	$\bar{4}2m$	$r_{41} = 8.77$ $r_{63} = 10.5$	$n_0 = 1.514$ $n_e = 1.472$ (at $0.5461 \mu\text{m}$)
Potassium dideuterium phosphate, KD_2PO_4 (KD*P)	$\bar{4}2m$	$r_{41} = 8.8$ $r_{63} = 26.4$	$n_0 = 1.508$ $n_e = 1.468$ (at $0.5461 \mu\text{m}$)
Lithium niobate, LiNbO_3	$3m$	$r_{13} = 9.6$ $r_{22} = 6.8$ $r_{33} = 30.9$ $r_{42} = 32.6$	$n_0 = 2.3410$ $n_e = 2.2457$ (at $0.5 \mu\text{m}$)
Lithium tantalate, LiTaO_3	$3m$	$r_{13} = 8.4$ $r_{22} = -0.2$ $r_{33} = 30.5$ $r_{51} = 20$	$n_0 = 2.176$ $n_e = 2.180$ (at 0.633 nm)
Barium titanate, BaTiO_3 ^b	$4mm$	$r_{13} = 19.5$ $r_{33} = 97$ $r_{42} = 1640$	$n_0 = 2.488$ $n_e = 2.424$ (at 514 nm)
Strontium barium niobate, $\text{Sr}_{0.6}\text{Ba}_{0.4}\text{NbO}_6$ (SBN:60)	$4mm$	$r_{13} = 55$ $r_{33} = 224$ $r_{42} = 80$	$n_0 = 2.367$ $n_e = 2.337$ (at 514 nm)
Zinc telluride, ZnTe	$\bar{4}3m$	$r_{41} = 4.0$	$n_0 = 2.99$ (at $0.633 \mu\text{m}$)

^a From a variety of sources. See, for example, Thompson and Hartfield (1978) and Cook and Jaffe (1979). The electrooptic coefficients are given in the MKS units of m/V. To convert to the cgs units of cm/statvolt each entry should be multiplied by 3×10^4 .

^b $\epsilon_{dc}^{\parallel} = 135$, $\epsilon_{dc}^{\perp} = 3700$.

Electro-optic modulators

Electro-optic modulators: Exploit second-order nonlinearities to modulate a beam of light by means of an electric signal.

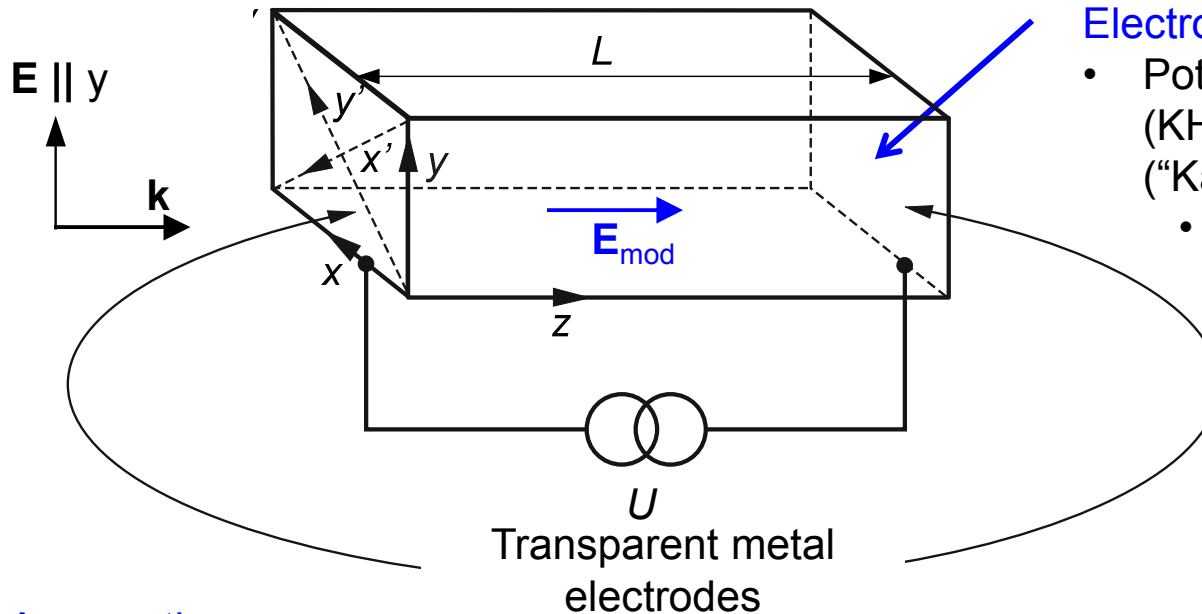


Longitudinal modulators:
Modulating electric field \mathbf{E}_{mod} applied parallel to the direction of light propagation

Transverse modulators:
 \mathbf{E}_{mod} perpendicular to the direction of light propagation.

Figures adapted Saleh/Teich, Fundamentals of Photonics

Longitudinal modulator: The Pockels cell



Electro-optic material, e.g.,

- Potassium dihydrogen phosphate (KH_2PO_4), also referred to as **KDP** (“Kalimudihydrogenphosphat”)
- Potassium dideuterium phosphate (KD_2PO_4); D denotes deuterium; short name **KD*P**
- Ammonium dihydrogen phosphate ($\text{NH}_4\text{H}_2\text{PO}_4$), short name **ADP**

Assumptions:

- Electro-optic material of **point group -42m**
 \Rightarrow **Uniaxial** impermeability tensor if $\mathbf{E}_{\text{mod}} = 0$,
 electro-optic tensor **restricted by crystal symmetry**
- Modulating voltage applied along z
- Light polarized along y, propagation along z
- Applied voltage U can be considered **static**, i.e., it remains constant during the propagation time of light through the electro-optic material

Uniaxial:

$$\eta = \begin{pmatrix} \frac{1}{n_o^2} & 0 & 0 \\ 0 & \frac{1}{n_o^2} & 0 \\ 0 & 0 & \frac{1}{n_e^2} \end{pmatrix}$$

Point group -42m:

$$\mathbf{r} = \begin{pmatrix} 0 & 0 & 0 \\ 0 & 0 & 0 \\ 0 & 0 & 0 \\ r_{41} & 0 & 0 \\ 0 & r_{41} & 0 \\ 0 & 0 & r_{63} \end{pmatrix}$$

Longitudinal modulator: The Pockels cell

Applied modulating field E_z transforms uniaxial crystal into a biaxial medium:

$$\eta(E_z) = \begin{pmatrix} \frac{1}{n_o^2} & r_{63}E_z & 0 \\ r_{63}E_z & \frac{1}{n_o^2} & 0 \\ 0 & 0 & \frac{1}{n_e^2} \end{pmatrix}$$

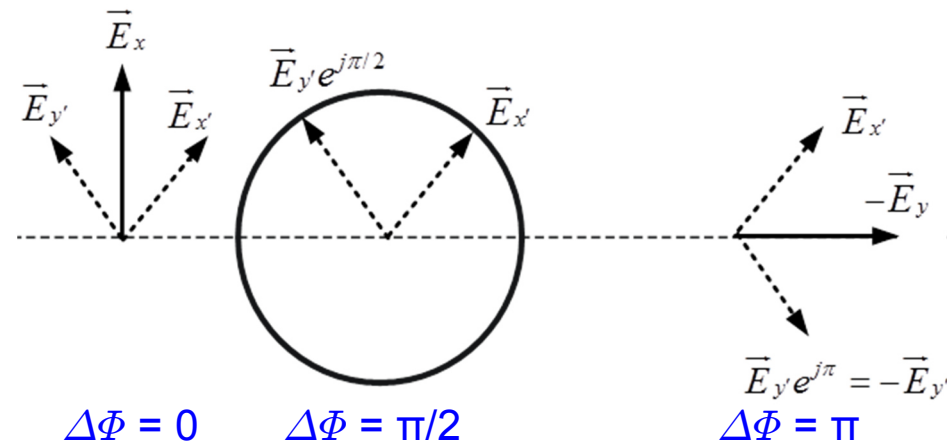
Transform indicatrix to new principal axes (X, Y, Z):

$$\begin{aligned} X &= \frac{1}{\sqrt{2}} (X' + Y') & n_{X'} &= n_o \left(1 + \frac{1}{2} r_{63} n_o^2 E_z \right) \\ Y &= \frac{1}{\sqrt{2}} (-X' + Y') & n_{Y'} &= n_o \left(1 - \frac{1}{2} r_{63} n_o^2 E_z \right) \\ Z &= Z' & n_{Z'} &= n_e \end{aligned}$$

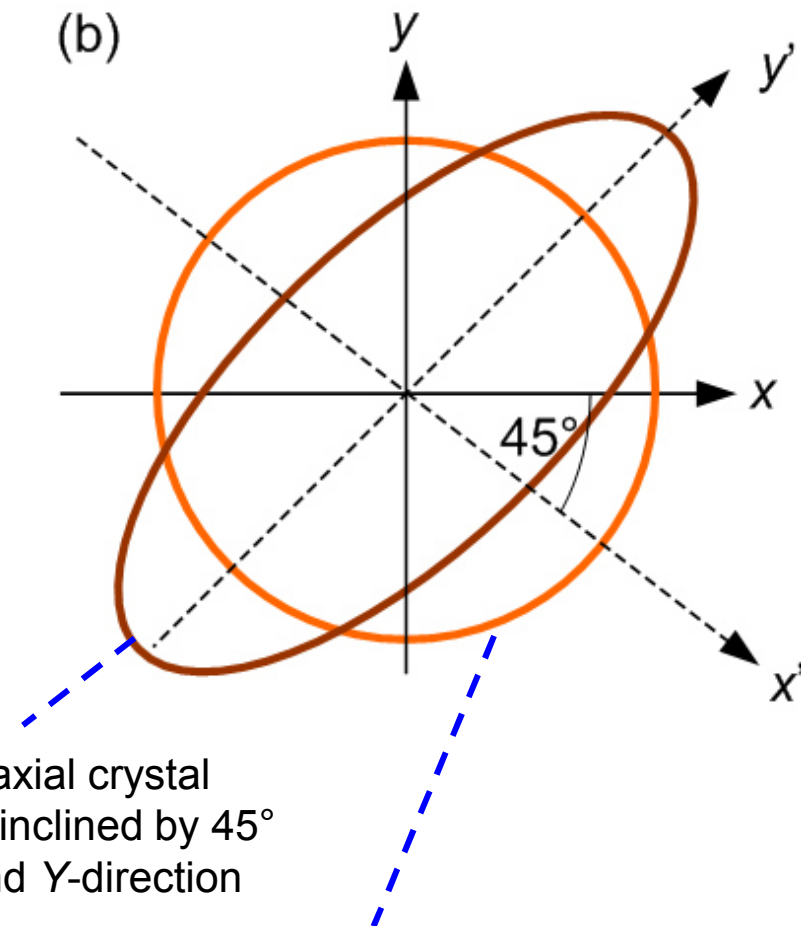
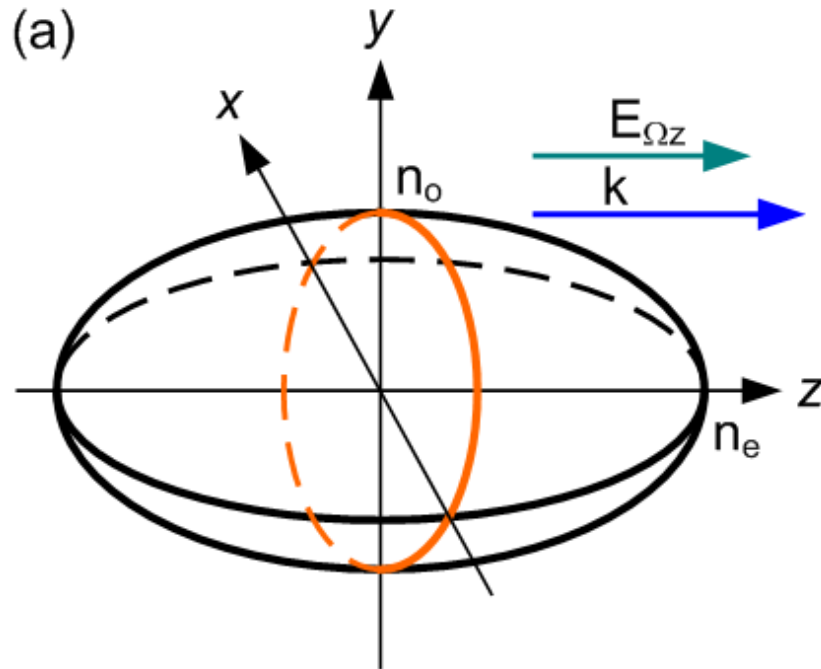
⇒ Normal modes are polarized at 45° with respect to x and y and experience a phase delay with respect to each other during propagation:

$$\Delta\Phi = \pi \frac{U}{U_\pi}$$

$$U_\pi = \frac{\lambda}{2r_{63}n_o^3}$$



Deformation of indicatrix by external electric field

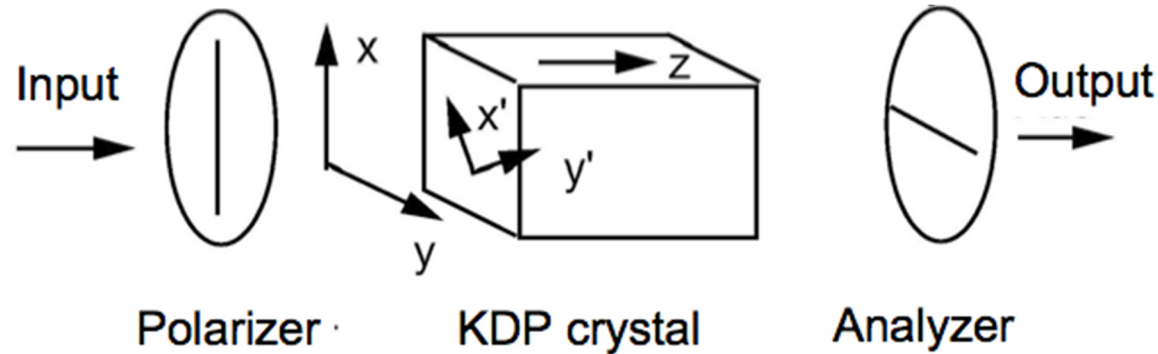


With external field ($E_{\Omega z}$): Biaxial crystal
 \Rightarrow Principal axes X' and Y' inclined by 45°
with respect to the X - and Y -direction

Without external field: Uniaxial crystal
 \Rightarrow Index ellipsoid rotationally symmetric
with respect to the z -axis

Turning the Pockels into an amplitude modulator

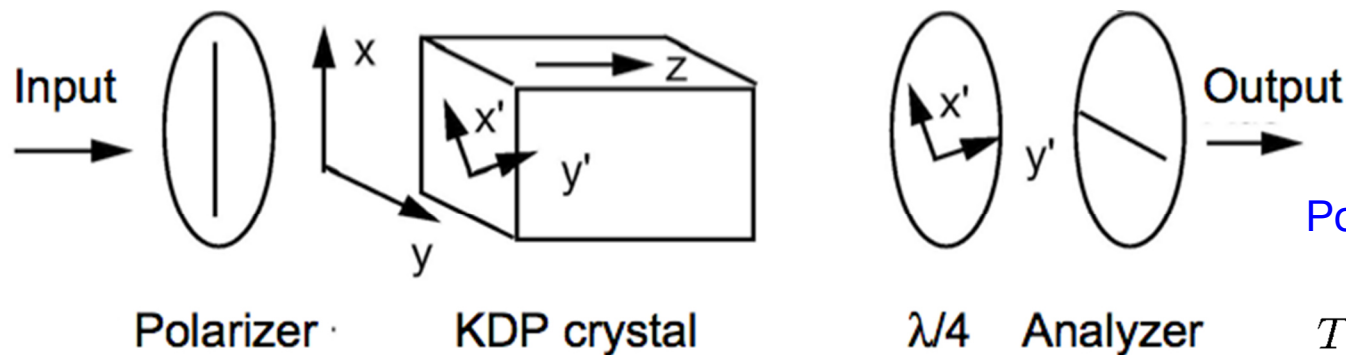
Insert polarizer after the Pockels cell:



Power transfer function:

$$T(U) = \sin^2\left(\frac{\pi U}{2U_\pi}\right)$$

Adjust operating point by quarter-wave plate:



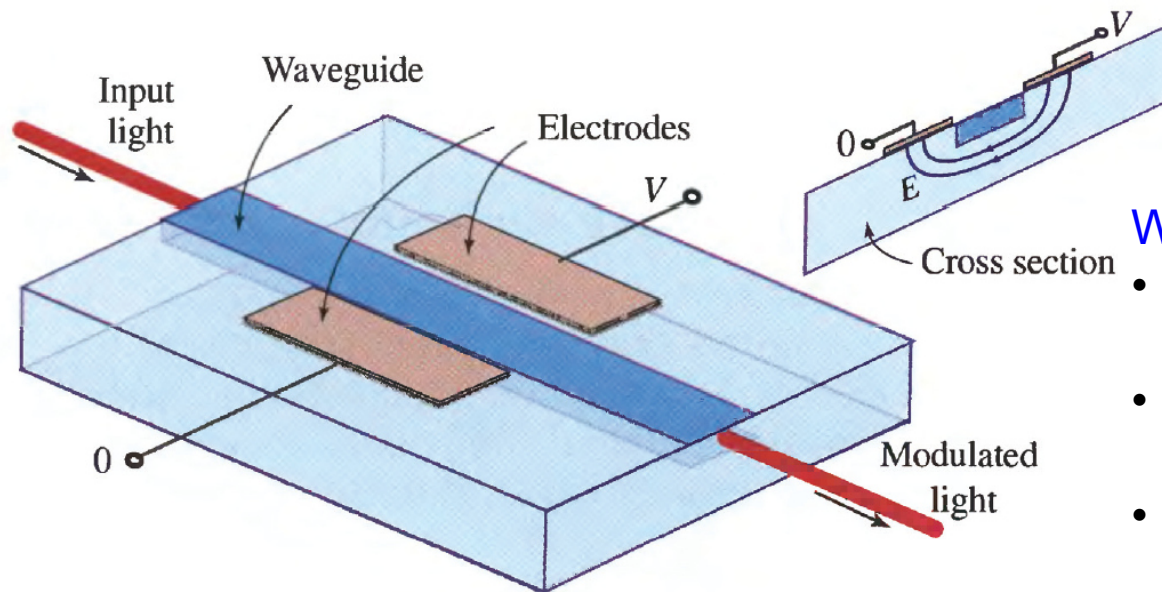
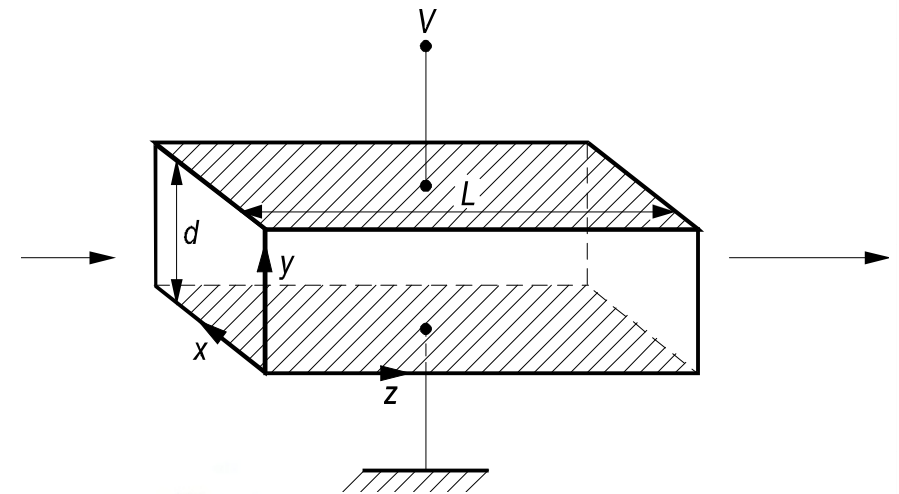
Power transfer function:

$$T(U) = \sin^2\left(\frac{\pi U}{2U_\pi} + \frac{\pi}{4}\right)$$

Power changes linearly with applied voltage.

Transverse modulator

- Modulating electric field **perpendicular to the direction of light propagation**
- **Problem for bulk devices:** Electrode separation d dictated by divergence of optical beam!



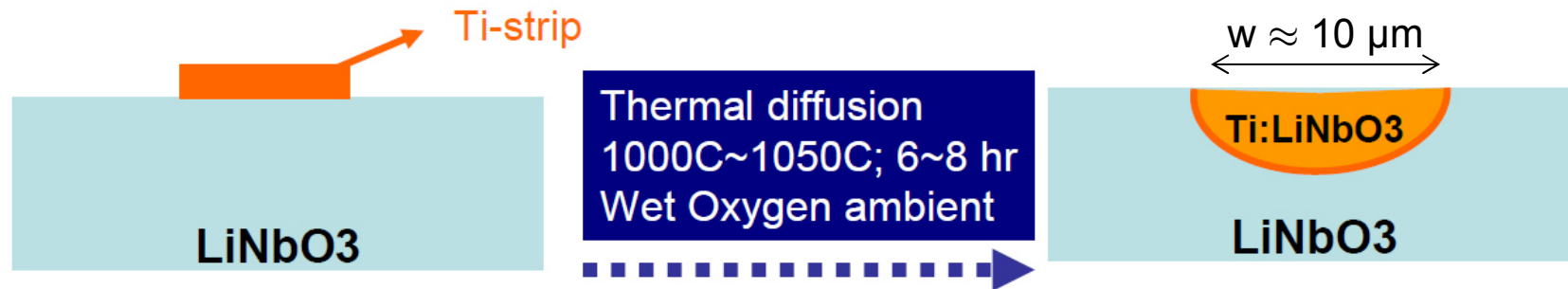
Waveguide-based devices:

- Electrode spacing of a few **micrometers**
- Interaction lengths of a few **centimeters**
- The workhorse of optical communications: **Integrated LiNbO₃ modulators**

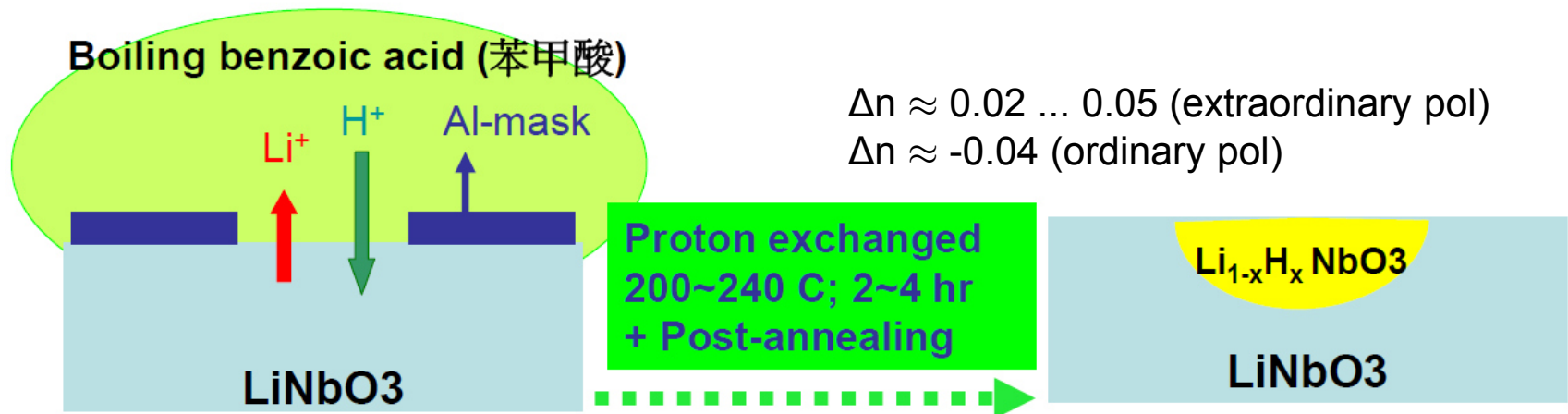
Figure adapted Saleh/Teich, Fundamentals of Photonics

The workhorse of optical communications: Integrated LiNbO₃ modulator

- **Ti-indiffused (TI) waveguides**



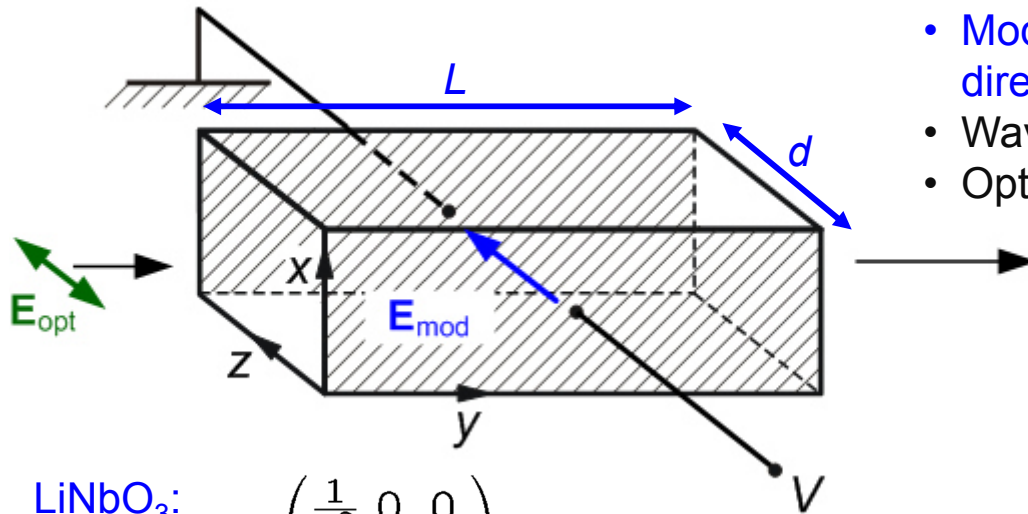
- **Proton-exchanged (PE) waveguides**



Note: Diffusion length along y-direction much larger (and much more uncertain) than along x- and z-direction

⇒ Waveguides usually oriented along y-direction!

Analysis of a transverse LiNbO₃ modulator



- Modulating electric field applied along z-direction
- Wave propagating in y-direction
- Optical mode polarized along z-direction

LiNbO₃:

$$\eta = \begin{pmatrix} \frac{1}{n_o^2} & 0 & 0 \\ 0 & \frac{1}{n_o^2} & 0 \\ 0 & 0 & \frac{1}{n_e^2} \end{pmatrix}, \quad n_o = 2.3410 \\ n_e = 2.2457$$

$$r = \begin{pmatrix} 0 & -r_{22} & r_{13} \\ 0 & r_{22} & r_{13} \\ 0 & 0 & r_{33} \\ 0 & r_{42} & 0 \\ r_{42} & 0 & 0 \\ -r_{22} & 0 & 0 \end{pmatrix}$$

$$r_{13} = 9.6 \frac{\text{pm}}{\text{V}} \\ r_{22} = 6.8 \frac{\text{pm}}{\text{V}} \\ r_{33} = 30.9 \frac{\text{pm}}{\text{V}} \\ r_{42} = 32.6 \frac{\text{pm}}{\text{V}}$$

External voltage along z: Material remains **uniaxial!**

$$\left(\frac{1}{n_o^2} + r_{13}E_z \right) X^2 + \left(\frac{1}{n_o^2} + r_{13}E_z \right) Y^2 + \left(\frac{1}{n_e^2} + r_{33}E_z \right) Z^2 = 1$$

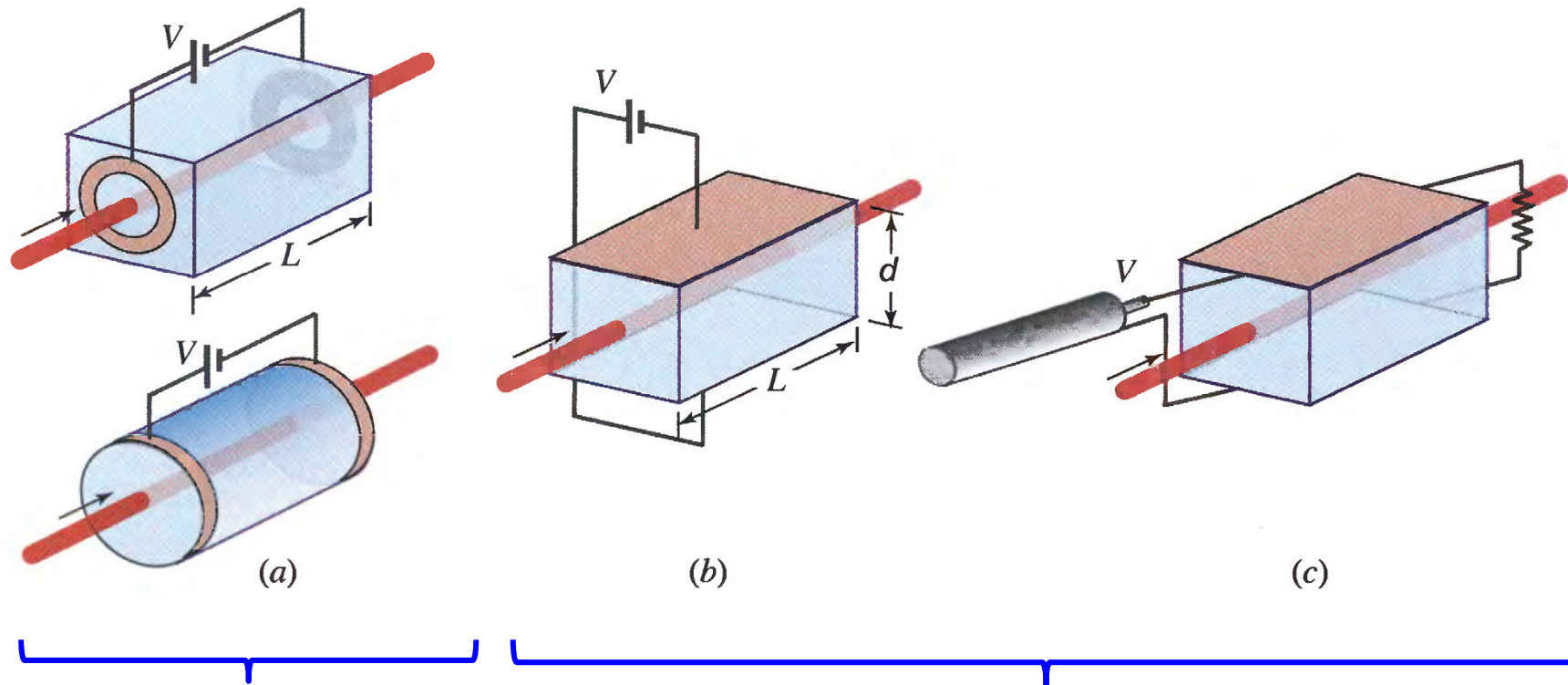
⇒ Refractive index change for plane wave polarized along z / phase shift / π -voltage:

$$\Delta n = -\frac{1}{2}n_e^3 r_{33}E_z \quad \Delta\Phi = \frac{1}{2}n_e^3 r_{33}E_z k_0 L \quad U_\pi = \frac{d \lambda_0}{L r_{33} n_e^3}$$

Lecture 9

Electro-optic modulators

Electro-optic modulators: Exploit second-order nonlinearities to modulate a beam of light by means of an electric signal.

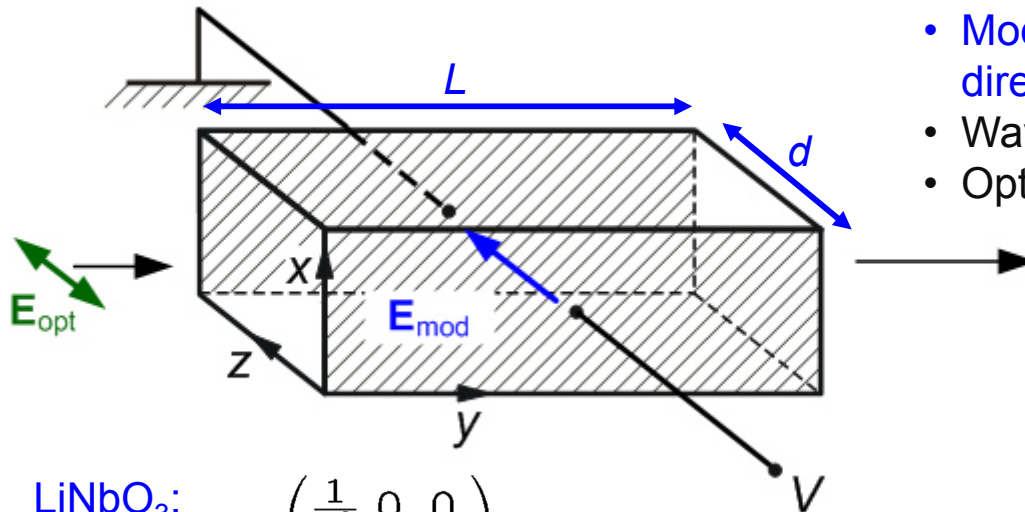


Longitudinal modulators:
Modulating electric field \mathbf{E}_{mod} applied parallel to the direction of light propagation

Transverse modulators:
 \mathbf{E}_{mod} perpendicular to the direction of light propagation.

Figures adapted Saleh/Teich, Fundamentals of Photonics

Analysis of a transverse LiNbO₃ modulator



- Modulating electric field applied along z-direction
- Wave propagating in y-direction
- Optical mode polarized along z-direction

LiNbO₃:

$$\eta = \begin{pmatrix} \frac{1}{n_o^2} & 0 & 0 \\ 0 & \frac{1}{n_o^2} & 0 \\ 0 & 0 & \frac{1}{n_e^2} \end{pmatrix}, \quad \begin{matrix} n_o = 2.3410 \\ n_e = 2.2457 \end{matrix}$$

$$r = \begin{pmatrix} 0 & -r_{22} & r_{13} \\ 0 & r_{22} & r_{13} \\ 0 & 0 & r_{33} \\ 0 & r_{42} & 0 \\ r_{42} & 0 & 0 \\ -r_{22} & 0 & 0 \end{pmatrix}$$

$$\begin{matrix} r_{13} = 9.6 \frac{\text{pm}}{\text{V}} \\ r_{22} = 6.8 \frac{\text{pm}}{\text{V}} \\ r_{33} = 30.9 \frac{\text{pm}}{\text{V}} \\ r_{42} = 32.6 \frac{\text{pm}}{\text{V}} \end{matrix}$$

External voltage along z: Material remains **uniaxial!**

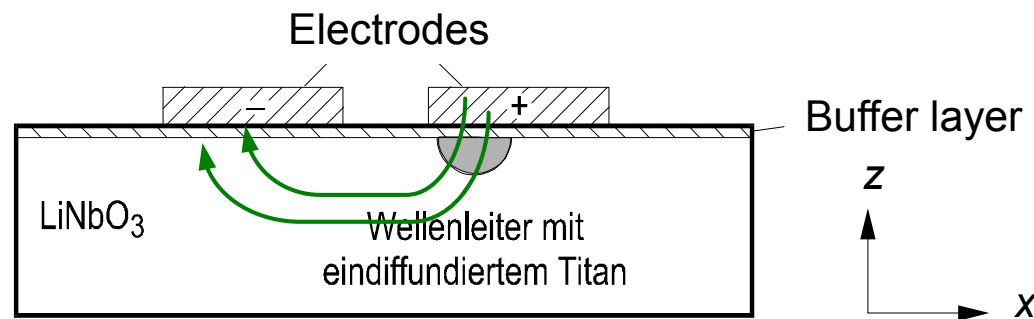
$$\left(\frac{1}{n_o^2} + r_{13}E_z \right) X^2 + \left(\frac{1}{n_o^2} + r_{13}E_z \right) Y^2 + \left(\frac{1}{n_e^2} + r_{33}E_z \right) Z^2 = 1$$

⇒ Refractive index change for plane wave polarized along z / phase shift / π -voltage:

$$\Delta n = -\frac{1}{2}n_e^3 r_{33}E_z \quad \Delta\Phi = \frac{1}{2}n_e^3 r_{33}E_z k_0 L \quad U_\pi = \frac{d \lambda_0}{L r_{33} n_e^3}$$

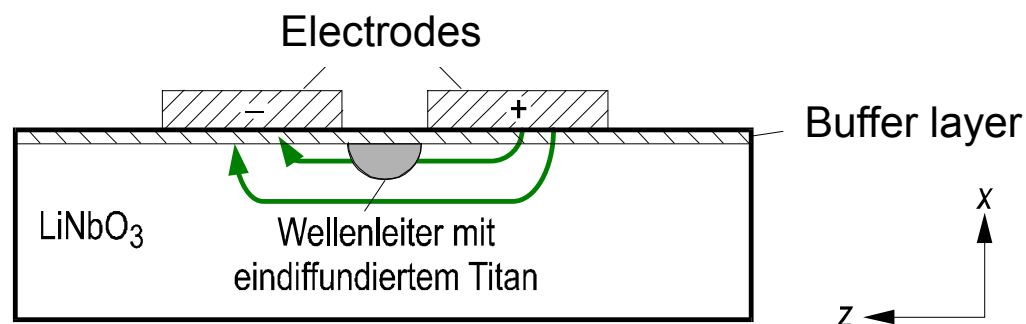
Technical realization: x-cut and z-cut geometry

z-cut geometry:



- Wafer surface normal to z-direction
- Modulating field oriented vertically (along z-direction)
- Waveguide oriented along y-direction
- “TM-polarization”, i.e., dominant electric field component of the optical mode oriented along z-direction

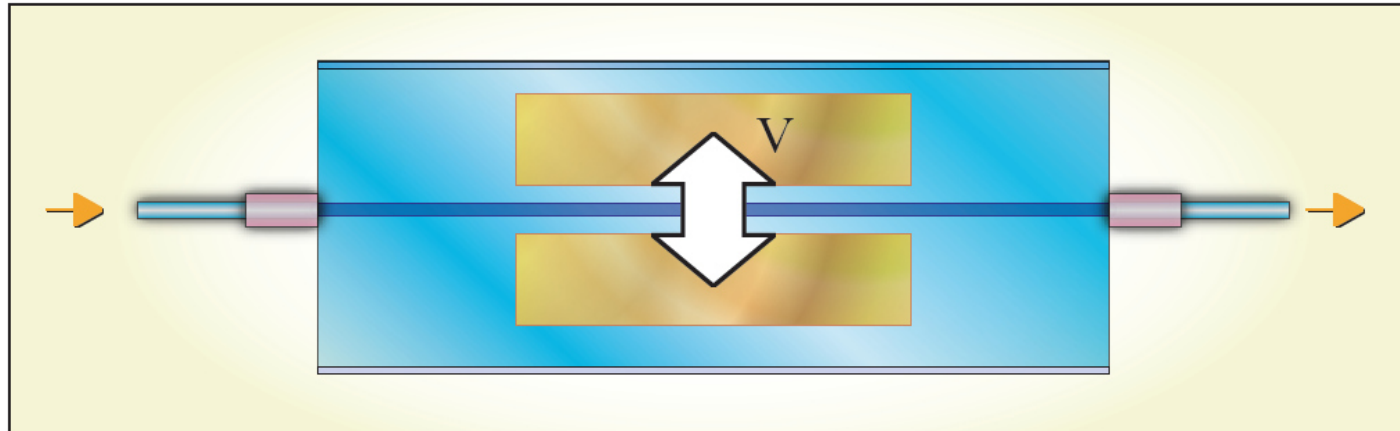
x-cut geometry:



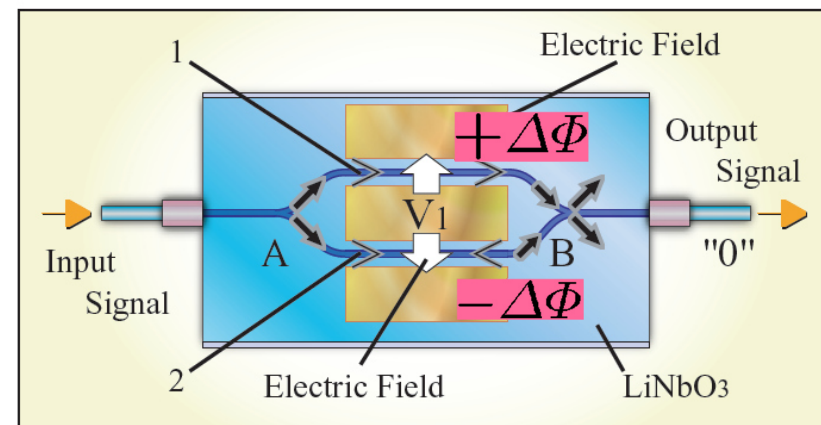
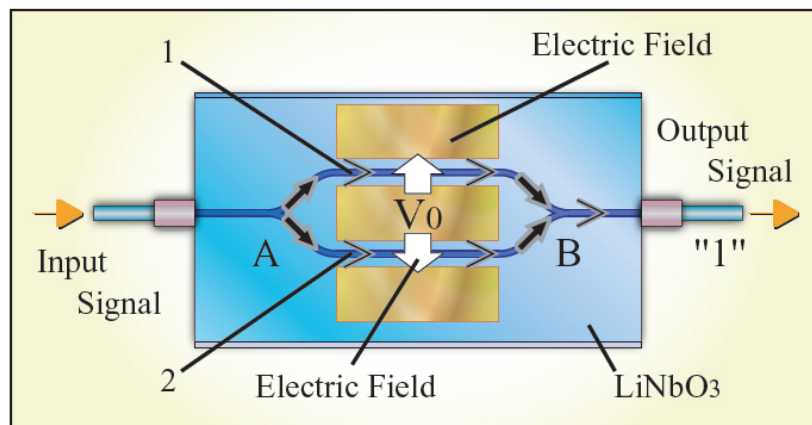
- Wafer surface normal to x-direction
- Modulating field oriented horizontally (along z-direction)
- Waveguide oriented along y-direction
- “TE-polarization”, i.e., dominant electric field component of the optical mode oriented along z-direction

The Mach-Zehnder Modulator (MZM)

So far: Phase modulator



Turning a phase modulator into an amplitude modulator: Mach-Zehnder Modulator (MZM)



Here: Push-pull configuration, i.e., antisymmetric phase shifts in both arms of the interferometer (same magnitude, opposite sign)

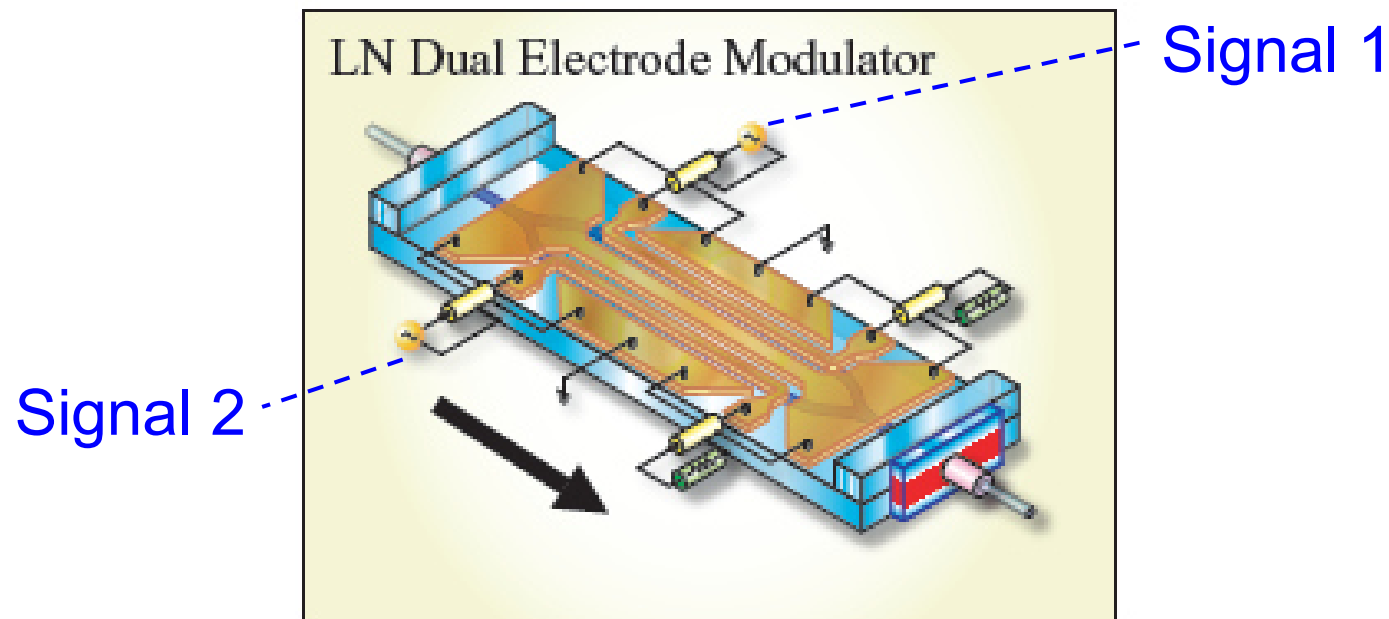
⇒ Chirp-free operation

Figures adapted from [Sumitomo Modulator Application Note](#).

Dual-drive Mach-Zehnder Modulator

Individual transmission line for each modulator arm

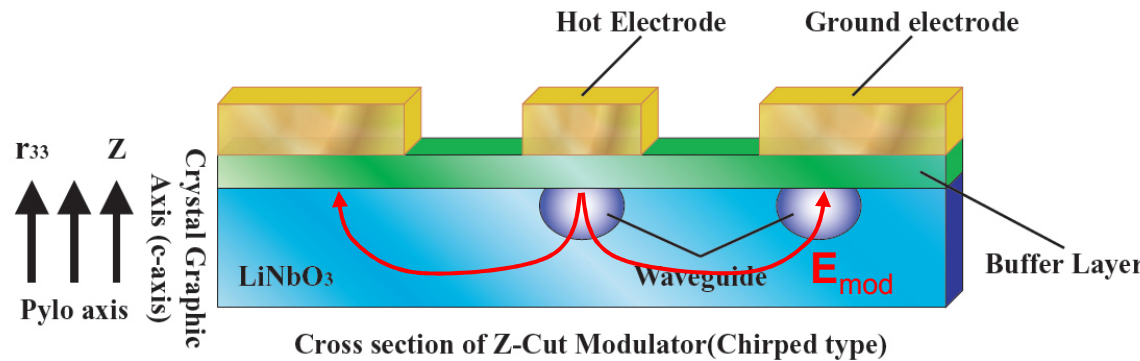
⇒ Dual-drive / dual-electrode configuration:



Figures adapted from [Sumitomo Modulator Application Note](#).

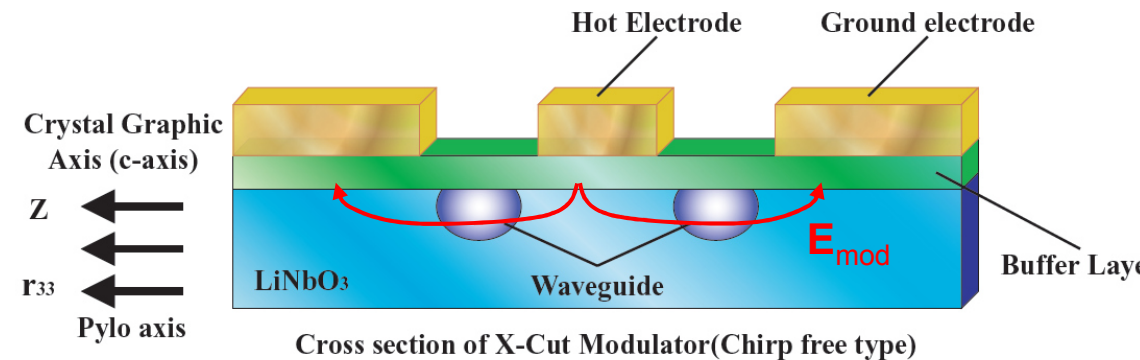
Push-pull modulation in z-cut and x-cut configuration

Combine push-pull modulator with **coplanar transmission line**:



z-cut:

- Electrodes placed on top of the waveguide
- Electric field flux concentrated for center electrode ("hot electrode")
- ⇒ Good overlap between optical field and RF field; high efficiency
- Reduced overlap for ground electrode
- ⇒ Asymmetric modulation; **slightly chirped output signal**

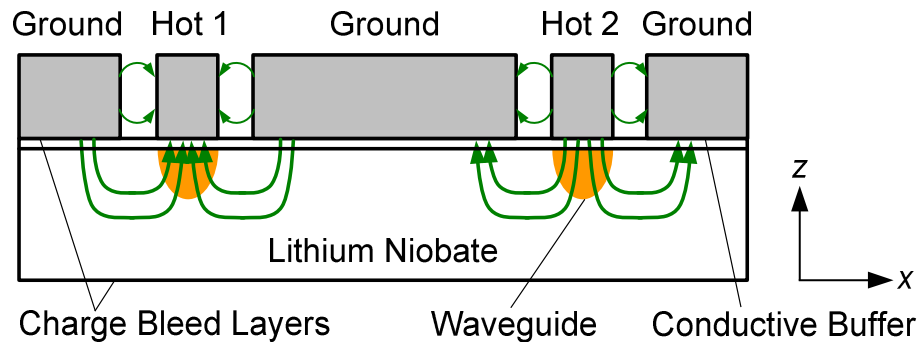


x-cut:

- Slightly decreased efficiency, but equal overlap for both arms
- ⇒ Antisymmetric modulation; **unchirped output signal**

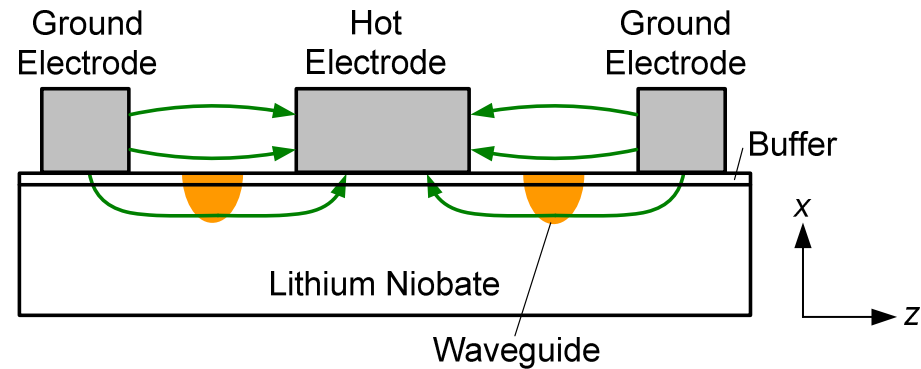
Figures adapted from [Sumitomo Modulator Application Note](#).

Two more examples...



z-cut dual-drive modulator:

- Good overlap of modulating RF-field and optical field
- ⇒ Low switching voltage, good electro-optic efficiency
- Push-pull-operation requires two RF-signals of identical amplitude but opposite sign



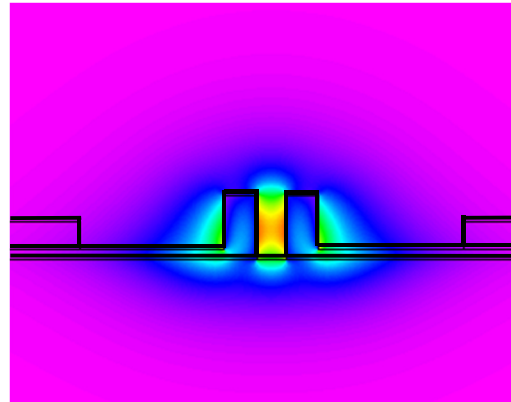
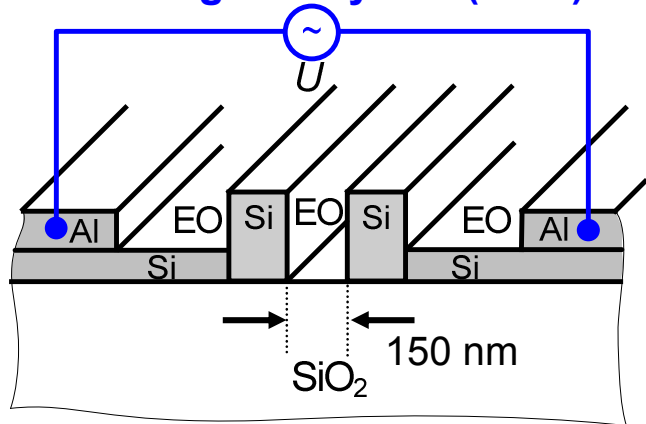
x-cut push-pull modulator:

- Push-pull operation with a single RF signal
- ⇒ Chirp-free modulation
- Needs approx. 20% higher voltage as compared to z-cut configuration

Ed L. Wooten *et al.*, IEEE J. Sel. Topics Quant. Electron. **6**, 69-82 (2000)

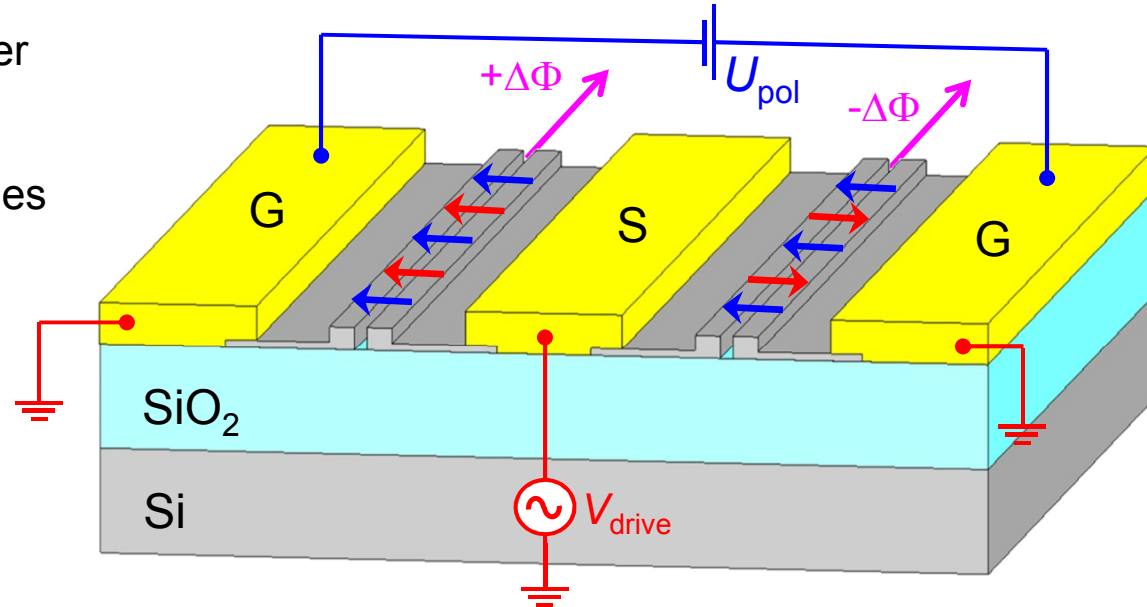
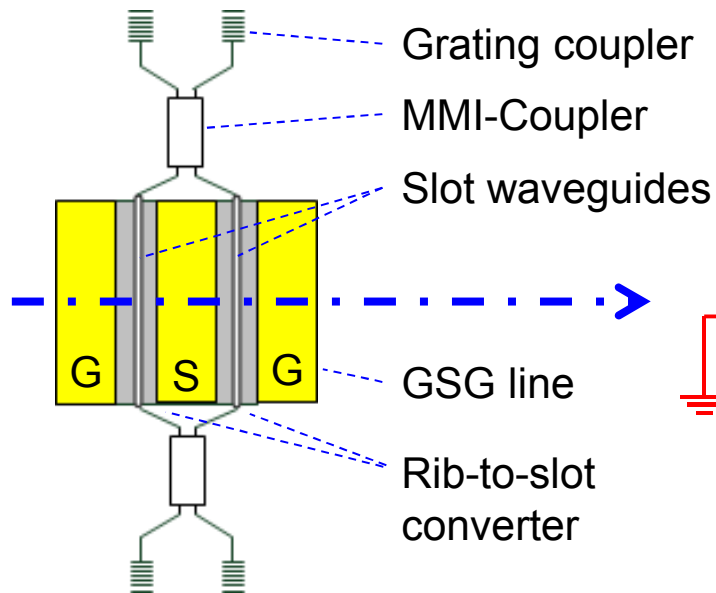
Ongoing research at IPQ: Silicon-based modulators

Silicon-organic hybrid (SOH) device: Silicon slot waveguide + organic electro-optic cladding

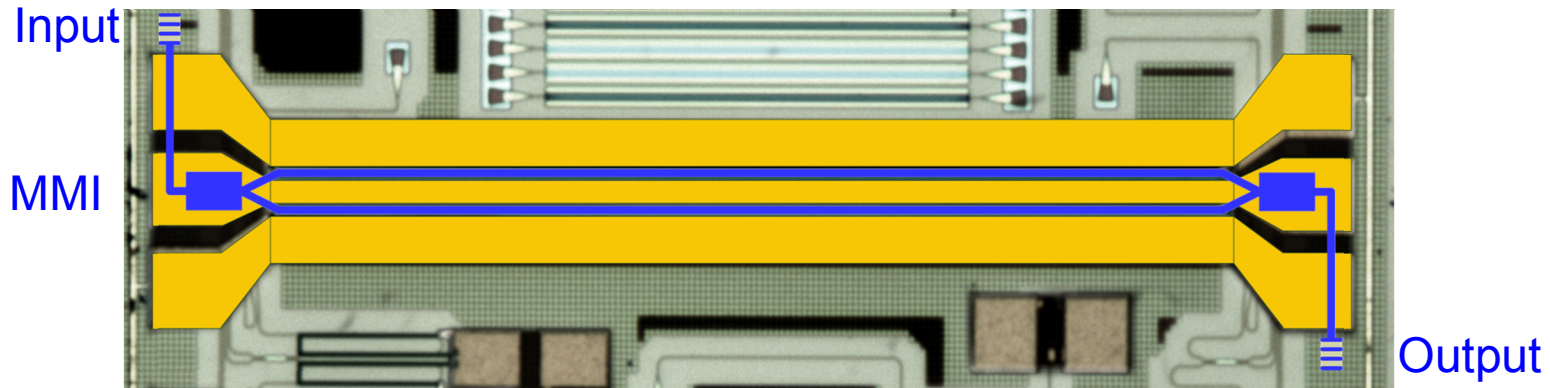


- Good overlap between optical field and RF field
- Small electrode spacing

Push-pull configuration:

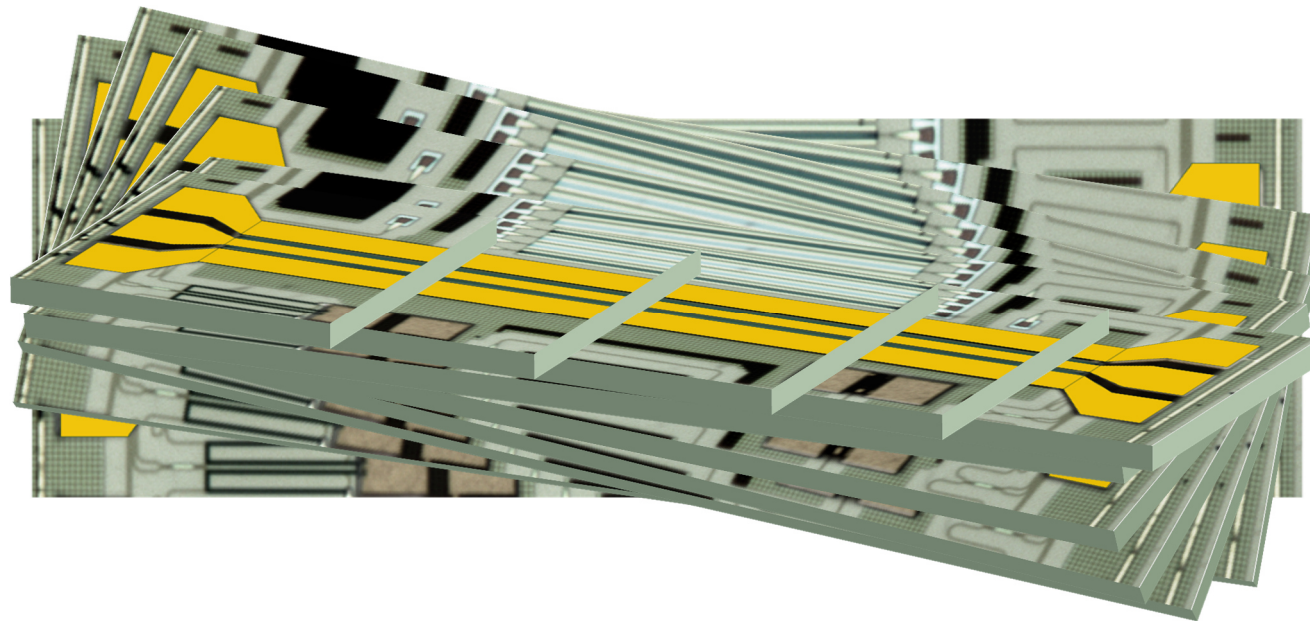


SOH Mach-Zehnder Modulators: Implementation

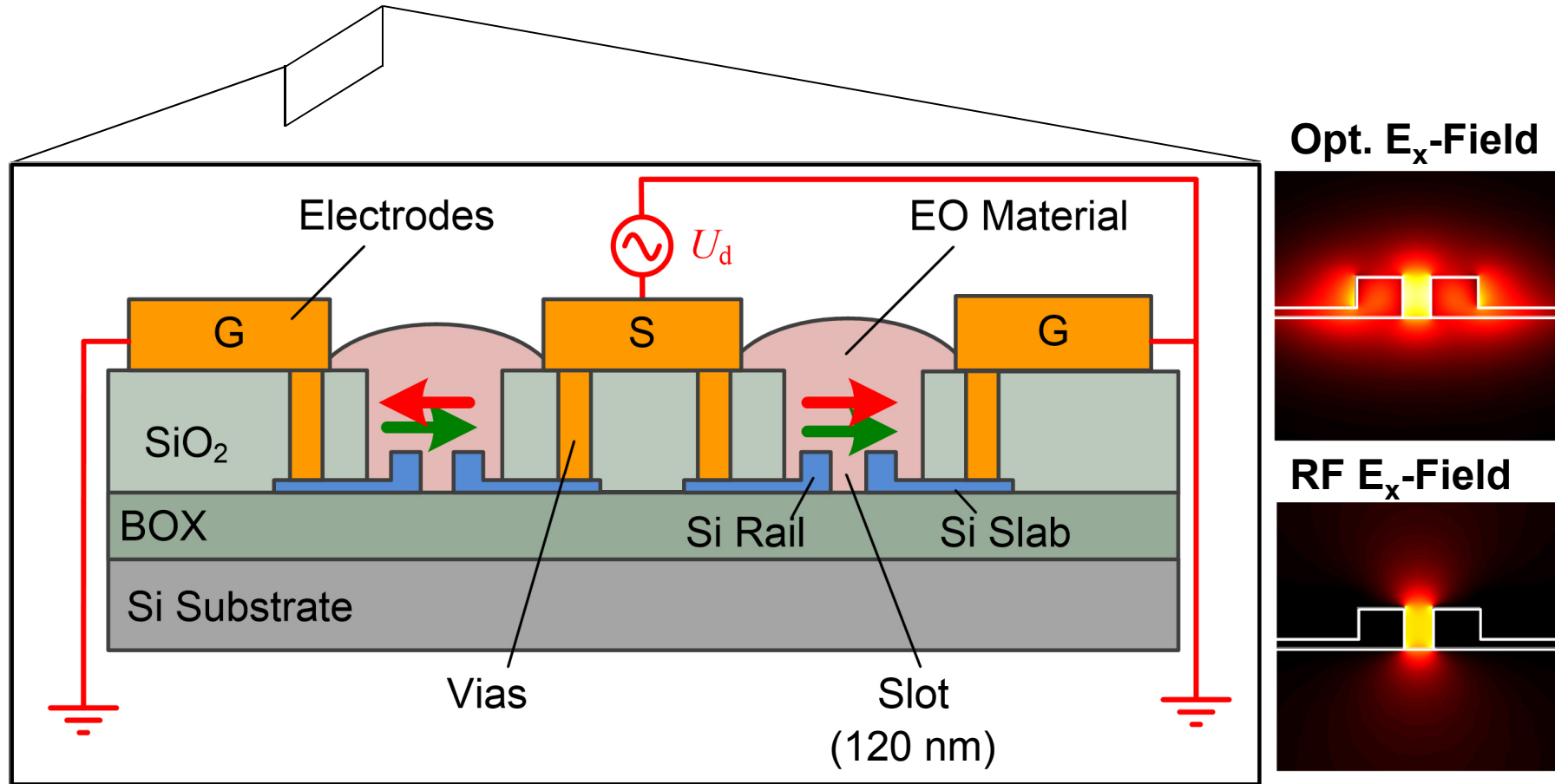


- Basic silicon photonic waveguide structures fabricated in standard silicon photonic line along with full portfolio of other devices (pn modulators, SiGe detectors *etc.*)
⇒ High integration density, high yield
- Organic EO materials deposited and poled in a post-processing step
⇒ No compatibility issues, efficient large-area processing

SOH Mach-Zehnder Modulators: Implementation



SOH Mach-Zehnder Modulators: Implementation

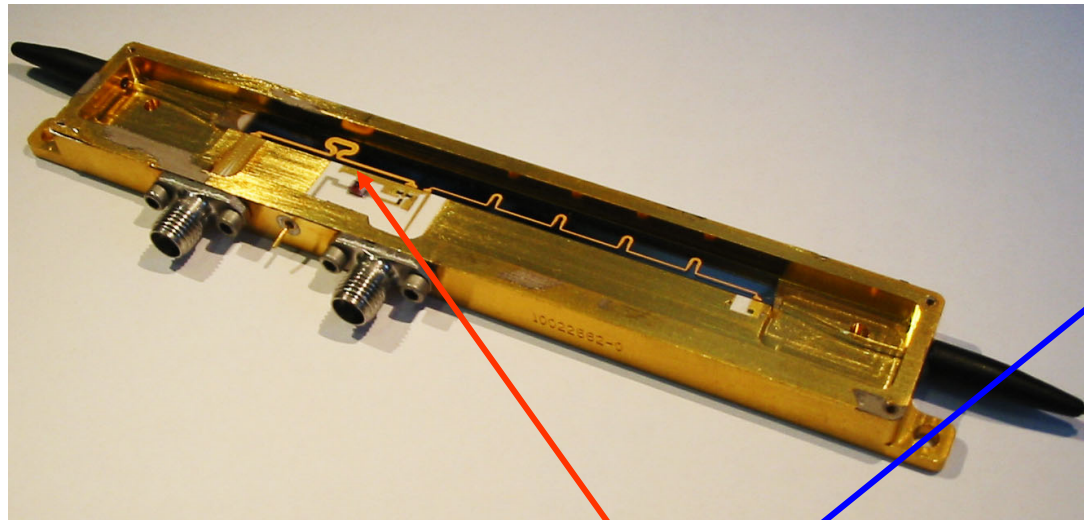


Chirp-free push-pull operation!

Koos *et al.*, J. Lightw. Technol. **34**, 256-268 (2016)

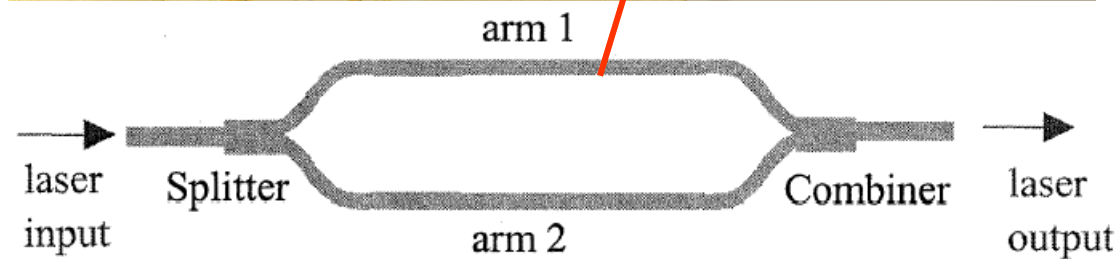
Koeber *et al.*, Light Sci Appl **4**, (2015)

Finally: A real device ...



State-of-the-art LiNbO_3 amplitude modulator

- X-cut push-pull configuration
- RF delay loops to match phase of RF line and optical signal



Sum-frequency generation and impact of phase mismatch

Recall: Evolution of complex field amplitudes during propagation through a nonlinear medium (SVEA)

$$\frac{\partial \underline{E}'(z', t', \omega_l)}{\partial z'} = -j \frac{\omega_l}{2\epsilon_0 c n} \underline{P}'_{\text{NL}}(z', t', \omega_l) e^{-j(k_{p,l} - k_l)z'}$$

Phase mismatch
↙

Now: Investigate impact of phase mismatch on interaction of three waves oscillating at frequencies ω_1 , ω_2 , and $\omega_3 = \omega_1 + \omega_2$.

Assume **fixed polarizations** along unit vectors \mathbf{e}_i :

$$\underline{\mathbf{E}}(z, t, \omega_i) = \underline{E}(z, t, \omega_i) \mathbf{e}_i, \quad \underline{\mathbf{P}}(z, t, \omega_3) = \underline{P}(z, t, \omega_3) \mathbf{e}_3,$$

$$\Rightarrow \begin{aligned} \frac{\partial \underline{E}(z, t, \omega_3)}{\partial z} &= -j \frac{\omega_3}{c n(\omega_3)} d_{\text{eff}} \underline{E}(z, t, \omega_1) \underline{E}(z, t, \omega_2) e^{-j\Delta k z}, \\ \frac{\partial \underline{E}(z, t, \omega_1)}{\partial z} &= -j \frac{\omega_1}{c n(\omega_1)} d_{\text{eff}} \underline{E}(z, t, \omega_3) \underline{E}^*(z, t, \omega_2) e^{j\Delta k z}, \\ \frac{\partial \underline{E}(z, t, \omega_2)}{\partial z} &= -j \frac{\omega_2}{c n(\omega_2)} d_{\text{eff}} \underline{E}(z, t, \omega_3) \underline{E}^*(z, t, \omega_1) e^{j\Delta k z}. \end{aligned}$$

where $\Delta k = k_1 + k_2 - k_3$ **Wave vector mismatch**

$$d_{\text{eff}} = \frac{1}{2} \sum_{q,r,s} \mathbf{e}_{3,q} \chi_{q:r,s}^{(2)}(\omega_3 : \omega_1, \omega_2) \mathbf{e}_{1,r} \mathbf{e}_{2,s}$$

**Effective 2nd-order
nonlinear susceptibility**

Phase matching considerations

Zero phase mismatch: Linear increase of converted amplitude (depletion at ω_1 and ω_2 neglected):

$$\underline{E}(L, t, \omega_3)|_{\Delta k=0} \approx -j \frac{\omega_3}{cn(\omega_3)} d_{\text{eff}} \underline{E}(0, t, \omega_1) \underline{E}(0, t, \omega_2) L$$

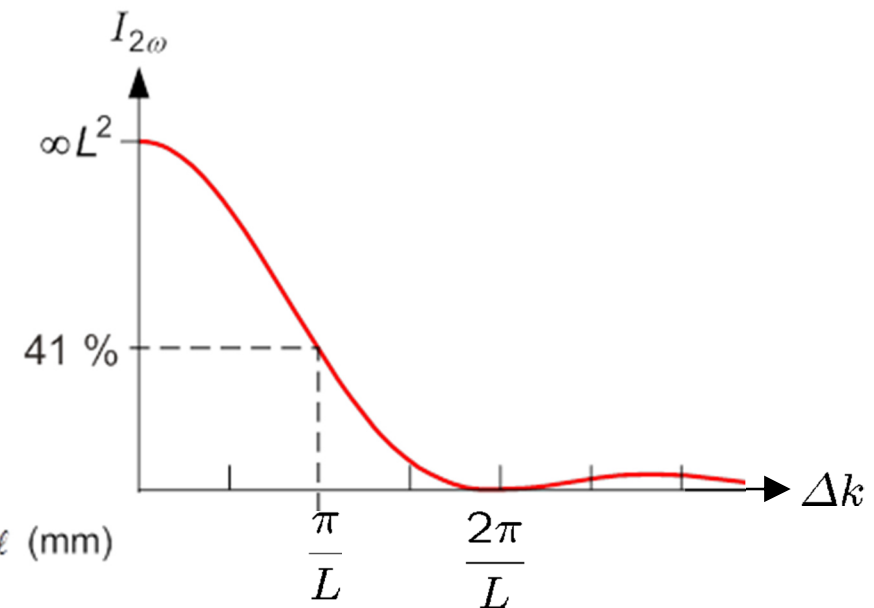
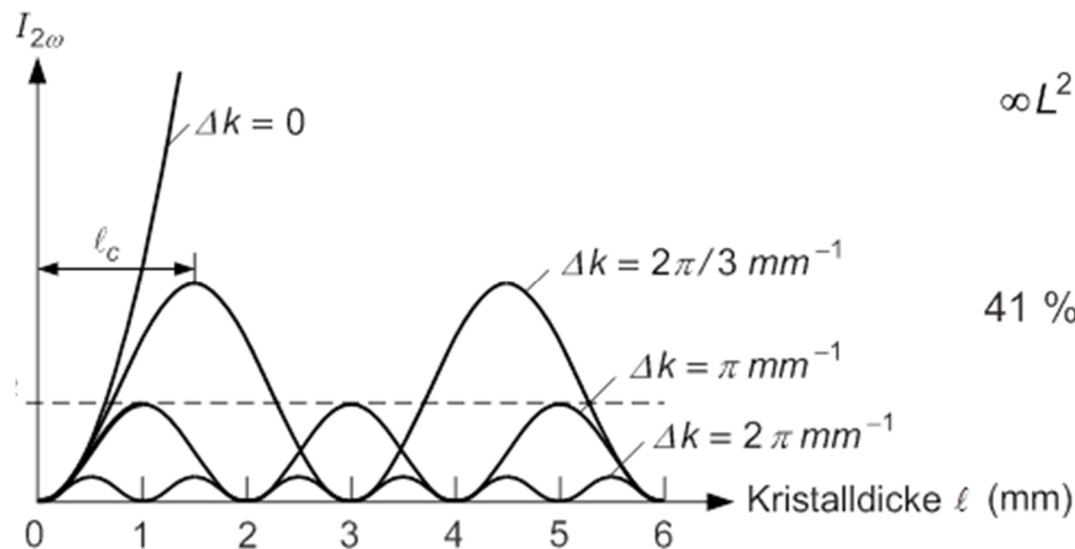
Non-zero phase mismatch: Oscillatory behavior

$$\underline{E}(L, t, \omega_3)|_{\Delta k \neq 0} = -j \frac{\omega_3}{cn(\omega_3)} d_{\text{eff}} \underline{E}(0, t, \omega_1) \underline{E}(0, t, \omega_2) \frac{2}{\Delta k} \sin\left(\frac{\Delta k L}{2}\right) e^{-j\frac{\Delta k L}{2}}.$$

⇒ Considerable decrease of the power conversion efficiency:

$$\left| \frac{\underline{E}(L, t, \omega_3)|_{\Delta k \neq 0}}{\underline{E}(L, t, \omega_3)|_{\Delta k=0}} \right|^2 = \frac{\sin^2\left(\frac{\pi L}{2 L_{\text{coh}}}\right)}{\left(\frac{\pi L}{2 L_{\text{coh}}}\right)^2}.$$

$$L_{\text{coh}} = \frac{\pi}{\Delta k}.$$



Lecture 10

Sum-frequency generation and impact of phase mismatch

Recall: Evolution of complex field amplitudes during propagation through a nonlinear medium (SVEA) Phase mismatch

$$\frac{\partial \underline{E}'(z', t', \omega_l)}{\partial z'} = -j \frac{\omega_l}{2\epsilon_0 c n} \underline{P}'_{\text{NL}}(z', t', \omega_l) e^{-j(k_{p,l} - k_l)z'}$$

Now: Investigate impact of phase mismatch on interaction of three waves oscillating at frequencies ω_1 , ω_2 , and $\omega_3 = \omega_1 + \omega_2$.

Assume **fixed polarization directions** along unit vectors \mathbf{e}_i :

$$\underline{\mathbf{E}}(z, t, \omega_i) = \underline{E}(z, t, \omega_i) \mathbf{e}_i, \quad \underline{\mathbf{P}}(z, t, \omega_3) = \underline{P}(z, t, \omega_3) \mathbf{e}_3,$$

$$\begin{aligned} \Rightarrow \frac{\partial \underline{E}(z, t, \omega_3)}{\partial z} &= -j \frac{\omega_3}{c n(\omega_3)} d_{\text{eff}} \underline{E}(z, t, \omega_1) \underline{E}(z, t, \omega_2) e^{-j\Delta k z}, \\ \frac{\partial \underline{E}(z, t, \omega_1)}{\partial z} &= -j \frac{\omega_1}{c n(\omega_1)} d_{\text{eff}} \underline{E}(z, t, \omega_3) \underline{E}^*(z, t, \omega_2) e^{j\Delta k z}, \\ \frac{\partial \underline{E}(z, t, \omega_2)}{\partial z} &= -j \frac{\omega_2}{c n(\omega_2)} d_{\text{eff}} \underline{E}(z, t, \omega_3) \underline{E}^*(z, t, \omega_1) e^{j\Delta k z}. \end{aligned}$$

where $\Delta k = k_1 + k_2 - k_3$ Wave vector mismatch

$$d_{\text{eff}} = \frac{1}{2} \sum_{q,r,s} \mathbf{e}_{3,q} \chi_{q:r,s}^{(2)}(\omega_3 : \omega_1, \omega_2) \mathbf{e}_{1,r} \mathbf{e}_{2,s}$$

Effective 2nd-order
nonlinear susceptibility

Phase matching considerations

Zero phase mismatch: Linear increase of converted amplitude (depletion at ω_1 and ω_2 neglected):

$$\underline{E}(L, t, \omega_3)|_{\Delta k=0} \approx -j \frac{\omega_3}{cn(\omega_3)} d_{\text{eff}} \underline{E}(0, t, \omega_1) \underline{E}(0, t, \omega_2) L$$

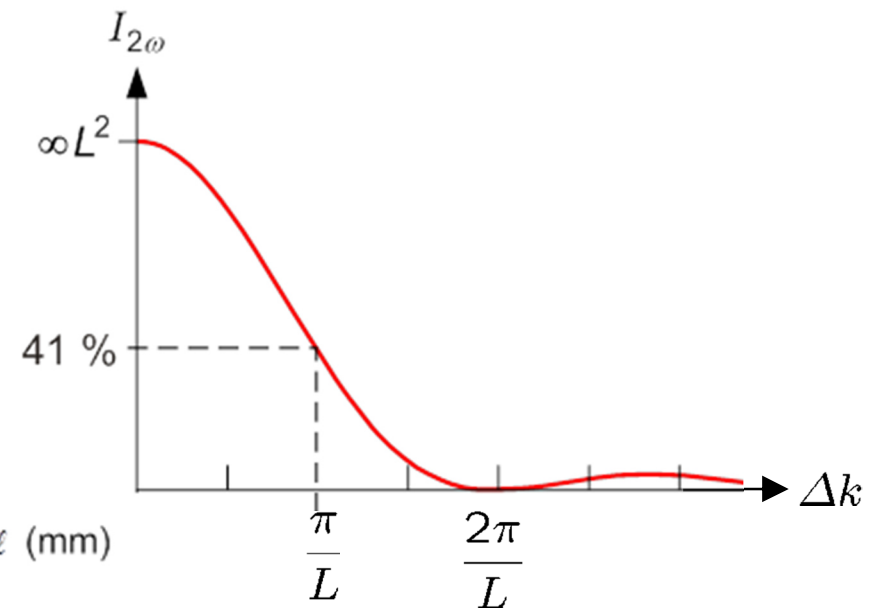
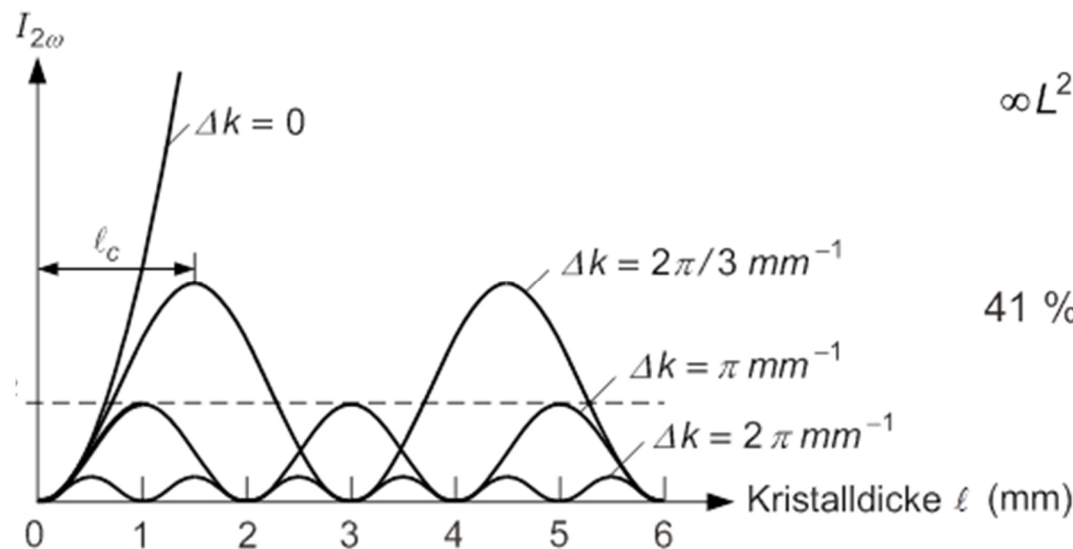
Non-zero phase mismatch: Oscillatory behavior

$$\underline{E}(L, t, \omega_3)|_{\Delta k \neq 0} = -j \frac{\omega_3}{cn(\omega_3)} d_{\text{eff}} \underline{E}(0, t, \omega_1) \underline{E}(0, t, \omega_2) \frac{2}{\Delta k} \sin\left(\frac{\Delta k L}{2}\right) e^{-j\frac{\Delta k L}{2}}$$

⇒ Considerable decrease of the power conversion efficiency:

$$\left| \frac{\underline{E}(L, t, \omega_3)|_{\Delta k \neq 0}}{\underline{E}(L, t, \omega_3)|_{\Delta k=0}} \right|^2 = \frac{\sin^2\left(\frac{\pi L}{2 L_{\text{coh}}}\right)}{\left(\frac{\pi L}{2 L_{\text{coh}}}\right)^2}$$

$$L_{\text{coh}} = \frac{\pi}{\Delta k}$$



Phase matching concepts

Phase matching conditions:

$$\text{SFG: } \omega_1 n(\omega_1) + \omega_2 n(\omega_2) - \omega_3 n(\omega_3) = 0$$

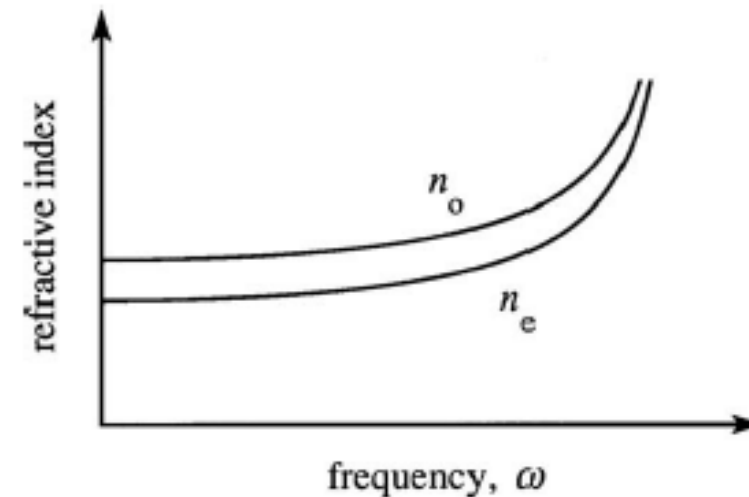
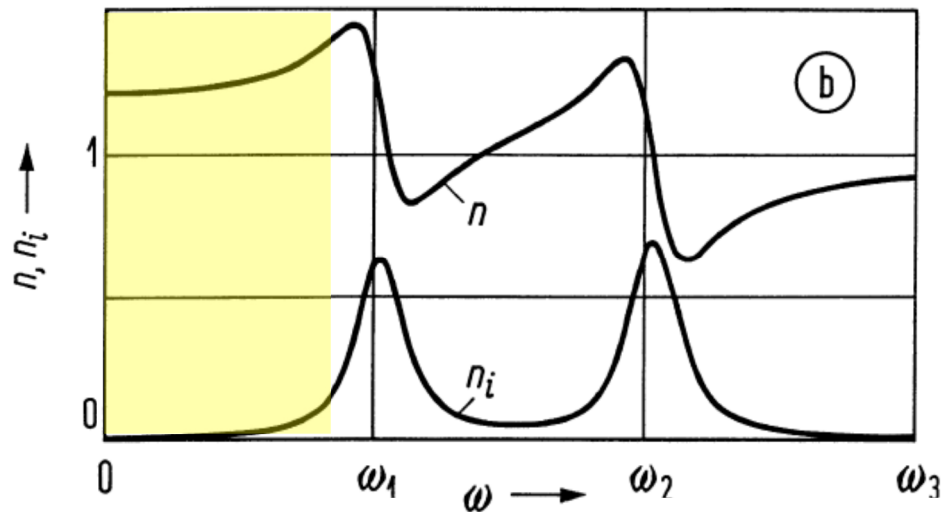
$$\text{SHG: } n(\omega_1) = n(2\omega_1)$$

Mostly: Materials operated below resonance frequencies

⇒ Normal (phase velocity) dispersion, i.e., refractive index increases with frequency

⇒ Phase matching conditions cannot be fulfilled.

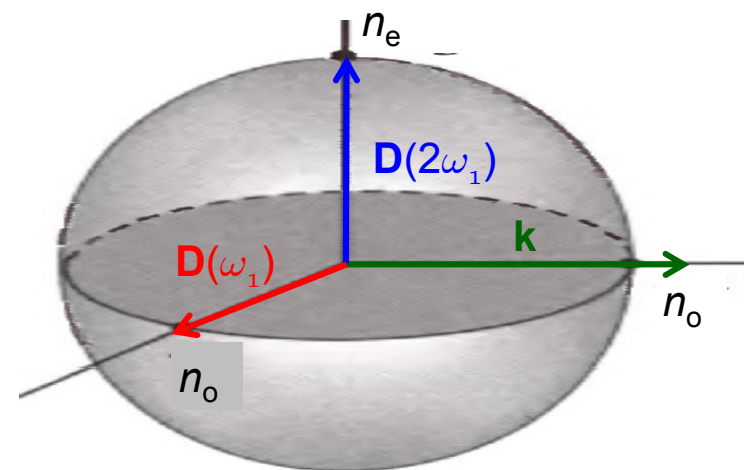
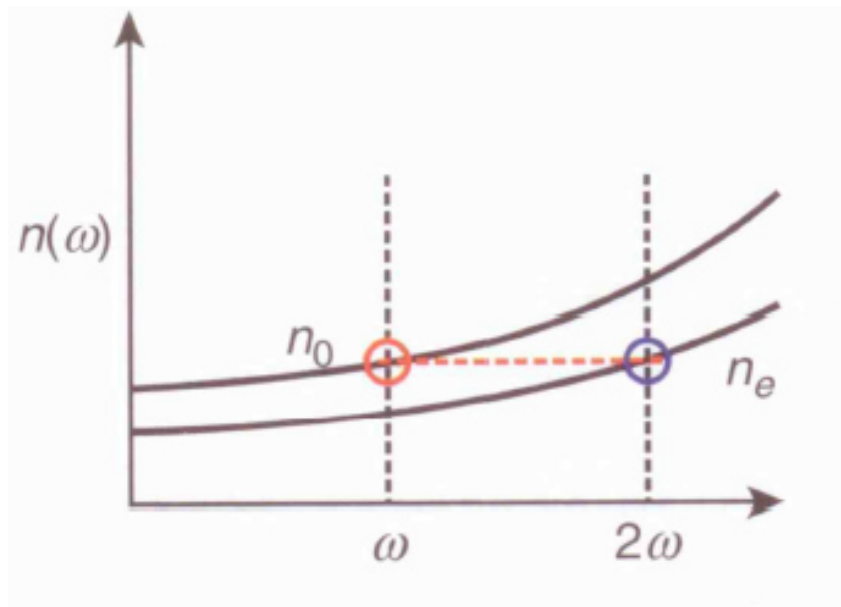
Idea: Exploit birefringence for phase matching!



Type-1 phase matching in negative-uniaxial crystal

Type-1 phase matching: Lower-frequency components have the same polarization

Second-harmonic generation (SHG): $n_e(2\omega_1) = n_o(\omega_1)$ $[oo \rightarrow e]$



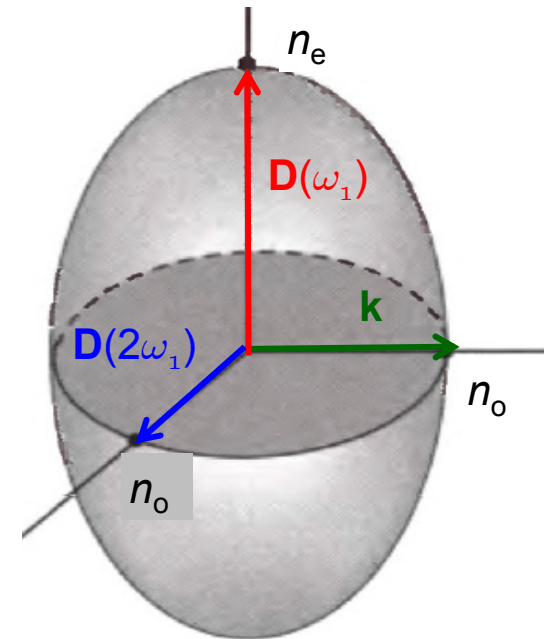
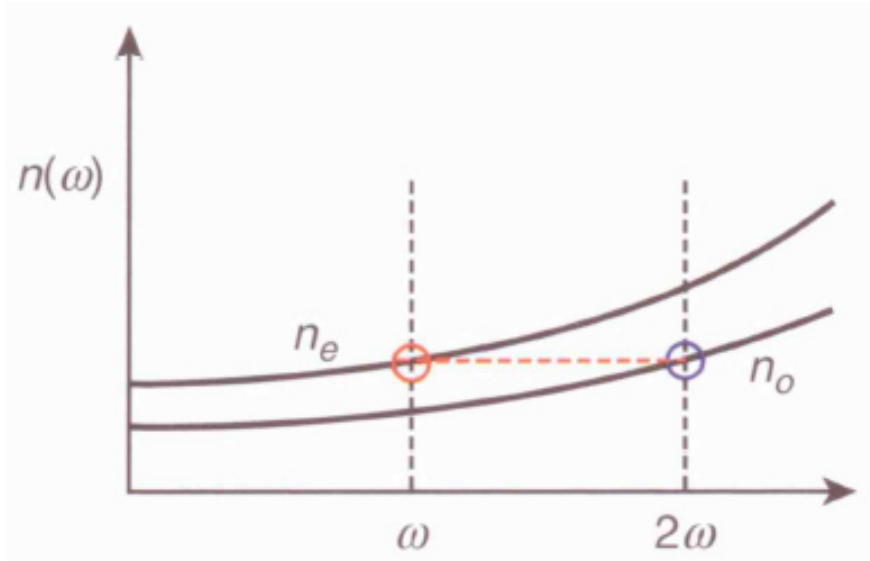
Sum-frequency generation (SFG):

$$\omega_3 n_e(\omega_3) = \omega_1 n_o(\omega_1) + \omega_2 n_o(\omega_2) \quad [oo \rightarrow e]$$

Figures adapted from Stegeman, Nonlinear Optics
and Saleh-Teich, Fundamentals of Photonics

Type-1 phase matching in positive-uniaxial crystal

Second-harmonic generation (SHG): $n_o(2\omega_1) = n_e(\omega_1)$ $[ee \rightarrow o]$



Sum-frequency generation (SFG):

$$\omega_3 n_o(\omega_3) = \omega_1 n_e(\omega_1) + \omega_2 n_e(\omega_2) \quad [ee \rightarrow o]$$

Figures adapted from Stegeman, Nonlinear Optics and Saleh-Teich, Fundamentals of Photonics

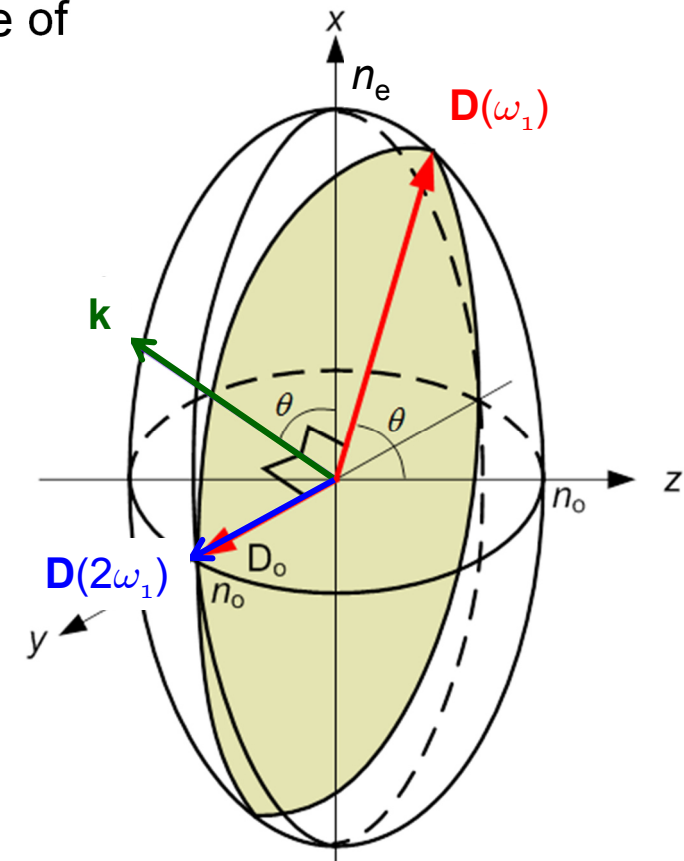
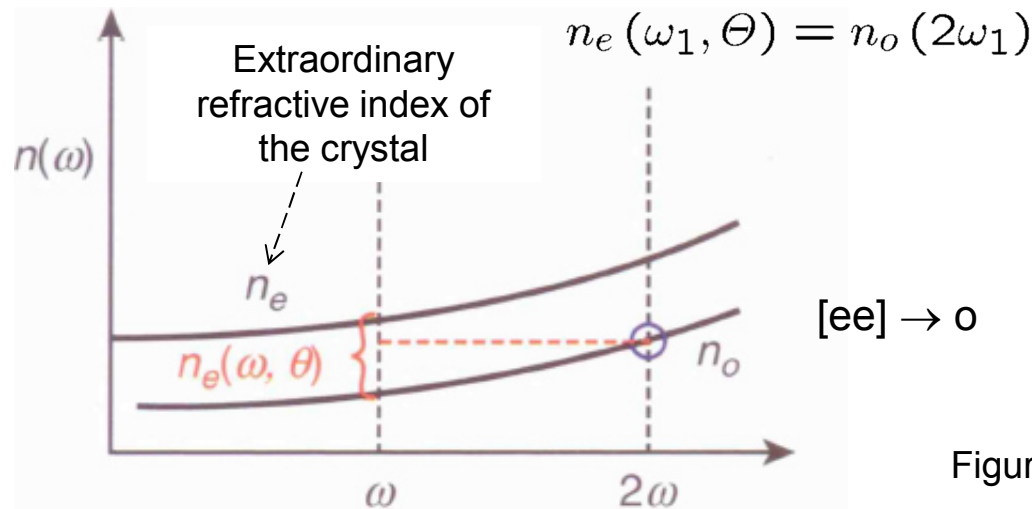
Type-1 phase matching: Tuning options

Temperature tuning:

- Birefringence is temperature-dependent
⇒ Phase-matching by varying the temperature of the crystal!
- Example LiNbO_3 : Strong temperature dependence of birefringence.

Angle tuning:

- Adjust propagation direction of the involved light beams to obtain phase matching
- **Example:** Second-harmonic generation in a **positive-uniaxial** crystal



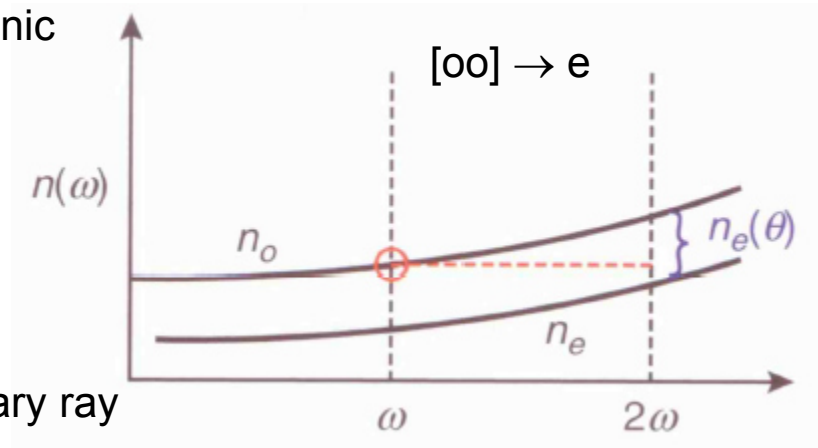
Figures adapted from Stegeman, Nonlinear Optics and Saleh-Teich, Fundamentals of Photonics

Type-1 phase matching: Calculation of propagation angle

Example: Type-1 phase matching for second-harmonic generation in a **negative-uniaxial** crystal

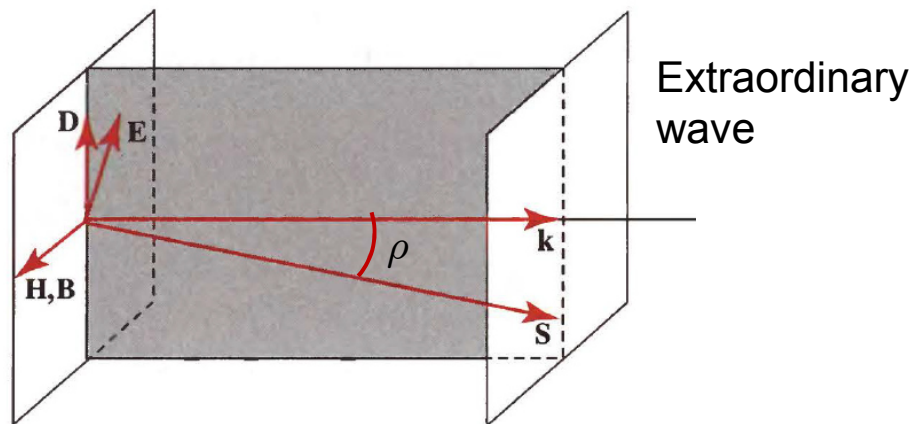
$$n_e(2\omega_1, \Theta_p) = n_o(\omega_1)$$

$$\Rightarrow \tan \Theta_p = \frac{n_e(2\omega_1)}{n_o(2\omega_1)} \sqrt{\frac{n_o^2(2\omega_1) - n_o^2(\omega_1)}{n_o^2(\omega_1) - n_e^2(2\omega_1)}}$$

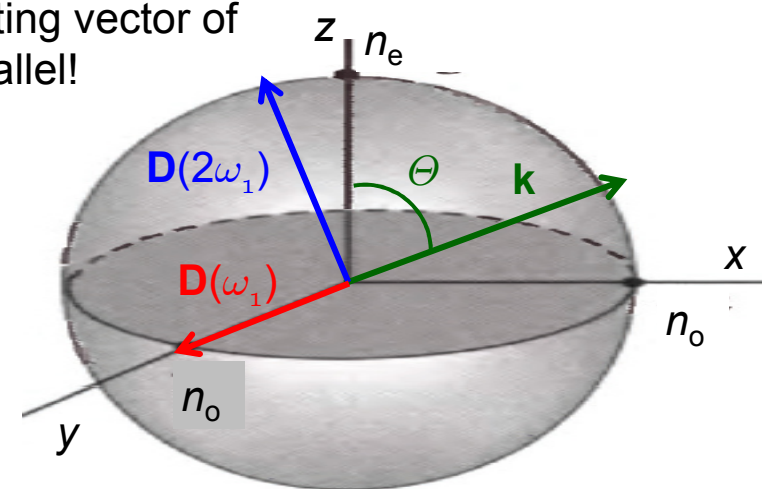


Problem: Walk-off between ordinary and extraordinary ray

Recall: Poynting vector and wave vector of the extraordinary ray are not parallel, and hence the Poynting vector of the fundamental and the second harmonic are not parallel!



$$\cos(\rho) = \frac{n_e^2(2\omega_1) \cos^2(\Theta_p) + n_o^2(2\omega_1) \sin^2(\Theta_p)}{\sqrt{n_e^4(2\omega_1) \cos^2(\Theta_p) + n_o^4(2\omega_1) \sin^2(\Theta_p)}}$$



Figures adapted from Stegeman, Nonlinear Optics and Saleh-Teich, Fundamentals of Photonics

Type-2 phase matching

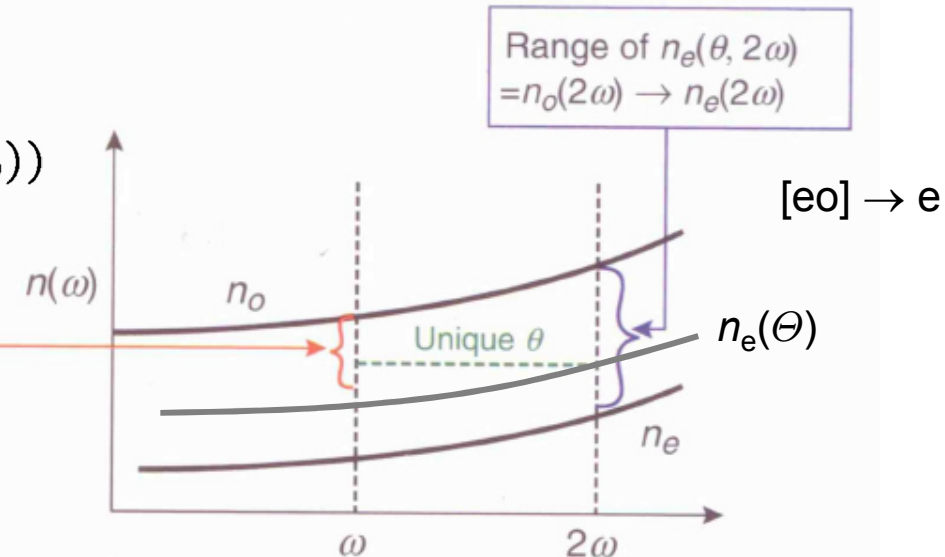
For strong birefringence: Type-1 phase-matching would overcompensate phase velocity mismatch and require large propagation angles

⇒ Type-2 phase matching: Lower-frequency components have different polarizations

Negative-uniaxial crystal:

$$n_e(2\omega_1, \Theta_p) = \frac{1}{2} (n_o(\omega_1) + n_e(\omega_1, \Theta_p))$$

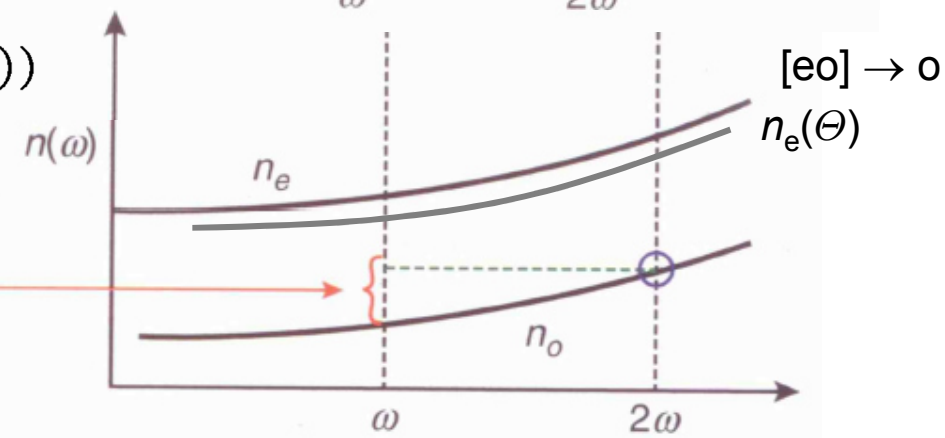
$$\text{Range of } \frac{1}{2}[n_o(\omega) + n_e(\theta, \omega)] = n_o(\omega) \rightarrow \frac{1}{2}[n_o(\omega) + n_e(\omega)]$$



Positive-uniaxial crystal:

$$n_o(2\omega_1) = \frac{1}{2} (n_o(\omega_1) + n_e(\omega_1, \Theta_p))$$

$$\text{Range of } \frac{1}{2}[n_o(\omega) + n_e(\theta, \omega)] = n_o(\omega) \rightarrow \frac{1}{2}[n_o(\omega) + n_e(\omega)]$$

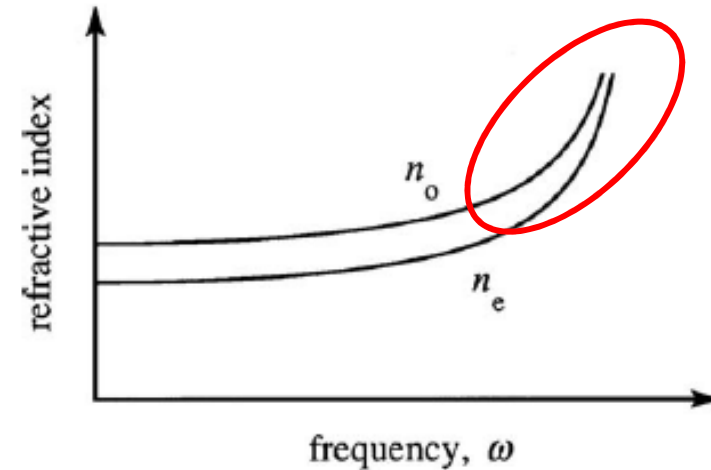
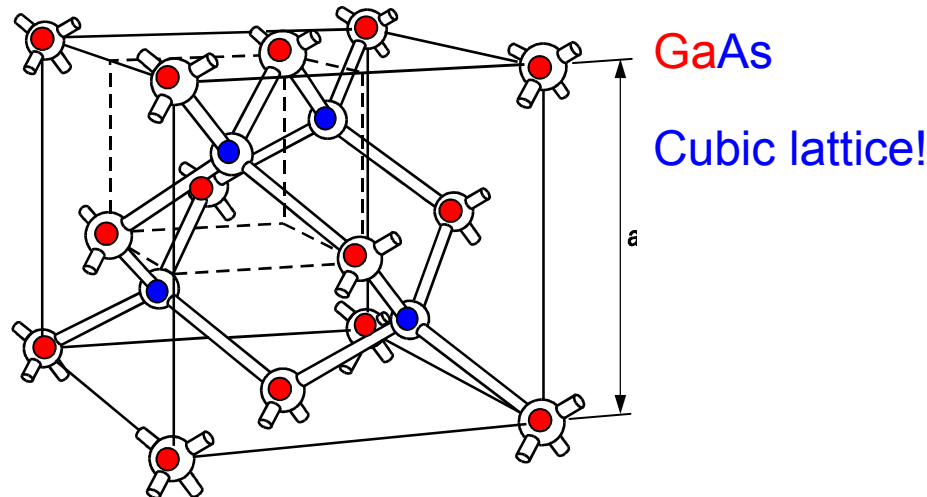


Figures adapted from Stegeman, Nonlinear Optics

Quasi-phase-matching

In some cases we cannot use birefringence to achieve phase matching:

- Nonlinear material is **not birefringent**
- Birefringence **too weak / dispersion too strong**, e.g., at short wavelengths



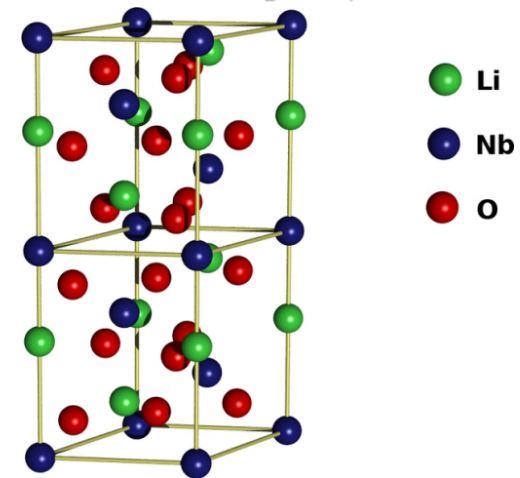
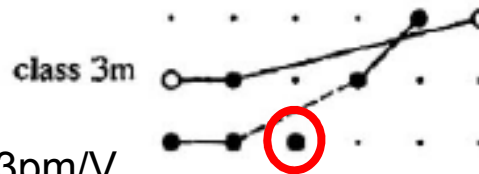
- Exploit **strong d_{33} coefficient**; this requires waves that are polarized in the same direction

LiNbO₃:

$$d_{22} \approx 3 \text{ pm/V}$$

$$d_{31} \approx -5 \text{ pm/V}$$

$$d_{33} \approx -25 \text{ pm/V}$$



Figures adapted from Boyd, Nonlinear Optics

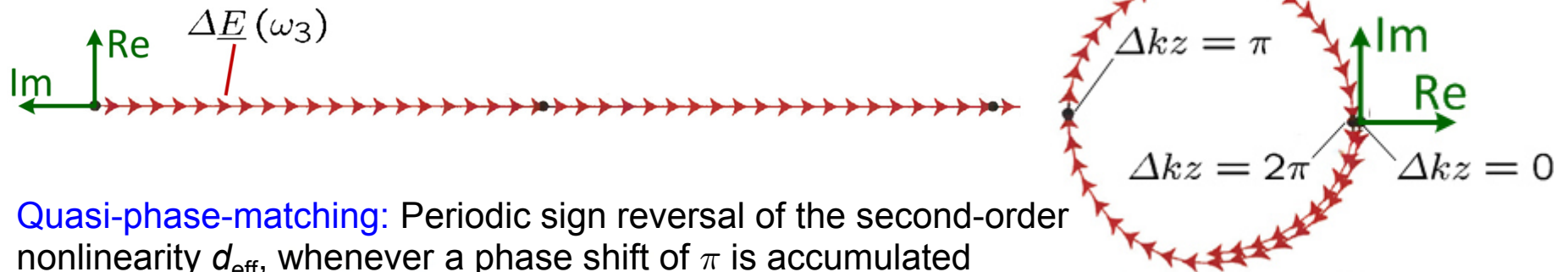
The principle of quasi-phase-matching (QPM)

Problem of phase mismatch: Continuous change of phase of new contributions along z .

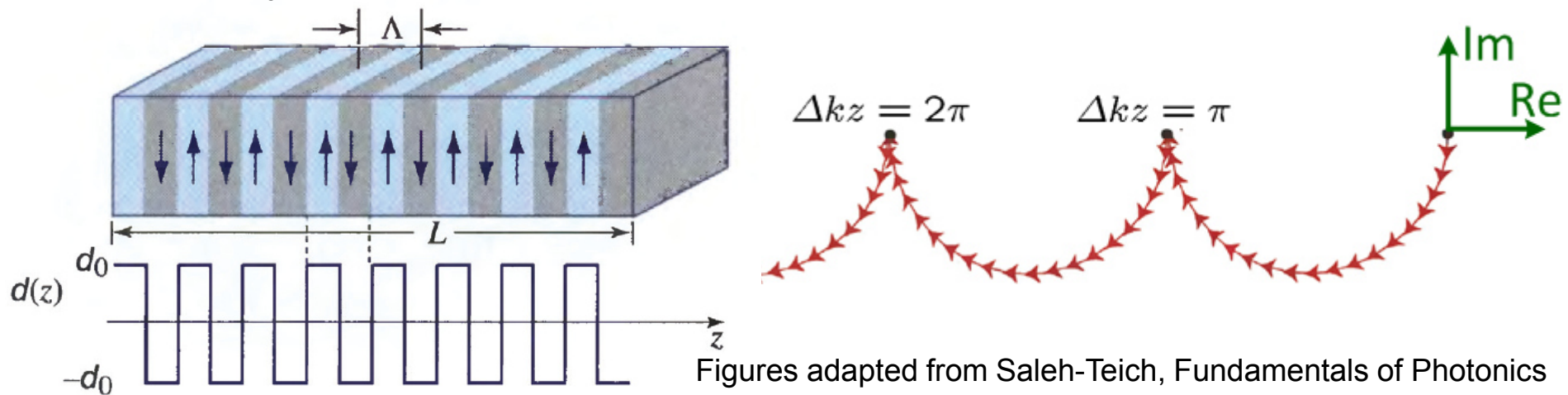
$$\frac{\partial \underline{E}(z, t, \omega_3)}{\partial z} = -j \frac{\omega_3}{c n(\omega_3)} d_{\text{eff}} \underline{E}(z, t, \omega_1) \underline{E}(z, t, \omega_2) e^{-j\Delta k z},$$

Phase matching: $\Delta k = 0$

Phase mismatch: $\Delta k \neq 0$

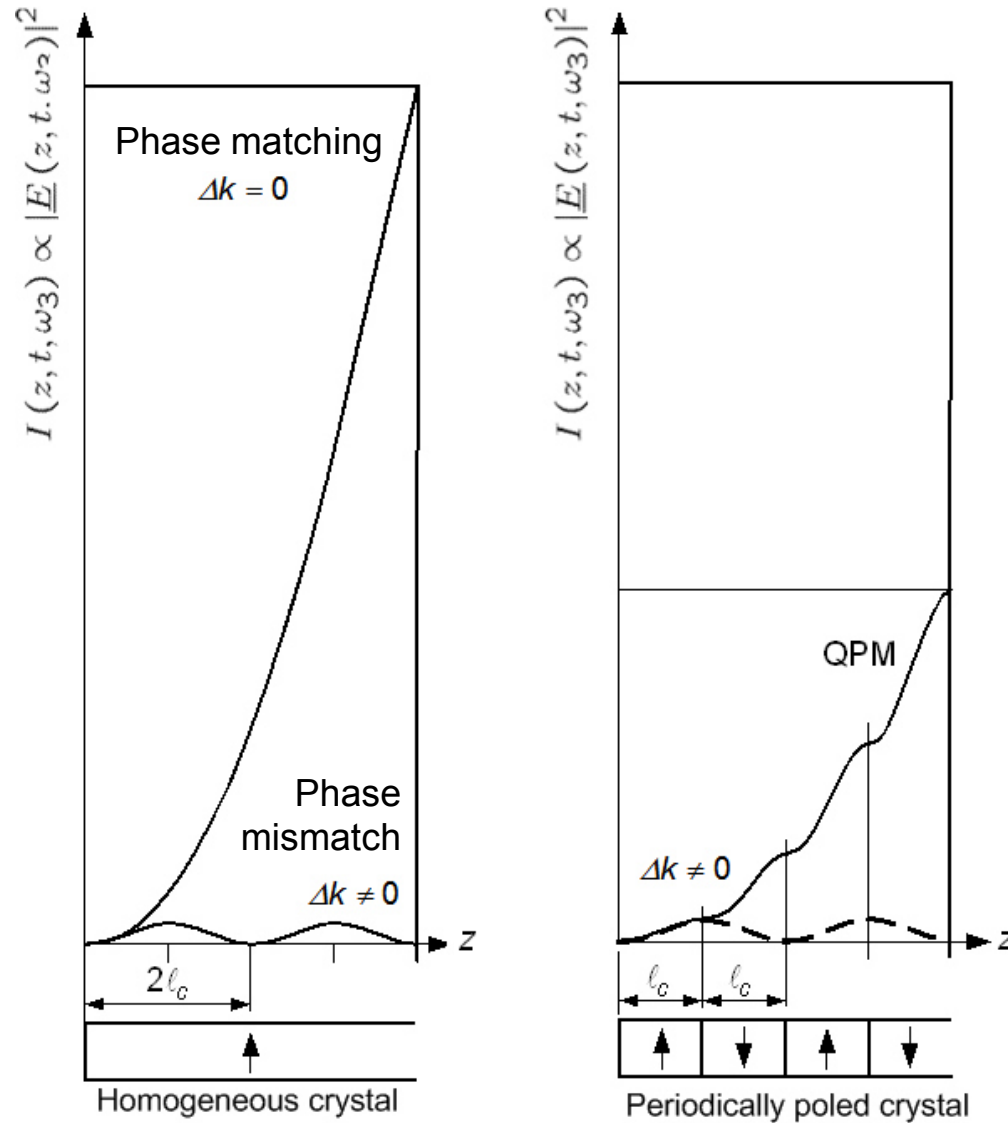


Quasi-phase-matching: Periodic sign reversal of the second-order nonlinearity d_{eff} , whenever a phase shift of π is accumulated



Figures adapted from Saleh-Teich, Fundamentals of Photonics

Quasi-phase-matching (QPM)



Evolution of converted wave amplitude $I(z, t, \omega) \propto |E(z, t, \omega)|^2$ along z .

$$l_c = L_{\text{coh}} = \frac{\pi}{\Delta k}$$

Quasi-phase-matching: Sign reversal after L_{coh} (additional phase shift of π)

Quasi-phase-matching (QPM)

Evolution of converted wave amplitude $E(z,t,\omega)$ along z :

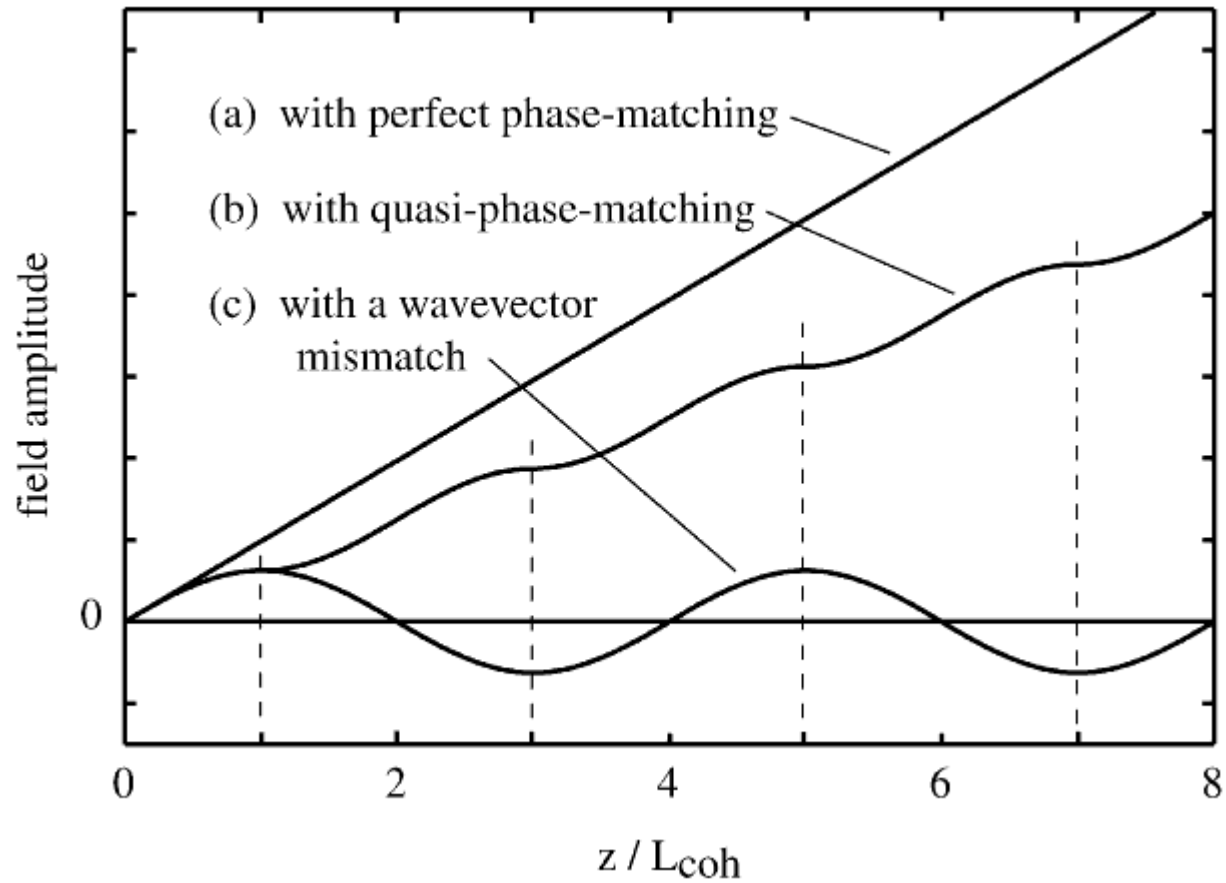


Figure adapted from Boyd, Nonlinear Optics

Evolution of converted wave along z:

$$\frac{\partial \underline{E}(z, t, \omega_3)}{\partial z} = -j \frac{\omega_3}{c n(\omega_3)} d_{\text{eff}} \underline{E}(z, t, \omega_1) \underline{E}(z, t, \omega_2) e^{-j\Delta k z},$$

Introduce periodic effective second-order nonlinearity: $d_{\text{eff}}(z + \Lambda) = d_{\text{eff}}(z)$

$$d_{\text{eff}}(z) = \sum_m d_m e^{jm \frac{2\pi}{\Lambda} z},$$

$$\frac{\partial \underline{E}(z, t, \omega_3)}{\partial z} = -j \frac{\omega_3}{c n(\omega_3)} \sum_m d_m \underline{E}(z, t, \omega_1) \underline{E}(z, t, \omega_2) e^{-j\left(\Delta k - m \frac{2\pi}{\Lambda}\right) z},$$

Phase-matching by first-order interaction (m=1): $\Lambda = \frac{2\pi}{\Delta k}$,

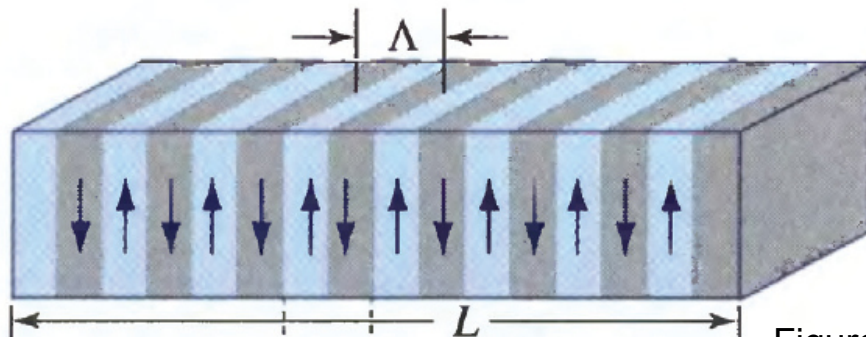


Figure adapted from Saleh-Teich, Fundamentals of Photonics

Principle:

- Lithium Niobate is a ferroelectric crystal, i.e., each unit cell in the crystal has a small electric dipole moment, depending on the positions of the niobium and lithium atoms in the unit cell.
- A strong electric field (~ 22 kV/mm) can locally invert the crystal structure and flip the orientation of the dipole moment and of the second-order nonlinear susceptibility tensor.

Fabrication of PPLN:

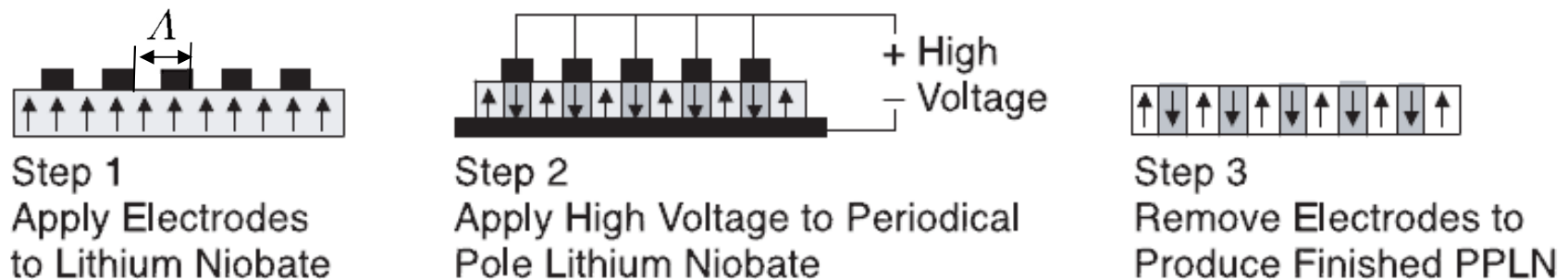


Figure adapted from Thorlabs, Tutorial on Periodically Poled Lithium Niobate (PPLN) , www.thorlabs.com

The Manley-Rowe relations

Consider interaction of 3 waves oscillating at frequencies ω_1 , ω_2 , and $\omega_3 = \omega_1 + \omega_2$:

$$\frac{\partial \underline{E}(z, t, \omega_3)}{\partial z} = -j \frac{\omega_3}{cn(\omega_3)} d_{\text{eff}} \underline{E}(z, t, \omega_1) \underline{E}(z, t, \omega_2) e^{-j\Delta kz},$$

$$\frac{\partial \underline{E}(z, t, \omega_1)}{\partial z} = -j \frac{\omega_1}{cn(\omega_1)} d_{\text{eff}} \underline{E}(z, t, \omega_3) \underline{E}^*(z, t, \omega_2) e^{j\Delta kz},$$

$$\frac{\partial \underline{E}(z, t, \omega_2)}{\partial z} = -j \frac{\omega_2}{cn(\omega_2)} d_{\text{eff}} \underline{E}(z, t, \omega_3) \underline{E}^*(z, t, \omega_1) e^{j\Delta kz}.$$

Intensity: $I(z, t, \omega_i) = \frac{1}{2} \epsilon_0 cn(\omega_i) |\underline{E}(z, t, \omega_i)|^2.$

⇒ Evolution of intensities along z:

$$\frac{\partial I(z, t, \omega_3)}{\partial z} = -\epsilon_0 \omega_3 d_{\text{eff}} \text{Im} \left\{ \underline{E}^*(z, t, \omega_1) \underline{E}^*(z, t, \omega_2) \underline{E}(z, t, \omega_3) e^{j\Delta kz} \right\}$$

$$\frac{\partial I(z, t, \omega_2)}{\partial z} = \epsilon_0 \omega_2 d_{\text{eff}} \text{Im} \left\{ \underline{E}^*(z, t, \omega_1) \underline{E}^*(z, t, \omega_2) \underline{E}(z, t, \omega_3) e^{j\Delta kz} \right\}$$

$$\frac{\partial I(z, t, \omega_1)}{\partial z} = \epsilon_0 \omega_1 d_{\text{eff}} \text{Im} \left\{ \underline{E}^*(z, t, \omega_1) \underline{E}^*(z, t, \omega_2) \underline{E}(z, t, \omega_3) e^{j\Delta kz} \right\}$$

The Manley-Rowe relations

Conclusions:

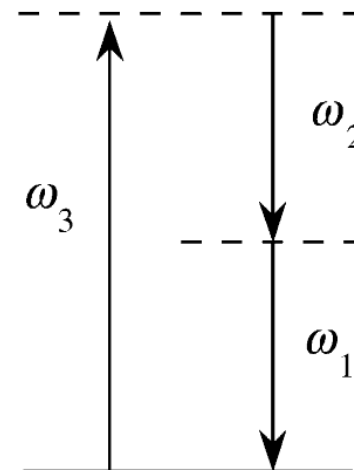
- Total intensity does not change along z

$$\frac{\partial}{\partial z} (I(z, t, \omega_1) + I(z, t, \omega_2) + I(z, t, \omega_3)) = 0.$$

- Change of photon fluxes are connected:

$$\frac{\partial}{\partial z} \left(\frac{I(z, t, \omega_1)}{\hbar\omega_1} \right) = \frac{\partial}{\partial z} \left(\frac{I(z, t, \omega_2)}{\hbar\omega_2} \right) = -\frac{\partial}{\partial z} \left(\frac{I(z, t, \omega_3)}{\hbar\omega_3} \right)$$

⇒ Generation of a photon at ω_1 is always accompanied by generation of a photon at ω_2 and annihilation of a photon at ω_3 (and vice versa)



Lecture 11

The Manley-Rowe relations

Consider interaction of 3 waves oscillating at frequencies ω_1 , ω_2 , and $\omega_3 = \omega_1 + \omega_2$:

$$\frac{\partial \underline{E}(z, t, \omega_3)}{\partial z} = -j \frac{\omega_3}{cn(\omega_3)} d_{\text{eff}} \underline{E}(z, t, \omega_1) \underline{E}(z, t, \omega_2) e^{-j\Delta kz},$$

$$\frac{\partial \underline{E}(z, t, \omega_1)}{\partial z} = -j \frac{\omega_1}{cn(\omega_1)} d_{\text{eff}} \underline{E}(z, t, \omega_3) \underline{E}^*(z, t, \omega_2) e^{j\Delta kz},$$

$$\frac{\partial \underline{E}(z, t, \omega_2)}{\partial z} = -j \frac{\omega_2}{cn(\omega_2)} d_{\text{eff}} \underline{E}(z, t, \omega_3) \underline{E}^*(z, t, \omega_1) e^{j\Delta kz}.$$

Intensity: $I(z, t, \omega_i) = \frac{1}{2} \epsilon_0 cn(\omega_i) |\underline{E}(z, t, \omega_i)|^2.$

⇒ Evolution of intensities along z:

$$\frac{\partial I(z, t, \omega_3)}{\partial z} = -\epsilon_0 \omega_3 d_{\text{eff}} \text{Im} \left\{ \underline{E}^*(z, t, \omega_1) \underline{E}^*(z, t, \omega_2) \underline{E}(z, t, \omega_3) e^{j\Delta kz} \right\}$$

$$\frac{\partial I(z, t, \omega_2)}{\partial z} = \epsilon_0 \omega_2 d_{\text{eff}} \text{Im} \left\{ \underline{E}^*(z, t, \omega_1) \underline{E}^*(z, t, \omega_2) \underline{E}(z, t, \omega_3) e^{j\Delta kz} \right\}$$

$$\frac{\partial I(z, t, \omega_1)}{\partial z} = \epsilon_0 \omega_1 d_{\text{eff}} \text{Im} \left\{ \underline{E}^*(z, t, \omega_1) \underline{E}^*(z, t, \omega_2) \underline{E}(z, t, \omega_3) e^{j\Delta kz} \right\}$$

The Manley-Rowe relations

Conclusions:

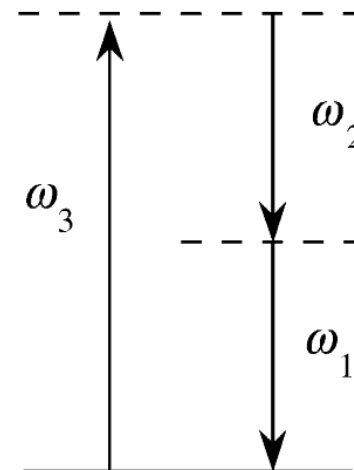
- Total intensity does not change along z

$$\frac{\partial}{\partial z} (I(z, t, \omega_1) + I(z, t, \omega_2) + I(z, t, \omega_3)) = 0.$$

- Change of photon fluxes are connected:

$$\frac{\partial}{\partial z} \left(\frac{I(z, t, \omega_1)}{\hbar\omega_1} \right) = \frac{\partial}{\partial z} \left(\frac{I(z, t, \omega_2)}{\hbar\omega_2} \right) = -\frac{\partial}{\partial z} \left(\frac{I(z, t, \omega_3)}{\hbar\omega_3} \right)$$

⇒ Generation of a photon at ω_1 is always accompanied by generation of a photon at ω_2 and annihilation of a photon at ω_3 (and vice versa)



Consider difference frequency generation with strong pump wave at $\omega_3 = \omega_1 + \omega_2$

Assumptions: - Phase matching: $\Delta k = 0$
- Strong pump at frequency ω_3
 \Rightarrow Pump depletion can be neglected, $\underline{E}(z, t, \omega_3) = \underline{E}(0, t, \omega_3)$

Coupled differential equations:

$$\frac{\partial \underline{E}(z, t, \omega_1)}{\partial z} = -j \frac{\omega_1}{c n(\omega_1)} d_{\text{eff}} \underline{E}(0, t, \omega_3) \underline{E}^*(z, t, \omega_2),$$
$$\frac{\partial \underline{E}(z, t, \omega_2)}{\partial z} = -j \frac{\omega_2}{c n(\omega_2)} d_{\text{eff}} \underline{E}(0, t, \omega_3) \underline{E}^*(z, t, \omega_1).$$

General solution:

$$\underline{E}(z, t, \omega_1) = \underline{E}_a \cosh(\kappa z) + \underline{E}_b \sinh(\kappa z),$$
$$\underline{E}(z, t, \omega_2) = -j \sqrt{\frac{\omega_2 n(\omega_1)}{\omega_1 n(\omega_2)} \frac{\underline{E}(0, t, \omega_3)}{|\underline{E}(0, t, \omega_3)|}} (\underline{E}_a^* \sinh(\kappa z) + \underline{E}_b^* \cosh(\kappa z))$$

where $\kappa^2 = \frac{\omega_1 \omega_2 d_{\text{eff}}^2}{c^2 n(\omega_1) n(\omega_2)} |\underline{E}(0, t, \omega_3)|^2.$

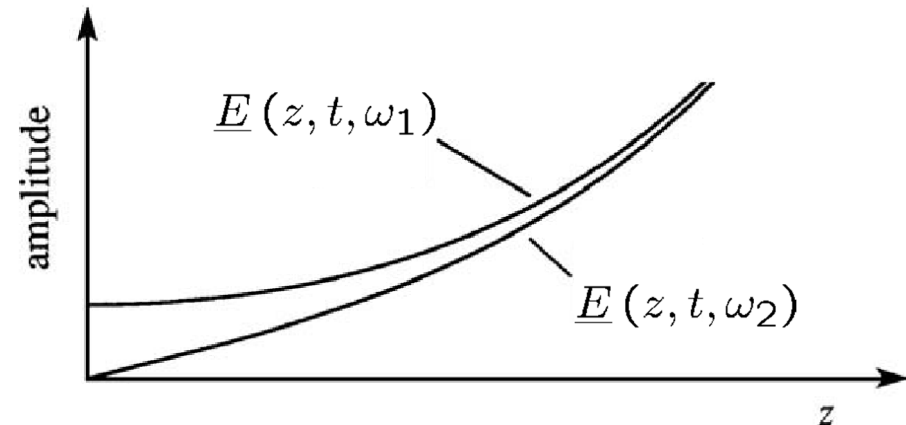
Optical parametric amplifier (OPA):

Launch signal at frequency ω_1 :

$$\underline{E}(0, t, \omega_1) = \underline{E}_1$$

$$\underline{E}(0, t, \omega_2) = 0.$$

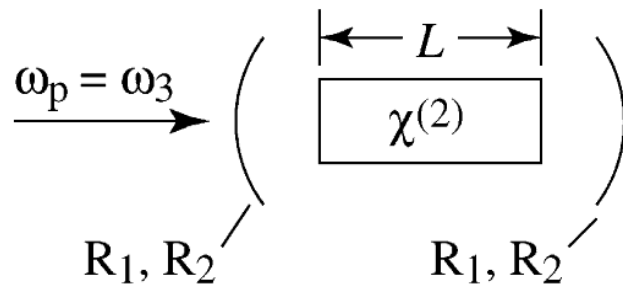
⇒ Parametric amplification of signal at ω_1 and generation of idler wave at ω_2 :



Signal:
$$\underline{E}(z, t, \omega_1) = \underline{E}_1 \cosh(\kappa z),$$

Idler:
$$\underline{E}(z, t, \omega_2) = -j \sqrt{\frac{\omega_2 n(\omega_1)}{\omega_1 n(\omega_2)}} \frac{\underline{E}(0, t, \omega_3)}{|\underline{E}(0, t, \omega_3)|} \underline{E}_1^* \sinh(\kappa z).$$

Optical parametric oscillator (OPO): Add mirrors to form an optical resonator

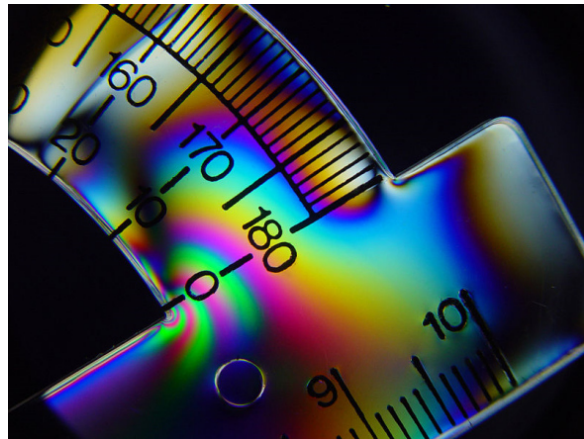


Note: Oscillation at ω_1 and ω_2 starts from “noise” (zero-point fluctuations) at the frequencies for which phase matching is fulfilled.

⇒ Wavelength can be adjusted by tuning phase-matching conditions!

Acousto-optics and photon-phonon interactions

Elasto-optic effect and strain



Visualization of the **elasto-optic effect**: The medium becomes birefringent under strain, leading to interference fringes in a polarized-light image.

Quantitative description: **Strain tensor**

$$\sigma_{kl} = \frac{1}{2} \left(\frac{\partial u_k}{\partial x_l} + \frac{\partial u_l}{\partial x_k} \right)$$

where $u = (u_1, u_2, u_3)$ denotes the **vectorial displacement** of a volume element (dx, dy, dz) at a position $(x_1, x_2, x_3) = (x, y, z)$.

A few examples ($x_1 = x, x_2 = y, x_3 = z, u_1 = U, u_2 = V$):

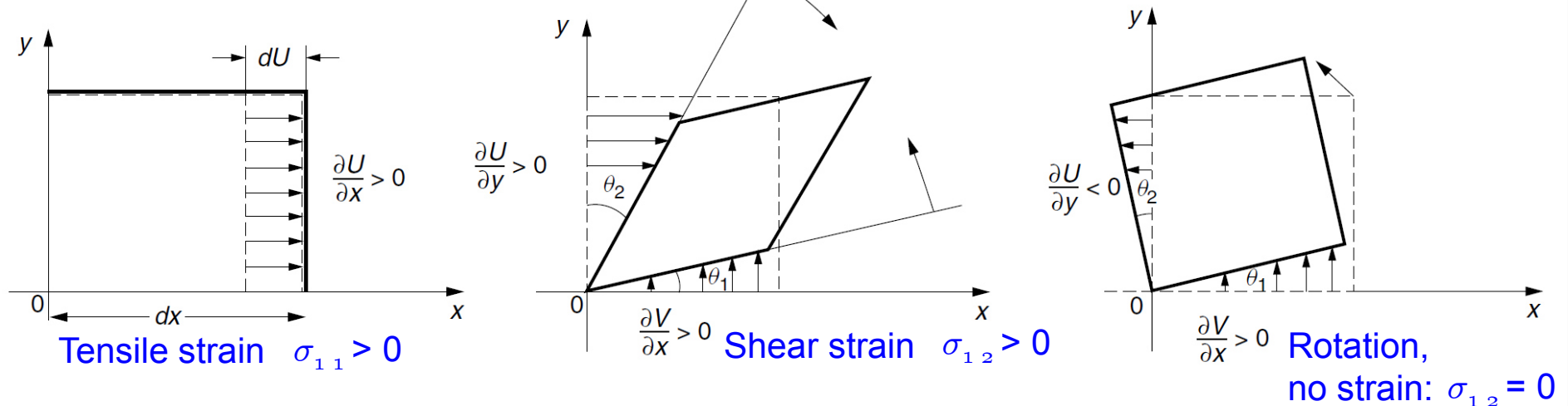
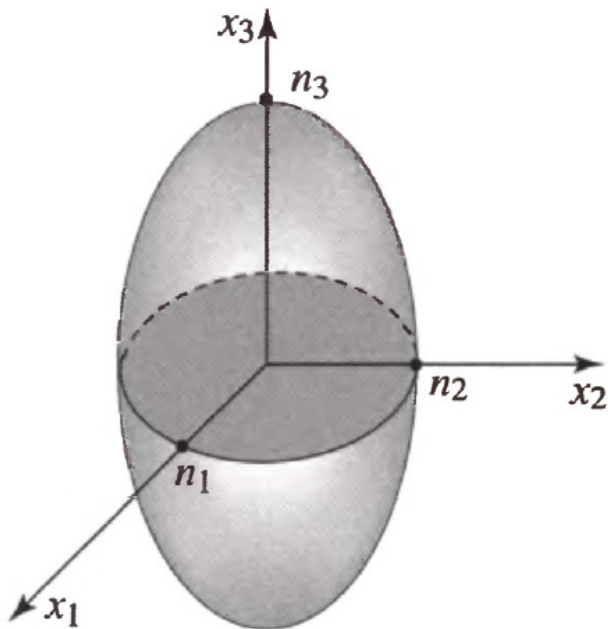


Figure adapted from Iizuka, Elements of Photonics

Recall: **Anisotropic media** are characterized by the electric impermeability tensor η_{ij} and the associated **index ellipsoid**

$$\sum_{i,j} \eta_{ij} X_i X_j = 1$$



Strain-induced changes $\Delta\eta_{ij}$ of the **impermeability tensor** elements are related to the various elements of the **strain tensor** by the **fourth-rank elasto-optic tensor** p_{ijkl}

$$\eta_{ij}(\sigma_{kl}) = \eta_{ij}(0) + \sum_{kl} p_{ijkl} \sigma_{kl}$$

Contracted notation:

ij/kl	11	22	33	23, 32	13, 31	12, 21
I/K	1	2	3	4	5	6

⇒ Elasto-optic tensor can be written as a **6 x 6 matrix**

$$\Delta\eta_I = p_{IK} \sigma_K$$

Crystal symmetries further restrict elements of p_{IK} .

Figure adapted from Saleh-Teich, Fundamentals of Photonics

Elasto-optic tensors of different materials

Name of Substance	Chemical Symbol	Photoelastic Constant	Index of Refraction	Wavelength (μm)	Crystal Symmetry	Elasto-optic Tensor
Fused silica	SiO ₂	$p_{11} = 0.121$ $p_{12} = 0.270$ $p_{44} = p_{55} = p_{66}$ $= \frac{1}{2}(p_{11} - p_{12})$	$n = 1.457$	0.63	Isotropic	$\begin{bmatrix} p_{11} & p_{12} & p_{12} & 0 & 0 & 0 \\ p_{12} & p_{11} & p_{12} & 0 & 0 & 0 \\ p_{12} & p_{12} & p_{11} & 0 & 0 & 0 \\ 0 & 0 & 0 & p_{44} & 0 & 0 \\ 0 & 0 & 0 & 0 & p_{55} & 0 \\ 0 & 0 & 0 & 0 & 0 & p_{66} \end{bmatrix}$
Water	H ₂ O	$p_{11} = 0.31$ $p_{12} = 0.31$ $p_{44} = p_{55} = p_{66}$ $= \frac{1}{2}(p_{11} - p_{12})$	$n = 1.33$	0.63	Isotropic	$\begin{bmatrix} p_{11} & p_{12} & p_{12} & 0 & 0 & 0 \\ p_{12} & p_{11} & p_{12} & 0 & 0 & 0 \\ p_{12} & p_{12} & p_{11} & 0 & 0 & 0 \\ 0 & 0 & 0 & p_{44} & 0 & 0 \\ 0 & 0 & 0 & 0 & p_{55} & 0 \\ 0 & 0 & 0 & 0 & 0 & p_{66} \end{bmatrix}$
Gallium arsenide	GaAs	$p_{11} = -0.165$ $p_{12} = -0.140$ $p_{44} = -0.061$	$n_x = n_y = n_z = 3.42$	1.15	$\bar{4}3m$	$\begin{bmatrix} p_{11} & p_{12} & p_{12} & 0 & 0 & 0 \\ p_{12} & p_{11} & p_{12} & 0 & 0 & 0 \\ p_{12} & p_{12} & p_{11} & 0 & 0 & 0 \\ 0 & 0 & 0 & p_{44} & 0 & 0 \\ 0 & 0 & 0 & 0 & p_{44} & 0 \\ 0 & 0 & 0 & 0 & 0 & p_{44} \end{bmatrix}$
Zinc sulfide	β -ZnS	$p_{11} = 0.091$ $p_{12} = -0.01$ $p_{44} = 0.075$	$n_x = n_y = n_z = 2.352$	0.63		$\begin{bmatrix} p_{11} & p_{12} & p_{12} & 0 & 0 & 0 \\ p_{12} & p_{11} & p_{12} & 0 & 0 & 0 \\ p_{12} & p_{12} & p_{11} & 0 & 0 & 0 \\ 0 & 0 & 0 & p_{44} & 0 & 0 \\ 0 & 0 & 0 & 0 & p_{44} & 0 \\ 0 & 0 & 0 & 0 & 0 & p_{44} \end{bmatrix}$
Lithium niobate	LiNbO ₃	$p_{11} = -0.02$ $p_{12} = 0.08$ $p_{13} = 0.13$ $p_{14} = -0.08$ $p_{31} = 0.17$ $p_{33} = 0.07$ $p_{41} = -0.15$ $p_{44} = 0.12$ $p_{66} = \frac{1}{2}(p_{11} - p_{12})$	$n_x = n_y = 2.286$ $n_z = 2.20$	0.63	$3m$	$\begin{bmatrix} p_{11} & p_{12} & p_{13} & p_{14} & 0 & 0 \\ p_{12} & p_{11} & p_{13} & -p_{14} & 0 & 0 \\ p_{31} & p_{31} & p_{33} & 0 & 0 & 0 \\ p_{41} & -p_{41} & 0 & p_{44} & 0 & 0 \\ 0 & 0 & 0 & 0 & p_{44} & p_{41} \\ 0 & 0 & 0 & 0 & p_{14} & p_{66} \end{bmatrix}$

Figure adapted from Iizuka, Elements of Photonics

Elasto-optic tensors of different materials

Name of Substance	Chemical Symbol	Photoelastic Constant	Index of Refraction	Wavelength (μm)	Crystal Symmetry	Elasto-optic Tensor
Lithium tantalate	LiTaO ₃	$p_{11} = -0.08$ $p_{12} = -0.08$ $p_{13} = 0.09$ $p_{14} = -0.03$ $p_{31} = 0.09$ $p_{33} = -0.044$ $p_{41} = -0.085$ $p_{44} = 0.02$ $p_{66} = \frac{1}{2}(p_{11} - p_{12})$	$n_x = n_y = 2.176$ $n_z = 2.180$	0.63	3m	
Rutile	TiO ₂	$p_{11} = -0.011$ $p_{12} = 0.172$ $p_{13} = -0.168$ $p_{31} = -0.096$ $p_{33} = -0.058$ $p_{44} = 0.0095$ $p_{66} = \pm 0.072$	$n_x = n_y = 2.585$ $n_z = 2.875$	0.63	$\bar{4}2m$	
Potassium dihydrogen phosphate (KDP)	KH ₂ PO ₄	$p_{11} = 0.251$ $p_{12} = 0.249$ $p_{13} = 0.246$ $p_{31} = 0.225$ $p_{33} = 0.221$ $p_{44} = -0.019$ $p_{66} = -0.058$	$n_x = n_y = 1.51$ $n_z = 1.47$	0.63	$\bar{4}2m$	$\begin{bmatrix} p_{11} & p_{12} & p_{13} & 0 & 0 & 0 \\ p_{12} & p_{11} & p_{13} & 0 & 0 & 0 \\ p_{31} & p_{31} & p_{33} & 0 & 0 & 0 \\ 0 & 0 & 0 & p_{44} & 0 & 0 \\ 0 & 0 & 0 & 0 & p_{44} & 0 \\ 0 & 0 & 0 & 0 & 0 & p_{66} \end{bmatrix}$
				0.51 0.63		
				0.59 0.63		

Figure adapted from Iizuka, Elements of Photonics

Elasto-optic tensors of different materials

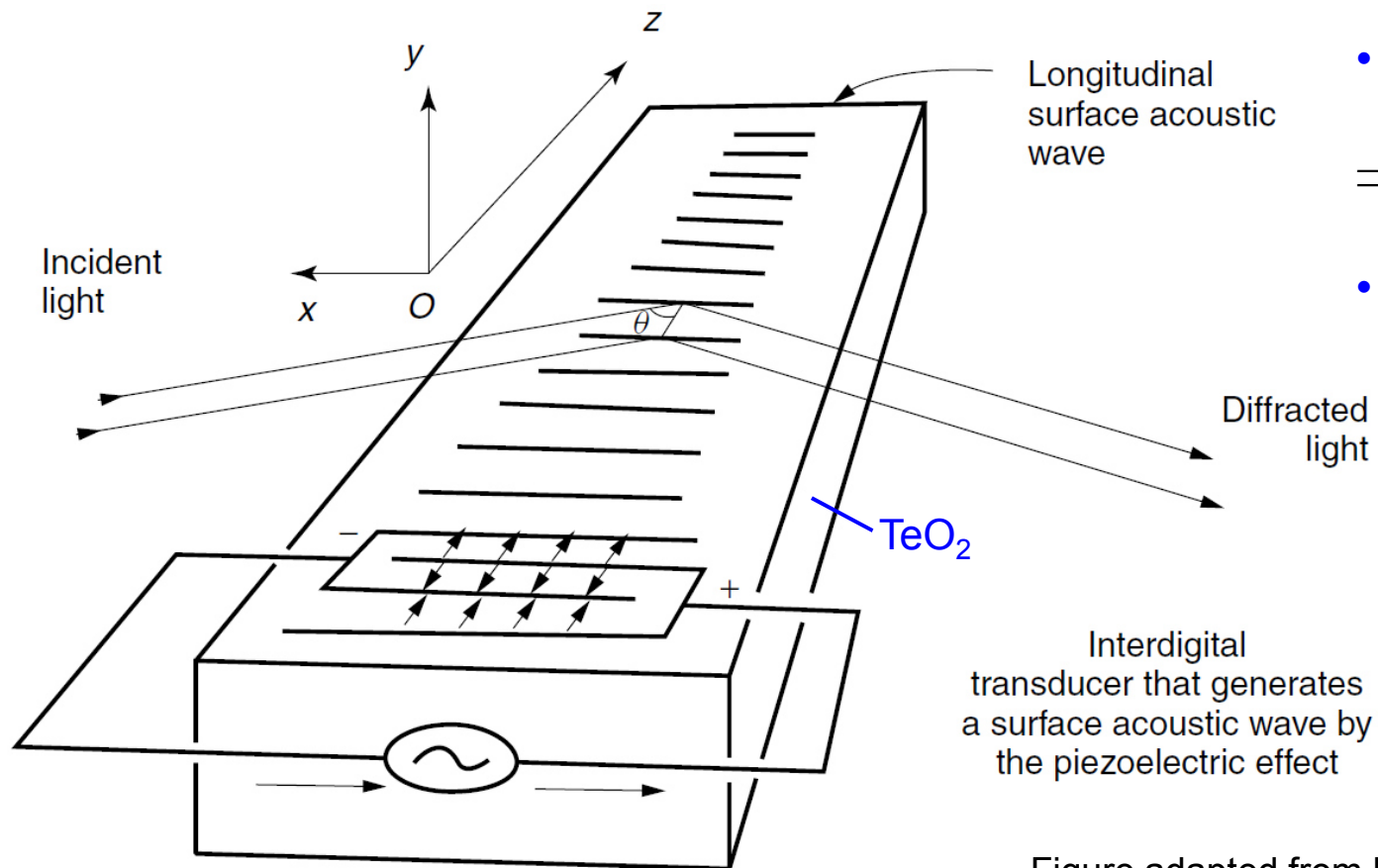
Name of Substance	Chemical Symbol	Photoelastic Constant	Index of Refraction	Wavelength (μm)	Crystal Symmetry	Elasto-optic Tensor
Ammonium dihydrogen phosphate (ADP)	NH ₄ H ₂ PO ₄ or ADP	$p_{11} = 0.302$	$n_x = n_y = 1.52$ $n_z = 1.48$	0.63	$\bar{4}2m$	$\begin{bmatrix} p_{11} & p_{12} & p_{13} & 0 & 0 & 0 \\ p_{12} & p_{11} & p_{13} & 0 & 0 & 0 \\ p_{31} & p_{31} & p_{33} & 0 & 0 & 0 \\ 0 & 0 & 0 & p_{44} & 0 & 0 \\ 0 & 0 & 0 & 0 & p_{44} & 0 \\ 0 & 0 & 0 & 0 & 0 & p_{66} \end{bmatrix}$
		$p_{12} = 0.246$		0.59		
		$p_{13} = 0.236$		0.59		
		$p_{31} = 0.195$				
		$p_{33} = 0.263$				
		$p_{44} = -0.058$				
		$p_{66} = -0.075$				
Tellurium dioxide	TeO ₂	$p_{11} = 0.0074$	$n_x = n_y = n_z = 2.35$	0.63	$\bar{4}2m$	$\begin{bmatrix} p_{11} & p_{12} & p_{13} & 0 & 0 & 0 \\ p_{12} & p_{11} & p_{13} & 0 & 0 & 0 \\ p_{31} & p_{31} & p_{33} & 0 & 0 & 0 \\ 0 & 0 & 0 & p_{44} & 0 & 0 \\ 0 & 0 & 0 & 0 & p_{44} & 0 \\ 0 & 0 & 0 & 0 & 0 & p_{66} \end{bmatrix}$
		$p_{12} = 0.187$				
		$p_{13} = 0.340$				
		$p_{31} = 0.090$				
		$p_{33} = 0.240$				
		$p_{44} = -0.17$				
		$p_{66} = -0.046$				

Figure adapted from Iizuka, Elements of Photonics

Acousto-optic modulator

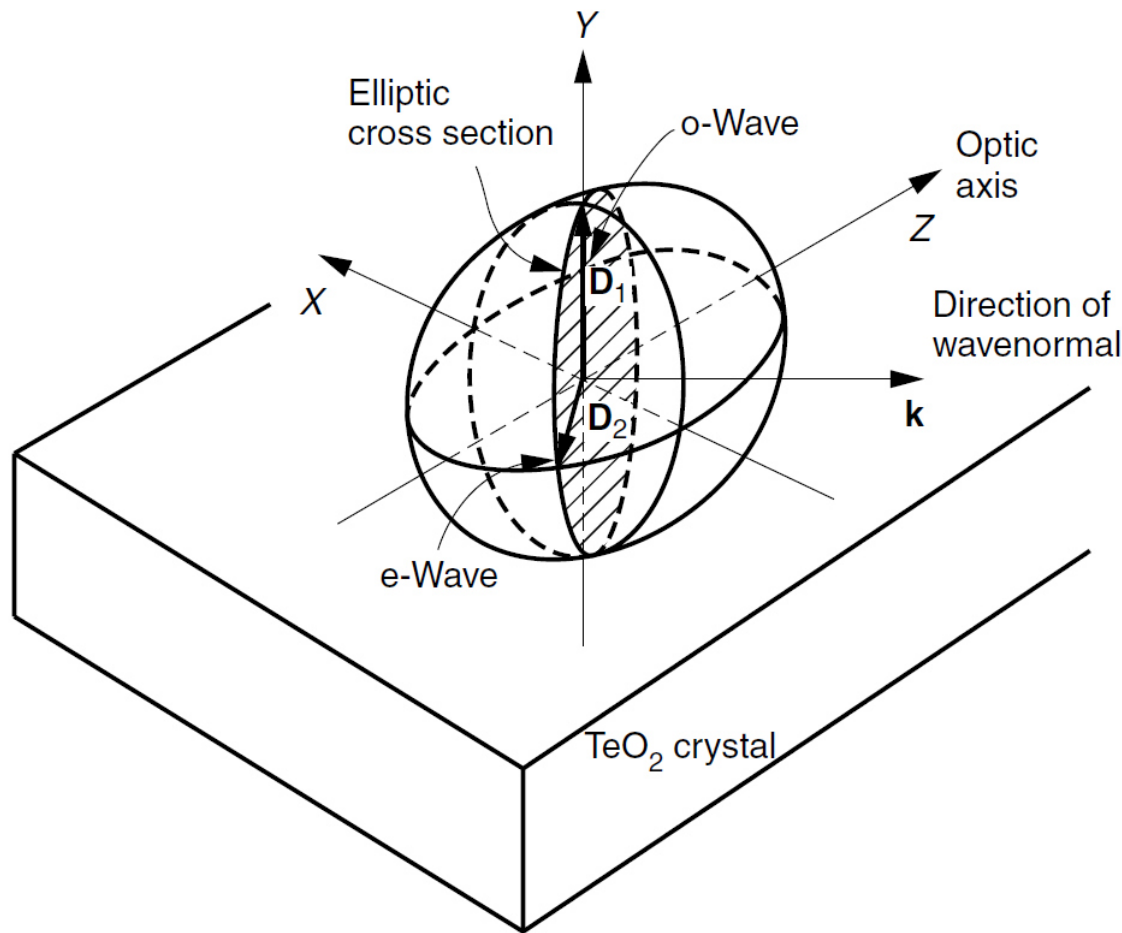
Acousto-optic effect: Strain induced by an acoustic wave
=> “Wave-like” variation of refractive index

Example: Surface-acoustic wave (SAW) modulator based on TeO_2



- **Acoustic wave** launched along z
=> Tensile strain along the z -direction
- **Optical wave** launched in (x,z) -plane, polarized along y
(Note: $p_{23} = p_{13}$)

Figure adapted from Iizuka, Elements of Photonics



Strain-induced birefringence corresponds to that of a uniaxial crystal

$$n_x = n_y = n_0 - \frac{1}{2}n_0^3 p_{13} \sigma_3$$

$$n_z = n_0 - \frac{1}{2}n_0^3 p_{33} \sigma_3.$$

Spatio-temporal variation of refractive index:

$$n(\mathbf{r}, t) = n_0 + \Delta n(\mathbf{r}, t),$$

$$\Delta n(\mathbf{r}, t) = \Delta n_0 \cos(\Omega t - \mathbf{q}\mathbf{r}).$$

where $|\mathbf{q}| = \frac{\Omega}{v_s}$.

Phase velocity of the sound wave within the medium

Figure adapted from Iizuka, Elements of Photonics

Coupled-wave equations

Dielectric displacement for small index perturbation:

$$\underline{\mathbf{D}}(\mathbf{r}, t) \approx \epsilon_0 \left(n_0^2 \underline{\mathbf{E}}(\mathbf{r}, t) + 2n_0 \Delta n(\mathbf{r}, t) \underline{\mathbf{E}}(\mathbf{r}, t) \right).$$

Wave equation for acousto-optic interaction:

$$\nabla^2 \underline{\mathbf{E}}(\mathbf{r}, t) - \frac{n_0^2}{c^2} \frac{\partial^2 \underline{\mathbf{E}}(\mathbf{r}, t)}{\partial t^2} = \frac{2n_0}{c^2} \frac{\partial^2 (\Delta n(\mathbf{r}, t) \underline{\mathbf{E}}(\mathbf{r}, t))}{\partial t^2}.$$

Slowly varying envelope approximation (in space only!):

$$\underline{\mathbf{E}}(\mathbf{r}, t) = \sum_l \underline{\mathbf{E}}(\mathbf{r}, \omega_l) \mathbf{e}_l e^{j(\omega_l t - \mathbf{k}_l \mathbf{r})}.$$

$$\text{where } |\nabla^2 \underline{\mathbf{E}}(\mathbf{r}, \omega_l)| \ll |\mathbf{k}_l \cdot \nabla \underline{\mathbf{E}}(\mathbf{r}, \omega_l)|.$$

Coupled-wave equation for space-dependent wave amplitudes:

$$\sum_l [-2j\mathbf{k}_l \cdot \nabla \underline{\mathbf{E}}(\mathbf{r}, \omega_l)] \mathbf{e}_l e^{j(\omega_l t - \mathbf{k}_l \mathbf{r})} = \frac{2n_0}{c^2} \sum_l \frac{\partial^2}{\partial t^2} (\Delta n(\mathbf{r}, t) \underline{\mathbf{E}}(\mathbf{r}, \omega_l) \mathbf{e}_l e^{j(\omega_l t - \mathbf{k}_l \mathbf{r})}).$$

Launch wave at frequency ω_0 , consider evolution of amplitude at $\omega_1 = \omega_0 + \Omega$:

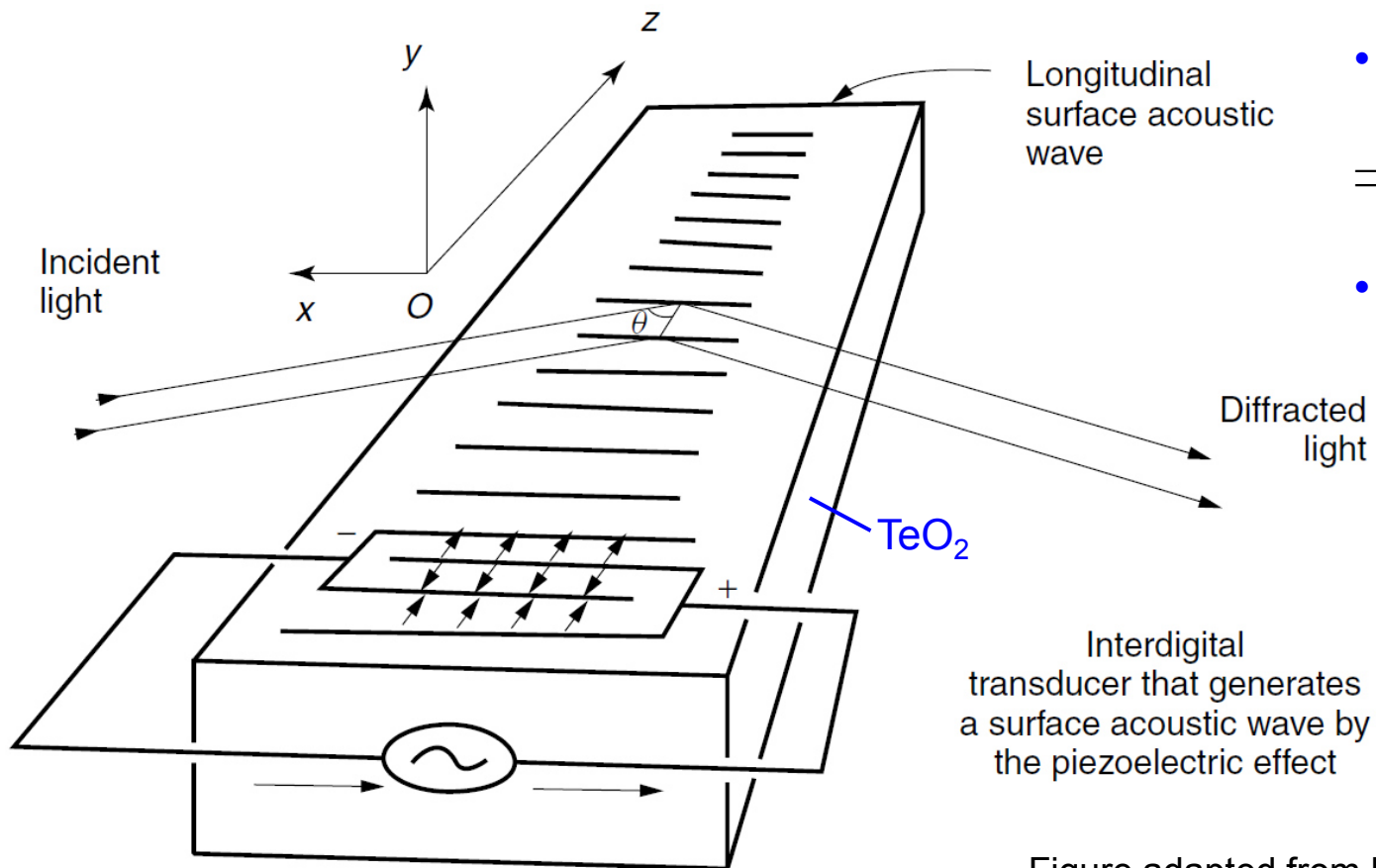
$$\mathbf{k}_1 \cdot \nabla \underline{\mathbf{E}}(\mathbf{r}, \omega_1) = -j \frac{1}{2} (\mathbf{e}_1 \cdot \mathbf{e}_0) \frac{\omega_1^2}{c^2} n_0 \Delta n_0 \underline{\mathbf{E}}(\mathbf{r}, \omega_0) e^{-j(\mathbf{k}_0 + \mathbf{q} - \mathbf{k}_1) \mathbf{r}}.$$

Lecture 12

Acousto-optic modulator

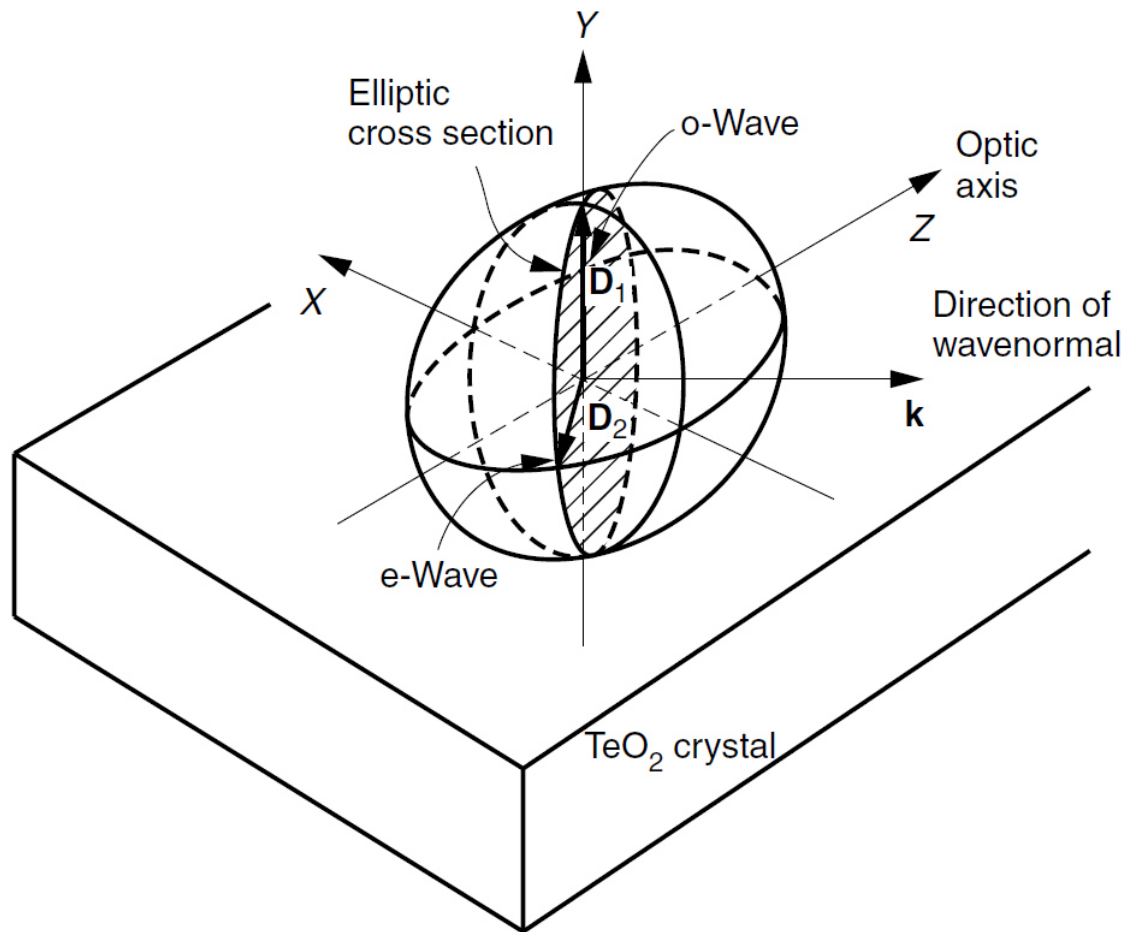
Acousto-optic effect: Strain induced by an acoustic wave
=> “Wave-like” variation of refractive index

Example: Surface-acoustic wave (SAW) modulator based on TeO_2 (strong $p_{13} = p_{23}$)



- **Acoustic wave** launched along z
=> Tensile strain along the z-direction
- **Optical wave** launched in (x.z)-plane, polarized along y

Figure adapted from Iizuka, Elements of Photonics



Strain-induced birefringence corresponds to that of a uniaxial crystal

$$n_x = n_y = n_0 - \frac{1}{2}n_0^3 p_{13} \sigma_3$$

$$n_z = n_0 - \frac{1}{2}n_0^3 p_{33} \sigma_3.$$

Spatio-temporal variation of refractive index:

$$n(\mathbf{r}, t) = n_0 + \Delta n(\mathbf{r}, t),$$

$$\Delta n(\mathbf{r}, t) = \Delta n_0 \cos(\Omega t - \mathbf{q}\mathbf{r}).$$

where $|\mathbf{q}| = \frac{\Omega}{v_s}$.

Phase velocity of the sound wave within the medium

Figure adapted from Iizuka, Elements of Photonics

Dielectric displacement for small index perturbation:

$$\underline{\mathbf{D}}(\mathbf{r}, t) \approx \epsilon_0 \left(n_0^2 \underline{\mathbf{E}}(\mathbf{r}, t) + 2n_0 \Delta n(\mathbf{r}, t) \underline{\mathbf{E}}(\mathbf{r}, t) \right).$$

Wave equation for acousto-optic interaction:

$$\nabla^2 \underline{\mathbf{E}}(\mathbf{r}, t) - \frac{n_0^2}{c^2} \frac{\partial^2 \underline{\mathbf{E}}(\mathbf{r}, t)}{\partial t^2} = \frac{2n_0}{c^2} \frac{\partial^2 (\Delta n(\mathbf{r}, t) \underline{\mathbf{E}}(\mathbf{r}, t))}{\partial t^2}.$$

Slowly varying envelope approximation:

$$\underline{\mathbf{E}}(\mathbf{r}, t) = \sum_l \underline{E}(\mathbf{r}, \omega_l) \mathbf{e}_l e^{j(\omega_l t - \mathbf{k}_l \mathbf{r})}.$$

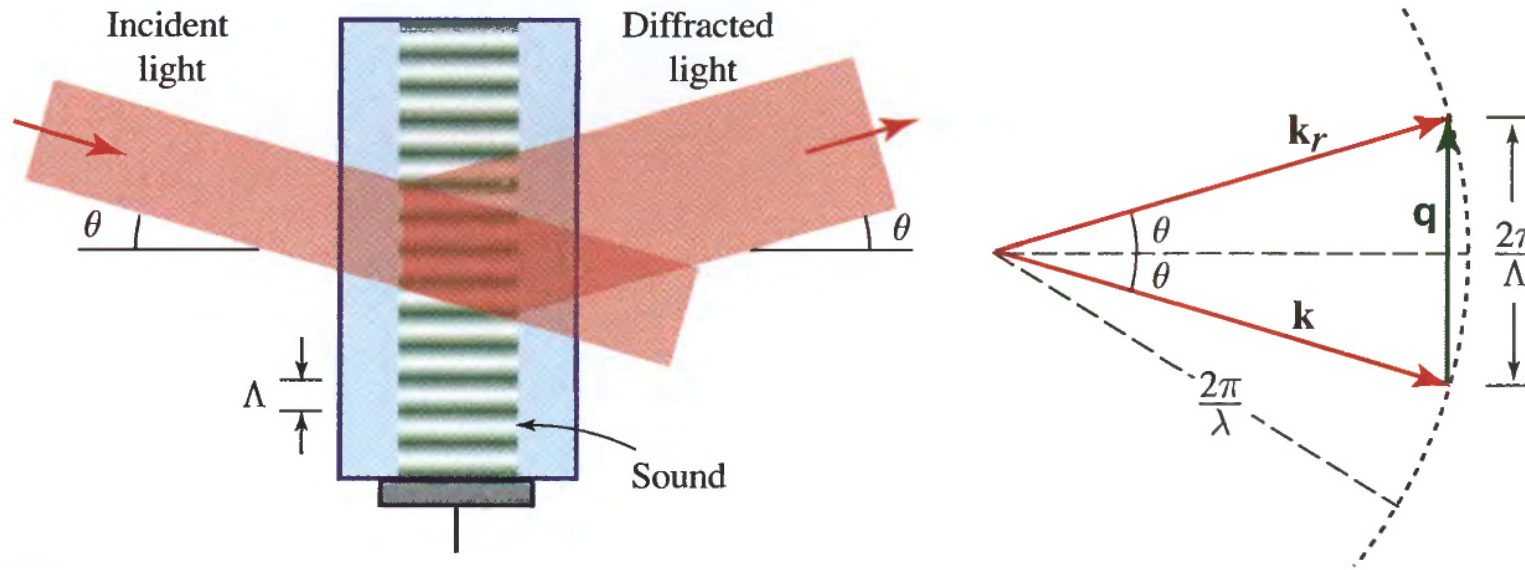
$$\text{where } |\nabla^2 \underline{E}(\mathbf{r}, \omega_l)| \ll |\mathbf{k}_l \cdot \nabla \underline{E}(\mathbf{r}, \omega_l)|.$$

Coupled-wave equation for space-dependent wave amplitudes:

$$\sum_l [-2j\mathbf{k}_l \cdot \nabla \underline{E}(\mathbf{r}, \omega_l)] \mathbf{e}_l e^{j(\omega_l t - \mathbf{k}_l \mathbf{r})} = \frac{2n_0}{c^2} \sum_l \frac{\partial^2}{\partial t^2} (\Delta n(\mathbf{r}, t) \underline{E}(\mathbf{r}, \omega_l) \mathbf{e}_l e^{j(\omega_l t - \mathbf{k}_l \mathbf{r})}).$$

Launch wave at frequency ω_0 , consider evolution of amplitude at $\omega_1 = \omega_0 + \Omega$:

$$\mathbf{k}_1 \cdot \nabla \underline{E}(\mathbf{r}, \omega_1) = -j \frac{1}{2} (\mathbf{e}_1 \cdot \mathbf{e}_0) \frac{\omega_1^2}{c^2} n_0 \Delta n_0 \underline{E}(\mathbf{r}, \omega_0) e^{-j(\mathbf{k}_0 + \mathbf{q} - \mathbf{k}_1) \mathbf{r}}.$$



Phase matching:

$$\mathbf{k}_1 = \mathbf{k}_0 + \mathbf{q} \quad \text{where} \quad |\mathbf{k}_0| \approx |\mathbf{k}_1|$$

$$\sin \Theta_B = \frac{|\mathbf{q}|}{2|\mathbf{k}_0|} = \frac{\lambda/n_0}{2\Lambda}$$

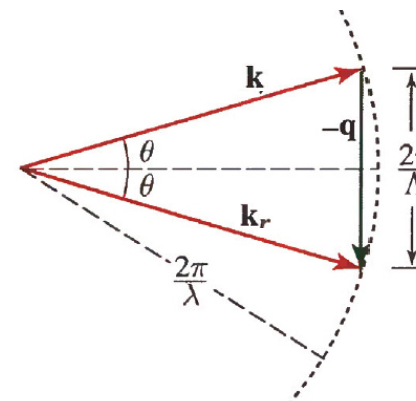
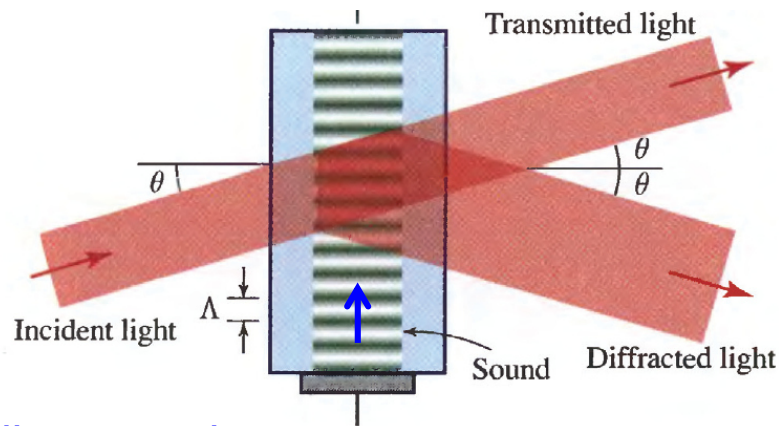
Bragg angle: Reflections from neighboring wavefronts of the acoustic wave experience a relative phase delay of 2π and hence interfere constructively

Figure adapted from Saleh-Teich, Fundamentals of Photonics

Down-conversion and deflection from a standing wave

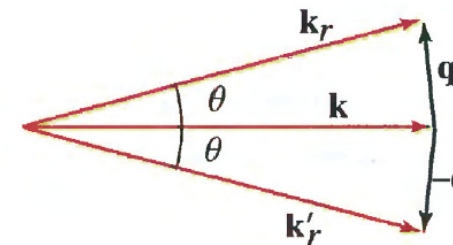
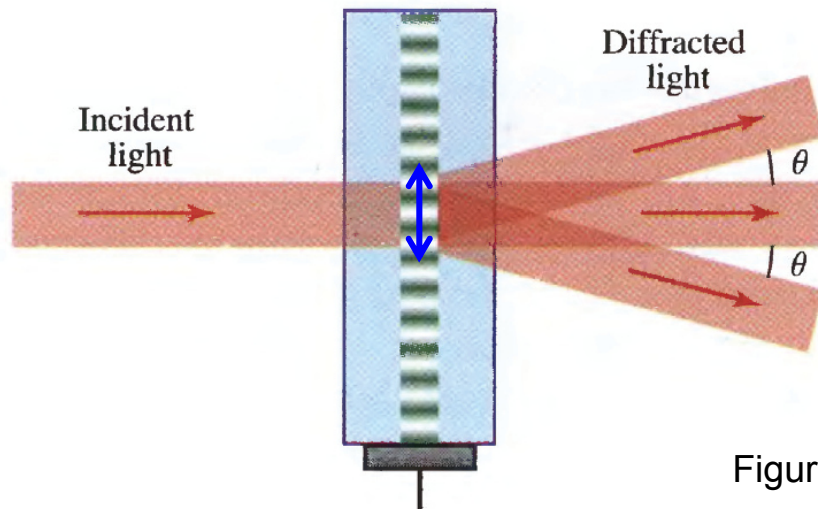
“Co-propagation” of incident light and sound wave

⇒ Down-conversion



Standing sound wave

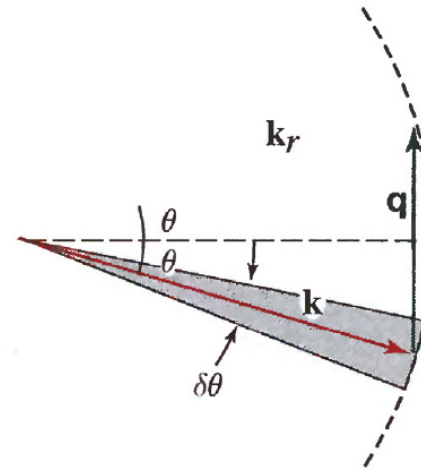
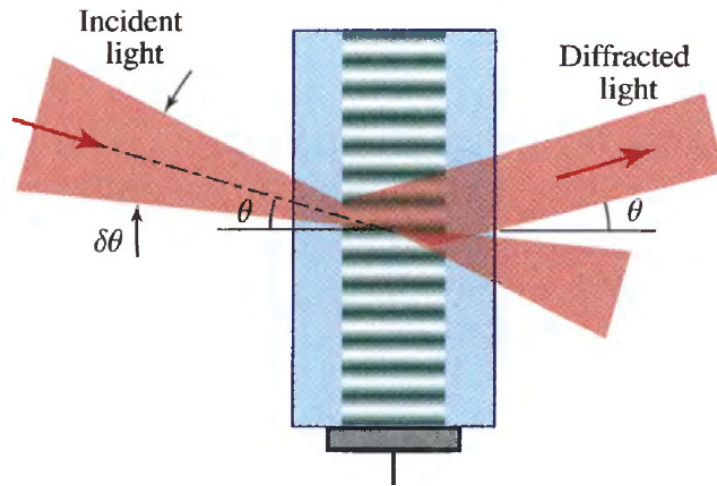
⇒ Diffraction in two directions



Figures adapted from Saleh-Teich, Fundamentals of Photonics

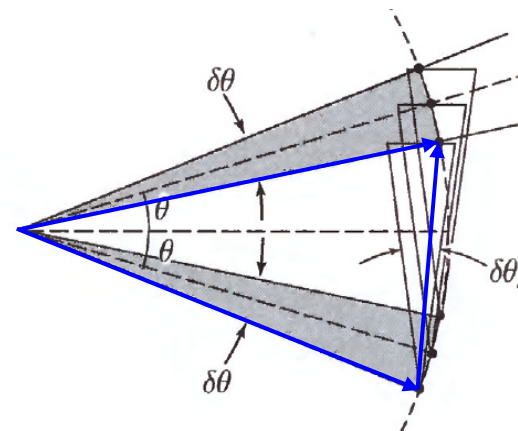
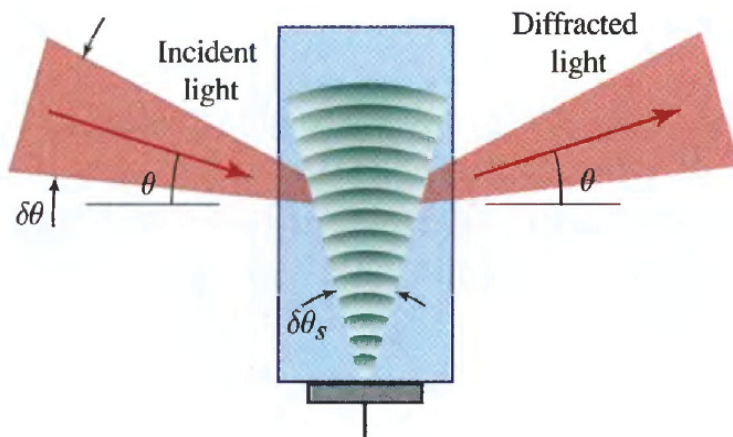
Bragg diffraction of beams

Diffraction of an optical beam from an acoustic plane wave



Only one plane-wave component satisfies the Bragg condition.

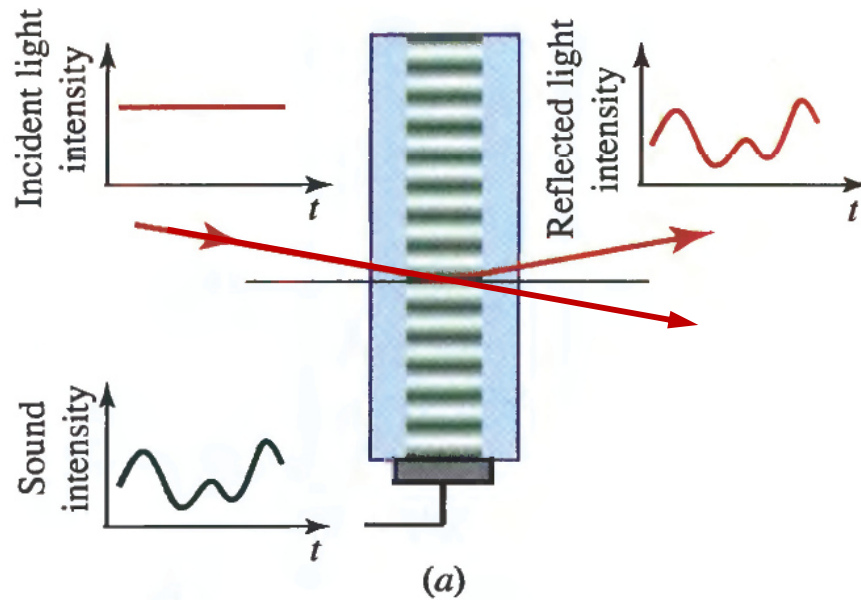
Diffraction of an optical beam from an acoustic beam



For sufficiently large $\delta\theta_s$, every incident plane wave finds an “acoustic match”.

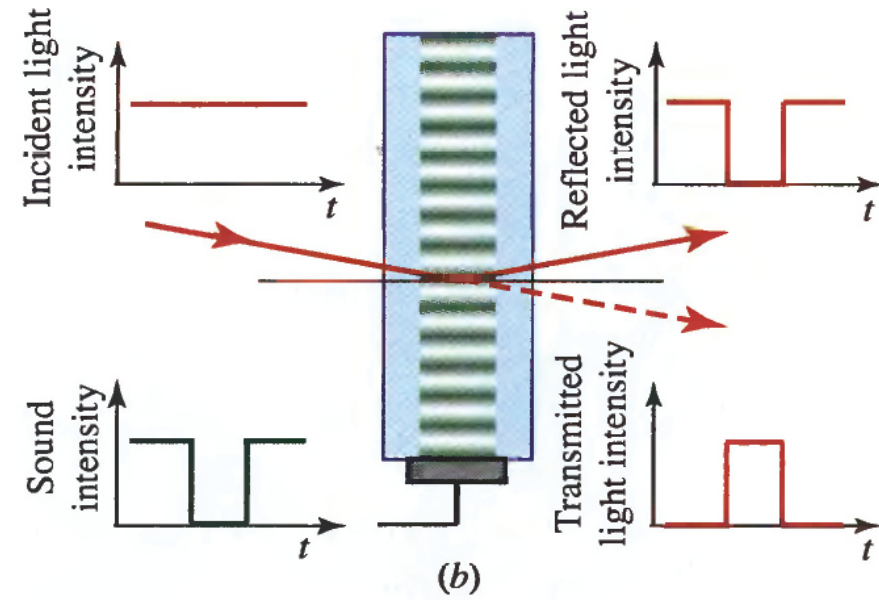
Figures adapted from Saleh-Teich, Fundamentals of Photonics

Acousto-optic modulators



Analogue acousto-optic modulator:

For weak acoustic waves, the intensity of the refracted light is proportional to the intensity of the acoustic wave.



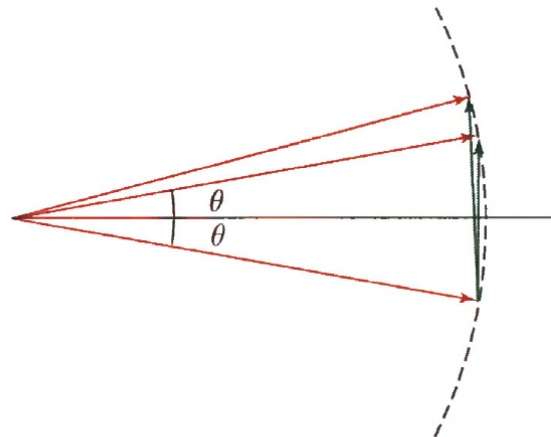
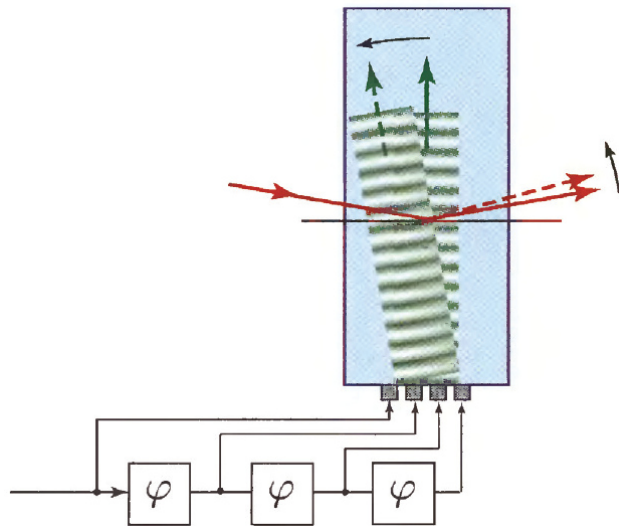
Acousto-optic switch:

At high acoustic intensities, total reflection occurs, and the reflected beam can be turned on and off by switching the sound wave on and off.

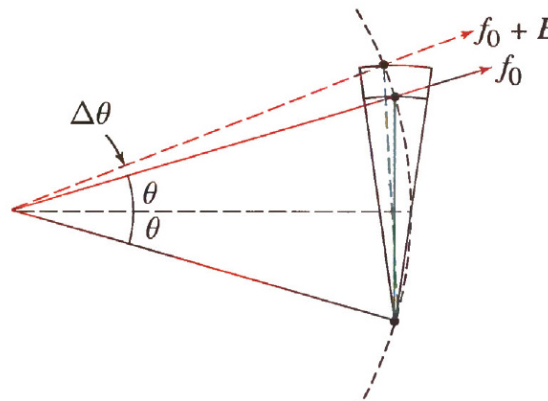
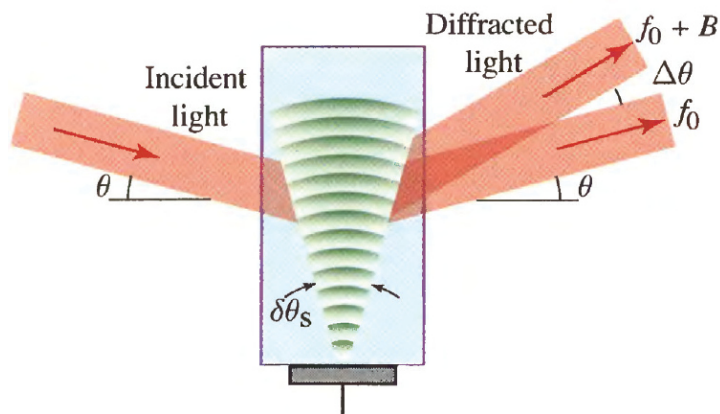
Figures adapted from Saleh-Teich, Fundamentals of Photonics

Acousto-optic beam scanners

Deflection (approximation for small angles): $2\theta_B = \frac{c/n\omega}{v_s \Omega}$



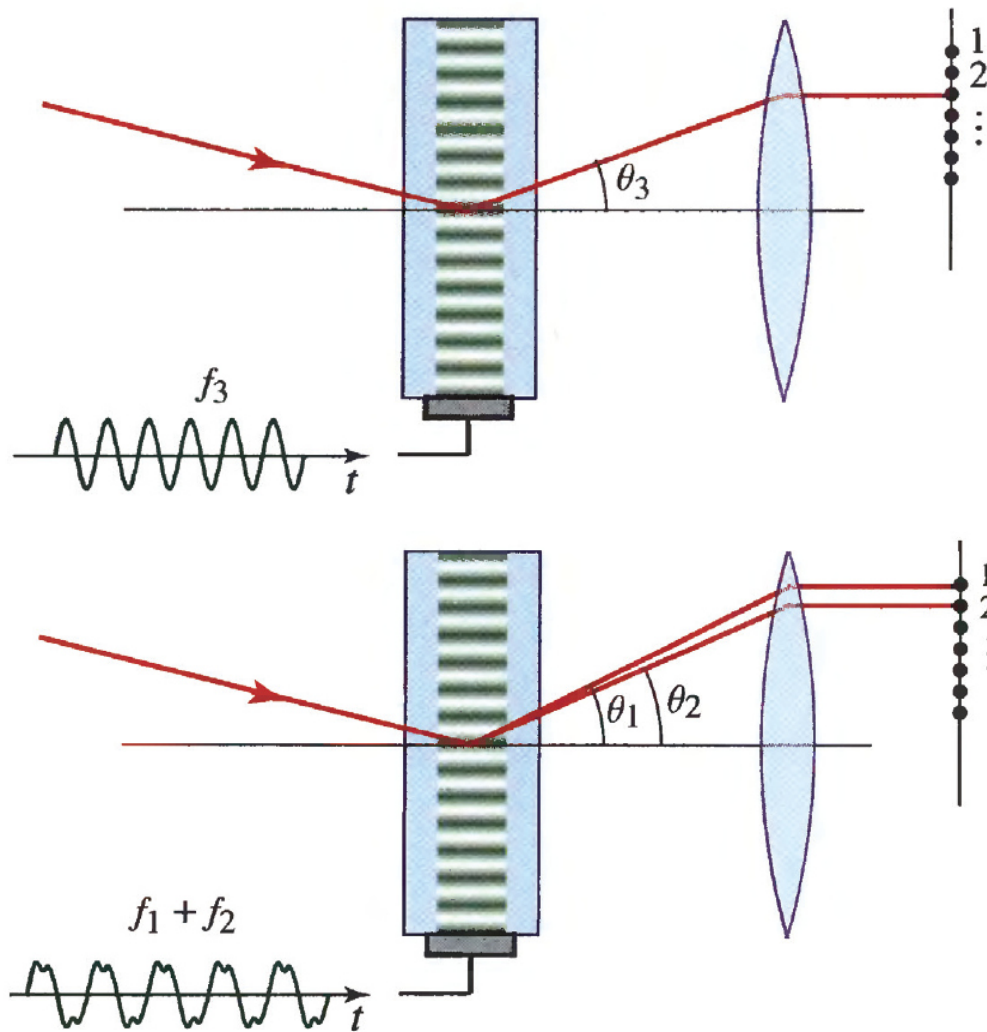
Phased array of acoustic transducers:
 Simultaneous variation of the angle of incidence and the acoustic frequency to maintain phase matching.



Diverging sound beam:
 Variation of frequency sufficient; incoming light wave always “finds” an acoustic plane-wave component with the matching propagation direction.

Figures adapted from Saleh-Teich, Fundamentals of Photonics

Acousto-optic space switches



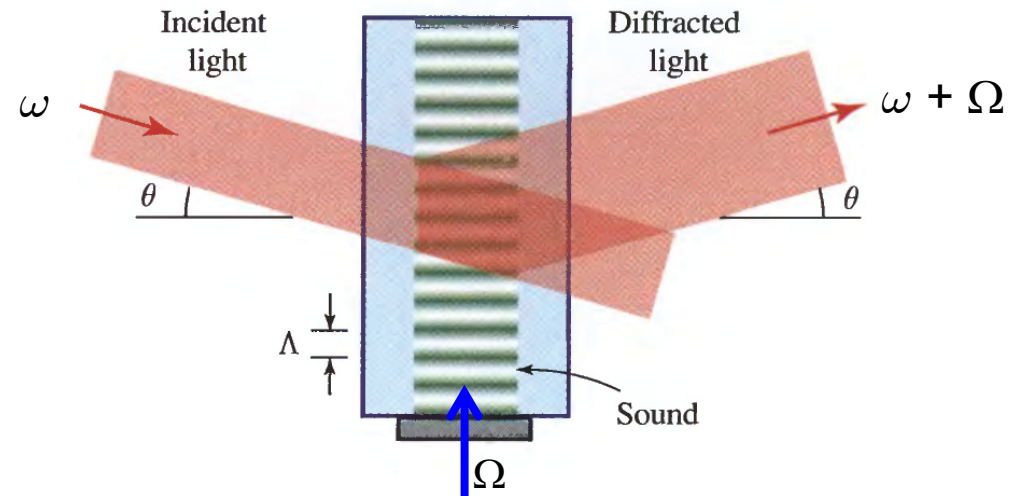
Splitting of incident optical beam by using acoustic drive signals that comprise various frequency components

Figure adapted from Iizuka, Elements of Photonics

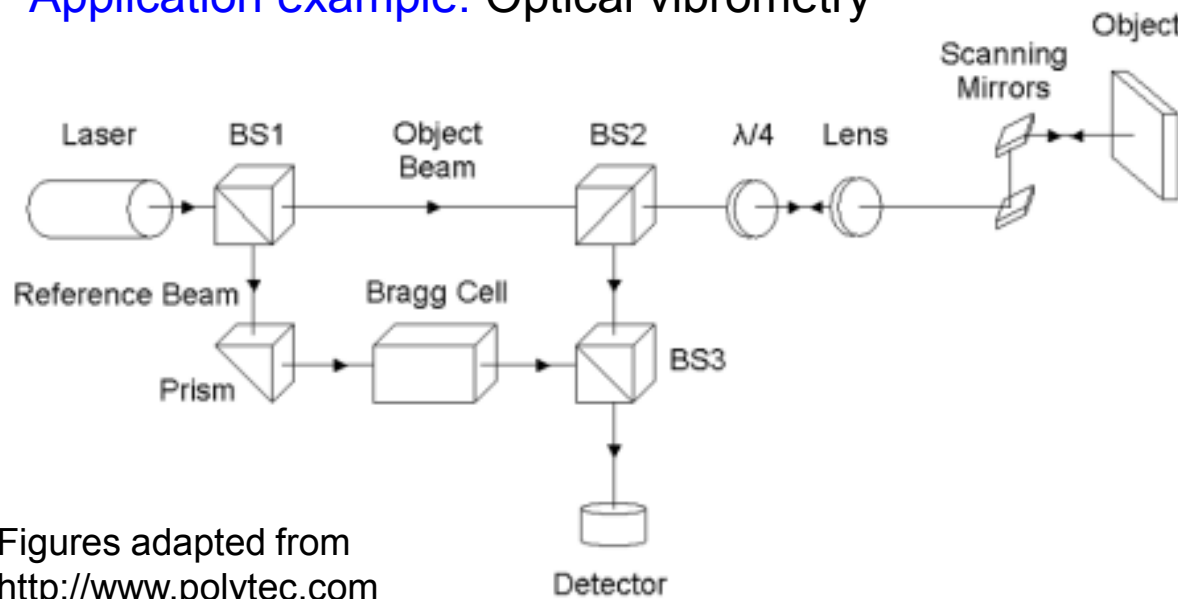
Frequency shifter (“Bragg cell”)

Note: Bragg-reflected light is shifted up or down by the frequency of the sound wave.

⇒ Use as **frequency shifter**, e.g., used for highly sensitive heterodyne detection



Application example: Optical vibrometry



Figures adapted from <http://www.polytec.com>

Interaction of photons and phonons

Quantum interpretation:

- **Light wave** of angular frequency ω and wavevector \mathbf{k} corresponds to stream of photons of energy $\hbar\omega$ and momentum $\hbar\mathbf{k}$.
- **Acoustic wave** of angular frequency Ω and wavenumber \mathbf{q} can be regarded as a stream of phonons of energy $\hbar\Omega$ and momentum $\hbar\mathbf{q}$.
- **Acousto-optic effects** correspond to interaction photons with phonons, whereby new photons with frequency ω_s and wavevectors \mathbf{k}_s can be generated.
- **Energy and momentum conservation require**

$$\omega_s = \omega + \Omega,$$

$$\mathbf{k}_s = \mathbf{k} + \mathbf{q}$$

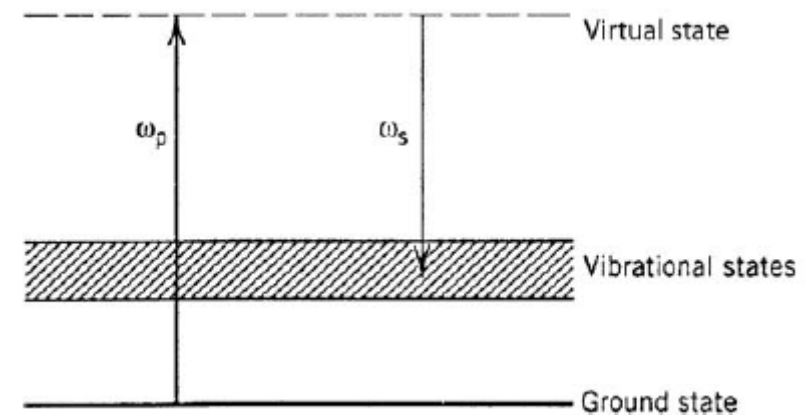
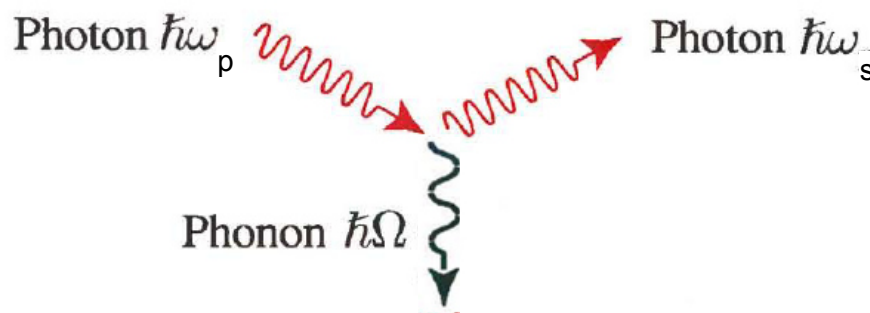


Figure adapted from Saleh-Teich, Fundamentals of Photonics

Acoustic and optical phonons

Simple model:
Diatomic linear chain

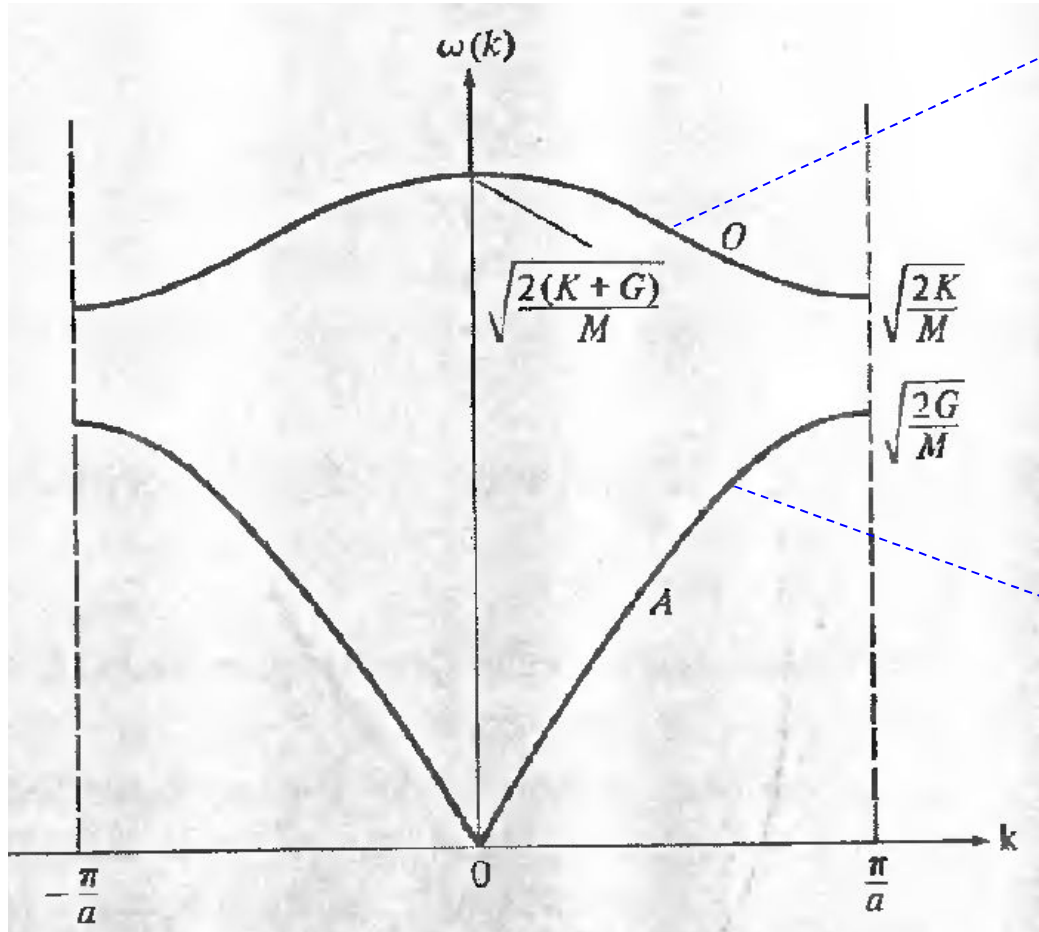
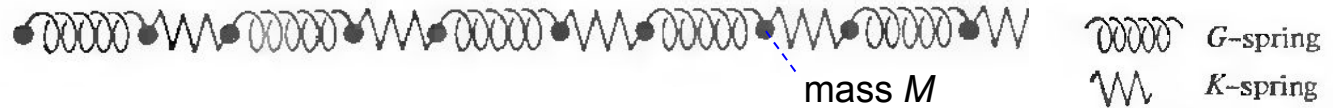


Figure adapted from Ashcroft/Mermin, Solid State Physics

Optical phonons:

- Motion of neighbouring atoms „out of phase“
- Localized vibrational normal modes of molecules
- Bigger energy than acoustic phonons
- Energy approximately independent of momentum

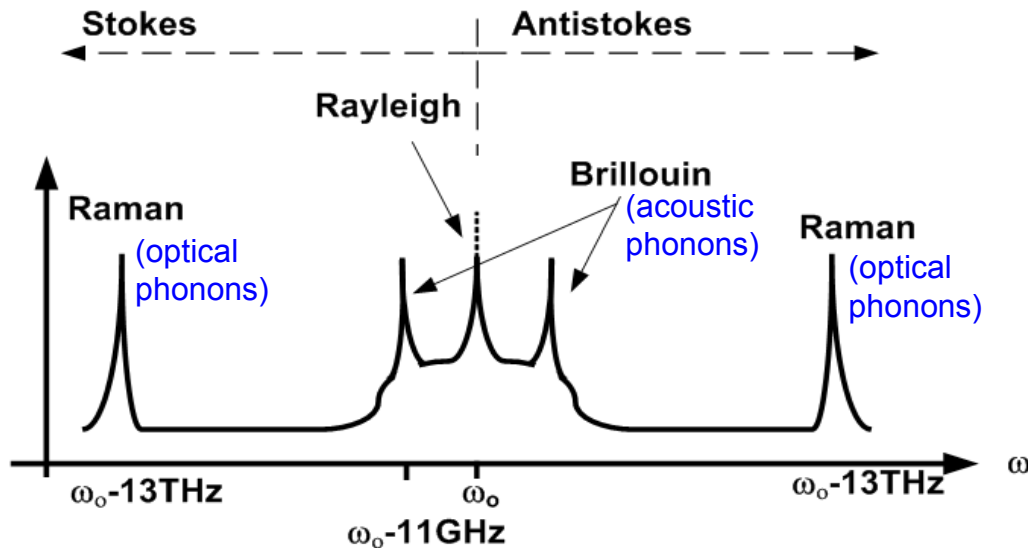


Acoustic phonons:

- Neighbouring atoms move „in phase“
- “Traveling sound waves”
- Energy small; approximately proportional to momentum



Interaction of photons and phonons in optical fibers



Raman Stokes Raman Anti-Stokes Brillouin Stokes

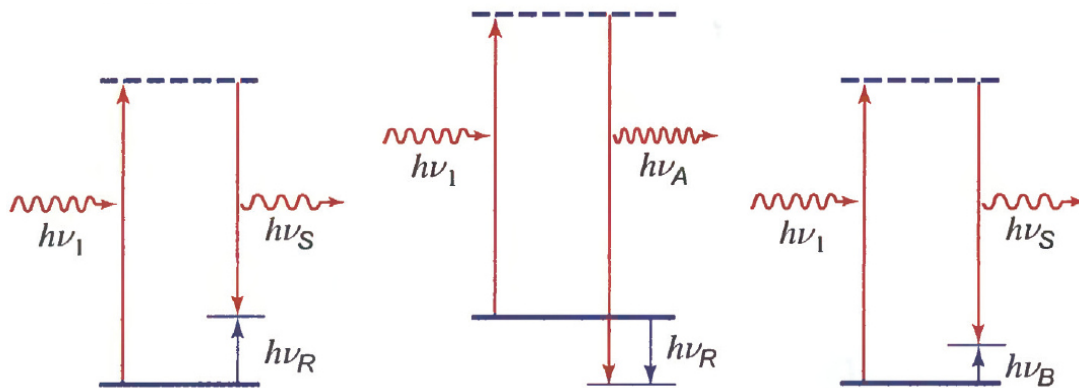


Figure adapted from Saleh-Teich, Fundamentals of Photonics

Rayleigh scattering:

- Scattering due to localized fluctuations of optical density
- No frequency shift

Brillouin scattering:

- Scattering due to interactions with acoustic phonons
- Small frequency shift (~ 11 GHz in silica fibers)
- Only in backward direction

Raman scattering:

- Scattering due to interactions with optical phonons
- Large frequency shift (~ 13 THz in silica fibers)
- Scattering in forward and backward direction

Stokes process:

Photon loses energy during interaction

Anti-Stokes process:

Photon gains energy during interaction

Brillouin scattering

- Interaction of light with a traveling sound wave (**acoustic phonons**)
- Only in **backward direction**
- Brillouin shift:

$$f_B = \frac{\Omega_B}{2\pi} = 2n \frac{v_s}{c} f$$

- **Silica fiber:**

$$f_B \approx 11 \text{ GHz},$$

gain bandwidth 50 MHz ... 100 MHz

- **Brillouin shift depends on local strain and temperature of the fiber**
 \Rightarrow Application in “distributed sensing”

Stimulated Brillouin scattering (SBS):

- Interference of incident and scattered wave lead to beat signal and generates an acoustic wave with frequency f_B via the process of electrostriction
 \Rightarrow **Positive feedback leads to “stimulated scattering”**
- Quantitative model:

$$\frac{dI_p}{dz} = -g_B I_p I_s - \alpha I_p,$$

$$\frac{dI_s}{dz} = g_B I_p I_s + \alpha I_s,$$

$$g_B(\Omega) = g_B(\omega_p - \omega_s) \quad \text{Brillouin gain}$$

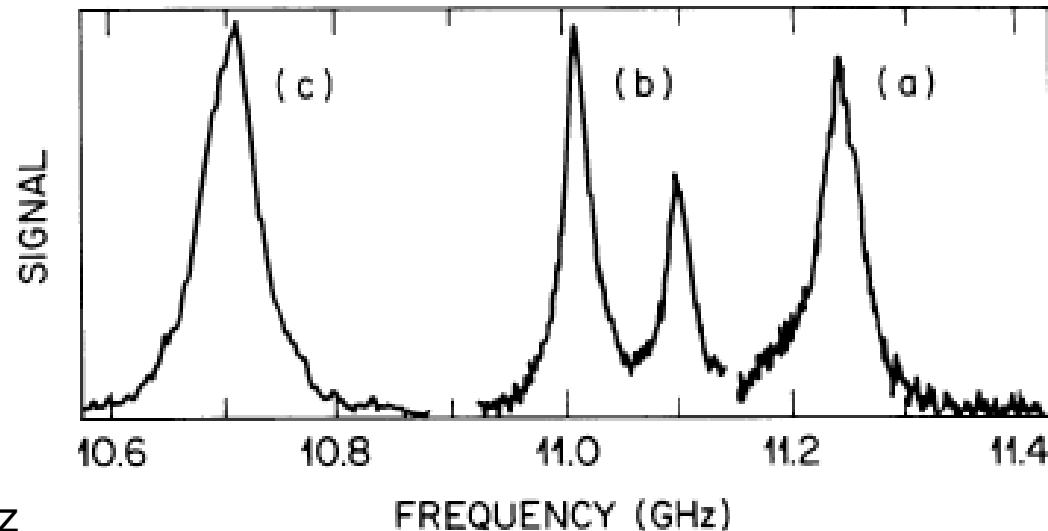


Figure adapted from Agrawal, Nonlinear Fiber Optics

Raman scattering

- Interaction of light with vibrational states of the material molecules or atoms (optical phonons)
- Scattering in both forward and backward direction
- Silica fibers:
 - Raman shift ~ 13 THz
 - Large gain bandwidth (~ 10 THz) due to amorphous structure of the fibers (local inhomogeneities \Rightarrow Broadening of vibrational energy states)

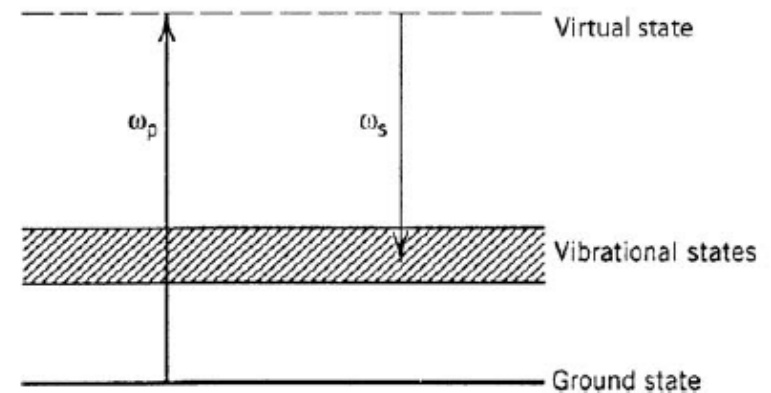
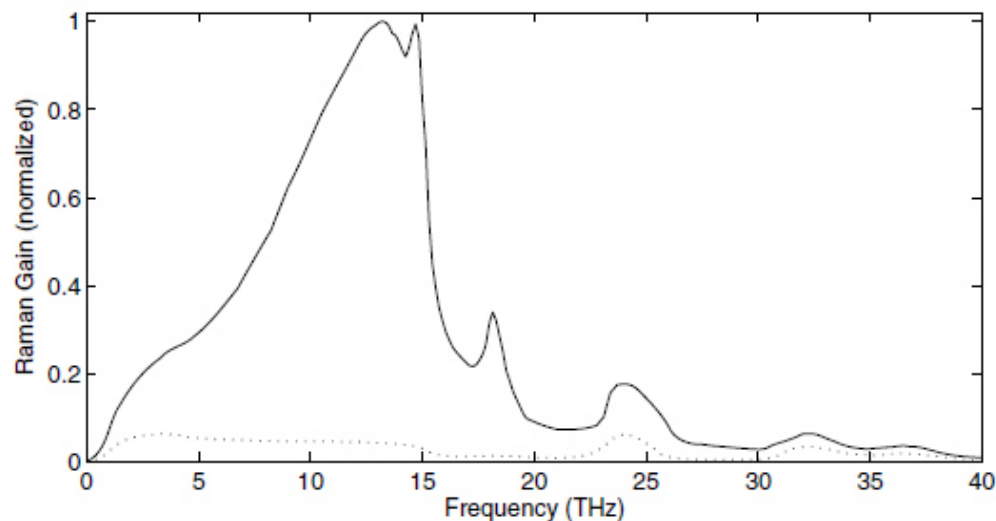


Figure adapted from Agrawal, Fiber-Optic Communication Systems

Stimulated Raman scattering and Raman amplifier

- Scattered wave interferes with the incoming wave, generating a beat signal at the Raman frequency.
- ⇒ New phonons generated by electrostriction, which further enhance Raman scattering

⇒ Positive feedback

- Quantitative model:

$$\frac{dI_s}{dz} = g_R I_p I_s - \alpha_s I_s, \quad g_R(\Omega) = g_R(\omega_p - \omega_s)$$

$$\frac{dI_p}{dz} = -\frac{\omega_p}{\omega_s} g_R I_p I_s - \alpha_p I_p,$$

Raman gain

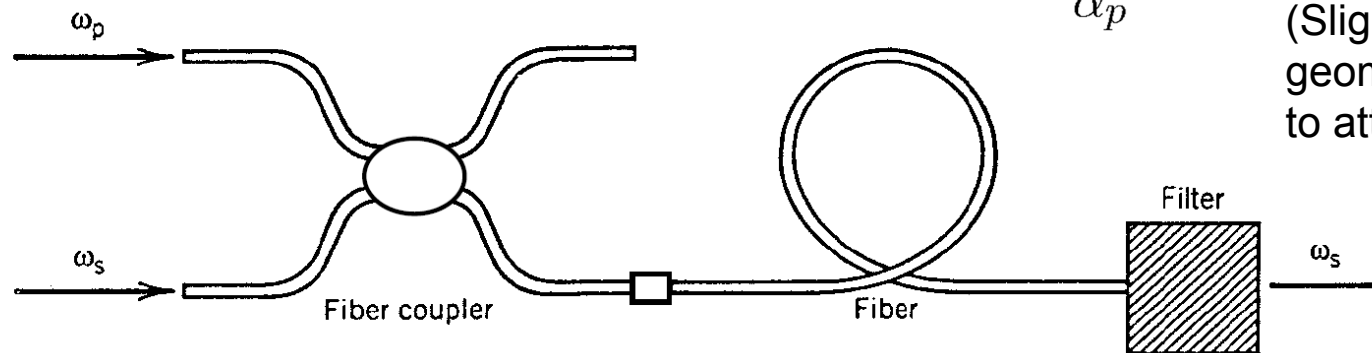
- Raman amplifier:

Small-signal approximation: Neglect Raman-induced depletion of the pump wave

$$I_s(L) = I_s(0) e^{-\alpha_s L} G_R, \quad \text{where } G_R = e^{g_R I_p(0) L_{\text{eff}}}. \quad \text{Gain}$$

$$L_{\text{eff}} = \frac{1 - e^{-\alpha_p L}}{\alpha_p}.$$

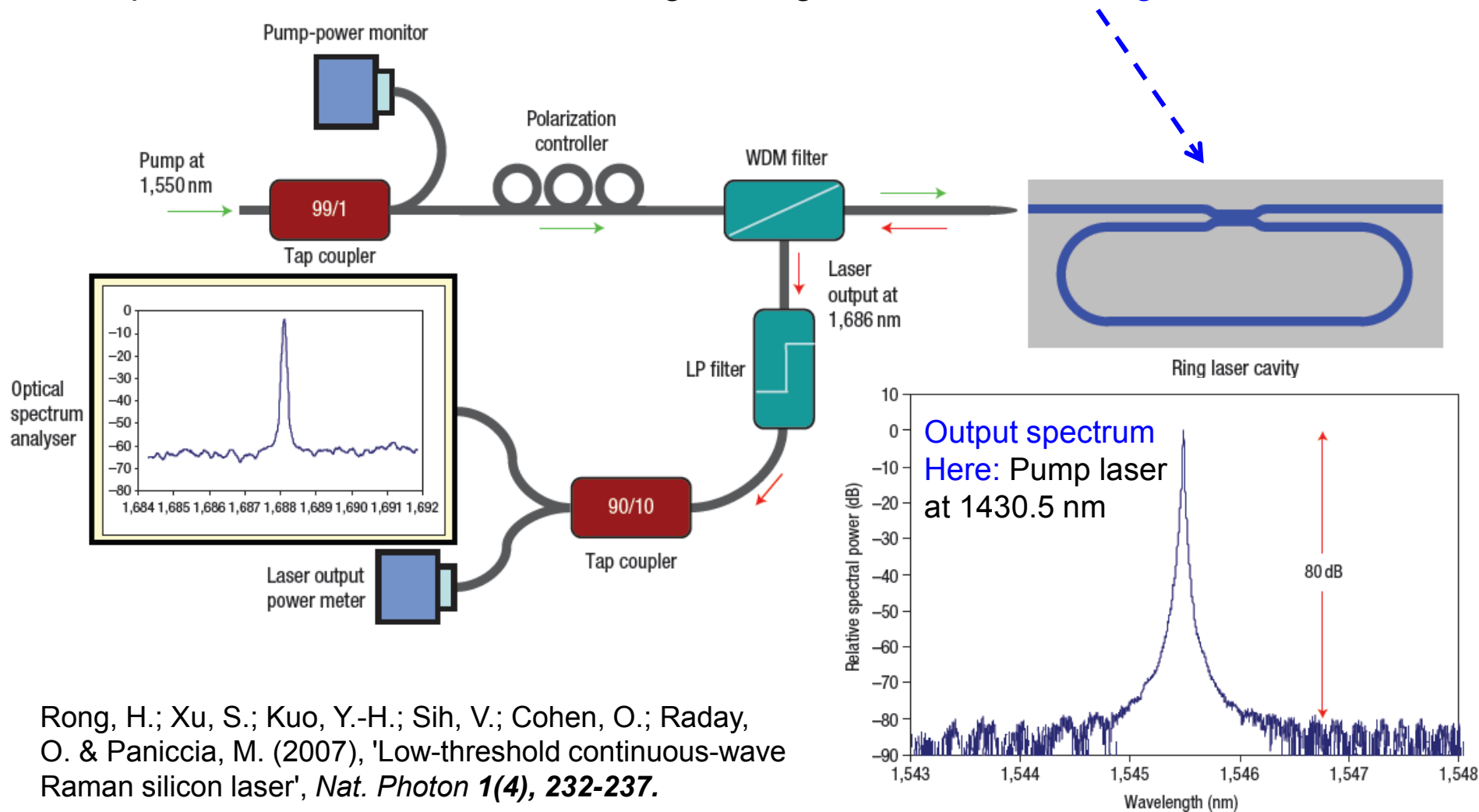
Effective length
(Slightly shorter than geometrical length L due to attenuation of pump)



Example: Raman laser on silicon

Challenge: Light emission on silicon (indirect bandgap!)

⇒ Exploit stimulated Raman scattering in a high-Q **silicon microring resonator**:



Rong, H.; Xu, S.; Kuo, Y.-H.; Sih, V.; Cohen, O.; Raday, O. & Paniccia, M. (2007), 'Low-threshold continuous-wave Raman silicon laser', *Nat. Photon* **1(4)**, 232-237.

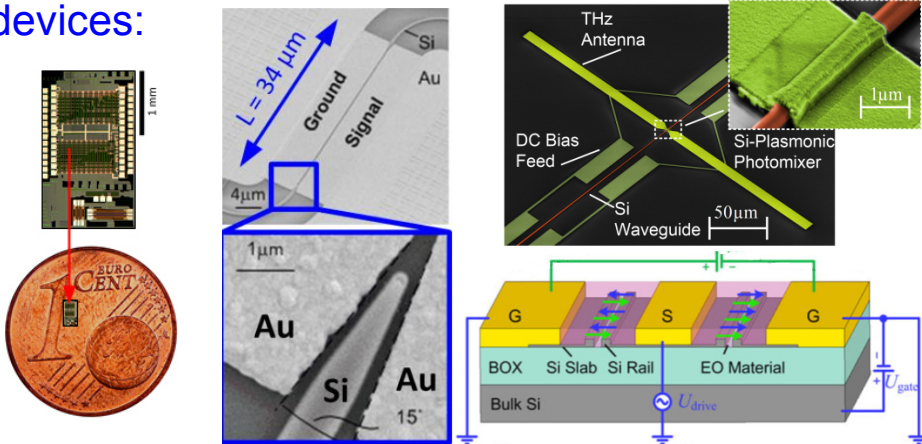
Lecture 13

IPQ Lab Tour

Tuesday, 17. July 2018, 10:30 – 11:15 AM (instead of the NLO lecture)

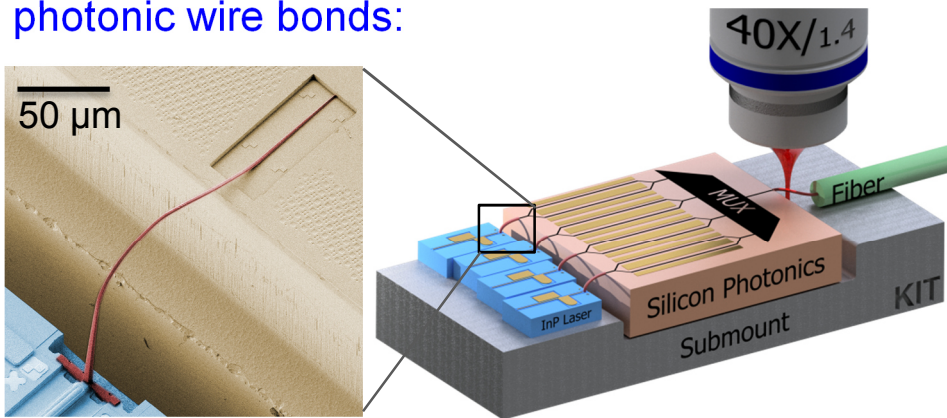
Meeting point: Building 30.10, Room 3.42 (IPQ seminar room)

Photonic integration, plasmonics and THz devices:

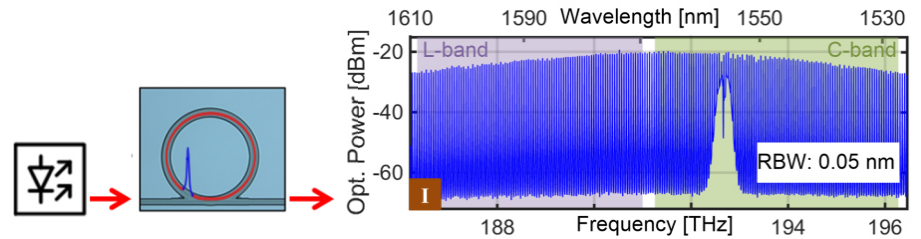


Muehlbrandt *et al.*, *Optica* **3**, 741-747 (2016)

3D-nanoprinting by two-photon lithography/
photonic wire bonds:

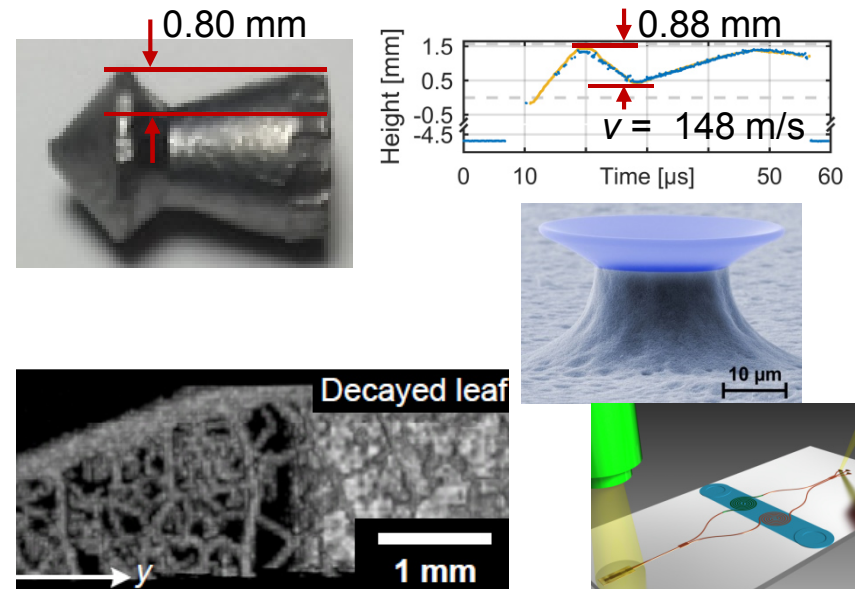


Frequency combs and optical communications:



Marin *et al.*, *Nature* **546**, 274–279 (2017)

Metrology, sensing und biophotonics:

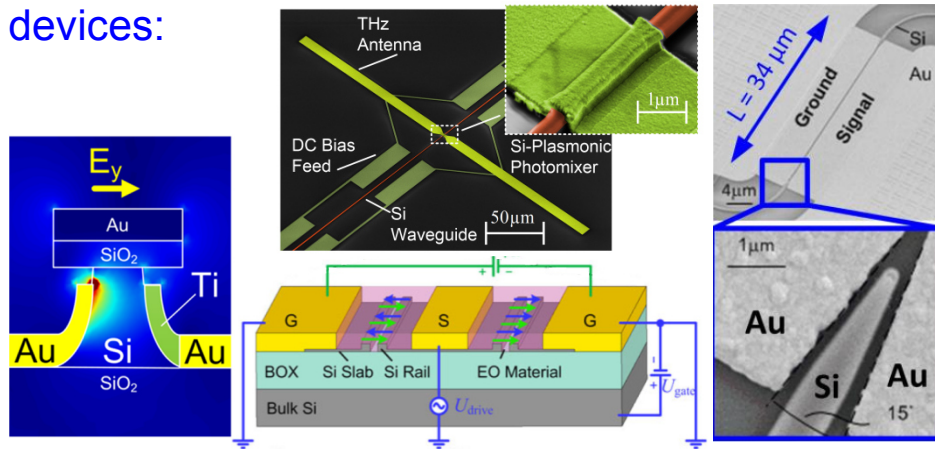


IPQ Lab Tour

Tuesday, 17. July 2018, 10:30 – 11:15 AM (after the NLO tutorial)

Meeting point: Building 30.10, Room 3.42 (IPQ seminar room)

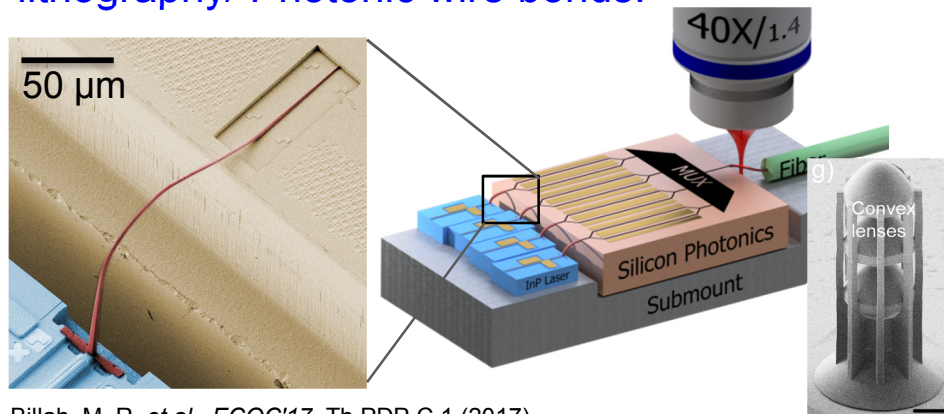
Photonic integration, plasmonics and THz devices:



Muehlbrandt, S. *et al.*, *Optica* **3**, 741 (2016).

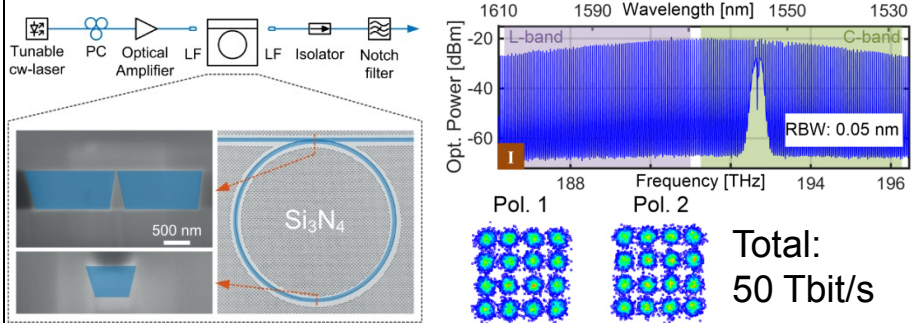
3D-Nanoprinting by two-photon lithography/ Photonic wire bonds:

vanguard
PHOTONICS



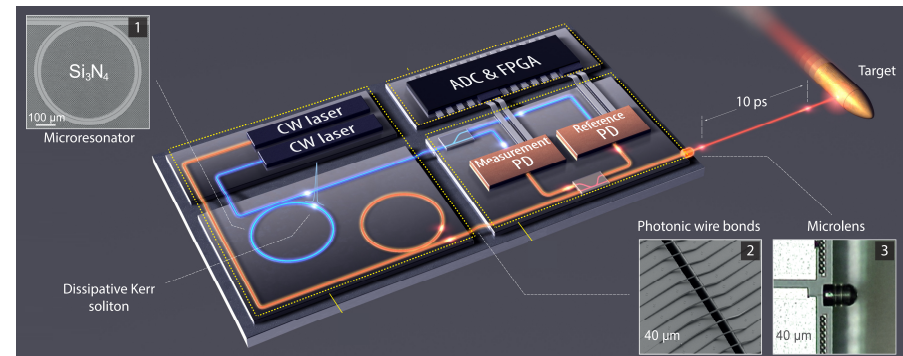
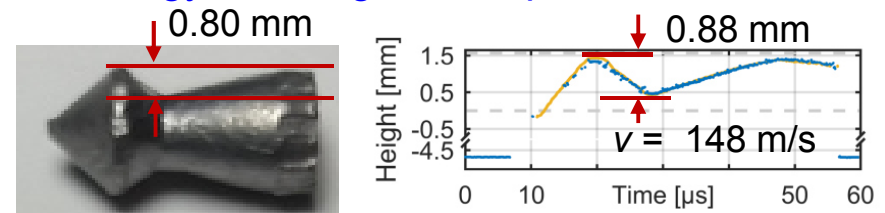
Billah, M. R. *et al.*, *ECOC'17*, Th.PDP.C.1 (2017)

Frequency combs and optical communications:



Marin-Palomo, P. *et al.*, *Nature* **546**, 274–279 (2017).

Metrology, sensing und biophotonics:



Trocha, P. *et al.*, *Science* **359**, 887-891 (2018)

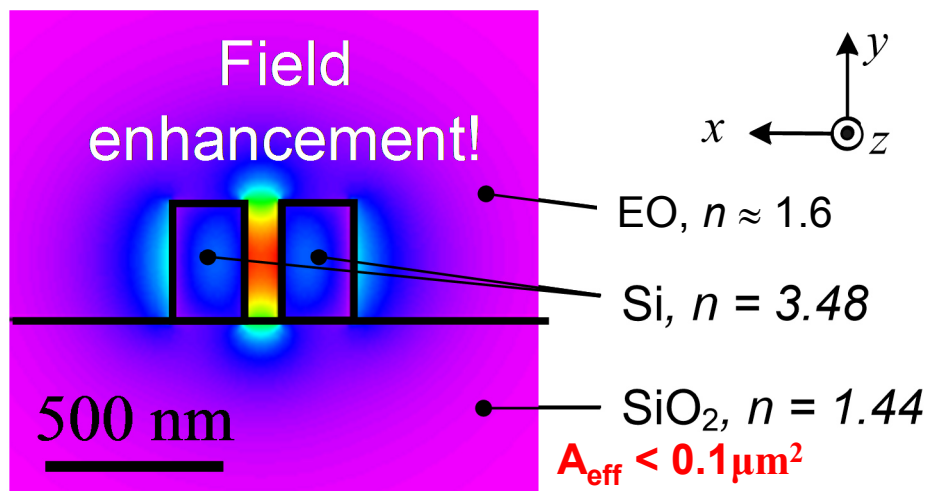
Third-order nonlinearities

- Dominate in many materials (e.g., if second-order nonlinear effects are absent)
- Can be strong for high intensities and/or large interaction lengths
- **Note:** Some third-order nonlinear optical effects are inherently phase-matched (SPM, XPM)!

Examples:

Nanophotonic waveguides:

- Strong confinement: Small effective cross section (diameter $< 1 \mu\text{m}$)
⇒ Large intensities!
- Typically mm-scale interaction lengths



Optical fibers:

- Core diameter $\approx 10 \mu\text{m}$
- Interaction over several kilometres!

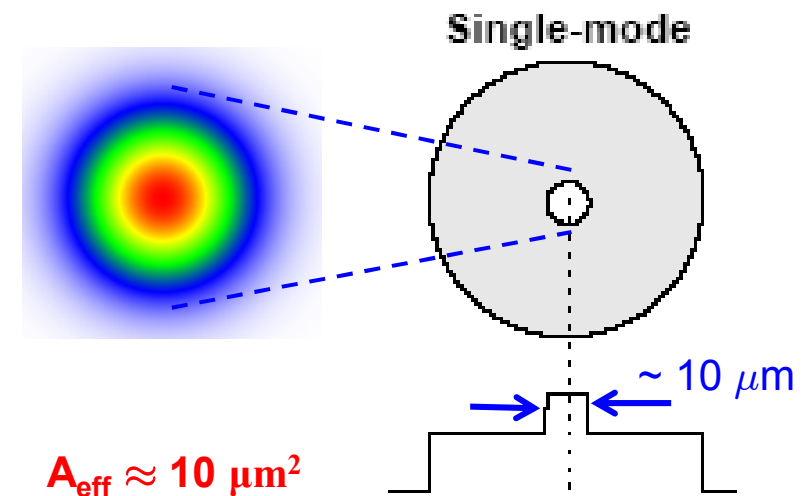
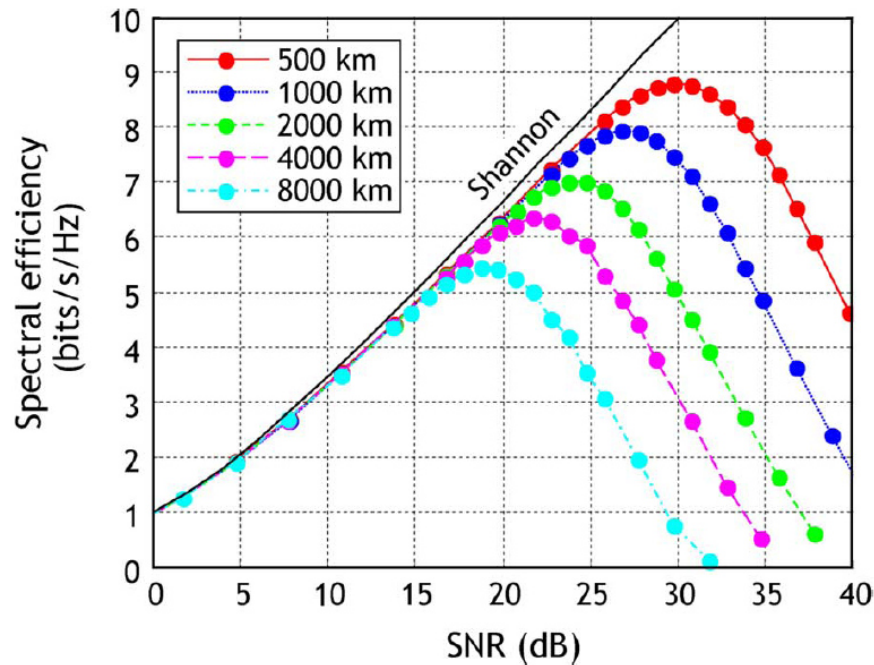


Figure adapted from:
<http://network.boerderie.com/fiber-optics/fiber.html>

Capacity of optical fibers is eventually limited by nonlinearities!

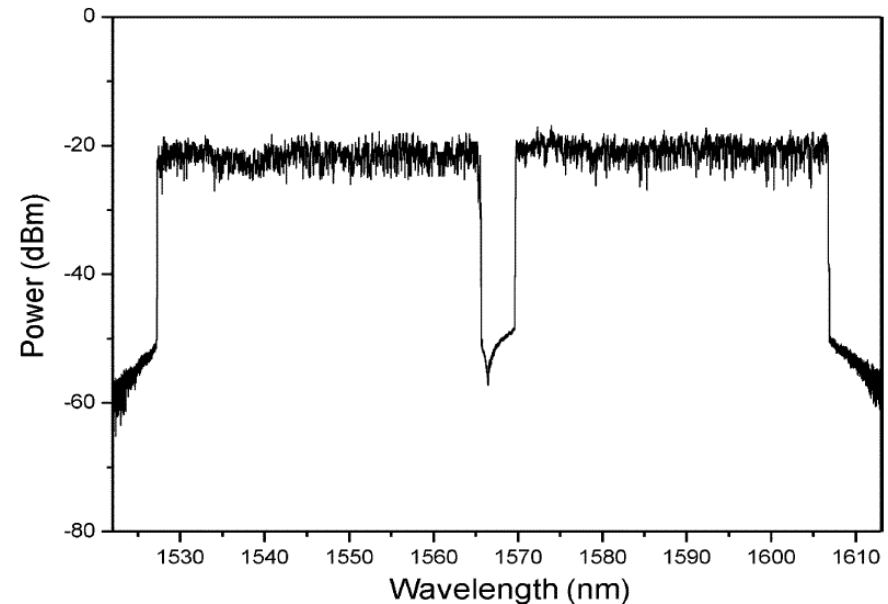
Capacity / spectral efficiency of optical fibers is limited by third-order nonlinearities



Essiambre *et al.*, 'Capacity Limits of Optical Fiber Networks', *Journal of Lightwave Technology* **28(4)**, 662 -701 (2010)

Record transmission speed over a single fiber core: 101.7 Tbit/s

- Transmission distance: 3 x 55 km
- Spectral efficiency: 11 bit/s/Hz
- Total power < 100 mW



Qian *et al.*, 'High Capacity/Spectral Efficiency 101.7-Tb/s WDM Transmission Using PDM-128QAM-OFDM Over 165-km SSMF Within C- and L-Bands', *Lightwave Technology, Journal of* **30(10)**, 1540-1548 (2012).

Waveguide modes for monochromatic waves:

Lossless z-invariant dielectric structure
 (“lossless homogeneous waveguide”):

$$n = n(x,y)$$

where $\text{Im}\{n\} = 0$ throughout space.

Eigenmodes: A lossless homogenous waveguide features a set of electromagnetic wave patterns which do not change their transverse shapes during propagation along z, so-called **eigenmodes**:

$$\underline{\mathbf{E}}(\mathbf{r}, t) = \underline{\mathcal{E}}(x, y, \omega) e^{j(\omega t - \beta(\omega)z)},$$

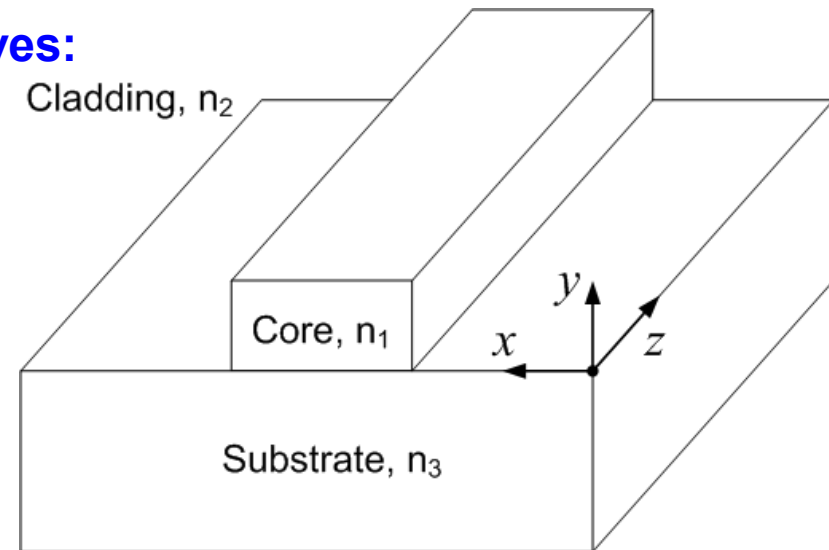
$$\underline{\mathbf{H}}(\mathbf{r}, t) = \underline{\mathcal{H}}(x, y, \omega) e^{j(\omega t - \beta(\omega)z)}$$

$\beta(\omega)$ Dispersion relation

⇒ **Maxwell’s equations for monochromatic guided modes** (to be solved numerically...):

$$(\nabla \times \underline{\mathcal{E}}(x, y, \omega)) - j\beta(\omega) \mathbf{e}_z \times \underline{\mathcal{E}}(x, y, \omega) = -j\omega\mu_0 \underline{\mathcal{H}}(x, y, \omega)$$

$$(\nabla \times \underline{\mathcal{H}}(x, y, \omega)) - j\beta(\omega) \mathbf{e}_z \times \underline{\mathcal{H}}(x, y, \omega) = j\omega\epsilon_0 n^2 \underline{\mathcal{E}}(x, y, \omega).$$



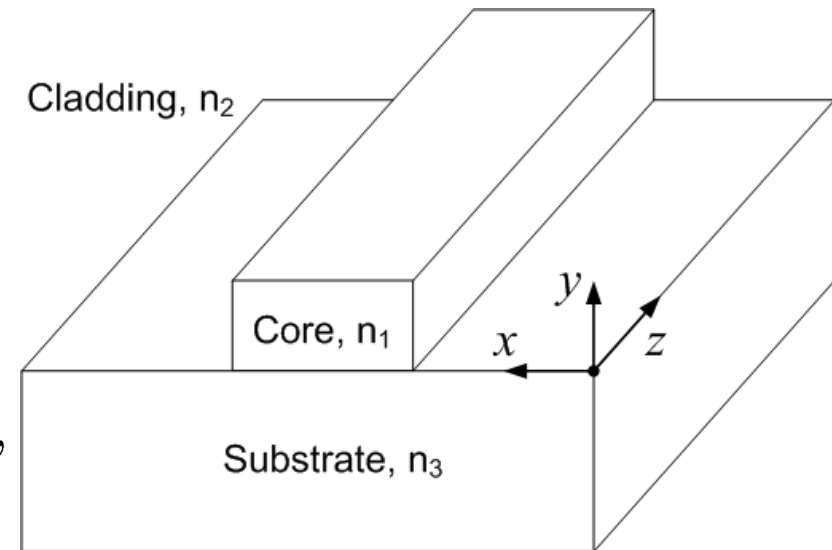
Further information:

Lecture „Optical waveguides and fibers (OWF)“
 ⇒ Winter term

Mode expansion: For a given frequency, *any* field pattern propagating along a waveguide can be expressed as a superposition of eigenmodes (**completeness**)

$$\underline{\mathbf{E}}(\mathbf{r}, t) = \sum_{\mu} \underline{A}_{\mu} \underline{\mathcal{E}}_{\mu}(x, y, \omega) e^{j(\omega t - \beta_{\mu}(\omega)z)},$$

$$\underline{\mathbf{H}}(\mathbf{r}, t) = \sum_{\mu} \underline{A}_{\mu} \underline{\mathcal{H}}_{\mu}(x, y, \omega) e^{j(\omega t - \beta_{\mu}(\omega)z)},$$



Orthogonality relation:

$$\frac{1}{4} \iint_{-\infty}^{\infty} \left(\underline{\mathcal{E}}_{\nu}(x, y) \times \underline{\mathcal{H}}_{\mu}^*(x, y) + \underline{\mathcal{E}}_{\mu}^*(x, y) \times \underline{\mathcal{H}}_{\nu}(x, y) \right) \cdot \mathbf{e}_z \, dx \, dy = \mathcal{P}_{\mu} \delta_{\nu\mu},$$

where $\mathcal{P}_{\mu} = \frac{1}{2} \iint_{-\infty}^{\infty} \text{Re} \left\{ \underline{\mathcal{E}}_{\mu}(x, y) \times \underline{\mathcal{H}}_{\mu}^*(x, y) \right\} \cdot \mathbf{e}_z \, dx \, dy.$

Further information: Lecture „Optical waveguides and fibers (OWF)“

⇒ Winter term

Time-domain description, based on slowly-varying envelopes:

$$\begin{aligned}\underline{\mathbf{E}}(\mathbf{r}, t) &= \underline{A}(z, t) \underline{\mathcal{E}}(x, y, \omega_c) e^{j(\omega_c t - \beta(\omega_c)z)}, \\ \underline{\mathbf{H}}(\mathbf{r}, t) &= \underline{A}(z, t) \underline{\mathcal{H}}(x, y, \omega_c) e^{j(\omega_c t - \beta(\omega_c)z)}\end{aligned}$$

Maxwell's equations:

$$\begin{aligned}\tilde{\underline{A}}(z, \omega - \omega_c) (\nabla \times \underline{\mathcal{E}}(x, y, \omega_c)) \\ + \left(\frac{\partial \tilde{\underline{A}}(z, \omega - \omega_c)}{\partial z} - j\beta(\omega_c) \tilde{\underline{A}}(z, \omega - \omega_c) \right) \mathbf{e}_z \times \underline{\mathcal{E}}(x, y, \omega_c) \\ = -j\omega\mu_0 \underline{\mathcal{H}}(x, y, \omega_c).\end{aligned}$$

Differential equation in frequency domain:

$$\frac{\partial \tilde{\underline{A}}(z, \omega - \omega_c)}{\partial z} + j(\beta(\omega) - \beta(\omega_c)) \tilde{\underline{A}}(z, \omega - \omega_c) = 0$$

Use Taylor expansion of dispersion relation about ω_c :

$$\beta(\omega) \approx \beta_c^{(0)} + (\omega - \omega_c)\beta_c^{(1)} + \frac{(\omega - \omega_c)^2}{2!}\beta_c^{(2)} + \frac{(\omega - \omega_c)^3}{3!}\beta_c^{(3)} + \dots,$$

where $\beta_c^{(i)} = \left. \frac{d^i \beta(\omega)}{d\omega^i} \right|_{\omega=\omega_c}$.

Differential equation in the time domain:

$$\frac{\partial \underline{A}(z, t)}{\partial z} + \beta_c^{(1)} \frac{\partial \underline{A}(z, t)}{\partial t} - j \frac{1}{2} \beta_c^{(2)} \frac{\partial^2 \underline{A}(z, t)}{\partial t^2} + \dots = 0.$$

Introduce retarded time frame:

$$t' = t - \beta_c^{(1)} z,$$

$$z' = z,$$

$$\underline{A}(z, t) = \underline{A}'(z, t - \beta_c^{(1)} z).$$

Simplified differential equation:

$$\frac{\partial \underline{A}'(z', t')}{\partial z'} - j \frac{1}{2} \beta_c^{(2)} \frac{\partial^2 \underline{A}'(z', t')}{\partial t'^2} + \dots = 0.$$

Example: Propagation of a Gaussian impulse through a dispersive waveguide

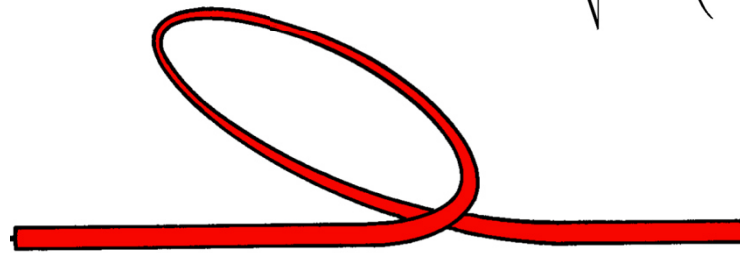
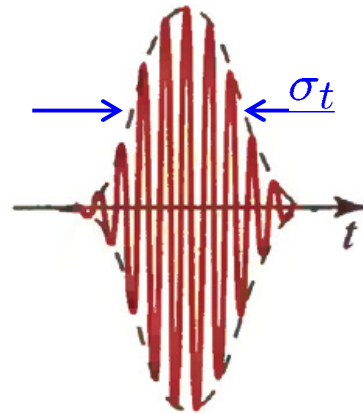
Solve corresponding DEq. in the frequency domain:

$$\tilde{\underline{A}}(z, \omega) = \tilde{\underline{A}}(0, \omega) e^{-j \frac{1}{2} \beta_c^{(2)} \omega^2 z}.$$

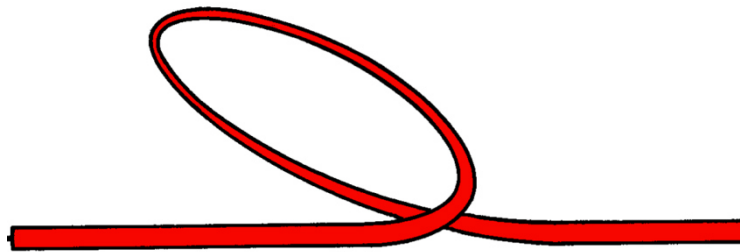
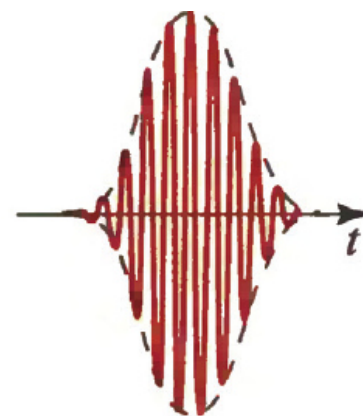
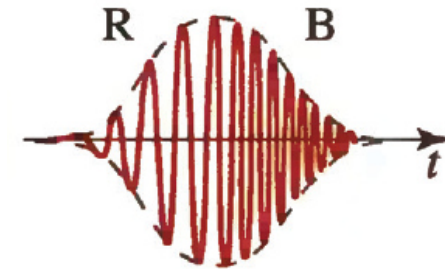
Dispersive broadening of a Gaussian Impulse

$$\underline{A}(0, t) = \underline{A}_0 e^{-\frac{t^2}{2\sigma_t^2}},$$

$$\underline{A}(z, t) = \underline{A}_0 \sqrt{\frac{2\pi\sigma_t^2}{2\pi(\sigma_t^2 - j\beta_c^{(2)}z)}} e^{-\frac{(\sigma_t^2 - j\beta_c^{(2)}z)t^2}{2(\sigma_t^4 + (\beta_c^{(2)}z)^2)}}.$$



Normal GVD: $\beta_c^{(2)} > 0$



Anomalous GVD: $\beta_c^{(2)} < 0$

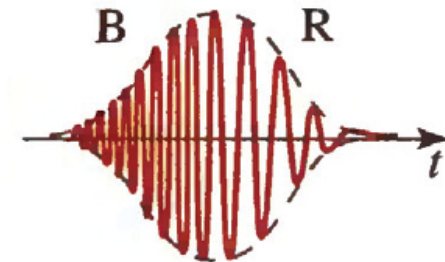


Figure adapted from: Saleh, B. E. A. & Teich, M. C. (2007), *Fundamentals of Photonics*, John Wiley & Sons, Hoboken, NJ.

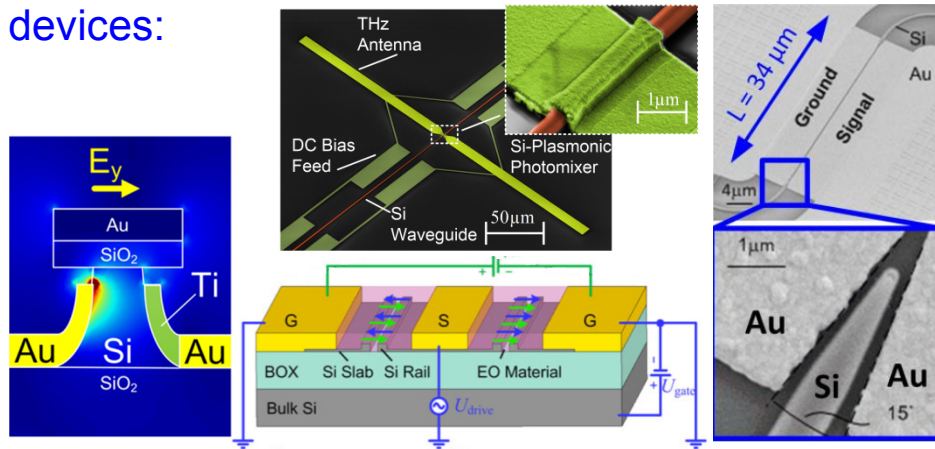
Lecture 14

IPQ Lab Tour

Tuesday, 17. July 2018, 10:30 – 11:15 AM (after the NLO tutorial)

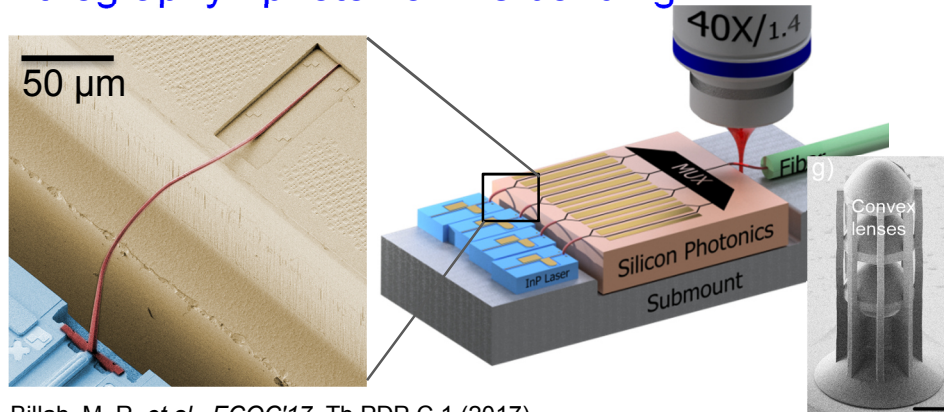
Meeting point: Building 30.10, Room 3.42 (IPQ seminar room)

Photonic integration, plasmonics and THz devices:



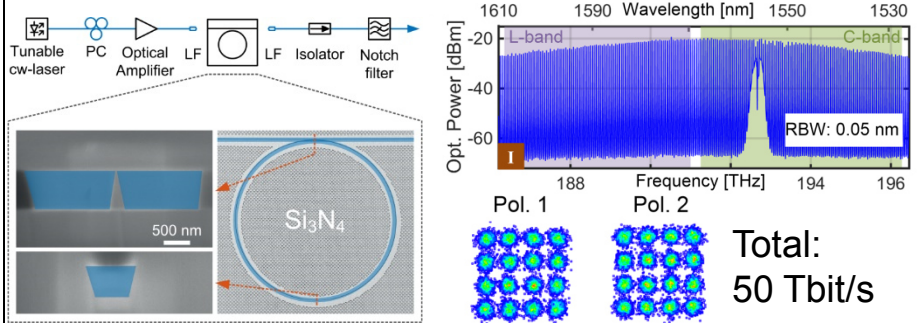
Muehlbrandt, S. *et al.*, *Optica* **3**, 741 (2016).

3D-Nanoprinting by two-photon lithography / photonic wire bonding: **vanguard PHOTONICS**



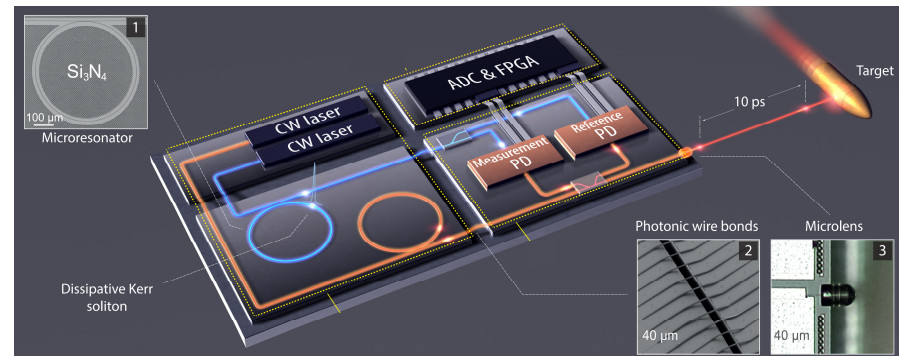
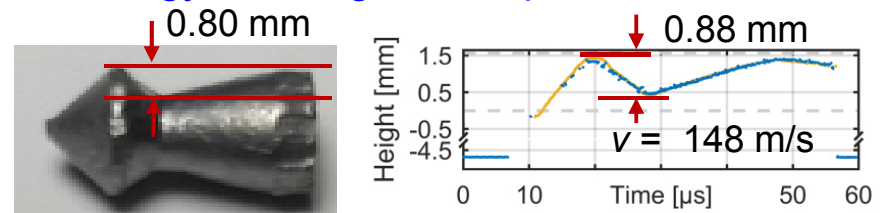
Billah, M. R. *et al.*, *ECOC'17*, Th.PDP.C.1 (2017)

Frequency combs and optical communications:



Marin-Palomo, P. *et al.*, *Nature* **546**, 274–279 (2017).

Metrology, sensing und biophotonics:



Trocha, P. *et al.*, *Science* **359**, 887-891 (2018)

Differential equation in the time domain:

$$\frac{\partial \underline{A}(z, t)}{\partial z} + \beta_c^{(1)} \frac{\partial \underline{A}(z, t)}{\partial t} - j \frac{1}{2} \beta_c^{(2)} \frac{\partial^2 \underline{A}(z, t)}{\partial t^2} + \dots = 0.$$

Introduce retarded time frame:

$$t' = t - \beta_c^{(1)} z,$$

$$z' = z,$$

$$\underline{A}(z, t) = \underline{A}'(z, t - \beta_c^{(1)} z).$$

Simplified differential equation:

$$\frac{\partial \underline{A}'(z', t')}{\partial z'} - j \frac{1}{2} \beta_c^{(2)} \frac{\partial^2 \underline{A}'(z', t')}{\partial t'^2} + \dots = 0.$$

Example: Propagation of a Gaussian impulse through a dispersive waveguide

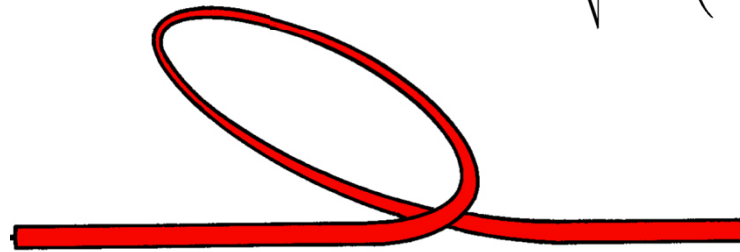
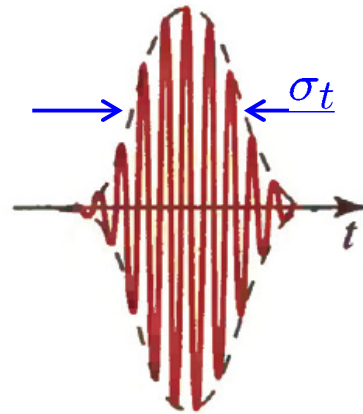
Solve corresponding DEq. in the frequency domain:

$$\tilde{\underline{A}}(z, \omega) = \tilde{\underline{A}}(0, \omega) e^{-j \frac{1}{2} \beta_c^{(2)} \omega^2 z}.$$

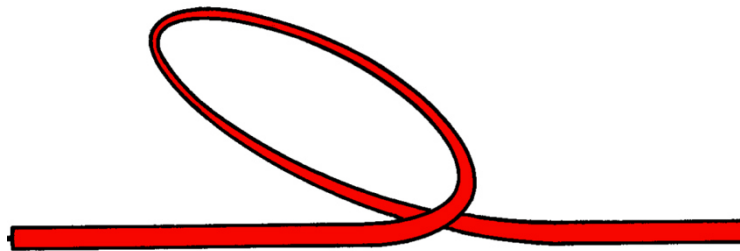
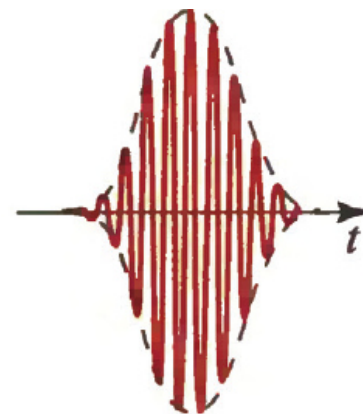
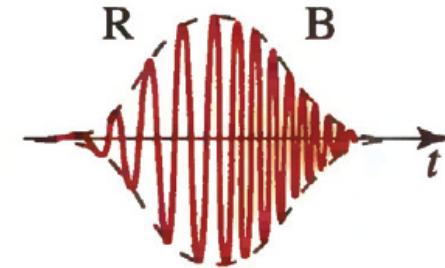
Dispersive broadening of a Gaussian Impulse

$$\underline{A}(0, t) = \underline{A}_0 e^{-\frac{t^2}{2\sigma_t^2}},$$

$$\underline{A}(z, t) = \underline{A}_0 \sqrt{\frac{2\pi\sigma_t^2}{2\pi(\sigma_t^2 - j\beta_c^{(2)}z)}} e^{-\frac{(\sigma_t^2 - j\beta_c^{(2)}z)t^2}{2(\sigma_t^4 + (\beta_c^{(2)}z)^2)}}.$$



Normal GVD: $\beta_c^{(2)} > 0$



Anomalous GVD: $\beta_c^{(2)} < 0$

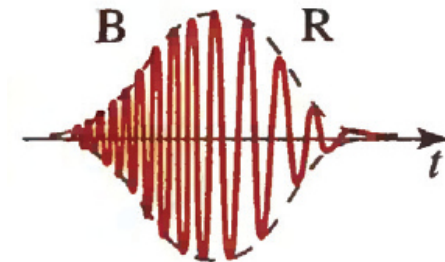


Figure adapted from: Saleh, B. E. A. & Teich, M. C. (2007), *Fundamentals of Photonics*, John Wiley & Sons, Hoboken, NJ.

Now: Consider joint influence of dispersion and optical nonlinearities

Maxwell's equations:

$$\nabla \times \mathbf{H}(\mathbf{r}, t) = \epsilon_0 n^2 \frac{\partial}{\partial t} \mathbf{E}(\mathbf{r}, t) + \frac{\partial}{\partial t} \mathbf{P}_{\text{NL}}(\mathbf{r}, t),$$

$$\nabla \times \mathbf{E}(\mathbf{r}, t) = -\mu_0 \frac{\partial}{\partial t} \mathbf{H}(\mathbf{r}, t).$$

General SVEA mode ansatz:

$$\mathbf{E}(\mathbf{r}, t) = \frac{1}{2} \sum_{m=-M}^M \sum_{\mu} \underline{A}_{\mu}(z, t, \omega_m) \frac{\underline{\mathcal{E}}_{\mu}(x, y, \omega_m)}{\sqrt{\mathcal{P}_{\mu}}} e^{j(\omega_m t - \beta_{\mu}(\omega_m) z)},$$

$$\mathbf{H}(\mathbf{r}, t) = \frac{1}{2} \sum_{m=-M}^M \sum_{\mu} \underline{A}_{\mu}(z, t, \omega_m) \frac{\underline{\mathcal{H}}_{\mu}(x, y, \omega_m)}{\sqrt{\mathcal{P}_{\mu}}} e^{j(\omega_m t - \beta_{\mu}(\omega_m) z)},$$

↖
↖
↖

Various frequencies
(generated by optical nonlinearities)
 ↖
 Various modes
(coupled by optical nonlinearities)
 ↖
 Power normalization

where $\mathcal{P}_{\mu} = \frac{1}{2} \iint_{-\infty}^{\infty} \text{Re} \{ \underline{\mathcal{E}}_{\mu}(x, y) \times \underline{\mathcal{H}}_{\mu}^*(x, y) \} \cdot \mathbf{e}_z \, dx \, dy.$

$$\mathbf{P}_{\text{NL}}(\mathbf{r}, t) = \frac{1}{2} \sum_{m=-M}^{+M} \underline{\mathbf{P}}_{\text{NL}}(\mathbf{r}, t, \omega_m) e^{j\omega_m t},$$

Insert mode ansatz into Maxwell's equations in the frequency domain:

Recall: $\nabla \times (\Phi \mathbf{F}) = \Phi (\nabla \times \mathbf{F}) + (\nabla \Phi \times \mathbf{F})$

$$\begin{aligned} \Rightarrow \sum_{\mu} \tilde{A}_{\mu}(z, \omega - \omega_m, \omega_m) e^{-j\beta_{\mu}(\omega_m)z} & \left[\nabla \times \frac{\mathcal{H}_{\mu}(x, y, \omega_m)}{\sqrt{\mathcal{P}_{\mu}}} \right] \\ + \frac{\partial}{\partial z} \left[\tilde{A}_{\mu}(z, \omega - \omega_m, \omega_m) e^{-j\beta_{\mu}(\omega_m)z} \right] \mathbf{e}_z \times & \frac{\mathcal{H}_{\mu}(x, y, \omega_m)}{\sqrt{\mathcal{P}_{\mu}}} \\ - j\omega \epsilon_0 n^2 \tilde{A}_{\mu}(z, \omega - \omega_m, \omega_m) \frac{\mathcal{E}_{\mu}(x, y, \omega_m)}{\sqrt{\mathcal{P}_{\mu}}} e^{-j\beta_{\mu}(\omega_m)z} & = j\omega \tilde{P}_{\text{NL}}(\mathbf{r}, \omega - \omega_m, \omega_m) \\ \sum_{\mu} \tilde{A}_{\mu}(z, \omega - \omega_m, \omega_m) e^{-j\beta_{\mu}(\omega_m)z} & \left[\nabla \times \frac{\mathcal{E}_{\mu}(x, y, \omega_m)}{\sqrt{\mathcal{P}_{\mu}}} \right] \\ + \frac{\partial}{\partial z} \left[\tilde{A}_{\mu}(z, \omega - \omega_m, \omega_m) e^{-j\beta_{\mu}(\omega_m)z} \right] \mathbf{e}_z \times & \frac{\mathcal{E}_{\mu}(x, y, \omega_m)}{\sqrt{\mathcal{P}_{\mu}}} \\ + j\omega \mu_0 \tilde{A}_{\mu}(z, \omega - \omega_m, \omega_m) \frac{\mathcal{H}_{\mu}(x, y, \omega_m)}{\sqrt{\mathcal{P}_{\mu}}} e^{-j\beta_{\mu}(\omega_m)z} & = 0. \end{aligned}$$

Signal propagation in third-order nonlinear waveguides

Recall: $\underline{\mathcal{E}}_\mu(x, y, \omega_m)$ and $\underline{\mathcal{H}}_\mu(x, y, \omega_m)$ are guided modes of the linear waveguide!

$$\Rightarrow \begin{aligned} \left(\nabla \times \frac{\underline{\mathcal{E}}_\mu(x, y, \omega)}{\sqrt{\mathcal{P}_\mu}} \right) &= j\beta_\mu(\omega) \mathbf{e}_z \times \frac{\underline{\mathcal{E}}_\mu(x, y, \omega)}{\sqrt{\mathcal{P}_\mu}} - j\omega\mu_0 \frac{\underline{\mathcal{H}}_\mu(x, y, \omega)}{\sqrt{\mathcal{P}_\mu}}, \\ \left(\nabla \times \frac{\underline{\mathcal{H}}_\mu(x, y, \omega)}{\sqrt{\mathcal{P}_\mu}} \right) &= j\beta_\mu(\omega) \mathbf{e}_z \times \frac{\underline{\mathcal{H}}_\mu(x, y, \omega)}{\sqrt{\mathcal{P}_\mu}} + j\omega\epsilon_0 n^2 \frac{\underline{\mathcal{E}}_\mu(x, y, \omega)}{\sqrt{\mathcal{P}_\mu}}. \end{aligned}$$

Insert into derived relations:

Note: $\underline{\mathcal{E}}_\mu(x, y, \omega) \approx \underline{\mathcal{E}}_\mu(x, y, \omega_m)$ for $\omega \approx \omega_m$

$$\sum_\mu \left[\frac{\partial \tilde{\underline{A}}_\mu(z, \omega - \omega_m, \omega_m)}{\partial z} + j(\beta_\mu(\omega) - \beta_\mu(\omega_m)) \tilde{\underline{A}}_\mu(z, \omega - \omega_m, \omega_m) \right] \mathbf{e}_z \times \frac{\underline{\mathcal{H}}_\mu(x, y, \omega_m)}{\sqrt{\mathcal{P}_\mu}} e^{-j\beta_\mu(\omega_m)z} = j\omega \tilde{\underline{\mathbf{P}}}_{\text{NL}}(\mathbf{r}, \omega - \omega_m, \omega_m)$$

$$\sum_\mu \left[\frac{\partial \tilde{\underline{A}}_\mu(z, \omega - \omega_m, \omega_m)}{\partial z} + j(\beta_\mu(\omega) - \beta_\mu(\omega_m)) \tilde{\underline{A}}_\mu(z, \omega - \omega_m, \omega_m) \right] \mathbf{e}_z \times \frac{\underline{\mathcal{E}}_\mu(x, y, \omega_m)}{\sqrt{\mathcal{P}_\mu}} e^{-j\beta_\mu(\omega_m)z} = 0$$

Recall: Orthogonality relation

$$\frac{1}{4} \iint_{-\infty}^{\infty} (\underline{\mathcal{E}}_\mu(x, y) \times \underline{\mathcal{H}}_\nu^*(x, y) + \underline{\mathcal{E}}_\nu^*(x, y) \times \underline{\mathcal{H}}_\mu(x, y)) \cdot \mathbf{e}_z \, dx \, dy = \mathcal{P}_\mu \delta_{\nu\mu},$$

Dot-multiply with $[-\underline{\mathcal{E}}_\nu^*(x, y, \omega_m)]$ and $\underline{H}_\nu^*(x, y, \omega_m)$ and add resulting relations

$$\Rightarrow \sum_{\mu} \left[\frac{\partial \tilde{A}_\mu(z, \omega - \omega_m, \omega_m)}{\partial z} + j(\beta_\mu(\omega) - \beta_\mu(\omega_m)) \tilde{A}_\mu(z, \omega - \omega_m, \omega_m) \right] \left[\frac{\underline{\mathcal{E}}_\mu(x, y, \omega_m) \times \underline{H}_\nu^*(x, y, \omega_m) + \underline{\mathcal{E}}_\nu^*(x, y, \omega_m) \times \underline{H}_\mu(x, y, \omega_m)}{\sqrt{\mathcal{P}_\mu}} \right] e_z e^{-j\beta_\mu(\omega_m)z} = -j\omega \tilde{\mathbf{P}}_{\text{NL}}(\mathbf{r}, \omega - \omega_m, \omega_m) \cdot \underline{\mathcal{E}}_\nu^*(x, y, \omega_m)$$

Integrate over the entire (x,y)-plane and make use of orthogonality relation

$$\Rightarrow \left[\frac{\partial \tilde{A}_\nu(z, \omega - \omega_m, \omega_m)}{\partial z} + j(\beta_\nu(\omega) - \beta_\nu(\omega_m)) \tilde{A}_\nu(z, \omega - \omega_m, \omega_m) \right] e^{-j\beta_\nu(\omega_m)z} = -\frac{j\omega}{4\sqrt{\mathcal{P}_\nu}} \iint_{-\infty}^{\infty} \tilde{\mathbf{P}}_{\text{NL}}(\mathbf{r}, \omega - \omega_m, \omega_m) \cdot \underline{\mathcal{E}}_\nu^*(x, y, \omega_m) dx dy$$

Use Taylor expansion of the propagation constant $\beta_\nu(\omega)$ about the carrier frequency ω_m

$$\beta(\omega) \approx \beta_c^{(0)} + (\omega - \omega_c)\beta_c^{(1)} + \frac{(\omega - \omega_c)^2}{2!}\beta_c^{(2)} + \frac{(\omega - \omega_c)^3}{3!}\beta_c^{(3)} + \dots,$$

Transform back to the time domain ...

$$\begin{aligned} \Rightarrow & \left[\frac{\partial \underline{A}_\nu(z, t, \omega_m)}{\partial z} + \beta_c^{(1)} \frac{\partial \underline{A}_\nu(z, t, \omega_m)}{\partial t} - j \frac{1}{2} \beta_c^{(2)} \frac{\partial^2 \underline{A}_\nu(z, t, \omega_m)}{\partial t^2} \right] e^{j(\omega_m t - \beta_\nu(\omega_m) z)} \\ & = -\frac{1}{4\sqrt{\mathcal{P}_\nu}} \frac{\partial}{\partial t} \left(\iint_{-\infty}^{\infty} \underline{\mathbf{P}}_{\text{NL}}(\mathbf{r}, t, \omega_m) \cdot \underline{\mathcal{E}}_\nu^*(x, y, \omega_m) dx dy e^{j\omega_m t} \right) \end{aligned}$$

Introduce retarded time frame:

$$\begin{aligned} t' &= t - \beta_c^{(1)} z, \\ z' &= z, \\ \underline{A}(z, t) &= \underline{A}'(z, t - \beta_c^{(1)} z). \end{aligned}$$

$$\begin{aligned} \Rightarrow & \left[\frac{\partial \underline{A}_\nu(z, t, \omega_m)}{\partial z} - j \frac{1}{2} \beta_c^{(2)} \frac{\partial^2 \underline{A}_\nu(z, t, \omega_m)}{\partial t^2} \right] e^{-j\beta_\nu(\omega_m) z} \\ & = -\frac{j\omega_m}{4\sqrt{\mathcal{P}_\nu}} \iint_{-\infty}^{\infty} \underline{\mathbf{P}}_{\text{NL}}(\mathbf{r}, t, \omega_m) \cdot \underline{\mathcal{E}}_\nu^*(x, y, \omega_m) dx dy. \end{aligned}$$

(primes skipped ...)

Description of nonlinear polarization

Recall: $\underline{\mathbf{P}}^{(3)}(\omega_m) = \frac{1}{4} \epsilon_0 \sum_{\mathbb{S}(\omega_m)} \underline{\chi}^{(3)}(\omega_m : \omega_l, \omega_p, \omega_o) : \underline{\mathbf{E}}(\omega_l) \underline{\mathbf{E}}(\omega_p) \underline{\mathbf{E}}(\omega_o)$

where $\mathbb{S}(\omega_m) = \left\{ (l_1, \dots, l_n) \mid \omega_{l_1} + \dots + \omega_{l_n} = \omega_m \right\}$.

⇒ For SPM (one frequency component at ω_m only, excitation only by dominant mode ν):

$$\underline{\mathbf{P}}_{\text{NL}}(\mathbf{r}, t, \omega_m) = \frac{3}{4} \epsilon_0 \left(\underline{\chi}^{(3)}(\omega_m : \omega_m, -\omega_m, \omega_m) : \underline{\mathcal{E}}_\nu(x, y, \omega_m) \underline{\mathcal{E}}_\nu^*(x, y, \omega_m) \underline{\mathcal{E}}_\nu(x, y, \omega_m) \right) \frac{\underline{A}_\nu(z, t, \omega_m)}{\sqrt{\mathcal{P}_\nu}} \frac{\underline{A}_\nu^*(z, t, \omega_m)}{\sqrt{\mathcal{P}_\nu}} \frac{\underline{A}_\nu(z, t, \omega_m)}{\sqrt{\mathcal{P}_\nu}} e^{-j\beta_\nu(\omega_m)z}$$

⇒ Nonlinear Schrödinger Equation (NLSE):

$$\frac{\partial \underline{A}_\nu(z, t, \omega_m)}{\partial z} - j \frac{1}{2} \beta_c^{(2)} \frac{\partial^2 \underline{A}_\nu(z, t, \omega_m)}{\partial t^2} = -j\gamma |\underline{A}_\nu(z, t, \omega_m)|^2 \underline{A}_\nu(z, t, \omega_m),$$

where $\gamma_\nu(\omega_m) = \frac{3\omega_m \epsilon_0 \iint_{-\infty}^{\infty} \left[\underline{\chi}^{(3)} : \underline{\mathcal{E}}_\nu \underline{\mathcal{E}}_\nu^* \underline{\mathcal{E}}_\nu \right] \cdot \underline{\mathcal{E}}_\nu^* dx dy}{16 \mathcal{P}_\nu^2}$,

Nonlinearity parameter

⇒ Include waveguide losses:

$$\frac{\partial \underline{A}_\nu(\omega_m)}{\partial z} - j \frac{1}{2} \beta_c^{(2)} \frac{\partial^2 \underline{A}_\nu(\omega_m)}{\partial t^2} = -\frac{\alpha}{2} \underline{A}_\nu(\omega_m) - j\gamma |\underline{A}_\nu(\omega_m)|^2 \underline{A}_\nu(\omega_m),$$

Optical fibers:

- Low index contrast, i.e., index n of the cladding is usually very similar, $n \approx n_{\text{core}} \approx n_{\text{clad}}$
- Isotropic material
- Homogeneous nonlinearity, which does not change over the cross section

⇒ Transverse components of the mode fields may be approximated by a scalar function:

$$\underline{\mathcal{E}}_\nu(x, y, \omega_m) \approx F_\nu(x, y, \omega_m) \mathbf{e}_x,$$
$$\underline{\mathcal{H}}_\nu(x, y, \omega_m) \approx \frac{n}{Z_0} F_\nu(x, y, \omega_m) \mathbf{e}_y.$$

⇒ Simplified representation of nonlinearity parameter:

$$\gamma_\nu(\omega_m) \approx \frac{\omega_m n_2}{c A_{\text{eff}}},$$

where $n_2 = \frac{3Z_0}{4n^2} \chi^{(3)}$, Kerr coefficient

$$A_{\text{eff}} \approx \frac{\left(\iint_{-\infty}^{\infty} |F_\nu(x, y, \omega_m)|^2 dx dy \right)^2}{\iint_{-\infty}^{\infty} |F_\nu(x, y, \omega_m)|^4 dx dy}$$

Effective cross section

Nonlinear phase shift and spectral broadening

Neglect dispersion:
$$\frac{\partial \underline{A}(z, t)}{\partial z} = -j\gamma |\underline{A}(z, t)|^2 \underline{A}(z, t) - \frac{\alpha}{2} \underline{A}(z, t),$$

Solution ansatz:
$$\underline{A}(z, t) = \underline{A}_0(t) e^{j\Phi_{NL}(z, t)} e^{-\frac{\alpha}{2}z},$$

⇒ Nonlinear phase shift:
$$\Phi_{NL}(L, t) = -\gamma |\underline{A}_0(t)|^2 L_{\text{eff}},$$

where
$$L_{\text{eff}} = \frac{1 - e^{-\alpha L}}{\alpha}.$$

Effective length (slightly shorter than geometrical length due to waveguide losses)

Note:

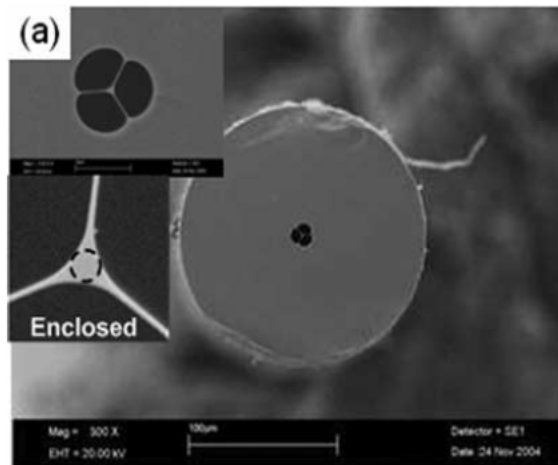
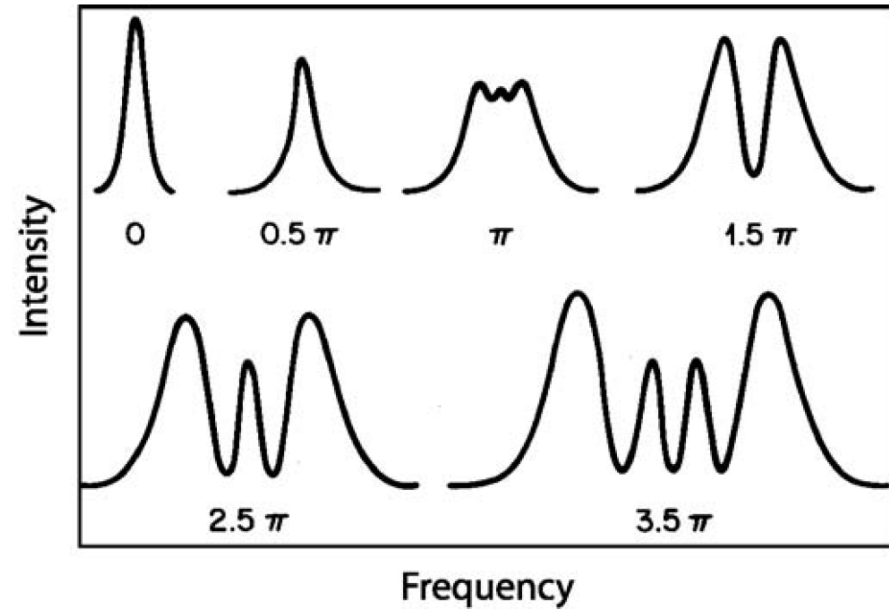
- SPM leaves the temporal pulse power envelope unchanged, but leads to **spectral broadening**
- Instantaneous frequency offset Ω negative near the leading edge of the pulse (red-shift) and positive near the trailing edge (blue-shift)
- **Interplay of SPM and anomalous GVD** can lead to pulse forms that do not change their envelope during propagation, so-called **solitons** (see next section!)



Figure adapted from: Saleh, B. E. A. & Teich, M. C. (2007), *Fundamentals of Photonics*, John Wiley & Sons, Hoboken, NJ.

Spectral broadening and supercontinuum generation

Spectral broadening of a Gaussian pulse for different maximum nonlinear phase shifts at the pulse peak



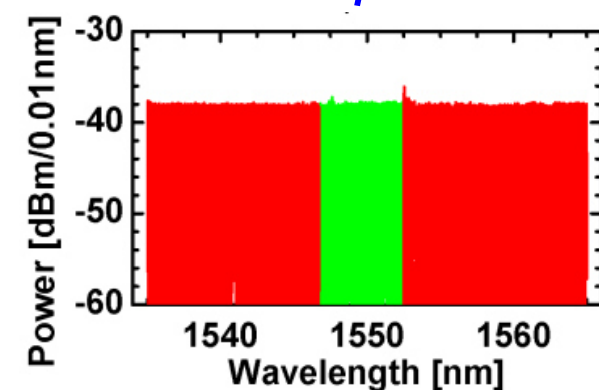
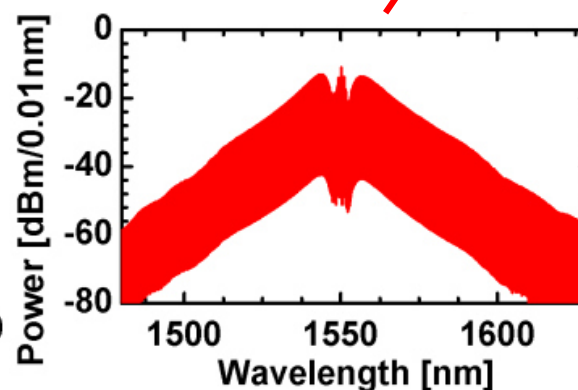
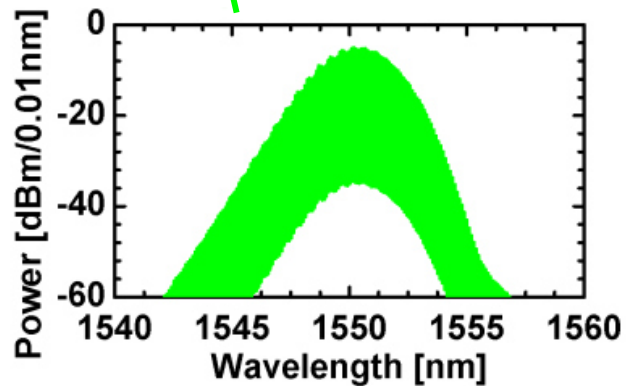
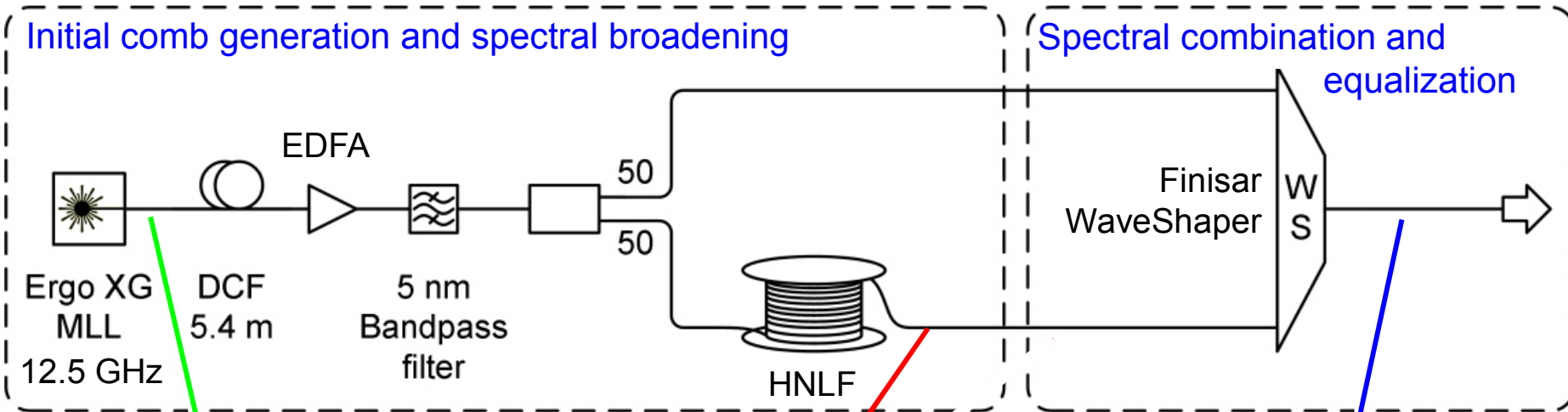
Supercontinuum generation in a highly nonlinear fiber with ultra-small mode field diameter



Frequency comb generation

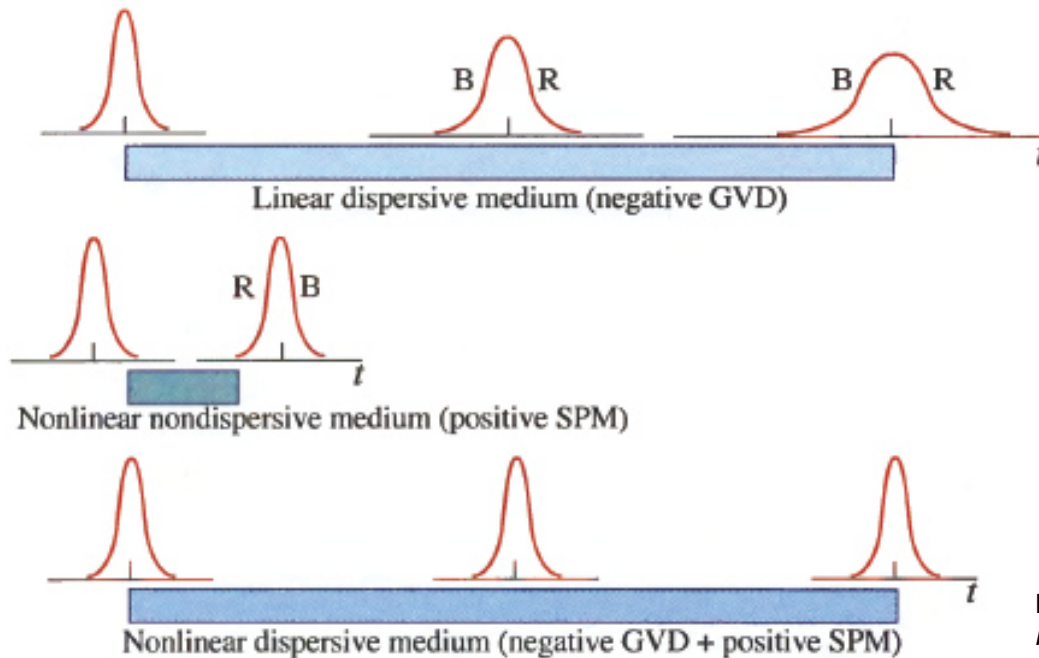
Mode-locked laser + spectral broadening in highly nonlinear fiber (HNLF)

Problem: Spectral dips for SPM-induced phase shifts of $\Delta\Phi \geq 1.5 \pi$



⇒ 325 carriers with 12.5 GHz spacing, linewidth < 10 kHz

Hillerkuss *et al.*, J. Opt. Commun. Netw. 4, 715–723 (2012)



Formation of solitons: Effects of anomalous group-velocity dispersion (GVD) and self-phase modulation cancel each other.

Figure adapted from: Saleh, B. E. A. & Teich, M. C. (2007), *Fundamentals of Photonics*, John Wiley & Sons, Hoboken, NJ.

Mathematical analysis: Start from NLSE, neglect losses

$$\frac{\partial \underline{A}(z, t)}{\partial z} - j \frac{1}{2} \beta_c^{(2)} \frac{\partial^2 \underline{A}(z, t)}{\partial t^2} = -j \gamma |\underline{A}(z, t)|^2 \underline{A}(z, t).$$

Solution ansatz: Real, z-independent envelope + z-dependent “global” phase shift

$$\underline{A}(z, t) = A_0(t) e^{j\Phi(z)}$$

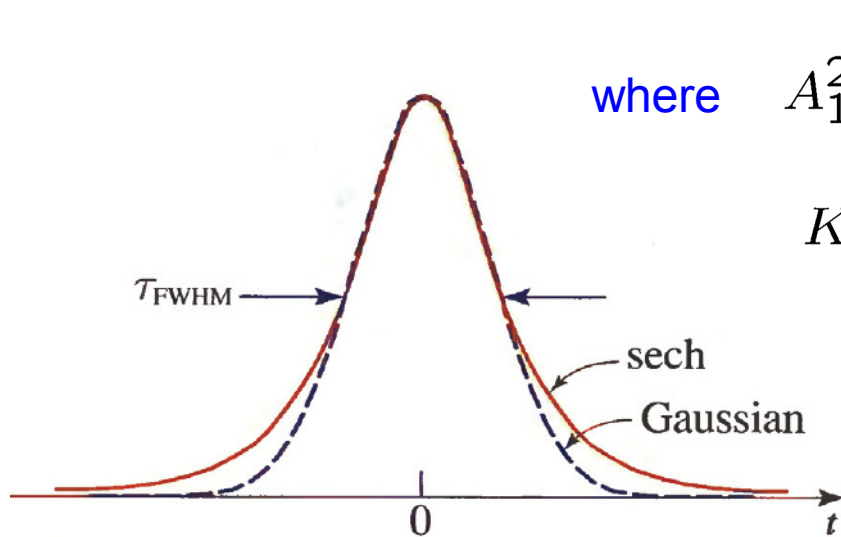
Separation of variables:

$$\Phi(z) = -Kz,$$

$$\frac{\partial^2 A_0(t)}{\partial t^2} = \frac{2}{\beta_c^{(2)}} \left(-K + \gamma A_0^2(t) \right) A_0(t),$$

Solution ansatz for time dependence: $A_0(t) = A_1 \operatorname{sech} \left(\frac{t}{T} \right),$

⇒ Total solution: $\underline{A}(z, t) = A_1 \operatorname{sech} \left(\frac{t}{T} \right) e^{-jKz},$



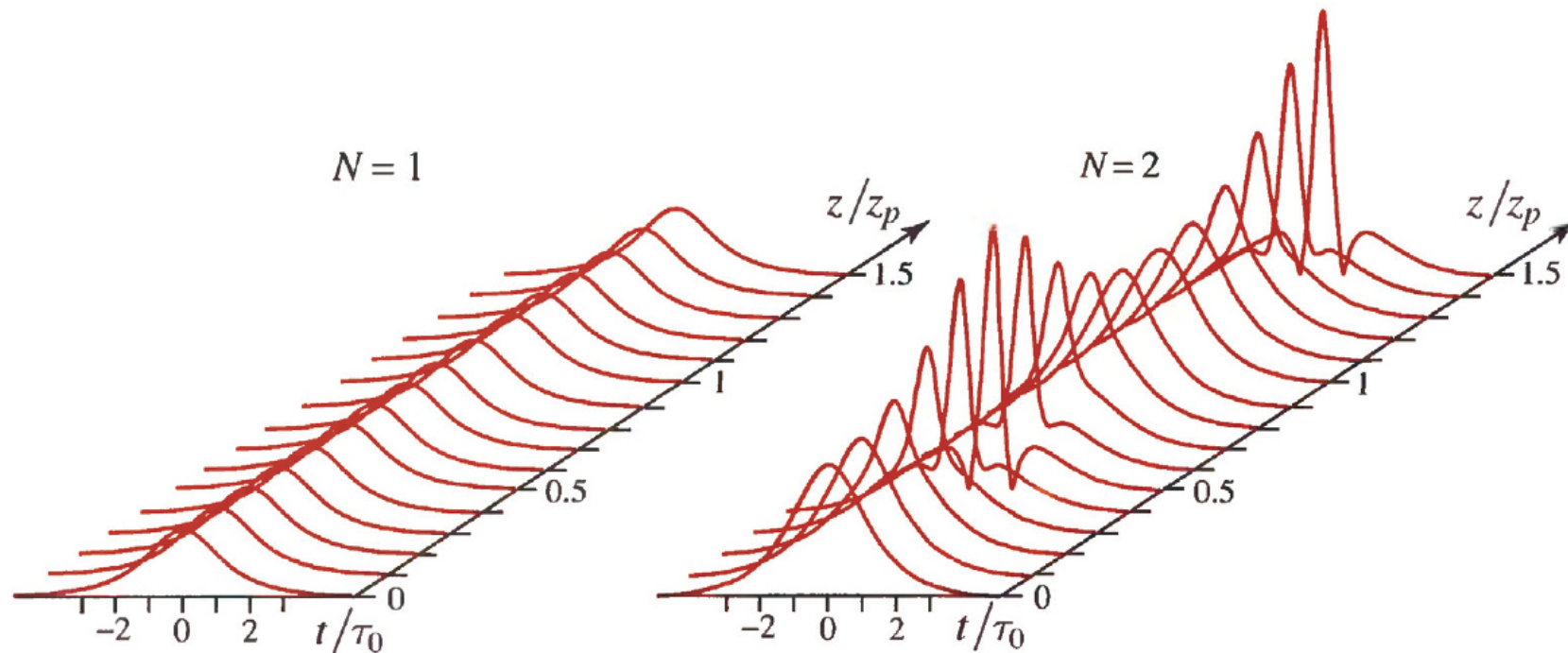
where $A_1^2 = \frac{-\beta_c^{(2)}}{\gamma T^2},$ Peak power (Note: $\beta_c^{(2)} < 0!$)

$K = \frac{1}{2} \gamma A_1^2.$ Global nonlinear phase shift

Note: Soliton duration T and peak power $|A_1|^2$ are linked to each other. The smaller T , the bigger the impact of dispersion, and the bigger the peak power $|A_1|^2$ must be to compensate the dispersion by SPM.

Figure adapted from: Saleh, B. E. A. & Teich, M. C. (2007), *Fundamentals of Photonics*, John Wiley & Sons, Hoboken, NJ.

Higher-order solitons



Fundamental soliton:
Real, z-invariant envelope

Higher-order soliton:
Complex envelope that reproduces itself periodically during propagation.

Figure adapted from: Saleh, B. E. A. & Teich, M. C. (2007), *Fundamentals of Photonics*, John Wiley & Sons, Hoboken, NJ.

Modulation instability

Modulation instability:

Nonlinear interaction transfers power from a **strong continuous-wave (cw)** signal to spectral sidebands. This may lead to the break-up of the cw signal into a train of pulses.

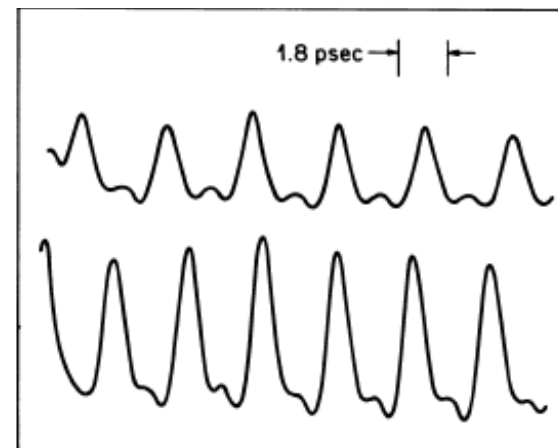
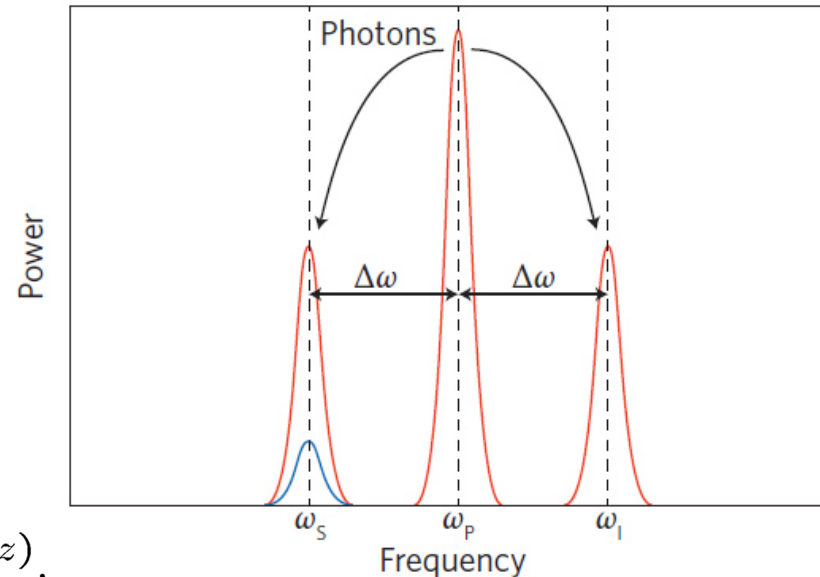
Assume a monochromatic wave propagating along an optical waveguide:

$$\mathbf{E}(\mathbf{r}, t) = \frac{1}{2} A_0 e^{j\Phi_{NL}(z)} \frac{\mathcal{E}(x, y, \omega_c)}{\sqrt{\mathcal{P}(\omega_c)}} e^{j(\omega_c t - \beta_c z)}$$

Ansatz: $\underline{A}(z, t) = A_0 e^{j\Phi_{NL}(z)}$

Solution: $\Phi_{NL}(z) = -\gamma |A_0|^2 z$

But: Is this solution stable? What happens to small perturbations $\Delta \underline{A}(z, t)$ of the solution? Do they increase or decay?



“Seeded” modulation instability using two different probe wavelengths

Figures adapted from Nature Photonics 6, 415–416 (2012), and from Agrawal, Nonlinear Fiber Optics

Ansatz: Continuous-wave solution which is perturbed by a small amplitude perturbation $\Delta \underline{A}(z,t)$

$$\underline{A}(z,t) = (A_0 + \Delta \underline{A}(z,t)) e^{-j\gamma |A_0|^2 z}$$

⇒ Linearize NLSE to obtain linear differential equation for the amplitude perturbation:

$$\frac{\partial \Delta \underline{A}(z,t)}{\partial z} = j \frac{1}{2} \beta_c^{(2)} \frac{\partial^2 \Delta \underline{A}(z,t)}{\partial t^2} - j\gamma |A_0|^2 (\Delta \underline{A}(z,t) + \Delta \underline{A}^*(z,t))$$

Time- and space-harmonic ansatz:

$$\Delta \underline{A}(z,t) = C_1 e^{j(\Omega t - Kz)} + C_2 e^{-j(\Omega t - Kz)}$$

⇒ Linear equations for wave amplitudes C_1 and C_2 :

$$\begin{pmatrix} -K + \frac{1}{2} \Omega^2 \beta_c^{(2)} + \gamma |A_0|^2 & \gamma |A_0|^2 \\ \gamma |A_0|^2 & K + \frac{1}{2} \Omega^2 \beta_c^{(2)} + \gamma |A_0|^2 \end{pmatrix} \begin{pmatrix} C_1 \\ C_2 \end{pmatrix} = \begin{pmatrix} 0 \\ 0 \end{pmatrix}$$

Nontrivial solutions only if the determinant vanishes:

$$K = \pm \sqrt{\left(\frac{1}{2} \Omega^2 \beta_c^{(2)}\right)^2 + \Omega^2 \beta_c^{(2)} \gamma |A_0|^2}$$

Dispersion relation for the evolution of the perturbation

Dispersion and gain spectrum

Normal dispersion ($\beta_c^{(2)} > 0$): K real

⇒ Solution always stable

Anomalous dispersion ($\beta_c^{(2)} < 0$): K imaginary for $|\Omega| < \Omega_g = \sqrt{\frac{4\gamma |A_0|^2}{-\beta_c^{(2)}}}$

⇒ Solution unstable

Associated gain spectrum: $g(\Omega) = \left| \beta_c^{(2)} \right| \Omega \sqrt{\Omega_g^2 - \Omega^2}$

Gain spectra for three power levels of the cw signal. The so-called “nonlinear length” is given by

$$L_{NL} = (\gamma |A_0|^2)^{-1}$$

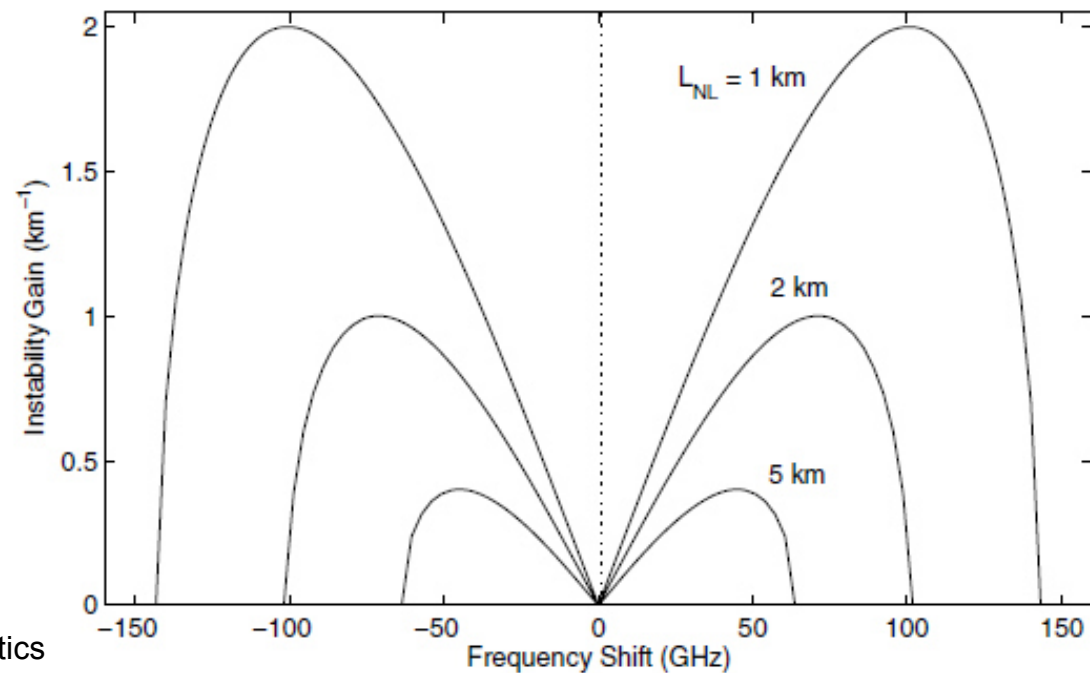


Figure adapted from Agrawal, Nonlinear Fiber Optics

Ansatz: Continuous-wave solution which is perturbed by a small amplitude perturbation $\Delta \underline{A}(z,t)$

$$\underline{A}(z,t) = (A_0 + \Delta \underline{A}(z,t)) e^{-j\gamma |A_0|^2 z}$$

⇒ NLSE leads to differential equation for the amplitude perturbation:

$$\frac{\partial \Delta \underline{A}(z,t)}{\partial z} = j \frac{1}{2} \beta_c^{(2)} \frac{\partial^2 \Delta \underline{A}(z,t)}{\partial t^2} - j\gamma |A_0|^2 (\Delta \underline{A}(z,t) + \Delta \underline{A}^*(z,t))$$

Time- and space-harmonic ansatz:

$$\Delta \underline{A}(z,t) = C_1 e^{j(\Omega t - Kz)} + C_2 e^{-j(\Omega t - Kz)}$$

⇒ Linear equations for wave amplitudes C_1 and C_2 :

$$\begin{pmatrix} -K + \frac{1}{2} \Omega^2 \beta_c^{(2)} + \gamma |A_0|^2 & \gamma |A_0|^2 \\ \gamma |A_0|^2 & K + \frac{1}{2} \Omega^2 \beta_c^{(2)} + \gamma |A_0|^2 \end{pmatrix} \begin{pmatrix} C_1 \\ C_2 \end{pmatrix} = \begin{pmatrix} 0 \\ 0 \end{pmatrix}$$

Nontrivial solutions only if the determinant vanishes:

$$K = \pm \sqrt{\left(\frac{1}{2} \Omega^2 \beta_c^{(2)}\right)^2 + \Omega^2 \beta_c^{(2)} \gamma |A_0|^2}$$

Dispersion relation for the evolution of the perturbation

Dispersion and gain spectrum

Normal dispersion ($\beta_c^{(2)} > 0$): K real

⇒ Solution always stable

Anomalous dispersion ($\beta_c^{(2)} < 0$): K imaginary for $|\Omega| < \Omega_g = \sqrt{\frac{4\gamma |A_0|^2}{-\beta_c^{(2)}}}$

⇒ Solution unstable

Associated gain spectrum: $g(\Omega) = \left| \beta_c^{(2)} \right| \Omega \sqrt{\Omega_g^2 - \Omega^2}$

Gain spectra for three power levels of the cw signal. The so-called “nonlinear length” is given by

$$L_{NL} = (\gamma |A_0|^2)^{-1}$$

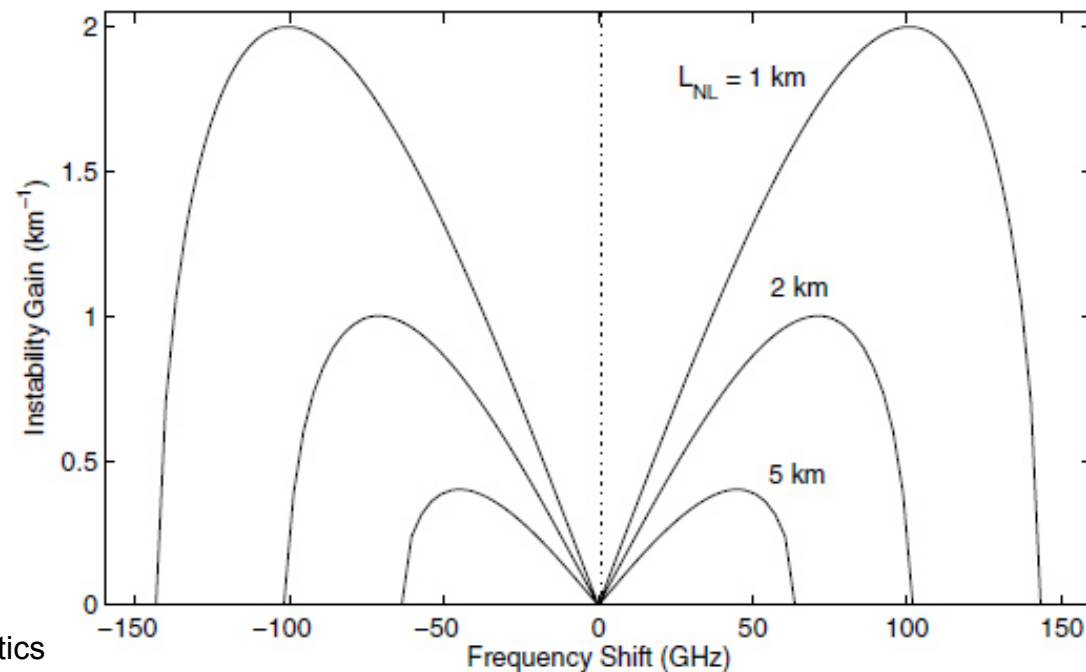
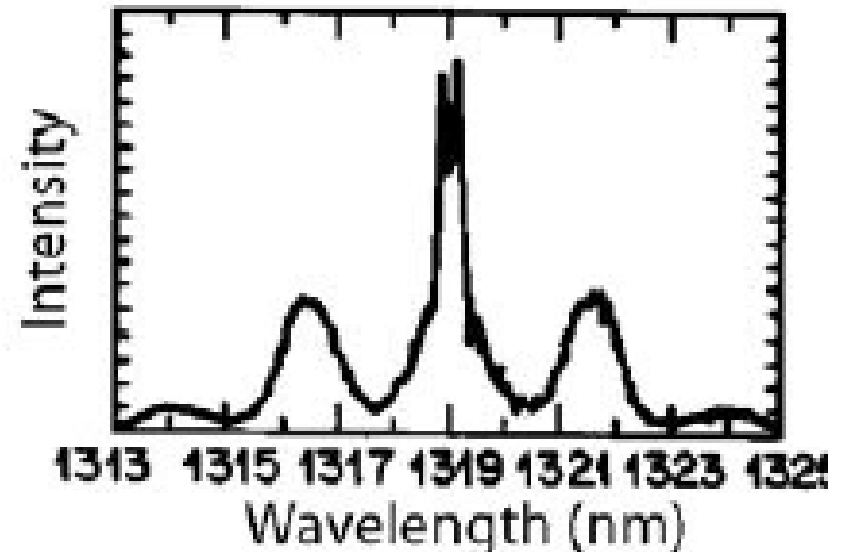


Figure adapted from Agrawal, Nonlinear Fiber Optics

Modulation instability in optical fibers

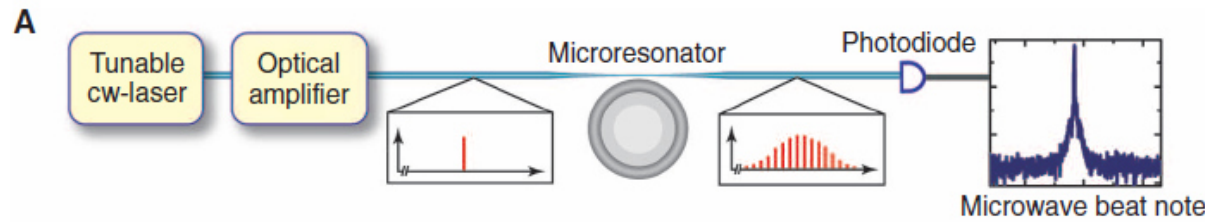
- Gain spectrum of modulation instability is (approximately) **symmetric** with respect to the cw signal
- **Our analysis:** Modulation instability gain always present to the optical carrier
- **Real fiber:** Modulation instability gain only visible if it overcomes **propagation loss**



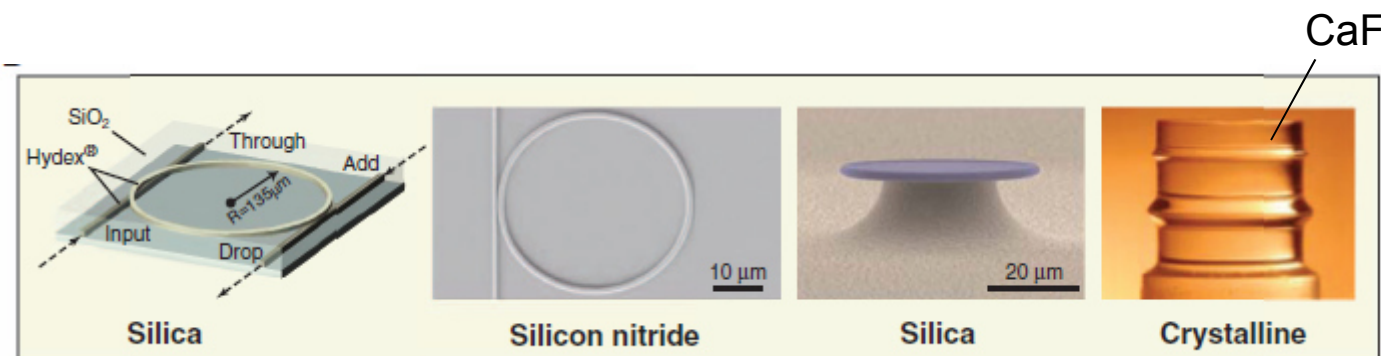
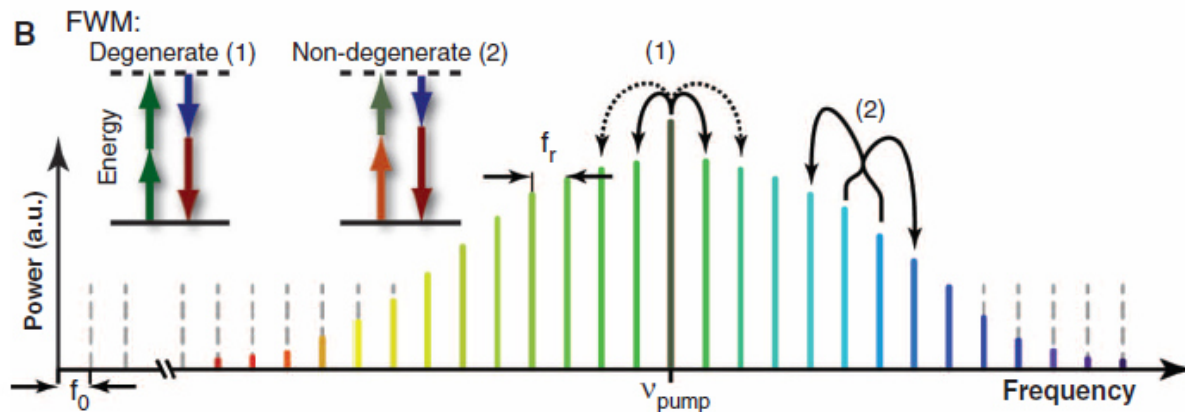
Sidebands at fiber output occurring as a consequence of modulation instability.

Figures adapted from Agrawal, Nonlinear Fiber Optics

Modulation instability and Kerr comb generation in optical microresonators



High-Q optical resonator “stores” sideband photons and enables generation of further sidebands by four-wave mixing
 ⇒ Broadband frequency combs

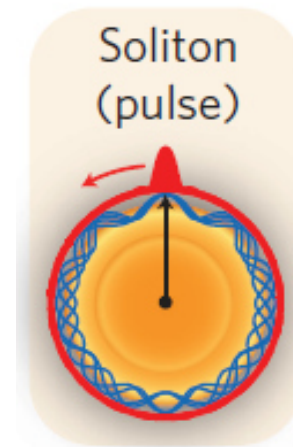
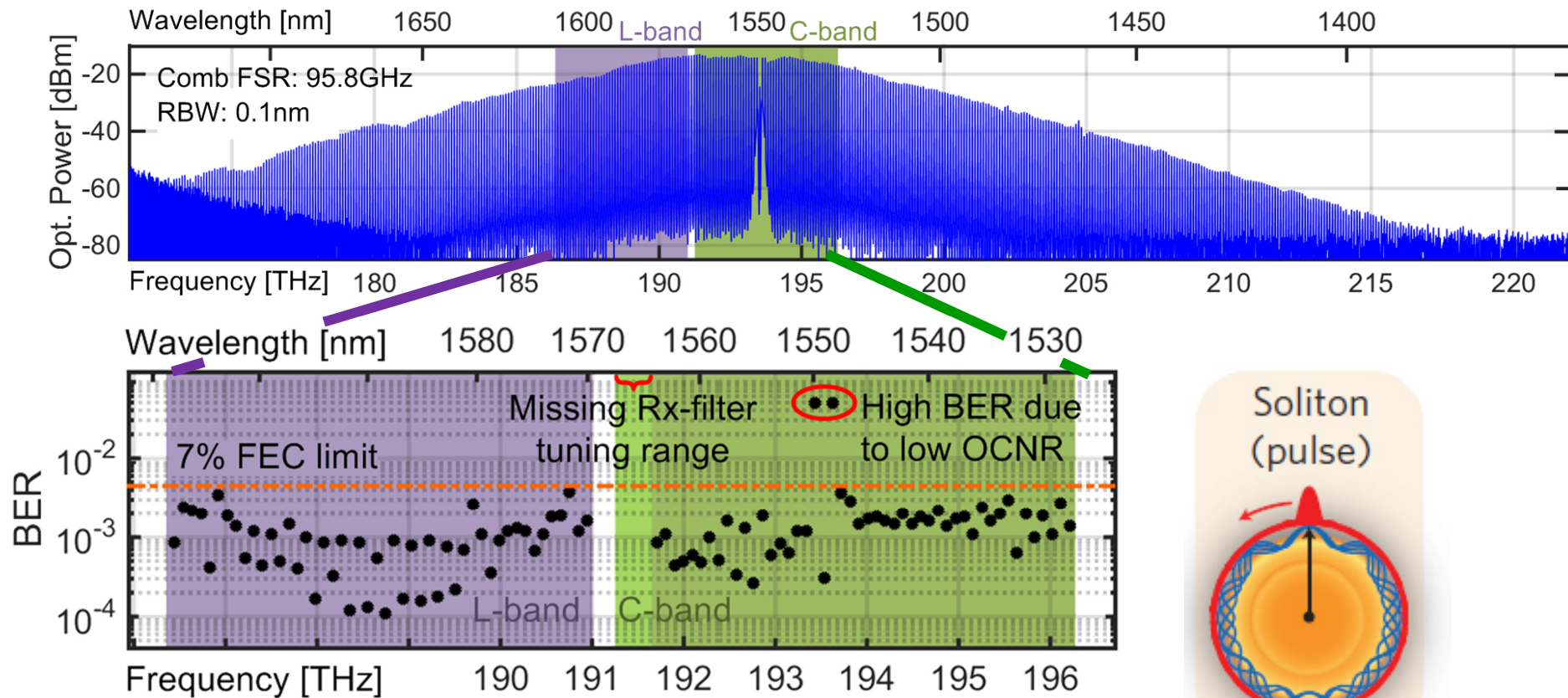


Key:

- Low-loss / high-Q resonators with large transparency window
- Anomalous group-velocity dispersion

Figures adapted from Nature Photonics 6, 415–416 (2012)

Kerr soliton comb generation and data transmission



Superposition of all resonator modes leads to formation of a cavity soliton

> 100 comb lines in C and L-band
 Aggregate net data rate: up to 50 Tbit/s

Marin *et al.*, Nature **546**, 274–279 (2017)

Summary

Linear and nonlinear optics

- Maxwell's equations in linear and nonlinear optics
- Linear and nonlinear dielectric polarization
- Kramers-Kronig relations
- Wave propagation in linear and nonlinear optics
- Slowly-varying envelope approximation
- Retarded time frames
- Overview of various second- and third-order nonlinear processes
- Kerr effect and intensity-dependent refractive index
- Parametric and nonparametric processes

The nonlinear optical susceptibility

- Formal definition and tensor notation
- Properties of the nonlinear optical susceptibility tensor
- Spatial symmetry and Neumann's principle
- Contracted notation

Second-order nonlinear effects

- Permittivity and impermeability tensor
- Biaxial, uniaxial, and isotropic crystals

- Index ellipsoid
- Wave propagation in anisotropic crystals
- Linear electro-optic effect / Pockels effect
- Electro-optic modulators
- LiNbO₃ modulator: Principle and technical realization
- Mach-Zehnder modulators
- Impact of phase mismatch in various second-order nonlinear effects
- Phase matching concepts: Type-1, type-2, quasi-phase-matching
- The Manley-Rowe relations
- Parametric amplifiers and oscillators

Acousto-optics and photon-phonon interactions

- Elasto-optic effect and tensor representation
- Acousto-optic modulators and related devices
- Acoustic and optical phonons
- Brillouin and Raman scattering
- Raman amplifier and laser

Third-order nonlinearities

- Impact of third-order nonlinearities on transmission links
- Signal propagation in linear and nonlinear optical waveguides

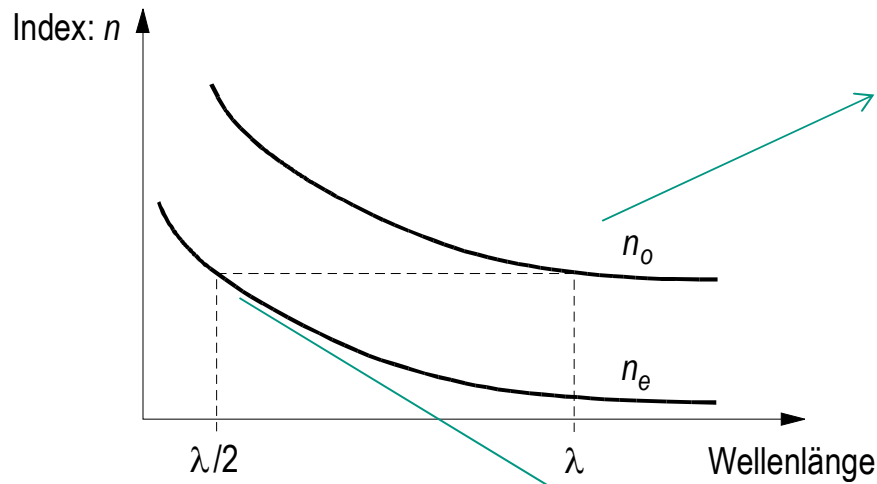
Summary III

- Nonlinear Schrödinger equation and interplay of nonlinearity and dispersion
- Spectral broadening in optical fibers
- Optical solitons

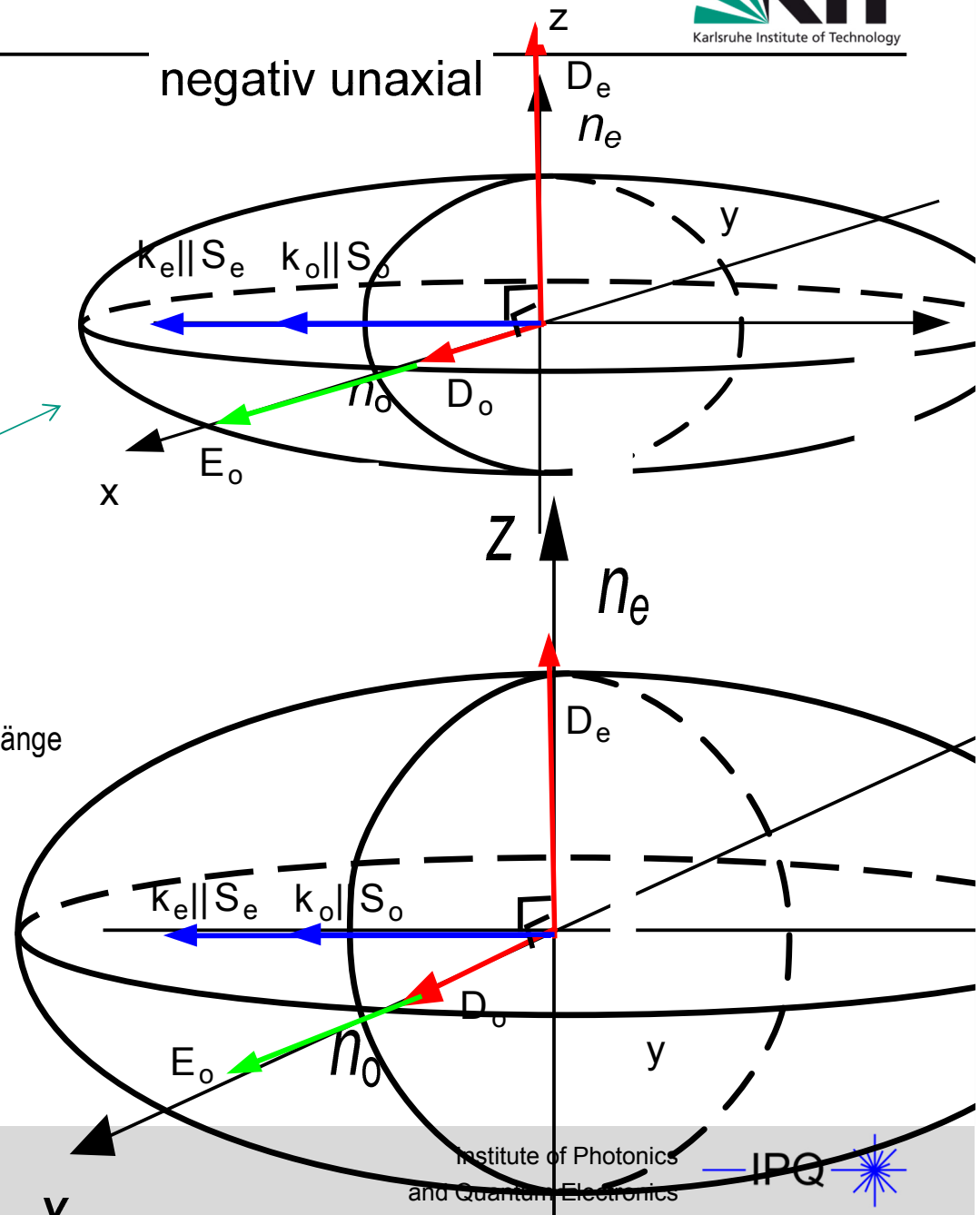
Lecture 14

Non-critical phase matching

Non-critical = 90° phase-matched



No energy walk-off
Finetuning via temperature



Critical phase match

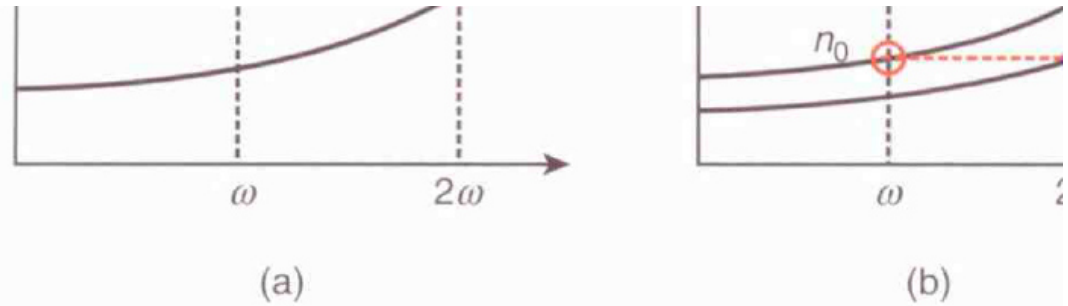
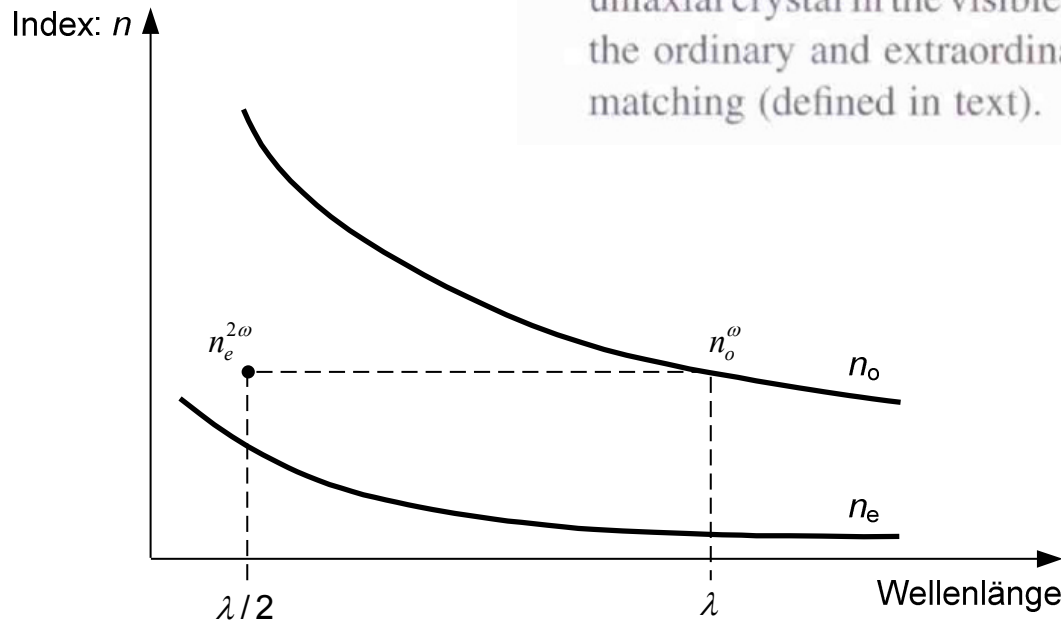
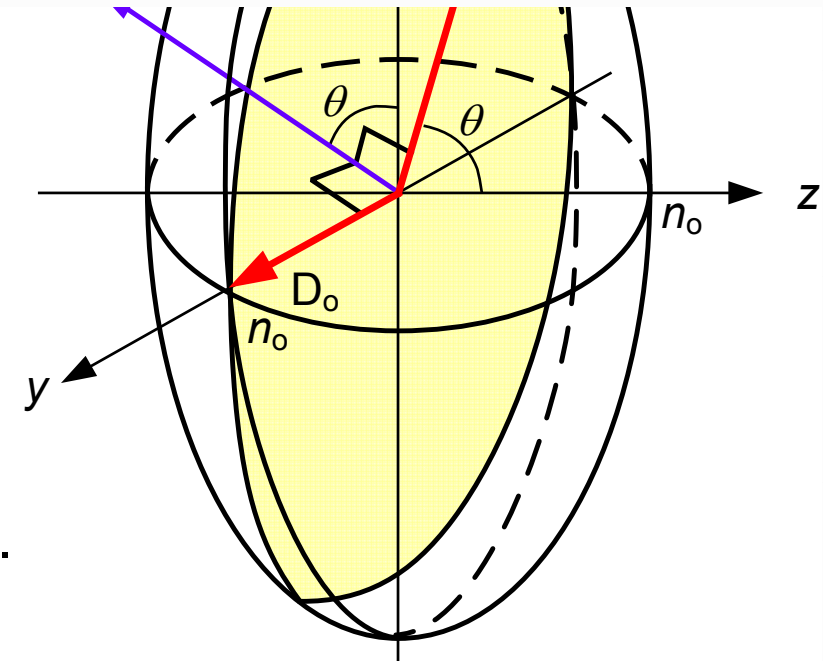


FIGURE 3.1 The dispersion in the refractive index for a (a) single polarized uniaxial crystal in the visible and near-infrared regions. n_o and n_e are the refractive indices for the ordinary and extraordinary polarizations. The case shown is for noncritical phase matching (defined in text).



Matching angle needs to be determined.
Energy walk-off



The walk-off angle can be derived from the indicatrix.

Critical phase matching – Type 2

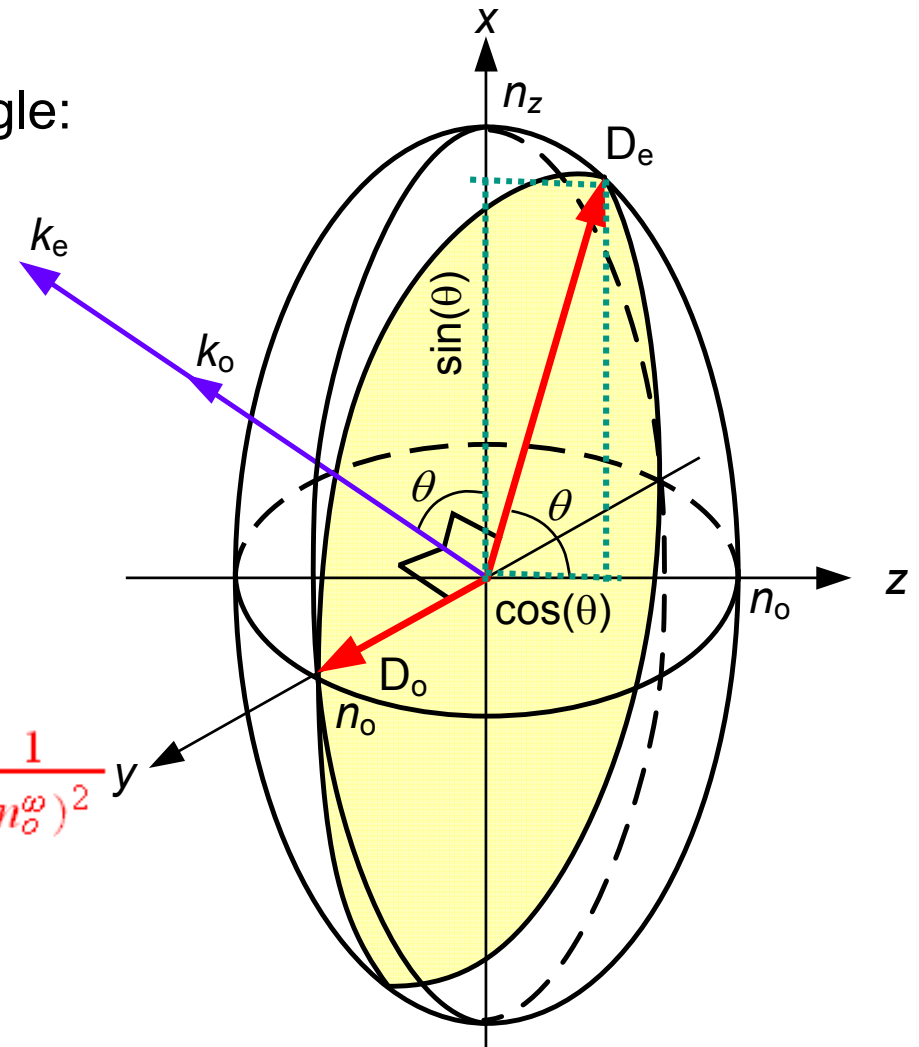
Determination of the phase matching angle:

The refractive index for a wavevector k :

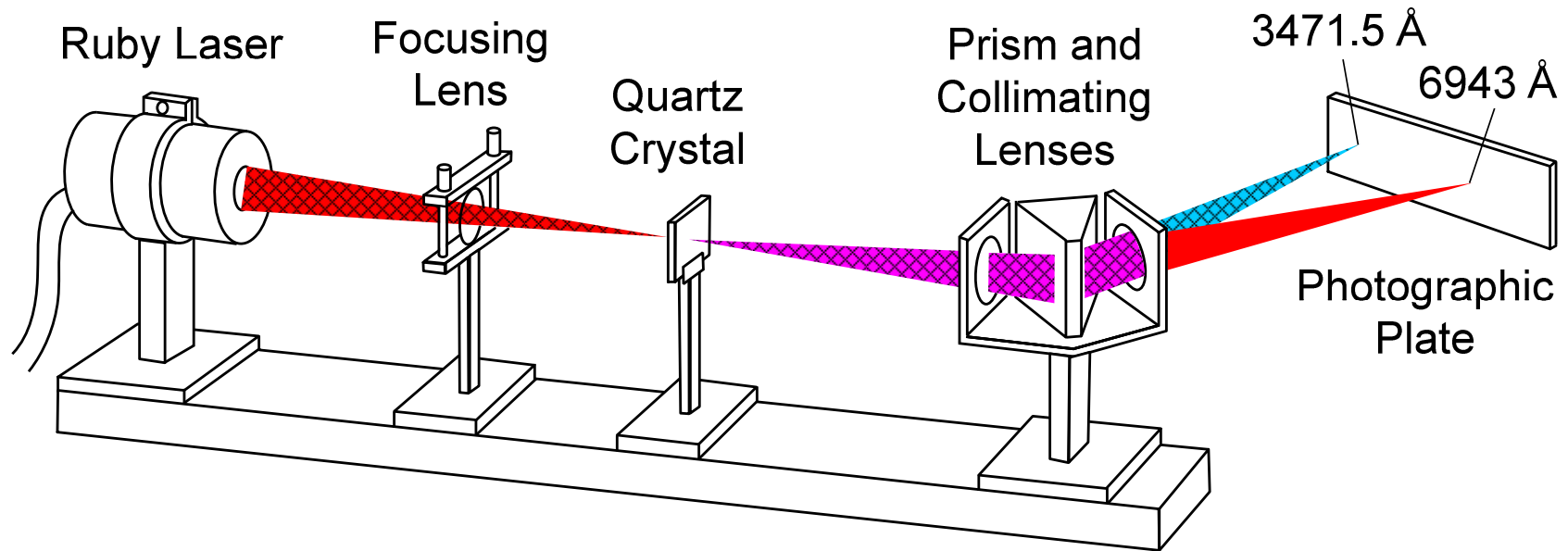
$$\frac{1}{n^2(\theta)} = \frac{\cos^2(\theta)}{n_o^2} + \frac{\sin^2(\theta)}{n_e^2}$$

The refractive index of generated and incident waves must match:

$$\frac{1}{(n_e^{2\omega}(\theta_p))^2} = \frac{\sin^2\theta_p}{(n_e^{2\omega})^2} + \frac{\cos^2\theta_p}{(n_o^{2\omega})^2} \stackrel{!}{=} \frac{1}{(n_o^\omega)^2}$$



Sum-frequency generation and impact of phase mismatch



Frequency Doubling Franken, 1961

Uncritical

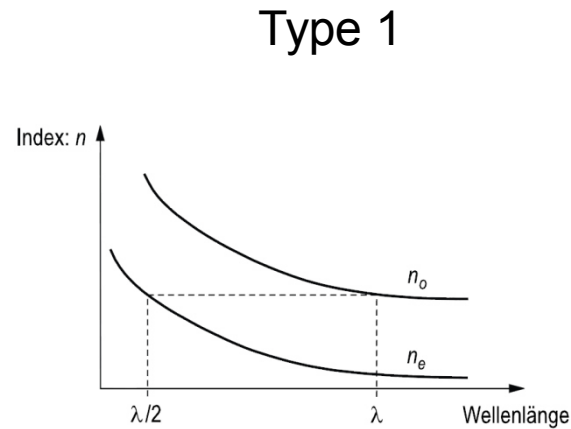


Abb. 4.6.: Nichtkritische Phasenanpassung

Critical

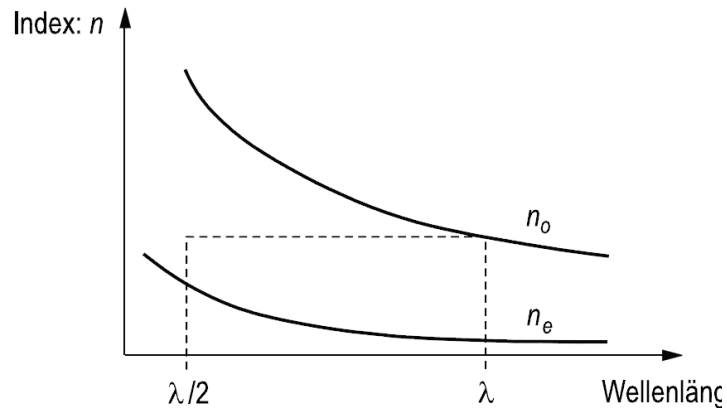


Abb. 4.7.: Typ I - kritische Phasenanpassung

Typ

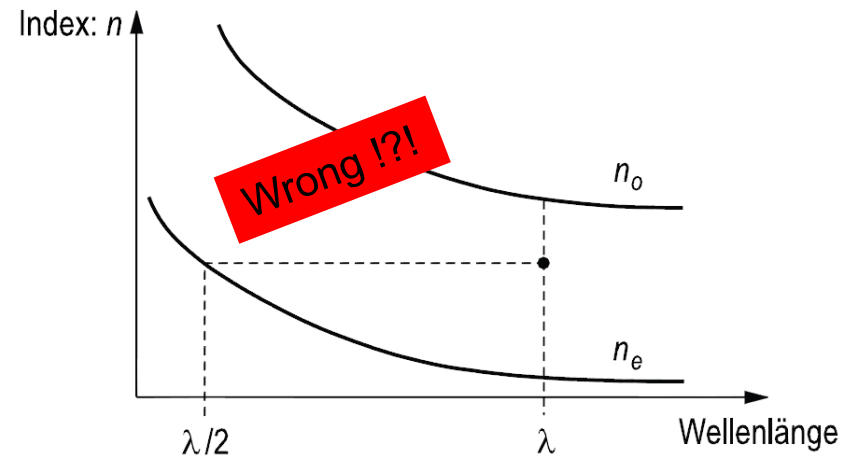
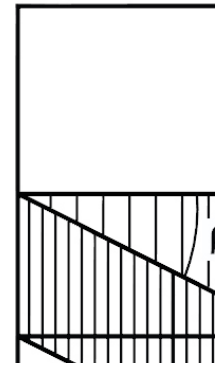


Abb. 4.9.: Typ II - kritische Phasenanpassung

